STUDIES ON ELECTROMECHANICAL SENSORS AND ACTUATORS BASED ON CONDUCTING POLYMERS

A THESIS
Submitted to the

UNIVERSITY OF PUNE (INDIA)

For the degree of

DOCTOR OF PHILOSOPHY (Ph.D.)

In
CHEMICAL ENGINEERING

By

SWARNENDU BIKAS KAR

Chemical Engineering Division
National Chemical Laboratory (NCL)
Pune – 411008 (INDIA)

August 2005

CERTIFICATE

Certified that the work incorporated in this Thesis entitled **"Studies on Electromechanical Sensors and Actuators based on Conducting Polymers"** submitted by **Mr. Swarnendu Bikas Kar**, was carried out by him under my supervision / guidance at the Chemical Engineering Division, National Chemical Laboratory, Pune-8. Such material as has been obtained from other sources has been duly acknowledged in this thesis.

August 2005

Dr. B.D.Kulkarni
Research Guide

CERTIFICATE

Certified that the work incorporated in this Thesis entitled **"Studies on Electromechanical Sensors and Actuators based on Conducting Polymers"** submitted by **Mr. Swarnendu Bikas Kar**, was carried out by him under my supervision / guidance at the Chemical Engineering Division, National Chemical Laboratory, Pune-8. Such material as has been obtained from other sources has been duly acknowledged in this thesis.

August 2005

Dr. S. Radhakrishnan
Research Co-Guide

ACKNOWLEDGEMENTS

I take this opportunity with deep sense of gratitude to record my sincere thanks to my research supervisors ***Dr. B. D. Kulkarni & Dr. S. Radhakrishnan****, for their keen interest, valuable guidance, drive towards perfection and constructive criticism during the course of this investigation. The fruitful discussions helped me to orient myself to analyze, design and execute scientific problems in the direction of the welfare of the mankind.*

I wish to thank ***Director, NCL, Pune,*** *for permitting me to do this research work, providing me the excellent facilities and permitting me to submit this work in the form of a PhD thesis.*

I take this opportunity to gratefully remember all my teachers, whose inspirations are always like a lighthouse.

I wish to thank my labmates Arindam, Dr.Shivkalyan, Francis, Ramanujan, Santhosh, Subramanyam, Pradip, Shreejit, Narendra, Radhakrishnan, Dr.R.C.Patil, Dr.S.D.Deshpande, Raut, Shalaka, and Jaykarna for their willing co-operation extended to me in various stages of this work.

It will be injustice if I have not mentioned the great help provided by some of my friends to complete the characterization and compounding part of this thesis. I wish to thank Suresh P.R, Santosh H.L, Raman, Prakash, N. Pawaskar, Gaikewad for their unstinted support and help

There are so many other friends whose support has been helpful for me to take challenges and to improve. It is difficult to name all of them. My heartfelt thanks to all.

I would like to give full credit to my parents for every achievement I had in my life. Also I gratefully acknowledge the support of my sisters.

Financial assistance from the Council of Scientific and Industrial Research (CSIR), New Delhi, is gratefully acknowledged.

National Chemical Laboratory,

Pune. ***Swarnendu Bikas Kar***

DECLARATION

I hereby declare that the work incorporated in the thesis entitled "**Studies on Electromechanical Sensors and Actuators Based on Conducting Polymers**" submitted for the degree of Doctor of Philosophy to the University of Pune, has been carried out by me at the National Chemical Laboratory, Pune under the supervision of Dr. Dr. B. D. Kulkarni & Dr. S. Radhakrishnan. The work is original and has not been submitted in part or full by me for any other degree or diploma to this or any other university.

August-2005

National Chemical Laboratory
Pune-411 008

Swarnendu Bikas Kar
Research Student

DEDICATED TO
MY PARENTS & WELL WISHERS

CONTENTS

CHAPTER I: Introduction

CHAPTER II: Experimental

CHAPTER III: Theoretical Model

Results and Discussions

CHAPTER IV: Sensor

Piezo-Sensitivity of PVDF-PANI Blends

LIST OF ABBREVIATIONS

CP	-Conducting polymer
ICP	-Inherently conducting polymer
PA	- Polyacetylene
PT	- Polythiophene
PANI	-Polyaniline
EB	-Emeraldine base
ES	-Emeraldine salt
LEB	-Leucoemeraldine base
PPy	-Polypyrrole
HCl	-Hydrochloric acid
DBSA	-Dodecylbenzenesulfonic acid
M-P-M	-Metal-particle-metal
FL	- Fermi level
SCLC	-Space charge limited conduction
P-F	-Poole-Frenkel
TN	-Nordheim tunneling
SE	-Schottky emission
PANI-DBSA	-Polyaniline doped with dodecylbenzenesulfonic acid
PANI-HCl	-Polyaniline doped with hydrochloric acid
PANI-SBS(HCl)	-Polyaniline(doped with hydrochloric acid) and styrene butadiene styrene blends
PANI-SBS(DBSA)	-Polyaniline(doped with dodecylbenzenesulfonic acid) and styrene butadiene styrene blends
PANI-PVDF(HCl)	-Polyaniline(doped with hydrochloric acid) and polyvinylidene fluoride blends
PANI-PVDF(DBSA)	-Polyaniline(doped with dodecylbenzenesulfonic acid) and polyvinylidene fluoride blends
WXRD	-Wide angle X-RAY diffraction
SEM	-Scanning electron microscopy

BBM	-Bending beam method
Au	-Gold
MSA	-Methyl sulfonic acid
PTSA	-*p*-toluene sulfonic acid
CSA	-Camphor sulfonic acid
H_2SO_4	-Sulfuric acid
PET	-Polyethylene terephthalate
LDPE	-Low-density polyethylene
LLDPE	-Linear low-density polyethylene
PP	-Polypropylene
$LiClO_4$	-Lithium perchlorate

LIST OF SYMBOLS

β_{SE}	-Schottky coefficient
σ	-Stress
G	-Gauge factor
T	-Temperature
P/A	-Stress
$\in$	-Strain
μ	-Mobility of electron
t	-Time
q	-Charge
i	-Current
V	-Voltage
I	-Moment of inertia
m	-Mass
g	-Gravity
d	-Density of water
R	-Resistance
ρ	-Resistivity
σ	-Conductivity
Rp	-Resistance of matrix polymer
R_f	-Resistance of conducting particle
Np	-Number of M-P-M junction in parallel
Ns	-Number of M-P-M junction in series
B^2	-Cross sectional area of sensors
L	-Thickness of sensors
α	-Compressibility
S	-Sensitivity factor
P	-Applied load
d	-Interparticle separation
β	-Non linear function of mechanical property

N_{eff}	-Number of effective junction
$f(\varphi)$	-Volume fraction function
D	-Conducting particle diameter
ϕ	-Volume fraction of conducting particle
θ	-Bending angle
d_1	-Thickness of backing layer
d_2	-Thickness of conducting polymer
ρ	-Density
E	-Modulus of actuator
E_1	-Modulus of backing layer
E_2	-Modulus of conducting polymer
b	-Width of actuator film
p	-Combined force of gravitation and water pressure
W	-Total load on actuator
F	-Force
L	-Length of actuator
A	-Area of actuator
Δ	-Potential barrier height
n	-Non-linear function of current

Studies on Electromechanical Sensors and Actuators Based on Conducting Polymers

Abstract:

In the recent age of robotics and remote control systems, electro-mechanical devices play a very important role in many areas. Conducting polymers are important materials in electronic devices. These materials may be used in a large number of applications such as sensors, actuators, and displays etc., which are associated with their excellent reversible redox behavior. On the other hand, these materials also exhibit sensitivity to chemical, thermal and pressure environment which would be expected to make these useful as electro-mechanical sensors and actuators. Smart materials based on conducting polymers could be useful for robotics and remote control systems in various fields such as industrial control systems, aerospace, bio-medicals, drug delivery systems, etc.

For this purpose, detailed understanding in depth of the mechanism of piezo-sensitivity and actuation effect in conducting polymer blends and composites are essential. Firstly, theoretical model has been formulated for the sensor and actuator with conducting polymer placed in contact with another insulating polymer. Constitutive equations have been formulated considering series / parallel model of composite system, taking into account the modulus, thickness and various other parameters. The phenomenological model for piezo-sensor indicated that the piezo-resistivity in conducting polymer blends or composites takes into account the non-linear conduction process as well as non-linear dependence of mechanical response of the flexible matrix. Similarly, phenomenological model for conducting polymer bi-layer actuator indicated that there is an optimum value for the backing layer thickness as well as material modulus together with the thickness of the conducting polymer at which maximum bending is observed. The conducting polymer used were polyaniline and polypyrrole, the cheapest and most stable among all known organic conducting polymers. To improve the compatibility of polyaniline with insulating matrix, synthesized polyaniline (direct chemical method) was redoped with long chain organic acid as a dopant. Semiconducting composites were prepared with two different insulating matrices viz. styrene-butadiene co-polymer (SBS) and polyvinylidene

fluoride (PVDF). Current voltage characteristics of both composites with particular compositions are highly non linear in nature and shows highest piezo-sensitivity at that particular composition. The dopant ion also plays an important role since the phase morphology changes with the same. Phase segregated morphology shows higher piezo-sensitivity rather than more compatible morphology. In case of PVDF-PANI composites electrical poling at room temperature enhances piezo-sensitivity. In general, we use the term bending angle to refer to actuation. As the backing layer (insulating part of bi-layer actuator) thickness is decreased the bending angle increases for all types of backing layer. SBS shows maximum bending angle amongst the various polymers studied in comparable thickness values viz. co-polyester (Hytrel), low-density polyethylene (LDPE/LLDPE), polypropylene (PP), and polyester (PET). Modulus of the backing layer plays vital role in obtaining good actuation. The bending angle (θ_B) also passes through a maximum with conducting polymer (PPy) layer thickness. Dimension of actuator controlled the bending angle. Higher applied potential can cause more bending. Polypyrrole morphology also plays an important role in obtaining a higher bending angle. Very compact as well as fluffy types of morphology in PPy show lower bending angle. The (θ_B) was also measured in presence of different types of electrolytes in different solvents.

The present work is divided into six chapters–the first two chapters being (I) Introduction and (II) Experimental, which give the basic historical background of sensors and actuators and details of experimental methods used. The next three chapters are related to the research work on phenomenological model, synthesis as well as properties of these conducting polymer based materials. They give the results and discussions for phenomenological model for piezo sensors and bi-layer actuators in chapter III, role of non linear effect on piezo-sensitivity of SBS/PANI and PVDF/PANI blends in chapter IV, synthesis and actuation properties of PPy bi-layer actuator in chapter V respectively. The last chapter (VI) gives the summary and conclusions. Each chapter is described briefly as follows.

Chapter I. Introduction:

Chapter I of the thesis begin with an overview of the different types of the conducting polymers and their application in various fields. Historical background and an introduction to conducting polymers along with their classification, doping agents, types of doping are given. A brief review of conducting polymers are viz. most studied polypyrrole and polyaniline is given along with its method of synthesis (electrochemical and chemical synthesis), and their applications. The importance of polyaniline and polypyrrole amongst different conducting polymers is highlighted and their selection for the present work is justified. A short description to the sensors and actuators and their classification is presented here. A brief historical review of advantages of conducting polymer sensors and actuators, different relevant non-linear current voltage characteristics relating to composites systems is described. The detailed discussion on the non linear current voltage characteristics of semiconducting composites, non linear mechanical properties of the same, factors affecting piezo-sensitivity and the factors which govern the choice of a specific charge transport phenomena for a particular system are also discussed in this chapter. Different types of models related to piezo-sensors and actuators are described here. Importance of the different insulating materials acting as a matrix in sensor and backing layer in bi-layer actuators is also explained. A brief review of the importance of bi-layer actuator in artificial muscles and piezo-sensors in aerospace application are also given here. An overview of electrochemical system, types of electrochemical techniques, an introduction to the redox properties of conducting polymers and the origin of actuation of conducting polymers are also described. The last part of the chapter discusses the aim and scope of the present work

Chapter II. Experimental:

This chapter describes experimental techniques for the preparation of polyaniline and polypyrrole. The electrochemical set up used for synthesis of polypyrrole on gold-coated insulating matrix to prepare laminate (actuator sheet) is described here. This chapter is mainly divided into two sections as given below.

Section A: Sensor Fabrication and Testing

This section deals with two routes that were employed for synthesis of polyaniline with different dopants, like standard direct and indirect route (dedoping and re-doping method) and of solution blending of polyaniline with different insulating matrices. In the present work, two grades of polyaniline (PANI) were prepared by chemical route using HCl as a acidic doping agent and $(NH_4)_2S_2O_8$ as the oxidizing agent respectively in aqueous medium. In another set of experiments, the PANI obtained was treated with a base to neutralize the same and obtain emeraldine base PANI. This was then redoped with dodecylbenzene sulphonic acid (DBSA). Several blend compositions (PANI ranging from 5% to 30%) were prepared separately with insulating matrix polymer styrene-butadiene-styrene tri-block polymer (SBS) and polyvinylidene fluoride (PVDF). The – SBS-PANI (470 μm thick) and PVDF-PANI films (35 μm thick) were prepared by solvent casting method. The electrical properties, current voltage characteristics and piezo-response of conducting polymer blends have been investigated for SBS-PANI and PVDF-PANI composites containing two grades of polyaniline (PANI). The effect of mechanical deformation on the electrical property of the conducting polymer composites / blends were studied using a specially fabricated cell. The piezo-resistivity was measured in these samples by placing them between metal plates on which the mechanical load was applied through top electrode. In this present work, we have prepared poled PVDF-PANI composite films by applying electrical field (25-100 volt/cm^2) and placing it between the two electrodes in opposite directions. The average particle size and the interparticle distance in blends were determined using optical and electron microscopy.

Section B: *Actuator Fabrication and Measurement of Response*

This section presents the procedure for deposition of gold films on different polymer films (SBS, Hytrel, PET, PP, LDPE/LLDPE) by resistive heating and vacuum evaporation method. The experimental procedure employed in the electrochemical deposition of polypyrrole on various gold coated films, PET, Styrene Butadiene-Styrene (SBS) tri-block copolymer, Hytrel, PP and LDPE/LLDPE (called as backing layer) is described. Polymerization has been carried out in an aqueous bath containing 0.1M pyrrole and 0.1 M sulphuric acid along with platinum as counter electrode, saturated

calomel as reference electrode (SCE) and applying 0.65 V (vs SCE) constant potential, in a single pattern three electrode cell connected to a computerized potentio – galvanostat (EC2010 Lab India). The electrodes with deposited PPy films were removed, rinsed in distilled water and dried. The bi-layer films having wide range of polypyrrole thickness was prepared by applying constant potential for variable time period. Strips with the dimension of PPy/Au/backing layer area 2.5 cm length and 0.25 cm width were cut out from the laminate for bending test. Actuation measurement techniques are also presented here. The above actuator films were tested for actuation by measuring bending angle (degree) in 0.1(M) $LiClO_4$ dissolved in water applying -1.0 volt potential. Various types of electrolytes used are also reported here. Surface morphology of actuator laminate has been studied by scanning electron microscopy.

Chapter III , Theoretical Model:

In order to understand the ultimate performance limits of conducting polymer sensors and actuators and to predict their response for design purpose it is important to have models that describe their behaviour and provide a physical insight into the underlying physical mechanism for the same. This chapter is mainly divided into two sections as given below.

Section-I Sensor:

This section describes a phenomenological model for piezo-sensors. The conducting polymer composite or a phase separated immiscible blend can be considered as network of uniformly distributed conducting domains with thin insulating films between them. At each of these inter-domain junctions the current voltage characteristics are non-linear. The theory of electrical conductivity or resistivity of conducting composites, taking into account various non-linear conduction processes has been described. Amongst the different non-linear processes such as Schottky effect, Fowler Nordheim tunneling of charge carrier and Space charge limited conduction (SCLC), the piezo-sensitivity was found to be highest when SCLC was present. Following assumptions were made for the model : the effect of applied external pressure on such a composite is to mainly change the interparticle distance and thus cause modulation of resistivity, i.e. the applied load gets dissipated through deformation of the base polymer matrix, conducting particles are

assumed to be rigid, non-linearity of stress - strain relationship in a system contains heterogeneous two phase components. Constitutive equations have been formulated considering parallel model of composite system, taking into account the modulus, dimension of conducting particle, conducting particle loading & different types of conducting particles. A phenomenological model has been proposed for the piezo-resistivity in conducting polymer blends or composites which takes into account the non-linear conduction process as well as non-linear dependence of mechanical response of the flexible matrix. The conducting polymer blends exhibit piezo-sensitivity which is found to be dependent on composition, type of the matrix used, applied pressure etc. It has been shown that these materials exhibit high piezo-sensitivity at a certain concentration of conducting particles which also depends on the modulus of blends or composites, applied pressure and the particle / domain size of the conducting phase. The piezo-sensitivity is highest when space charge limited conduction is present. This theoretical model is able to explain many aspects of the piezo-sensitivity of conducting blends or composites.

Section-II , Actuator :

This section describes a phenomenological model for conducting polymer based actuators. Amongst the various types of configurations for the conducting polymer based actuators, the bi-layer type is more attractive since these are more sturdy and easy to prepare as well as handle. During these investigations a phenomenological model was established, considering the bi-layer as a cantilever beam with uniform bending pressure arising from applied current / potential on the electro-active polymer. Following assumptions were made for the model; conducting polymer is porous, allowing easy diffusion of ions and small molecules within it, the plane surface cross section remains plane on macroscopic scale, both conducting polymer and backing layer are isotropic and elastic , the strain in the conducting polymer layer is homogeneous along planes parallel to the interlayer junction, the change in Young's modulus of the conducting polymer is negligible during the doping / dedoping process , the bending force which arises from the ion insertion is uniformly exerted along length of the film , electrolyte pressure on the actuator film is negligible. Constitutive equations have been formulated considering parallel model of composite system, taking in to account the modulus,

thickness and co-operative deformation of the two layers. The correlation between the bending angle and the above parameters has been derived. The bending angle was calculated as a function of modulus and thickness of backing layer and conducting polymer layer respectively. It has been shown that there is an optimum for the backing layer thickness as well as the material modulus along with the thickness of the conducting polymer at which maximum bending is observed. .

Chapter- IV. Results and Discussion (Sensor) :

Electronically conducting polymers have attracted a great deal of interest in different types of sensors such as chemical gas sensors, opto-electronic sensors, tactile sensors etc. The electrical properties, current voltage characteristics and piezo-response of conducting polymer blends have been investigated with respect to composition for SBS-PANI and PVDF-PANI composites containing two grades of polyaniline (PANI).The change in resistivity of composites with volume fraction of polyaniline depends on the type of dopant and it is sharp for PANI-DBSA blends than that for HCl doped PANI. In the case of SBS-PANI blends ,the percolation threshold appears at about 10% PANI for HCl doped , while it is about 1% for DBSA doped PANI. In the case of PVDF-PANI blends for HCl doped PANI, the percolation threshold appears at about <10% PANI loading while for DBSA doped PANI, it is about 5% PANI. This is due to the particle size of the PANI used, the distribution of the added component, compatibility of the PANI etc. Optical and electron microscopy show that, the polyaniline particle size is very much smaller for DBSA than for HCl doped PANI. In this case, the inter-domain distance is much smaller for the same concentration of PANI than for HCl doped PANI.

The I-V Characteristics of these blends were investigated without any mechanical load applied to the sample. The I-V characteristics are almost non-linear in all cases but their nature changes with PANI concentration and nature of dopant. The I-V curves are mainly conforming to the SCLC mechanism while at higher concentrations, even tunneling type characteristics are observed. The present studies indicate that the piezo-sensitivity is higher for the compositions having SCLC type charge transport than ohmic or even the tunneling type conduction. This may arise from the lower dependence of current on thickness (here inter-particle gap “d”) and lack of charge storage in the same as

compared to the SCLC case. In the SCLC case, the charge stored under constant applied field can get liberated during the application of pressure due to overlap of the levels and /or increase of contact area giving rise to additional current in forward direction. During poling, the I-V nature of PVDF-PANI film changes more towards SCLC mechanism which was proved by log-log plot of I-V characteristics where, n value calculated upto 1 volt changes from 1.0 to a value 2.0 in higher voltage region >1 volt, which reflects SCLC type electronic conduction mechanism.

The piezo-sensitivity of SBS-PANI blends was measured but in case of PVDF-PANI blends it was measured before and after poling in electrical field 25KV/cm^2 for 90 min.) at room temperature. The pressure (P) dependence of resistance (R) in these cases followed the power law $R = KP^{-m}$ where, K is a constant and m is an exponent which depends on the composition of the sample. It is clearly seen from these values of K and m that the pressure dependence of the electrical resistance is highly non-linear and depends very much on the composition as well as the type of PANI incorporated in the blend. The piezo-sensitivity factor ($\sigma/ \sigma o = Ro/R$) is very much dependent on the concentration of the conducting phase. Average inter-particle distance (d) was calculated theoretically from the equation given for a uniformly dispersed two phase system as well as experimentally confirmed using SEM of cross-section of samples. The value of "d" decreases with increasing polyaniline loading. During application of external mechanical pressure load the interparticle distance changes giving rise to a rapid change in the electrical resistance For low polyaniline loading, d will be large but change in d is small where as at high PANI concentration, d tend to zero as the particles touch each other. Accordingly, the piezo-sensitivity will also change with to composition and it shows a maximum at a certain critical composition at which (d) is optimized. SBS-PANI blends with 15% PANI (HCl doped) loading shows more piezo-sensitive than other blends including DBSA dopant system whereas, PVDF-PANI blends with 10% PANI (HCl doped) loading shows more piezo-sensitive than other blends including DBSA dopant system in both the unpoled and poled condition. Poling in electric field shows very high piezo-sensitivity due to the appearance of a dipolar α phase and to some extent a newly generated highly polar β phase which is confirmed by FTIR and WAXD of PVDF-PANI

blends (5% PANI loading) comparing insignificant change in curves of PVDF without any polyaniline.

Chapter- V. Results and Discussion (Actuator):

Conducting polymer offers the promise of creating the flexible, low –mass actuators that can form the basic building blocks of artificial muscles. This chapter explains the selection of a particular backing layer, electrolyte, potential limit etc. in bi-layer type actuator. Conductive polymers typically function via the reversible counter ion insertion and expulsion that occurs during redox cycling. Oxidation and reduction occurs at the electrodes, inducing a considerable volume change mainly due to the exchange of ions with the electrolyte.

Bi-layer type actuators were fabricated. The conducting polymer coated electrodes were prepared by electrochemical polymerization of pyrrole in a single pattern three-electrode cell. The above actuator films were tested for actuation by measuring bending angle (degree).

Actuator films having a backing layer of SBS, Hytrel, PET and LDPE/LLDPE, PP were tested for actuation in 0.1 M solution of $LiClO_4$ applying -1.0 volt potential. It is evident that, as the backing layer thickness is decreased the bending angle increases for all polymers studied. At constant thickness, SBS shows maximum bending angle as compared to Hytrel, LDPE/LLDPE, PP, and PET. In each case, θ_B increases very rapidly after a certain thickness (called optimum thickness) which depends on the backing polymer. Optimum thickness was highest for SBS back layer actuator than Hytrel, LDPE/ LLDPE, PP and PET respectively. Also, the bending angle was highest for SBS back layer film than Hytrel, LDPE/ LLDPE, PP and PET of comparable thickness due to backing layer modulus value. Bending angle attains a steady value after a certain modulus value (500 MPa). It is also interesting to note that the modulus of the backing layer plays a vital role in obtaining good actuation. It is clear that the length to width ratio is also an important design parameter when improving the bending performance of actuators at these operating conditions. Higher ratio shows more non-linearity (higher slope) with bending angle. Actuator width is more influential than actuator length.

Bending angle passes through maxima with conducting polymer (PPy) layer thickness. Again, maxima depend on thickness and nature of the backing layer. In case of 25μm, 50 μm, 75μm and 100 μm thickness of PET backing layer maximum bending arises at 1.91 μm, 3.08 μm, 5.2 μm and 8.39 μm respectively. It follows the same trend for PP and LDPE/LLDPE with different numerical values. In this configuration, the bending force would increase with the increase of conducting polymer layer thickness but only up to certain value since beyond the critical limit, there will be an opposite force due to self-recovery. The backing layer will add to the recovery force and hence the bending angle will be maximum at certain thickness of the conducting polymer. With increasing conducting polymer layer thickness ions diffusion will slow down due to more path length traversed by the ions. With increase of backing layer thickness, maxima (bending angle) shifts towards higher PPy layer thickness. Force required to bend the actuator increases with increasing backing layer thickness. Higher conducting polymer thickness generates more electrochemical force due to greater redox reaction. Electrochemical stretching of higher CP thickness films would be very slow and small due to slow diffusion of dopant ions in the films.

Actuator films with PET backing layer were tested in different potential. Generally, bi-layer actuator exhibits mechanical bending response when excited by electrical voltage. Higher applied potential shows higher bending angle. At higher potential water electrolysis is likely to be taking place with oxygen gas produced at the anode and hydrogen gas at the cathode. This is not the main cause of bending (since deformation is observed at lower potential – 0.4 volt). Higher potential can cause blistering of the coating as well as de-bonding. The initial transient response is due to the charging of the PPy films, which behaves as a capacitor via ionic diffusion. Scanning electron microscopy shows porousness in actuator film after actuation testing. It indicates that SO_4^- escapes during dedoping and creates holes or porosity in PPy films. At higher potential, capacitance of the PPy films increases and so bending angle increases.

PPy was deposited in presence of H_2SO_4, DBSA and CSA. H_2SO_4 doped PPy actuator shows higher bending angle than the other two dopants. PPY actuator film prepared under an applied potential of 0.6 V shows higher bending angle than any other deposition

potential. Actuation behavior is also studied in different electrolytic conditions. Higher $LiClO_4$ concentration shows higher bending angle.

Chapter- VI. Summary and Conclusions:

The final chapter represents a summary of the work carried out and the results described in the thesis. The conducting polymer blends exhibit piezo-sensitivity which is found to be dependent on composition, type of the matrix used, applied pressure etc. A phenomenological model has been developed which takes in to account the non-linear conduction processes as well as the non-linear variations of mechanical response. This theoretical model is able to explain many aspects of the piezo-sensitivity of these blends or composites. Thus, the role of non-linear processes in piezo-resistivity of conducting polymers has been brought out clearly in the above model.

These studies indicate that SBS-PANI and PVDF-PANI conducting blends can be used for piezo-sensors but their composition has to be optimized for good performance. The blends containing 15 % & 10% of PANI appear to be best for these applications for SBS-PANI and PVDF-PANI respectively. However, the dopant ion and electrical poling also plays an important role since the phase morphology and configuration of insulating matrix phase changes with the same. In the case of DBSA doped PANI, the dopant acts as plasticizer and gives more compatible/finely dispersed blend. This type of morphology is not amenable for obtaining high piezo-sensitivity whereas the HCl doped PANI gives phase segregated morphology and better piezo-sensitivity. It may be pointed out that the conducting polymer blends which are essentially non-compatible behave more akin to composites. Thus, the non-linear characteristics of the electrical conduction as well as the mechanical deformation of the conducting polymer blend and composite affect the piezo-response leading to an optimum composition for highest sensitivity which depends on the modulus of the major matrix, particle / domain size of the dispersed phase as well as the type of conduction process.

A phenomenological model has been proposed for a conducting polymer based bi-layer type actuator which takes into account the nature of backing layer and gives the correlation between the modulus, & thickness of the supporting substrates on the actuation efficiency. It clearly brings out the fact that for a given condition of dopant ion,

applied potential and conducting polymer, there is an optimum thickness of the backing layer, its modulus as well as the thickness of the conducting polymer at which the actuation is maximum. It is clearly found that the model result is more influential with smaller thickness of backing layer and modulus of the same. The optimal design parameters are investigated to estimate the effect of varying experimental conditions on the response of the actuator. Thus, using this information, it is possible to adjust the parameters and choose appropriate materials for good actuating effect.

These studies indicate that SBS/Au/ PPy actuator shows highest bending angle than other bi-layer actuators due to its low modulus value. It can be used for actuators but its design parameters have to be optimized for good performance. Higher width of actuator would not show remarkable or efficient bending. It also indicates purpose of uses. For the purpose of lifting weight, PET/Au/PPy is the best than other type of actuator due to its high modulus. Very large dopant ions are also not efficient for good actuation. Solvent medium restricted the applied potential limit.

CHAPTER - I

Introduction

General Introduction

The last few decades have been marked by the growing importance of two classes of materials, viz. organic and inorganic semiconductors in various forms. Conducting polymers are important materials, which may be used in a large number of electronic devices such as light emitting diodes, field effect transistors etc. On the other hand, these materials also exhibit sensitivity to chemical, thermal and pressure environment, which would be expected to make them useful for various types of sensors and actuators. Smart materials based on conducting polymers could be useful for robotics and remote control systems in various fields such as industrial control systems, aerospace, bio-medicals, drug delivery systems, etc. In this context conducting polymers are now dominating the research areas of advanced materials.

Conducting Polymers-An Overview

1.1. History of Conducting Polymers

Conducting polymers are relatively new class of materials whose interesting metallic properties were first reported in 1977, with the discovery of electrically conducting polyacetylene (PA) [1]. This chance discovery occurred when a researcher accidentally added too much catalyst while synthesizing polyacetylene from acetylene gas, resulting shiny metallic substance rather than the expected black powder. This shiny semi-conducting material was subsequently partially oxidized with iodine or bromine vapors to give electrical conductivity values to up 10^4 $S.cm^{-1}$, which is in the metallic range [2]. The importance of this discovery was recognized in 2000 when the Nobel Prize for Chemistry was awarded to the scientists who discovered electrically conducting PA in 1977:

Alan MacDiarmid, Alan Heeger, and Hideki Shirakawa [3]. Since the discovery of PA, there has been much research into conducting polymers and many new conducting polymers have been synthesized. The most important, and common of these are polypyrrole (PPY) [4], polyaniline (PANI) [5], polythiophene (PT) [6] etc. the structures of these polymers are shown in Fig.1.1.1. There have been many potential applications suggested for these materials, including sensors [7-10], electro-chromic devices [11,12], corrosion inhibitor [13-15], supercapacitor [16,17], electromagnetic shielding [18-19], polymeric batteries [20-22], polymeric actuators [23-26], etc. These wide ranges of applications are possible in part due to the ability to alter the electrochemical, optical, chemical and mechanical properties of conducting polymer by changing the monomer and or dopant incorporated into the polymer.

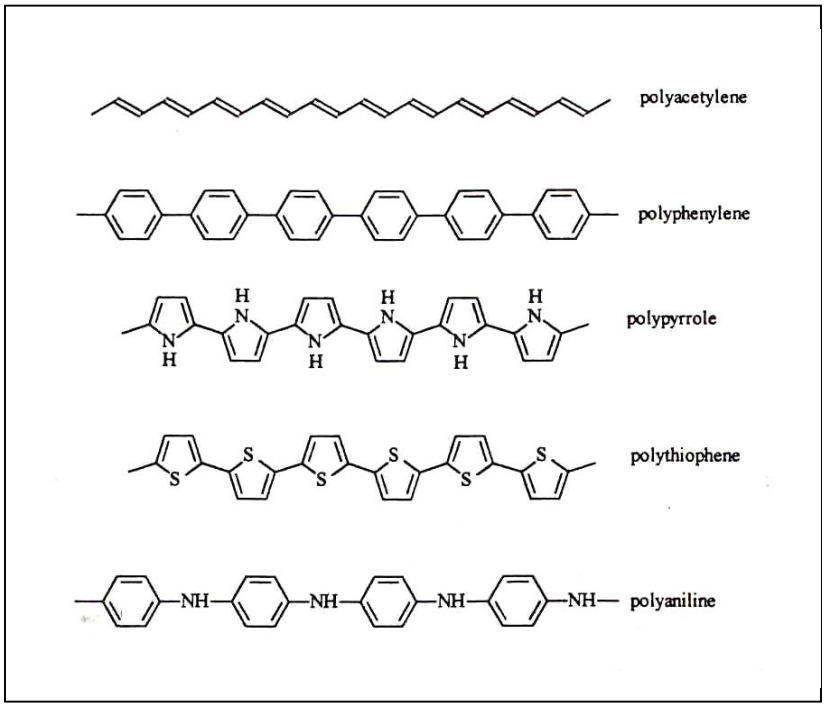

Figure-1.1.1. Examples of inherently conducting polymers

1.2. Classification of Conducting Polymers

Conducting polymers can be classified mainly into three types,

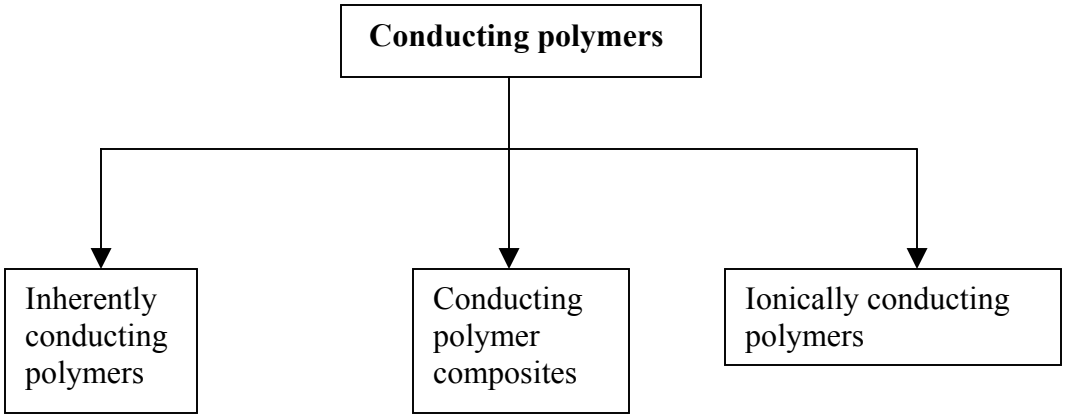

1.3. Doping

Doping of polymeric semiconductors is different from that in inorganic or traditional semiconductors [27]. Doping of conducting polymers involves random dispersion or aggregation of dopants in molar concentrations in the disordered structure of entangled chains and fibrils. The dopant concentrations may be as high as 50% [28]. Also incorporation of the dopant molecules in the quasi one-dimensional polymer systems considerably disturbs the chain order leading to reorganization of the polymer [29]. Doping of the polymer leads to the formation of conjugation defects, viz. solitons, polarons or bi-polarons in the polymer chain [30].

1.3.1. *Classification of Doping Agents*

Doping agents or dopants are either strong reducing agents or strong oxidizing agents. They may be neutral molecules or inorganic salts, which can be easily form ions. Thus, dopants may be classified as,

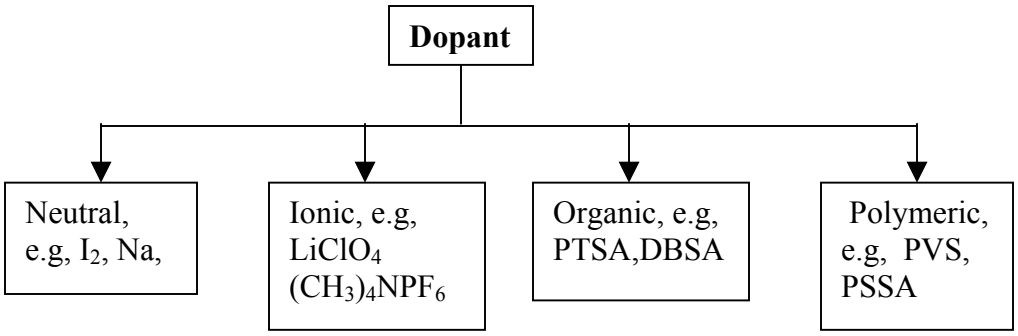

Natural dopants are converted into negative or positive ions with or without chemical modifications during the process of doping. Ionic dopants are either oxidized or reduced by an electron transfer with the polymer and the counter ion remains with the polymer to make the system neutral. Another type of ionic dopant involves the anion derived from the dissociation of the dopant molecule, which neutralizes the positive charge of the polymer during the electrochemical doping process. Organic dopants are anionic dopants, generally incorporated into polymers from aqueous electrolytes during anodic deposition of the polymer. Polymer dopants are functionalized polymer electrolytes containing amphiphilic anions.

1.3.2. *Effect of Doping on Conductivity*

Doping with acceptor or donor molecules causes a partial oxidation (p-doping) or reduction (n-doping) of the polymer molecule. As a result, positively or negatively charged quasi particles are created presumably polarons in the first step of doping. When doping proceeds, reactions among polaron take place, leading to energetically more favorable quasi-particles, i.e. a pair of charged solitons in materials with a degenerate ground state . At low dopant concentrations, the dopant molecules occupy random

positions between the chains. These dopant molecules further affect the electronic properties by their coulomb potential and by hybridization with the polymer π orbital. As polarons produced in this state has long lifetime, they are treated as quasi-particle. On this basis, Conwell et al.[31] has given an estimate of the density of free electrons at a doping level of about 5% and found a value for the free charges carrier density of about $3x10^{-24}$ m^{-3} or less at 300 K. Thus polarons have significantly lower mobility, which results in obtaining a moderate conductivity at low doping concentration. As the doping level is increased, the concentration of polarons goes up and they become crowded together, close enough for bipolaron formation to occur. It is at this point in the doping process that the conductivity undergoes a marked increase. Once the radical components of the polarons have combined to form π bonds, the remaining positive charges achieve high mobility along the chain.

1.4. Polyaniline (PANI)

Due to its ease of synthesis and processing, environmental stability, relatively high conductivity and cost economics, polyaniline is probably the most industrially important conducting polymer today [32-34]. Polyaniline is a typical phenylene based polymer having a chemically flexible -NH group in the polymer chain flanked by phenyl ring on either side. Polyaniline represents a class of macromolecules whose electrical conductivity can be varied from an insulator to a conductor by the redox process. This polymer can achieve its highly conductive state either through the protonation of the imine nitrogens or through the oxidation of amine nitrogens. For example the conducting state of PANI can be obtained in its 50% oxidized emeraldine state in aqueous acids like HCl and the

resulting material is a p-type semiconductor [35-37].

The method of synthesis depends on the intended application of the polymer. For bulk production chemical method, whereas for thin films and better patterns, electrochemical method is preferred.

1.5. Polypyrrole (PPy)

Polypyrrole is an inherently conductive polymer due to excluded π conjugation of electrons, which is stabilized by the heterocyclic group. PPy is an especially promising conductive polymer for commercial applications, owing to its high conductivity, good environmental stability and ease of synthesis. It is easy to prepare by standard electrochemical techniques and its surface charge characteristics can easily be modified by changing the dopant anion (X^-) that is incorporated into the material during synthesis. Polypyrrole was first synthesized in 1916 as black powder by oxidation of pyrrole. However, this powder was not highly conducting and it was intractable. Polypyrrole (Fig.1.1.2) is the first polymer for which electrically conducting film was made electrochemically [38, 39].

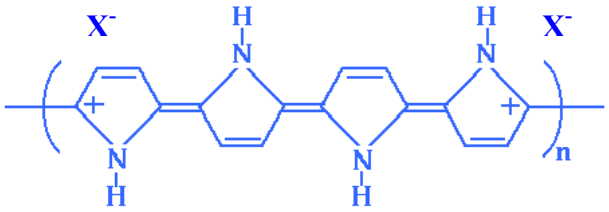

Figure-1.1.2. Structure of polypyrrole

1.6. Mechanical Behaviour of Polymers

Mechanical behaviour is in most general terms concerned with the deformations, which occur under loading. The deformations depend on geometrical shape of the sample or the way in which the load is applied. One of the simplest constitutive relations is Hooke's law, which relates the stress (σ) to the strain (ϵ) for the uniaxial deformation of an ideal elastic isotropic solid [40].

$$\sigma = E.\epsilon \qquad (1.0)$$

Where, E is the Young's modulus.

There are five important ways in which the mechanical behaviour of a polymer may deviate from that of an ideal elastic solid obeying Hooke's Law. Firstly, in elastic solid the deformations induced by loading are independent of the history or rate of application of the loads, whereas in polymer the deformations can be drastically affected by such considerations. This means that the simplest constitutive relation for a polymer should in general contain time or frequency as a variable in addition to stress and strain. Secondly, in elastic solid all the situations pertaining to stress and strain can be reversed. Thus, if a stress is applied, a certain deformation will occur. On removal of the stress, this deformation will disappear exactly. Thirdly, in an elastic solid obeying Hooke's law, which in its more general implications is the basis of small-strain elastic theory, the effects observed are linearly related to the influences applied. This is not generally true for polymers, but applies in many cases only as a good approximation for very small strains; in general the constitutive relations are non-linear. It is important to note that non-linearity is not related to recoverability.

Conducting Polymer Sensors

1.7. Introduction

A sensor allows detection, analysis, and recording of physical phenomenon that are difficult to otherwise measure by converting the phenomenon into a more convenient signal. Sensors convert physical measurements such as displacement, velocity, acceleration, force, pressure, chemical concentration, or flow rate into electrical signals. The value of the original physical parameter can be back calculated from the appropriate characteristics of the electrical signal (amplitude, frequency, pulse–width, etc). Electrical outputs are very convenient because there are well-known methods (and often) commercially available (off–the–shelf solution) for filtering and acquiring electrical signals for real–time or subsequent analysis.

Piezo-materials convert one form of energy into another, and are widely used in sensing applications. The tremendous growth in the use of microprocessors has propelled the demand for sensors in diverse applications. Today, Electromechanical Polymeric Sensors are among the fastest growing technology. This part provides an overview of modeling and properties of piezo-polymer.

1.7.1. *Sensors and Their Classification*

Sensor is a transducer that converts the measurund into signal. Sensors can be classified according to the nature of interaction, which means the basis of operation into three groups.

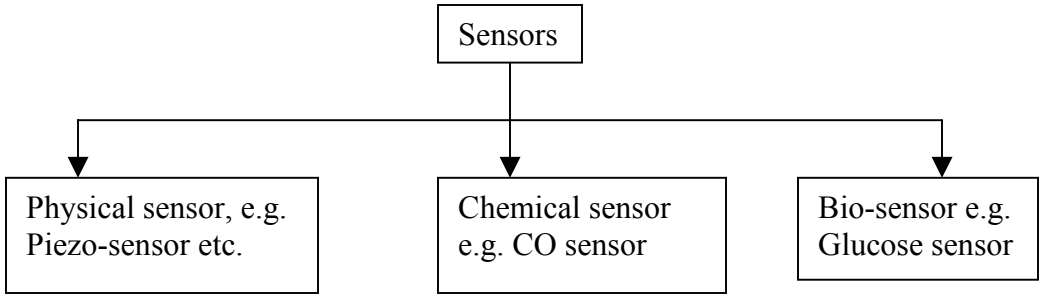

1.7.2. *Types of Piezo-materials*

Three main types of piezo-materials

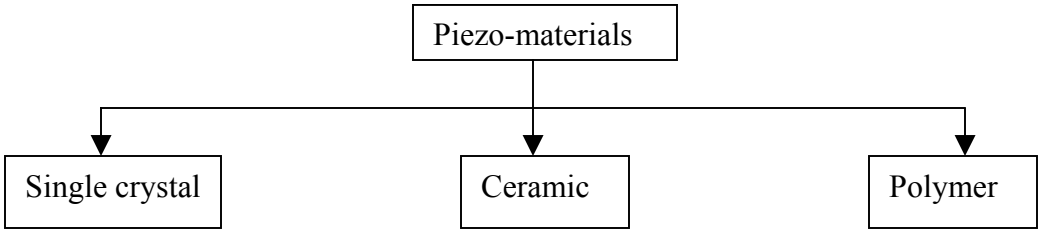

1.7.3. *Piezo-polymers-Background*

Piezoelectricity had always been associated with crystalline solids. So the suggestion, made in the 1920s of piezoelectric effects in non-crystalline materials would have indicated a significant discovery [41, 42]. In the 1950s, Japanese and Soviet workers initiated the substantial investigation of non-crystalline materials that would put these early observations on somewhat firm ground. Natural wood was the first polymeric material to give piezoelectric effect. The origin of this effect was ascribed to the piezoelectric property of crystallites of cellulose. Wood consists of oriented fibers in which many such crystallites are aligned along the fiber. Yasuda et al.[43] later found the piezoelectric constant of bone was more than twice that of wood. In this case, origin of the effect is thought to be uniaxial orientation of the crystalline micelle of collagen molecules, which

make up the hard outer layers bone. Japan was clearly the leader in the field of piezoelectric polymer studies at this time. Fukada, in the conclusions of his paper on the piezoelectric effect in wood, suggested, it might not be too absurd to imagine the creation of highly piezoelectric plastics which are artificially manufactured from linear high polymers. Fourteen years later, in 1969, Kawai announced that a new type piezoelectric effect has been discovered in elongated and polarized films of polymers [44]. The films were polarized in a manner similar to that described above in ceramics, but they were stretched to several times of their original length before applying the electric field. More than ten types of polymer were tested with a strong piezoelectric effect being found in six of them. Of these, PVDF was most active, with a piezoelectric strain constant d_{31} more than three times greater than the values measured for the other polymers. Another attraction of PVDF was that, along with poly (vinyl fluoride) and PVC, little change was observed in piezoelectric effect over the course of several months. These materials are obviously much more attractive for applications than polycarbonate, polyethylene, since piezoelectric effect of the later polymers had half-life of one to four days [44]. The large stable piezoelectric effect in PVDF sparked extensive development and it will be described in subsequent section.

1.7.4. *Theory of Piezoelectric Effect*

The Piezoelectricity of PVDF has been well-modeled [45]. The models assume the material consists of a crystalline and amorphous phase, with the two phases differing in their dielectric and elastic properties. The materials polarization is due to aligned dipolar chains in the crystalline and perhaps the surrounding amorphous regions. Injected charges

at the boundaries of the polarization zones also contribute to the polarization. There are three primary mechanisms which cause piezoelectricity in such a material. Fig. 1.2 shows direction of applied pressure.

A. Electrostrictive contribution:- The strain dependence of the dielectric constants of the crystalline and amorphous parts differ. In the presence of polarization, this produces a piezoelectric effect.

B. Dimensional contribution:- The elastic constants of the crystalline and amorphous region are different. This causes the polarization to have strain dependence, thereby, contributing to the piezoelectric activity

C. Crystal contribution:- The crystallites have an intrinsic piezoelectricity effect due to the strain dependence of their polarization.

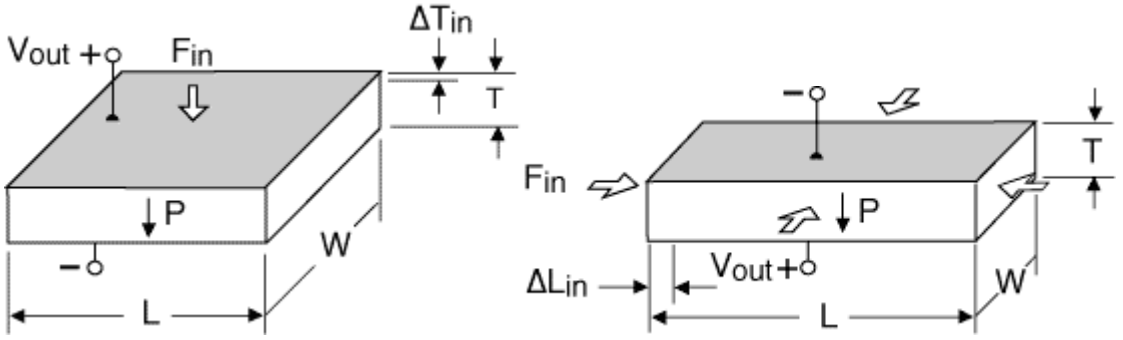

Longitudinal (d_{33}) Generator *Transverse (d_{31}) Generator, compressed on sides*

Figure-1.2. Schematic view of direction of applied pressure

1.7.5. *Poling and Polarization*

Most commonly available PVDF film consists of anti-polar α-crystallites. This must be processed in certain manner in order to generate β-crystalline form so that it becomes

useful in last ten years through an increased understanding of these processes [46]. Firstly, the film is uniaxially stretched 3-5 times of its original length at 60–65^{0}C. The material will re-crystallize as β-crystalline phase due to the packing of unit cells in parallel planes during the drawing [46]. Subsequent annealing of the sample will heal any damage due to stretching and will stabilize the film. Poling can be performed using either a thermal or a corona procedure.

In the case of poling (Fig 1.2.1), electrodes are first placed on the film, and then it is subjected to a field 50-80 Mv/m at 70–80^{0}C for about an hour. Dipoles are partially aligned in the crystalline regions in the field direction. The electric field is maintained, as the film is cooled at room temperature, stabilizing the polar alignment and causing a permanent polarization.

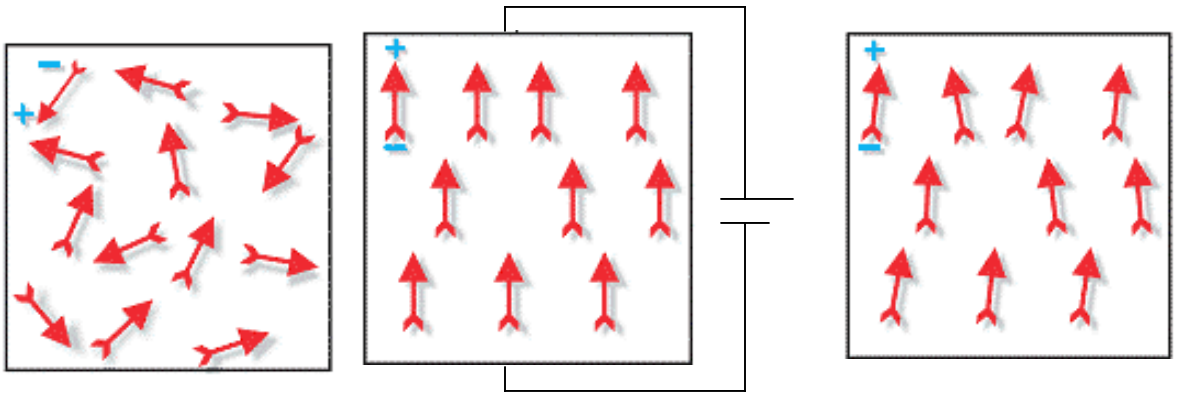

Random orientation of polar domain prior to polarization

Polarization in DC electric field (poling)

After removing electric field

Figure-1.2.1. Orientation of dipoles

For applied field upto 200 Mv/m, the polarization achieved is proportional to the field. For stronger fields a maximum polarization of about 20 mC/m^2 is reached [46]. This value

is considerably lower than that observed in ceramics piezoelectric[47], 400 mC/m^2. If weak electric fields are used, the resulting polarization is spatially non-uniform, greater piezoelectric activity is found near the positive electrode, which has been attributed to space–charge injection. Cz Pawlaczyk et al.[48] studied poling of PVDF polymer film to enhanced piezo-property.

1.7.6. *Advantages and Disadvantages of Piezo-polymer*

Piezo film is a compliant, lightweight, tough, and plastic. It is available in a wide variety of thicknesses and surface areas. Thus, it is vastly different in physical form from other well-known piezo active materials such as quartz and piezo-ceramics.

1.7.6.1. *Advantages*

i) Piezo film operates over an extremely wide frequency range (1-10 MHz).

ii) It has a wide dynamic range.

iii) It has low acoustic impedance.

iv) It has a higher dielectric strength than piezo-ceramic material (30 V/μm)

v) Its relatively high "electrical" impedance provides a complementary match to popular high-impedance (CMOS) circuits.

vi) Because, piezo film is thin, flexible plastic film, its elastic compliance is many times that of piezo-ceramics.

vii) Because, it is a high molecular weight fluoro-polymer (e.g. PVDF), it is mechanically strong and able to withstand extreme environmental conditions, including most solvents, acids, oxidants, and intense ultraviolet radiation.

viii) It can be easily cut and formed into complex shapes or prepared as a large area transducer. Sections of film can be readily adhered to each other or to other surfaces using commercial adhesives to make multi-layer devices.

ix) Materials and fabrication costs of piezo film (polymer) are generally lower than those of other piezo-active materials (ceramic).

1.7.6.2. *Disadvantages*

i) Because piezo film is a flexible compliant film, it is not a powerful electromechanical transmitter, particularly at low frequency. Thus, it will not operate well at a low frequency, large area, and acoustic speaker.

ii) The activity of piezo film decreases at elevated temperatures; therefore, its applications are limited to those operating under 100°C.

iii) It is sensitive to electromagnetic signals over a wide frequency. For certain applications, it is necessary to carefully shield the active side of the device from electromagnetic interference.

1.7.7. *Polyaniline Sensor*

The properties of polyaniline (PANI) sensors have been reported by a number of authors [49-51]. Electronically conductive PANI is the simple 1,4 coupling product of aniline. This coupling reaction is dominating in acidic media at pH 0-1. PANI can be prepared by both chemical and electrochemical routes [52].

1.7.7.1. *Chemical Synthesis*

The most preferred method for synthesis of polyaniline by chemical oxidative route involves the use of either hydrochloric or sulfuric acid with ammonium persulfate as an

oxidant in an aqueous solution [35,53]. Oxidative polymerization is a two-electron change reaction and hence, the persulfate requirement is one mole per mole of a monomer. However, the small quantity of oxidant is used to avoid oxidative degradation of the polymer formed. Chemical synthesis of PANI is given in scheme-1.

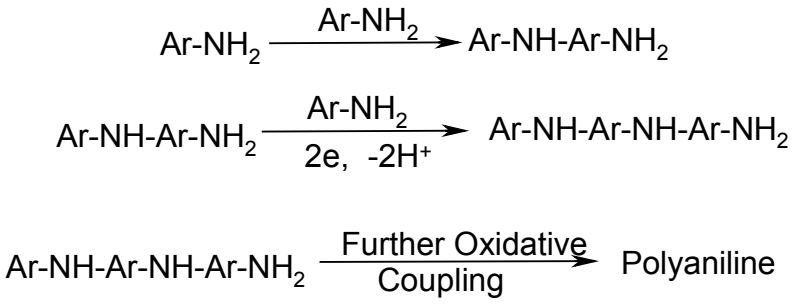

Scheme1. Mechanism of chemical synthesis of polyaniline

The synthesized polyaniline exists in various oxidation states; they are termed as (1) leucoemeraldine (2) emeraldine base (3) emeraldine salt and (4) pernigraniline shown schematically in the Fig. 1.2.2. Pron et al. [53] compared the electrical conductivity and the reaction yield of polyaniline, polymerized with four different oxidizing agents and at different aniline/oxidant ratios. These authors concluded that the redox potential of the oxidizing agent is not a dominant parameter in the chemical polymerization of aniline; most oxidizing agents gave similar results.

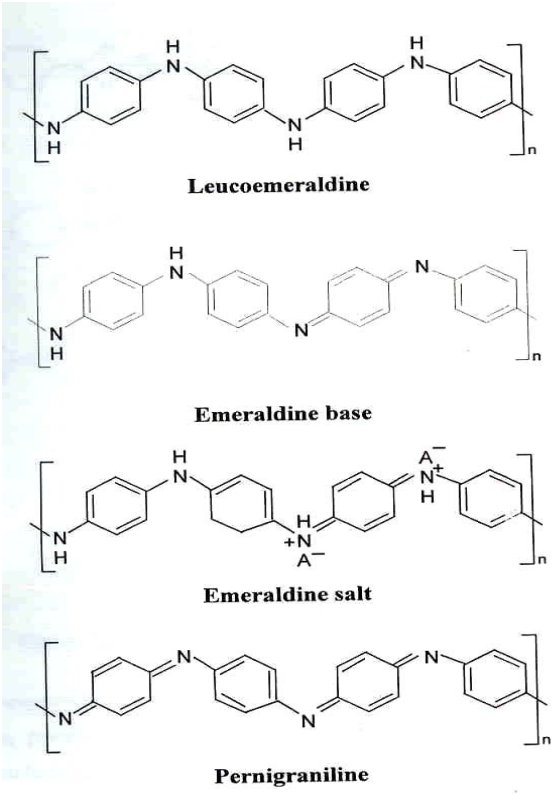

Figure-1.2.2. Various oxidation states of PANI

1.7.7.2. *Sensitivity*

Polyaniline, and its composites received a great deal of attention in recent years because of their potential for commercial applications in various fields such as electronics, sensors, etc.[54-55]. Considerable research efforts are now directed towards the development of sensors based on conducting polymer [56]. The electrical conductivity of these polymers used can be changed from insulating to metallic by chemical doping and they can be used to produce Schottky devices [57-59].

Piezo-resistivity studies have been mostly conducted on polymer filled with fillers that are electrically conducting. These composites are piezo-resistive sensors because strain

changes the proximity between the conducting filler units, thus affecting the electrical resistivity. Tension increases the distance between the filler units, thus increasing the resistivity; compression decreases this distance, thus decreasing the resistivity.

Hassan et al. [60] studied the effect of tensile deformation on the electrical conductivity of SRF black loaded styrene-butadiene rubber and showed that the equilibrium value of the electrical conductivity increased with deformation upto an elongation of 110% and then decreased with further increases of the extension. Bao et al.[61,64] monitored electrical conductivity of polyaniline as a function of pressure. According to him, primary effect of applying pressure is simple compression; this leads to reduce interchain separation with increasing pressure. Recently, Hong Q. et al.[53,65] reported piezo-resistivity of polyaniline–SBS composites and explained value of its largely dependent on composites preparative condition and nature of polyaniline. Radhakrishnan et al.[65-66] studied the dependence of the electrical resistivity of polypyrrole–SBS composites on mechanical deformations both in compression and extension modes. Origin of high piezo-sensitivity of polyaniline/TiO_2 system had been reported by Somani et al.[66] and showed that these composites exhibited high piezo-sensitivity at a certain polyaniline/TiO_2 composition. Radhakrishnan et al.[51] also studied piezo-resistivity of polyaniline and $BaTiO_3$ composites.

1.7.8. *Conducting Polymer Composites (CPC)*

These materials contain an electrically insulating polymer loaded with conductive filler. The concept of percolation can be used to understand the change in resistivity as a function of filler concentration in composites. It describes the conduction with the presence of electrically conducting paths between two filler particles. The number of

these paths will be dramatically destroyed below the critical volume fraction of filler. Direct current can flow along such materials only through continuous chains of filler particles [67]. The probability of finding such a structure depends on variety of factors, namely: quantity of filler, shape of filler particles and their compatibility with polymer, method of mixing etc. A choice of matrix is determined mainly by the operating conditions of a material and the desired physical-mechanical properties of composite. The value of the CPC conductivity does not depend only on a choice of polymer matrix.

1.7.8.1. *Conduction in CPC*

The blends and composites of the conducting polymers as discussed in the above section actually represent a heterogeneous mixture of two components. Hence, the different materials are in intimate contact in a polymer matrix and are dispersed uniformly throughout the matrix. The contact of the materials at the interface will strongly affect the electrical properties of the blends and composites on a macroscopic level. The dissimilarities in work function of the materials give rise to the formation of a potential barrier at the interface [68]. Various types of such junctions were fabricated in the past in the view of their potential use in electronic devices. The conducting polymers are p-type organic semi-conductors. Hence, the junctions formed at the interface of conducting polymers and inorganic materials in contact were termed as hetero-junctions. The Schottky diodes using polymers as an active material has been reported by several groups [69,70]. These new devices provided means of adding and removing charges to the polymer by injection and depletion that avoids chemical doping of the polymer and possible side reactions. These devices revealed novel physics that the characteristics of polymeric

devices are similar to the inorganic semiconductor devices. Thus the polymer films are amorphous and the devices have acceptable characteristics.

The electrical properties of the blends and composites are exclusively governed by the charge transport across the potential barrier formed at the interface of the materials. As discussed earlier, similarities can be drawn between the conducting polymer composites / blends and composites of inherently conducting polymers due to the fact that both represent filling of conducting material in the insulating counterpart. Hence, the charge transport in the conducting polymer composites is reviewed in the following section.

In general such composites may be considered to be metal-insulator–metal type of material (M-I-M) and therefore the conduction process at metal insulator interface should also be reviewed here.

According to Simmons et al.[71] the conductivity in insulator is often due to extrinsically rather than intrinsically bulk generated carriers. The intrinsic current (I) carried by an insulator is given by,

$$I = e\mu N_c F \exp\left[-\frac{E_g}{2KT}\right] \qquad (1.1)$$

Where e is the electronic charge, μ is charge density, F is field in the insulator, Nc the effective density of states in insulator, Eg the insulator energy band gap, K the Boltzman constant and T is the absolute temperature. When an electric field is applied across an insulator, if sufficient number of carriers are available to enter the insulator so as to replenish those, which are drawn out, then the I-V characteristics of sample will be dependent on the bulk limited. At high fields, or if the contact is blocking type then the current supplied through the electrodes to the insulator. Under this condition the I-V

characteristics of the sample will be controlled primarily by conditions existing at the cathode–insulator interface, this conduction process is referred to as being emission–limited or contact limited.

1.7.8.2. *Types of Contact*

The types of contact that can exist at a metal–insulator interface fall into three categories (i) ohmic contact, (ii) neutral contact, and (iii) blocking contact

(i) ohmic Contact–Mott Gurney Contact

In this case electrode work function (ψ_m) is smaller than the insulator work function (ψ_i) as shown in the Fig.1.2.3, and the electrode can readily supply electrons to the insulator as needed.

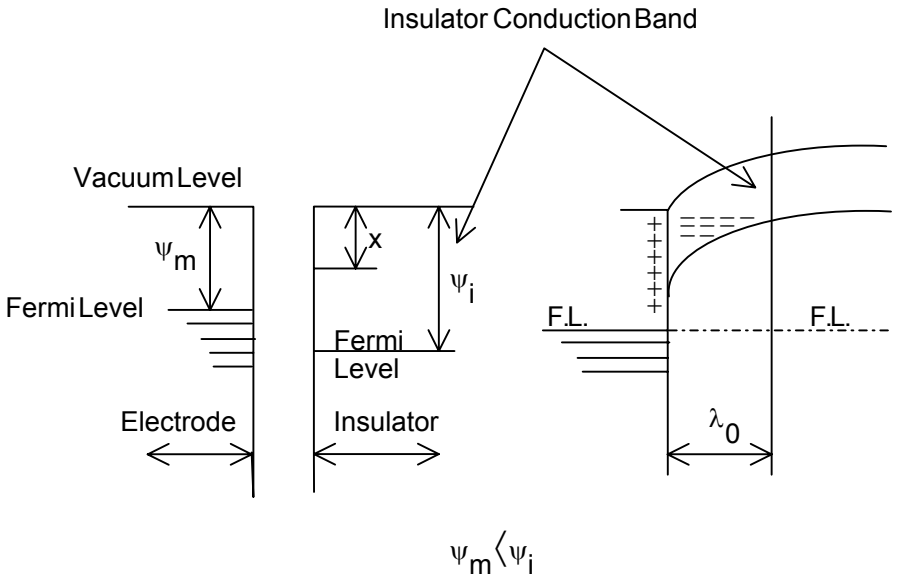

Figure-1.2.3. Energy diagram showing ohmic contact at M-I-M interface

Under these conditions, in order to satisfy thermal–equilibrium requirements, electrons are injected from the electrode into the conduction band of the insulator, thus giving rise

to a space–charge region in the insulator. This space charge region is shown in Fig 1.2.3 to extend a distance λ_o into the insulator, and is termed as the accumulation region.

(ii) Neutral Contact

In this case $(\psi_m) = (\psi_i)$, which means that the conduction band is flat right up to the interface, i.e. no band bending is present, as shown in Fig.1.2.4.

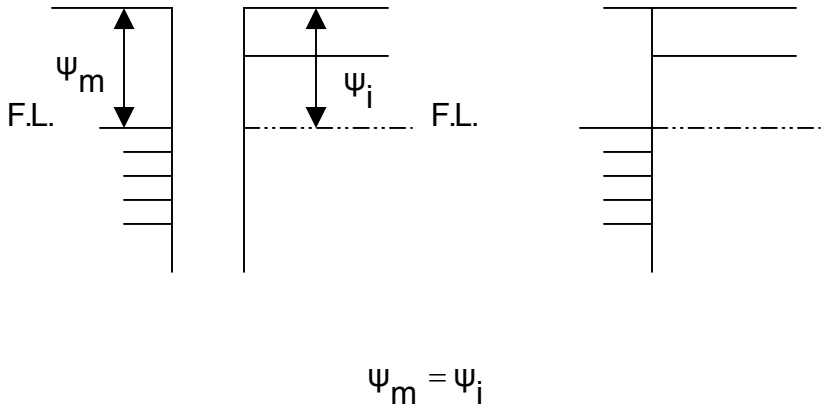

Figure-1.2.4. Energy diagram showing neutral contact at M-I-M interface

(iii) Blocking Contact–Schottky Barrier

A blocking contact (Fig.1.2.5) occurs when $(\psi_m) > (\psi_i)$, and in this case electrons flow from the insulator into the metal to establish thermal–equilibrium conditions. A space–charge region of positive charge, the depletion region, is thus created in the insulator and an equal negative charge resides on the metal electrode. As a result of the electrostatic interaction between the opposite charge regions, a local field exists within the surface of the insulator. This causes the bottom of the conduction band to downward until the fermi level within the bulk of the insulator lies ψ_I below the vacuum level. Various workers in this field of electrically conducting polymers have suggested different conduction process

as already mentioned early. A detailed review of the physical process involved in the mechanisms such as Tunnel effect, Poole–Frenkel effect and Space Charge Limited conduction is given here.

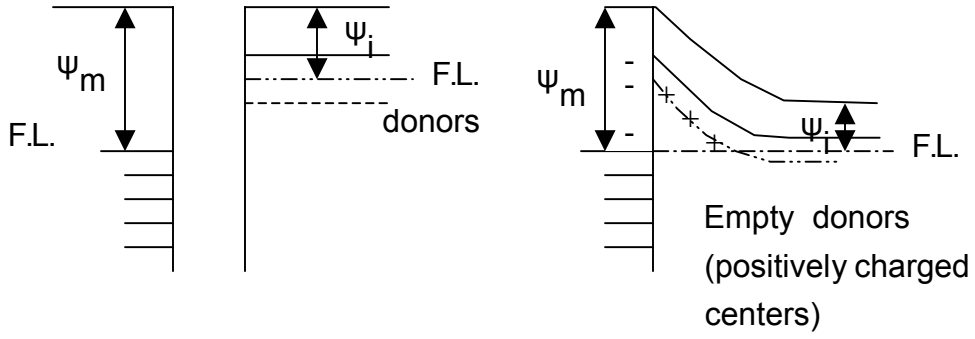

$\psi_m > \psi_i$

Figure-1.2.5. Energy diagram showing blocking contact at M-I-M interface

1.7.8.3. *Non-Linear Process in Electrical Conduction*

1.7.8.3.1. *Tunnel Effect*

If the energy of an electron is less than the interfacial potential barrier in a metal-insulator –metal junction upon which it is incident, the quantum–mechanical wave function $\psi_{(x)}$ of the electron has a finite value within the barrier (Fig.1.2.6). Since $\psi_{(x)}dx$ is the probability of finding electron within the incremental range x to x+dx, this means that the electron can penetrate the forbidden region of the barrier. The wave function decays rapidly with the depth of penetration of the barrier from the electrode-insulator interface and, for barrier of macroscopic thickness, is essentially zero at the opposite interface, indicating zero probability of finding the electron there. However, if the barrier is very thin (< 50 Å), the wave function has a nonzero value at the opposite interface. For this case, there is

a finite probability that the electron can pass from one electrode to the other by penetrating the barrier. When the electron passes from one electrode to the other by this process, it seems to be the electron as having tunneled through the barrier.

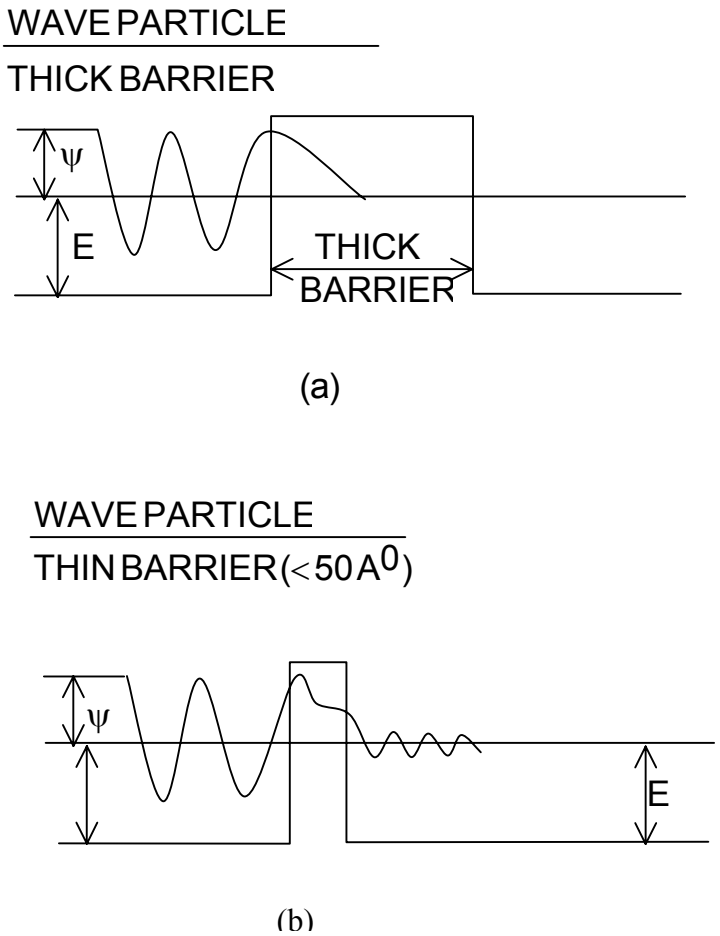

Figure-1.2.6. Quantum mechanical tunneling of an electron at M-I-M junction (a) at a thick barrier (b) at a thin barrier

The generalized formula gives the relationship connecting the tunnel current with the applied voltage for a barrier of arbitrary shape as,

$$I = I_0\left[\overline{\varphi}\exp\left(-A\overline{\varphi}^{1/2}\right) - \left(\overline{\varphi}+eV\right)\exp\left\{-A\left(\overline{\varphi}+eV\right)^{1/2}\right\}\right] \qquad (1.2)$$

Where, $I_o = \frac{e}{2\pi h(\beta\Delta s)^2}$ and $A = \frac{4\pi\beta\Delta s}{h}(2m)^{1/2}$

Δs = width of the barrier at the fermi level of the negatively biased electrode, $\overline{\varphi}$ = mean barrier height above the fermi level of the negatively biased electrode, h = Plancks constant, m = mass of the electrons, e = unit of electronic charge, β = a function barrier shape and is usually approximately equal to unity, a condition we will assume throughout, above equation becomes,

$$I = \frac{6.2x10^{10}}{(\Delta s)^2}\left[\overline{\varphi}\exp\left(-1.025\Delta s\overline{\varphi}^{1/2}\right) - (\overline{\varphi}+V)\exp\left\{-1.025\Delta s(\overline{\varphi}+V)^{1/2}\right\}\right] \qquad (1.3)$$

1.7.8.3.2. ***Poole–Frenkel Effect***

The Poole-Frankel effect (field assisted thermal ionization) is lowering of a coulombic potential barrier when it interacts with an electric field, as shown in Fig 1.2.7. This process is the bulk analog of the Schottky effect at an interfacial barrier. Since the potential energy of an electron in a coulombic field $-e^2/4\pi\varepsilon^o$ kx is four times than that of potential energy due to image force effects, the Poole-Frankel attenuation of a coulombic barrier $\Delta\varphi_{PF}$ is uniform electronic field is twice that due to the Schottky effect at a neutral barrier.

$$\Delta\varphi_{PF} = \left[\frac{e^3}{\pi \in_o K^*}\right]^{1/2} F^{1/2} = \beta_{PF}F^{1/2} \qquad (1.4)$$

This result was first applied by Frenkel et al.[72] to the host atoms in bulk semiconductors and insulators. He argued that ionization potential ε_o of the atoms in a solid are lowered an amount given by equation 1.4 in the presence of a uniform field–dependent conductivity of the form,

$$\sigma = \sigma_o \exp\left[\frac{\beta_{PF} F^{1/2}}{2KT}\right] \qquad (1.5)$$

Where $\sigma_o = [e\mu N_c \exp(- E_o / 2kT)]$ is the low field conductivity. The above equation may be written in the form,

$$J = J_o \exp\left[\frac{\beta_{PF} F^{1/2}}{2kT}\right] \qquad (1.6)$$

where, $J_o = \sigma_o F$ is the low field current density,

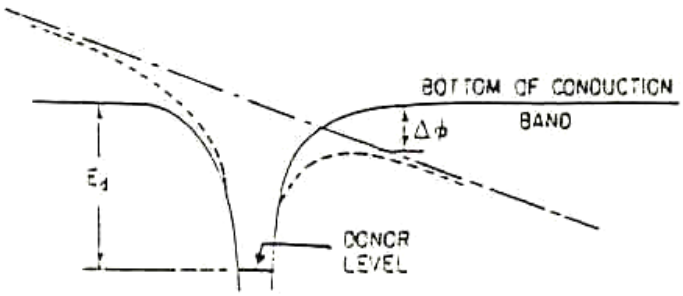

Figure-1.2.7. Lowering of coulombic potential barrier in P-F effect

It is interesting to note although $\Delta\varphi_{PF} = 2\Delta\varphi s$, where $\Delta\varphi s$ is the Schottky barrier, the coefficient of $F^{1/2}$ in the exponential is the same for both the Richardson–Schottky and Poole-Frenkel characteristics (i.e., $\beta_{PF}/2 = \beta_s$). Mead has suggested that since trap around in an insulator and that trap having a coulombic type barrier would experience the P–F effect at high fields, thereby increasing the probability of escape of an electron immobilized therein, the current density in thin film insulators containing shallow traps is given by,

$$J = J_o \exp\left[\frac{\beta_{PF} F^{1/2}}{kT}\right] \qquad (1.7)$$

Note in this case that the coefficient of $F^{1/2}$ is twice that in equation 1.6 and for this reason equation 1.7 is usually the form of P-F equation associated with thin film insulators rather than that given by equation 1.6.

From what has been said it follows that it should be possible to differentiate between the Schottky and P-F effects in thin-film insulator from their different rates of conductivity with field strength; viz., a plot of J vs $F^{1/2}$ /kT results in a straight line with slope β_s or β_{PF} depending upon whether the conduction process is Richardson-Schottky or Poole-Frenkel. These experimentally determined slopes can be compared with the theoretical β_s and β_{PF}, which can be calculated quite accurately provided the high frequency dielectric constant $K^* = n^2$, where n is the refractive index for the material.

Furthermore, if it is assumed that the insulator contains donor centers which known as the Fermi level this assumption is supported by the fact that the conductivity of the films continues to increase with increasing temperature above room temperature and shallow neutral traps (Fig. 1.2.7), the bulk J-V characteristics of the film is given by,

$$J = J_o \exp\left[\frac{\beta_{PF} F^{1/2}}{2kT}\right] \qquad (1.8)$$

where, $J_o = e\mu N_c \left[\frac{N_d}{N_t}\right]^{1/2} F \exp\left[-\frac{E_d + E_t}{2kT}\right]$

Thus, in this case the coefficient of $F^{1/2}$ /kt is β_{PF} /2 = β_s even though the conductivity is not electrode-limited, which explains the anomalous experimental results.

1.7.8.3.3. ***Space Charge Limited Conduction (SCLC)***

An insulator which does not contain donors and which is sufficiently thick to inhibit tunneling will not normally conduct significant current. However, if an ohmic contact is

made to the insulator, the space charge injected into the conduction band of the insulator is capable of carrying current, this process is termed SCL conduction. The results of the applied bias to an insulator having two Ohmic contacts on its surface are added positive charge to the anode and negative charge to the cathode. Thus, as the voltage bias increases, the net positive charge on the anode increases and that on the cathode decreases. Calling the charge on the cathode Q_1, that on the anode Q_2 and the negative space charge density p(x), the condition of charge neutrality demands that,

$$\int_0^s p(\chi)dx = Q_1 + Q_2 \qquad (1.9)$$

This equation may be rewritten as,

$$\int_0^{\lambda_m} p(\chi)d\chi + \int_{\lambda_m}^{L} p(\chi)d\chi = Q_1 + Q_2$$

Where λ_m is chosen such that

$$\int_0^{\lambda_m} p(\chi)d\chi = Q_1 \qquad (1.10)$$

and

$$\int_{\lambda_m}^{s} p(\chi)d\chi = Q_2 \qquad (1.11)$$

The insulator has thus been divided into two portions with λ_m as the boundary separating the two (Fig.1.2.8). The significance of equation 1.10 and 1.11 is that the positive charge on either contact is neutralized by an equal of negative charge contained between the contact and the plane at $x = \lambda_m$. Thus, the field in the insulator due to Q_1 and Q_2 is zero at $x = \lambda_m$, the net field there must be zero, as shown in Fig 1.2.8, and for this reason the plane at $x = \lambda_m$ is termed as the virtual cathode. The region $0 \geq x \geq \lambda_m$ is designed the

cathode region, and the region $\lambda_m \geq x \geq s$ the anode region. From consideration of equation 1.10 and 1.11 and the fact that Q_1 decreases and Q_2 increases with increasing voltage, it will be clear that the virtual cathode region decreases and the anode region increases. Eventually, when $Q_1 = 0$, the virtual cathode coincides with the physical cathode–insulator interface. Under this condition, then, the anode region extends throughout interface.

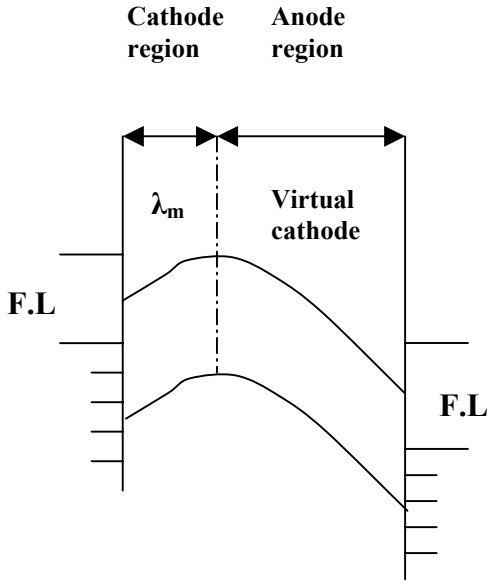

Figure-1.2.8. Energy diagram illustrating virtual cathode, cathode region, and anode region under space charge limited conduction

Thus, for further increasing voltage bias, the conduction process is no longer space charge limited, but rather it is emission–limited.

1.7.9. *Applications*

Because piezo film is a new form of transducer, many of its markets are developmental. Excellent progress is being made, however, resulting in improved designs for a number of electromechanical devices.

i) Switches

ii) Computer graphics

iii) Robotic tactile sensors

iv) IR detectors

v) Medical sensors

vi) Flow-meter

vii) Transducer

viii) Hydrophone

1.7.10. *Theoretical Model*

Modeling has become very important tool for structural design, analysis and research. The basic use of a model is to provide a physical understanding of a system. For a structural acoustic system this helps us to understand how structural motion results in pressure distributions in the acoustic fluid or how change in structural mass, stiffness damping effect the coupled acoustic field and vice versa. The model should be representative of the geometry of the system, and capture basic dynamic response properties such as model frequency, damping, residue and density reasonably well.

A significant improvement to the conceptual design model involves correlation with an actual system. Here, sensor modeling becomes vital to accurately capture the input/ output characteristics of the physical system. Correlation is achieved by modifying unknown or uncertain parameters to match data from the physical system. The modeling of sensors relies on the ability to characterize the electromechanical behaviour of the material in terms of forces or displacements around its contour.

Carmona et al.[73] has developed a model to predict the piezo-resistance of the conductor filled polymer composites close to threshold. Although his model can precisely fit the experimental data, it still has many disadvantages: (1) it is difficult to predict the effects of the influencing factors on the piezo-resistance quantitatively, especially the effects of filler particle diameter, matrix compressive modulus, etc.; and (2) it can not explain the time dependence of piezo-resistance. Xiao-Su–Yi et al.[74] explained time dependency peizo-resistance of conductor filled polymer composites based on tunneling conduction mechanism. But they did not consider effect of non-linearity on piezo-resistivity. Only Radhakrishnan et al.[66] described piezo-resistivity in terms of space charge limited conduction mechanism by considering conducting polymer composites model. But it can't predict preciously piezo-resistivity of polymer composites having non-linear mechanical properties at very low mechanical load and never discussed thoroughly why SCLC shows high piezo-resistivity than rest of conduction process. None of them consider nonlinear mechanical property of matrix polymer and affect of various nonlinear conduction phenomena, nature of composites (compatible or non-compatible) on piezo-sensitivity. So, we are focusing ourselves to develop phenomenological model considering all above mentioned drawbacks and construct experiment to prove it.

Conducting Polymer Actuators

1.8. Introduction

The development of materials and devices, which are able to imitate the performance of natural muscles in the direct conversion of electric energy into mechanical energy, has always been a challenge to the human being. Such a material should be able to connect to the main controlling system and hence conduct electricity change [75-78]. It should be able to work with electric pulse of few milivolts (natural muscles use a potential ≈175mV), it should experience a volume variation associated with conformational changes in the structure. It should also have the morphology and structure similar to natural muscles; thus the most likely that material will meet these requirements would be formed by macromolecular chemistry similar to proteins forming the natural muscles.

1.8.1 *Classification of Actuators*

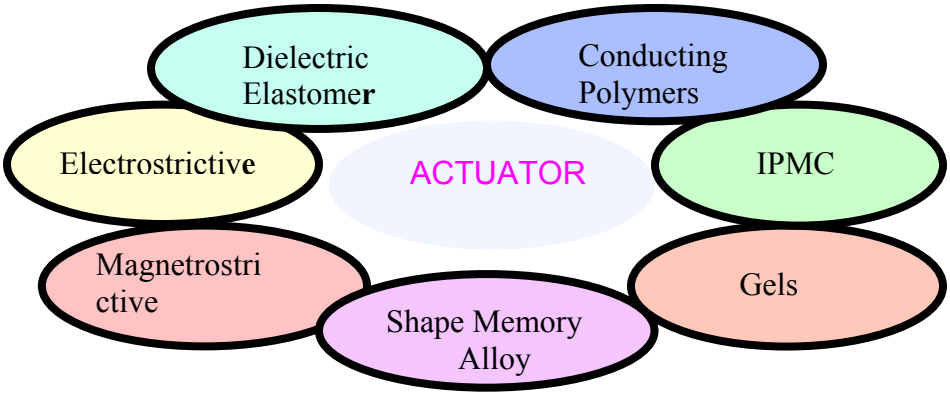

1.8.2. *Comparison of Properties of Different Actuators*

Actuation materials are finding increasing use to driving mechanisms, where electro-ceramics (EAC) and shape memory alloys (SMAs) and electro-active polymers (EAP)

are the main materials being used. EAC offer effective & compact actuation materials and they are incorporated into such mechanism as ultrasonic motors, inchworms, translators and manipulators. The performance parameters of these in actuator device are given in table1.1

Table 1.1 : Comparison of properties of various types of actuators.

Property	Electro-active polymer (EAP)	Shape memory alloy (SMA)	Electro-active Ceramic (EAC)
Actuation displacement (%)	>10	<8	0.1-0.3
Force (MPa)	0.1-3	About 700	30-40
Response speed	m-sec to sec	sec to min	m-sec to sec
Density	1-2.5 g/cc	5-6 g/cc	6-8 g/cc
Drive voltage	4-7 V	NA	50-800 V
Power consumption	mW	Watts	Watts
Fracture toughness	Resilient, elastic	Elastic	Fragile

1.8.3. *Advantages of Polymeric Actuators*

i) Can be synthesized in different forms.

ii) Comparatively easy to fabricate than inorganic materials.

iii) High strains can be possible.

iv) Flexible and easily mountable.

v) Can be adapted to existing technology electronics (coating, integration etc.).

vi) Low processing temperature and low cost.

vii) Easy to manipulate chemical composition/structure.

1.8.4. *Why Conducting Polymer as an Actuator*

Conducting polymers (e.g. polypyrrole and polyaniline) originally attracted attention because of their high and wide range of electronic conductivities (in special cases comparable with Cu). The polymers contain a conjugated, often one-dimensional backbone, and their properties usually depend on being oxidized or reduced by the introduction of anions or cations as dopants associated with the chain [79].

The accommodation of ions in the polymer also has consequences for their mechanical properties. The creation of charged electronic species on the chain can change the stiffness and the length of the individual polymer chains, and the incorporation of the sometimes-bulky counter-ions can increase the volume-especially when the ions are associated with co-intercalating solvent molecules. This opens the possibility for the reversible control of mechanical properties by the application of a voltage, and is the foundation for the interest in conducting polymers as electromechanical actuators.

1.8.5. *History of Conducting Polymer Actuators*

Baughman, Shacklette, & Elsenbaumer were the first to propose conducting polymer-based actuators. Latest several articles [80-81] from the research groups all over the world have been written on the subject of conducting polymer actuators. In the search for a system with the characteristics natural muscles at least approximately, the conjugated conducting polymers have emerged as the viable and interesting materials. In fact, the first actuator that received the name of an artificial muscle was based on a

conducting polymer (polypyrrole) and Otero et al.[24] in 1992 reported it. The history, description and various characteristics of conducting polymers such as PPy, PANI, etc. have been already given in the earlier sections of this chapter. These polymers can be doped i.e. incorporated with charged species, which either donate or accept electrons and hence make the materials conducting. This process can be reversed so that the polymer goes to non-conducting state. This process is also referred as oxidizing or reducing the conducting polymer. In electrochemical terminology it is called redox reaction process. In addition to the variation in conductivity, the state change of conjugated polymers due to doping can produce several effects, e.g. variations in polymer colors, volume and porosity, etc.[82-103]. These changes are related to the oxidation state of the polymer and are under electrochemical control: the neutral polymer, the reduced polymer, the oxidized polymer or any intermediate state can be reached by applying the appropriate potential. In this thesis we will concentrate on reversible and controllable volume changes in CP and their utilization in the fabrication of actuators.

1.8.5.1. ***Classification of C.P Actuators***

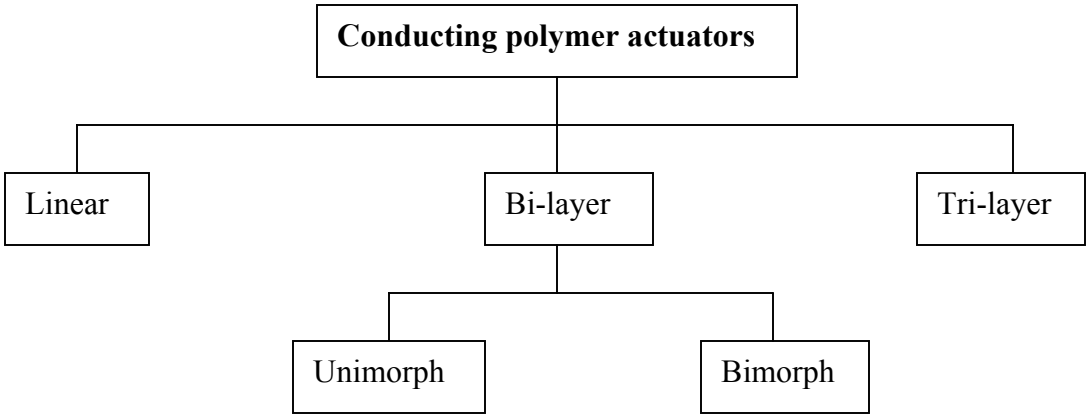

1.8.5.2. *Polypyrrole Actuator*

The properties of polypyrrole actuators have been reported by a number of authors[104-106]. The conductivity is very sensitive to conducting polymer structure. The structural information found from X-RAY diffraction measurements and the investigation of electronic state may eventually help to determine the mechanism responsible for charge induced actuation in polypyrrole .The overall morphology of PPy is very sensitive to synthesis condition.

1.8.5.2.1. *Synthesis*

All of the polypyrrole actuators reported in the literature are electrochemically synthesized. In such cases, about $1/3^{rd}$ of the monomers are charged [107]. The backbone charge is balanced by the presence of anions. In this state, polypyrrole is black in appearance and has a typical conductivities upto 10^{-2} $S.cm^{-1}$, reaching 10^{-3} $S.cm^{-1}$ when stretch aligned [108].

Generally, polypyrrole films are prepared by the electro-oxidation of pyrrole in one–compartment cell equipped with platinum working electrode, gold wire counter electrode and a sodium chloride calomel reference electrode (SCE). In a typical preparation, an acetonitrile solution containing 0.1 M $TEATBF_4$ plus ca 0.02 M pyrrole is employed [109]. A wide variety of solvents and electrolytes can be used, as the electrical resistance of the solution is not high and the nucleophilicity does not interfere with the polymerization reaction. These conditions can be maintained by selecting solutions where the electrolyte is highly dissociated and which are slightly acidic. Films of various thicknesses can be prepared by changing current density, time of deposition or monomer concentration.

Electro-polymerization of pyrrole and similar monomers differs from the other polymerization process, the electrode triggers chain growth and consequently this process requires very little electricity [110]. In the anodic oxidation of pyrrole to produce polypyrrole, the charged species of precursor initially formed by the continuous oxidation of the neutral monomer at the anode surface[111]. As a consequence, several electrochemical and chemical competitive reactions are possible near the electrode surface. The reaction mechanism of electrochemical synthesis of PPy is given in below (scheme-2).

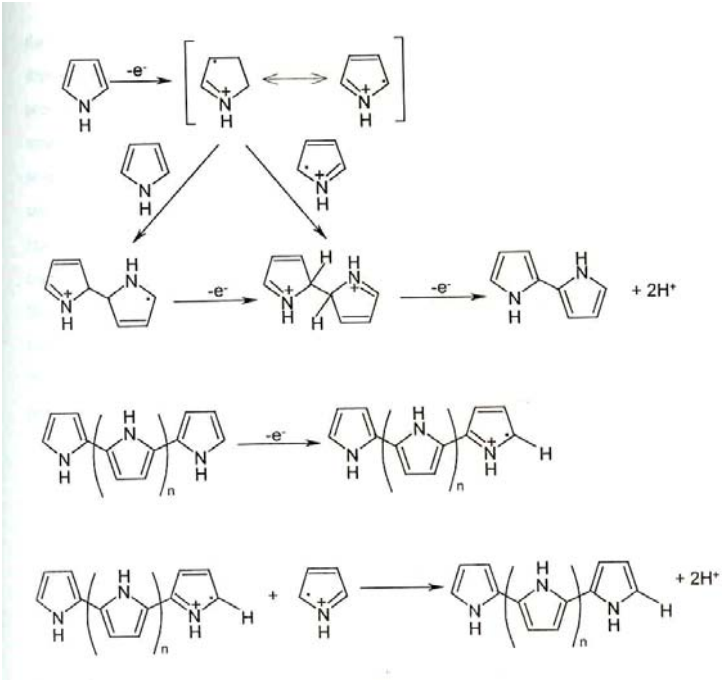

Scheme-2. Mechanism for the electro-polymerization of pyrrole

1.8.6. *Polymer Actuators - Mechanism and Principles of Operation*

There are various types of polymeric actuators: electrostrictive dielectric type, gel type and conducting polymer type. The mechanism and underlying principle for the actuation

i.e. change of shape, size or orientation depends on the type of actuator. Conducting polymer actuators are more versatile, but much more complicated to understand. The actuation relies on structural and volume changes occurring when the polymer is doped or undoped i.e. oxidized or reduced in an electrolyte. Different mechanisms have been proposed in the past to account for the actuation effect occurring during redox cycling of conducting polymers. Among all of them, redox mechanism is only well accepted. But, it has also some drawbacks; redox mechanism depends on diffusion of ions between conducting polymer film and electrolyte. Diffusion of ions is slow as compared to response time of actuator. So, another parallel phenomena is also occurring with redox phenomena. We will explain this phenomenon in chapter V.

1.8.6.1. *Electrochemical Oxidation/Reduction*

The construction of electromechanical devices based on conducting polymers is possible due to the volume changes taking place in these materials during their electrochemical oxidation / reduction.

Case-I

If the conducting polymer is grown in the presence of bulky anions (dodecylsulfate, dodecylbenzenesulfonate, etc.) or polyanions (polyvinylsulfonate, polystyrenesulfonate, etc.), mostly cations and solvent molecules are inserted and removed to compensate charge in the polymer. In this case, polymer volume increases during the reduction process and decreases in the oxidation process [112-118].

$$[(\text{Polymer})\ n(A^-)\ \ n\ (C^+)]_{\text{solid}}$$

$$\downarrow\uparrow$$

$$[(\text{Polymer})^{n+}\ n\ (A^-)]_{\text{solid}} + n\ (C^+)_{\text{solution}} + (ne^-)$$

Case-II

When conducting polymer is generated electrochemically in the presence of small anions (ClO_4^-, BF_4^-, Cl^-, etc.) mostly anion and solvent molecule motion is observed during the redox process. In this case, polymer volume increases during the oxidation and decreases in the reduction. However, apparent cation motion also becomes significant for higher oxidation and / or reduction states [118-121].

$$(\text{Polymer})_{\text{solid}} + n\,(A^-)\ \text{solution} \quad \uparrow\downarrow \quad [(\text{Polymer})^{n+}\ n\,(A^-)]_{\text{solid}} + (ne^-)_{\text{metal}}$$

Case-III

There is an intermediate situation that occurs when the conductive polymer is formed in the presence of medium-size anions (*p*-toluene sulfonate, napthalenesulfonate, etc.). In this case, simultaneous anion and cation motion are observed during the redox process and the volume change that occurs in the polymer is lower than in the preceding two cases [103, 122-124].

1.8.7. *Theoretical Model*

In order to understand the ultimate performance limits of conducting polymer actuators and to predict their response for design purpose it is important to have models that describe actuator behaviour.

A review of the literature [96,107,125] shows that several models have been proposed to explain the actuation behaviour of PPy in various oxidation states. Polypyrrole free

standing film undergoes redox reaction in electrolyte system and shows simultaneous shrinking or swelling. This volume change is usually small and can not be detected with ease. It is very likely that it is related to mass transport in the polymer phase [126]. An elucidation seems to be beneficial. In addition, the volume change must be taken into consideration for application purposes. The self-induced bending of a bi-layer strip, like a bimetal, has been considered for the study of small volume changes in one of the layers.

One of the first models proposed in this field was the theory of bi-layer strip (like bi-metal) by Q. Pei et.al [126-127]. However, they did not discuss the effect of thickness and modulus of both layers in depth. Another attempt made to develop a theoretical model was by T.F.Otero et al.[125]. They proposed effective active layer theory. According to them conducting polymer can be considered to have two layers, one is active and the other another is inactive (of same material backside). They have not considered the modulus of these two layers as different. This theory also was unable to explain maxima in bending angle in particular combination of thickness of bi-layer. None of them consider geometrical shape dependent actuation in bi-layer actuator. The geometrical shape must be taken into consideration when designing devices. Hence, it is essential to develop phenomenological model, which consider all the above-mentioned factors and corresponding experiments to prove the same.

1.8.8. *Advantages and Disadvantages of C.P Actuators*

Following the review of the most important CP actuators, the aim of this section is to analyze the general advantages and disadvantages of actuators based on conductive polymers.

1.8.8.1. *Advantages*

i) Conducting polymers (CP) are both ionic and electronic conductive materials that allow construction of CP actuators with a basic mechanism similar to natural muscles.

ii) Many conductive polymers are biocompatible and need low electric potentials.

iii) Conducting polymer is electrodeposited [128] on an electrode with defined favorable on unfavorable areas for polymer deposition.

iv) The strain or displacement of CP actuators is high.

1.8.8.2. *Disadvantages*

i) The actuation mechanism of a CP actuator is based on an ion exchange process between the conductive polymer film and the electrolytic medium (either electrolytic solution or dry/wet polymer electrolyte). This is the most important factor that controls and limits the response time of a CP actuator.

ii) The problem is both to find a good encapsulating material whose mechanical stiffness does not impede the actuator's movement and to avoid electronic conduction between conductive polymer and the counter electrode (which can be either a metallic electrode or a conductive polymer).

iii) Further, a delamination & degradation process that limited the actuator's lifetime was reported in CP actuators where a conductive polymer film was deposited onto a flexible plastic film sputtered with a thin layer of metal [129-130].

iv) Low linear strain of conductive polymer impedes the construction of effective linear CP actuators working in the same way as natural muscles.

1.9. Aim and Scope

It is observed from the above discussion that piezo-sensitivity and actuation can be achieved by using conducting polymers. Conducting polymer blends and composites are good for sensor whereas pristine conducting polymer deposited on flexible supports could be used for actuator. Dispersion is the most convenient way of making blends and composites, which one essential for processing these into different shapes. The dissimilarities in the work function of the constituent polymers give rise to the formation of junction in blends and composites giving rise to non-linear charge transport phenomena. However, the non-linear charge transport across the conducting polymer /insulating polymer interface has not been considered in the past for material used in sensors and actuators.

Hence, it is proposed in the present work to investigate the electromechanical response of conducting polymer blends and composites as well as the electrical charge transport characteristics and correlate the same through theoretical model. This thesis explores the development of conducting polymers for potential applications in sensors and actuators. It covers two major areas of conducting polymer. The first focuses on the development of conducting polymer composites for piezo-sensors, while the second area explores the development of conducting polymer-based materials showing high electromechanical response at low voltages.

The polymeric materials chosen for the present investigations are well known for their corresponding properties. Amongst conducting polymers, polyaniline is known to be stable, easy to synthesize and handle. Also, it can be mixed with a range of other

polymers such as polyvinyl chloride, polystyrene, polyethylene, etc. Flexible elastomers have been chosen for the present studies since these are not only easily deformed but also exhibit non-linear mechanical response. Polyvinylidene fluoride is well known for its piezoelectric properties and hence most ideally suited for the present investigations. The combination of these materials can lead to new synergistic effects which have not been reported before.

The main aim of the present studies is to bring out the engineering aspects of the design and development of the electromechanical sensors and actuators. In order to obtain good response characteristics it is essential not only to increase material properties but also consider the design, geometrical shape, size, aspect ratio, etc. The present work is an attempt to develop deeper understanding in these areas.

1.10. References

1. H.Shirakawa, E.J.Louis, AG.MacDiarmid, C.K.Chiang, A.J.Heeger, J.Chem.Soc. Chem.Comm.,1977,578.
2. C.K.Chiang, M.A.Druy, S.C.Gau, A.J.Heeger, E.J.Louis, A.G.MacDiarmid, J.Am.Chem.Soc.,**100**,1978,1013.
3. C.K.Chiang, C.R.Fincher, Jr.Y.W.Park, A.J.Heeger, H.Shirakawa, E.J.Louis, S.C.Gau, A.G.MacDiarmid, Phys.Rev.Lett., **39**,1977,1098.
4. T.A.Skotheim, Handbook of Conducting Polymers, Marcel Dekker, New York,1986, p-673.
5. W.R.Salaneck, I.Lundstrom, W.S.Haung, A.G.MacDiarmid, Synth.Met., **13**,1986,291.
6. K.Kaneto, Y.Kohno, K.Yoshino, Y.Inuishi, J.Chem.Soc.Chem.Comm., 1983,382.
7. G.G.Wallace, M.Smith, H.Zhao, Trends in Analytical Chemistry, **18(4)**,1999,245.
8. S.Cosnier, B.Galland, C.Gondran, A.Le Pellece, Electroanalysis, **10**,1998,808.
9. C.Kranz, H.Wohlschlager, H.L.Schmidt, W.Schuhmann, Electroanalysis, **10**,1998,546.
10. H.Korri–Youssofi, F.Garnier, P.Srivasta, P.Godillor, A.Yassar, J.Am.Chem.Soc., **119**,1997,7388.
11. B.P.Jelle, G.Hagen, S.Nodland, J.Electrochem.Soc., **140**,1993,3560.
12. R.J.Mortimer, J.Mater.Chem., **5**,1995,969.
13. N.Ahmad, A.G.Macdiarmid, Synth.Met., **78**,1996,103.
14. B.Wessling, Adv.Mater., **6**,1994,226.
15. R.Naugi, A.J.Framk, A.J.Nocic, J.Am.Chem.Soc.,**103**,1981,1849.
16. F.Jonas, G.Heywang, Electrochem.Acta. **39**,1994,1345.

17. G.Schopf, G.Kossmehl, Adv.Polymer Sci., **129**,1997,124.

18. V.T.Troung, A.R.Codd, M.Forsyth, J.Mater.Sci., **29**,1994,4331.

19. F.Legros, A.F.Lamer, Mat.Res.Bull., **19**,1984,1109.

20. H.Munstedt, G.Kohler, H.Mohwald, D.Naegde, R.Fly, G.Bitthin, E.Meissner, Synth.Met.,**18**,1987,259.

21. D.Naegele, R.Bitthin, Solid State Ionics, **28(30)**,1988,983.

22. H.S.Nalwa, Handbook of Organic Conductive Molecules and Polymers, John Wiley & Sons Ltd., New York,1997, Ch-12.

23. J. Kim, Y.B.Seo, Sang H.Choi, SPIE's Annual Symposium on Smart Materials II, Melbourne, Australia, **4934** 2002,158.

24. T.F.Otero, E.Angulo, J.Rodriguez, C.Santamaria, J.Electroana.Chem.**, 341**,1992,369.

25. K.Oguro,Y.Kawami, H.Takenaka, J.Micromachine Soc., **5**,1992,27.

26. J. Kim, Y.B.Seo, Smart Materials and Struc., **11**,2002,355.

27. A.G.MacDiarmid, R.J.Mammone, J.R.Krawczyk, S.J.Porter, Mol.Cryst.Liq.Cryst., **105**,1984,89.

28. J.J.D.Kroschwitz, Encyclopedia of Polymer Science & Engineering. John Wiley & Sons Ltd., New York,1982, p- 462.

29. T.J.Lewis, Faraday Discuss, Chem.Soc., **88**,1987,189.

30. S.S.Roth, Mater.Sci.Forum, **21**,1987,10.

31. E.M.Conwell, Phys.Rev., **33 B**,1986,3465.

32. J.Y.Shimano, A.G.MacDiarmid, Synth.Met.,**123**,2001,251.

33. E.M.Genies, A.Boyl, M.Lapkowski, C.Trintavis, Synth.Met., **36**,1990,139.

34. Y.Cao, A.Andretta, A.J.Heeger, P.Smith, Polymer, **30**,1989,2305.

35. J.C.Chiang, A.G.MacDiarmid, Synth.Met., **13**,1986,193.

36. J.L.Cadenas, H.Hu, Solar Energy Mat.Sol.Cells, **55**,1998,105.

37. A.G.MacDiarmid, J.C.Chiang, A.F.Richter, Synth.Met., **18**,1987,317.

38. W.Prissanaroon, N.Brack, P.J.Pigram, J.Liesegang, Synth.Met., **142**,2004,25.

39. A.Dallolia, Y.Dascola, V.Varacca, V.Bocchi, Comptes.Rendus, **C 267**,1986,433.

40. I.M.Ward, Mechanical Properties of Solid Polymers, John Wiley & Sons Ltd., New York,1983, Ch-2.

41. K.E.Brain, Proc.Phys.Soc., **36**,1924,81.

42. A.V.Subnikov, B.K.Brunovskij, Chem.Absr., **23(18)**,1929,4605.

43. E.Fukada, J.Yasuda, J.Phys.,Soc.Japan,**12(10)**,1957,1158.

44. H.Kawai, Jpn.J.Appl.Phys., **8** (7),1969,975.

45. G.M.Sessler, J.Acoust.Soc.Am, **70 (6)**,1981,1567.

46. Kynar, Piezo Film Technical Manual Pennwalt Corporation, Valley Forge, PA,1987, p-65.

47. J.P.Roberts, P.Popper, Piezoelectric Ceramics, Academic Press Inc., London, **3**,1971, p-317.

48. J.Kulek, Cz.Pawlaczyk, E.Markiewicz, J.Electrostatics, **56**,2002,135.

49. R.C.Patil, S.Radhakrishnan, S.Pethkar, R.Vijaymohanan, J.Mater.Res., **16(7)**,2001,1982.

50. Z.X.Bao, C.X.Liu, N.J.Pinto, Synth.Met., **87**,1997,147.

51. Hong-Quan Xie, Yong-Mei Ma, J.Appl.Polymer Sci., **77**,2000,2156.

52. A.G.MacDiarmid, J.C.Chiang, M.Halpern, W.S.Huang, S.L.Mu, N.L.Somasiri, S.I.Yaniger, Mol.Cryst.Liq.Cryst., **121**,1985,173.

53. A.Pron, F.Genoud, C.Menardo, M.Nechtschein, Synth.Met., **24**,1988,193.

54. K.Gurunathan, A.V.Murugan, R.Marimuthu, U.P.Mulik, D.P.Amalnerkar, Mater.Chem.Phys., **61**,1999,173.

55. G.Anitha, E.Subramanian, Sensors and Actuators, B: Chemical, (in Press).

56. D.N.Debarnot, F.P.Epaillard, Anal.Chim.Acta, **475**,2003,1.

57. H.Fuchigami, A.Tasumura, H.Kezka, Appl.Phys.Lett., **63**,1993,1372.

58. Y.Yang, A.J.Heeger, Nature, **372**,1995,498.

59. N.S.Saricitrci, L.Smilowitz, A.J.Heeger, F.Wudi, Science, **258**,1992,1474.

60. H.H.Hassan, S.A.Khairy, S.EI –Guiziri, M.E.Moeim, J.Appl.Polymer Sci., **42**,1991,2883.

61. S.Radhakrishnan, S.Chakne, P.N.Shelke, Materials Letters, **18**,1994,358.

62. S.Radhakrishnan, D.R.Saini, Polymer Int., **34**,1994,111.

63. Zhong-Xing Bao, C.X.Liu, N.J.Pinto, Synth.Met., **87**,1997,147.

64. Zhong-Xing Bao, F.Colon, N.J.Pinto, C.X..Liu, Synth.Met., **94**,1998,211.

65. Hong-Euan Xie, Yong-Mei Ma, Jun-Shi Guo, Polymer, **40**,1998,261.

66. P.R.Somani, R.Marimuthu, U.P.Mulik, S.R.Sainker, D.P.Amalnerkar, Synth.Met., **106**,1999,45.

67. A.T.Ponomarenko, V.G.Shevchenko, N.S.Enikolopyan, Advances in Polymer Sci., 1996,126.

68. S.Radhakrishnan, Polymer Comm., **26**,1986,153.

69. A.Assadi, C.Svensson, M.Willander, O.Inganas, J.Appl.Phys., **72**,1992,2900. J.Appl.Phys.Lett., **53**,1988,195.

70. H.Tomozawa, D.Braun, S.Phillipson, A.J.Heeger, Synth.Met., **28**,1989,687.

71. L.I.Maissel, R.Glang, Handbook of Thin Film Technology, McGraw–Hill, New York, 1976, Ch-14.

72. Frenkel, Phys.Rev., **54**,1938,647.

73. F.Carmona, R.Canet, P.Delhaes, J.Appl.Phys., **61**,1987,2550.

74. Xiang-wu Zhang, Y.Pan, Qiang Zheng, Xiao-Su YI, J.Polymer Sci., Part B: Polymer Phys., **38**,2000,2739.

75. Y.Bar-Cohen, S.P.Leary, K.Oguro, S.Tadokoro, J.S.Harrison, J.G.Smith, J.Su, SPIE 7th International Symposium on Smart Structures, 2000,140.

76. A.F.Huxley, Pro.Biophysics and Biophysical Chemistry, **7**,1957,255.

77. J.Spudich, Nature, **372**,1994,515.

78. M.Konyo, S.Tadokoro, T.Takamori, K.Oguro, IEEE International Conference on Robotics and Automation, 2000,3416.

79. S.Skaarup, K.West, L.M.W.K.Gunaratne, K.P.Vidanapathirana, M.A.Careem, Solid State Ionics, **136**,2000,577.

80. S.D.Deshpande, J.Kim, S.R.Yun, SPIE, San-Diago, USA, **5385**,2004,260.

81. M.A.De Paoli, A.Zanelli, M.Mastragostino, A.M.Rocco, J.Electroanal.Chem., **435**,1997,217.

82. S.D.Deshpande, J.Kim, S.R.Yun, Synth.Met., **149**,2005,53.

83. O.Inganas, J.Lundstrom, Synth.Met., **21**,1987,13.

84. J.D.Madden, R.A.Cush, T.S.Kanigan, C.J.Brenan, I.W.Hunter, Synth.Met., **105**,1999,16.

85. J.Kim, J.Y.Kim, S.J.Choe, SPIE's 7th Annual Symposium on Smart Structure and Materials, Newport Beach, CA, USA, **3987**,2000,203.

86. W.A.Jr.Gazotti, G.Casalbore-Miceli, A.Geri, M.A De Paoli, Adv.Mater., **10**,1998,60.

87. E.MGirotto, M.A.De Paoli, Adv.Mater., **41**,1998,1871.

88. M.Roemer, T.Kurzenknabe, E.Oestershutze, N.Nicoloso, Anal.Bional.Chem., **373**,2002,754.

89. R.H.Baughman, Macromol.Symp., **51**,1991,193.

90. T.F.Otero, E.Angulo, Solid State Ionics, **803**,1993,63.

91. E.Smela, S.Shimoda, Electrochim.Acta, **44**,1998,219.

92. E.Smela, N.Gadegaard, Avd.Mater., **11**,1999,953.

93. J.M.Sansinena, V.Olazabal, T.F.Otero, C.M.N.Poloda Fonseca, M.A.De Paoli, J.Chem.Soc.Chem.Comm., **22**,1997,17.

94. R.H.Baughman, Synth.Met., **78**,1996,339.

95. T.F.Otero, M.T.Cortes, Avd.Mater.,**15**,2003,279.

96. E.W.H.Jager, E.Smela, O.Inganas, Science, **290**,2000,1540.

97. E.W.H.Jager, O.Inganas, I.Lundstrom, Adv.Mater.,**13**,2001,76.

98. R.Owen, Chem.Soc.Rev., **26**,1987,259.

99. P.G.Bruce, J.Chem.Soc.Chem.Comm., **56**,1997,1817.

100. A.Davies, R.J.Hobson, M.J.Hudson, W.J.Macklin, R.J.J.Neat, J.Mater.Chem. **6**,1996,49.

101. T.F.Otero, M.J.Gonzalez-Tejera, J.Electroanal.Chem., **410**,1996,69.

102. A.Heller, Ac.Chem.Res., **14**,1981,154.

103. M.R.Gandhi, P.Murray, G.M.Spinks, G.G.Wallace, Synth.Met., **73**,1995,247.

104. T.F.Otero, E.Angulo, Solid State Ionics, **803**,1993,63.

105. J.M.Sansinema, V.Olazabal, T.F.Otero, C.M.N.Polo da Fonseca, M.A. De Paoli, J.Chem.Soc.Chem.Comm., **22**,1997,17.

106. R.H.Baughman, Synth.Met., **78**,1996,339.

107. C.K.Baker, R.A.John Reynolds, J.Electroana.Chemistry, **251**,1988,307.

108. K.Sato, M.Yamaura, T.Hagiwara, Synth.Met., **40**,1991,35.

109. A.F.Diaz, K.Kanazawa, G.P.Gardini, J.Chem.Soc.Chem.Comm.,1979,635.

110. T.F.Otero, Macromol.Chem.Rapid Comm., **5**,1984,125.

111. S.Sanyal, R.C.Bhakta, B.Nayak, Macromolecules, **18**,1985,1314.

112. T.Shimidzu, A.Ohtani, K.Honda, J.Electroanal.Chem., **224**,1987,123.

113. Q-X.Zhou, L.L .Miller, J.R.Valentine, J.Electroanal.Chem., **223**,1987,283.

114. G.Bidan, B.Ehui, M.Lapkowski, J.Phys.D, App.Phys. **21**,1988,1043.

115. K.Naoi, M.M.Lein, W.H.Smyrl. J.Electroanal.Chem., **272**,1989,273.

116. K.Naoi, M.M.Lein, W.H.Smyrl, J.Electrochem.Soc., **138 (2)**,1991,440.

117. C.M.Elliott, A.Kopelove, W.J.Albery, Z.Chen, J.Phys.Chem., **95**,1991,1743.

118. Ch.Baker, J.R.Reynolds, J.Phys.Chem., **95**,1991,4446.

119. H.Zhao, W.E.Price, G.G.Wallace, J.Electroanal.Chem., **334**,1992,111.

120. R.C.D.Peres, M-A.De Paoli, R.M.Torresi, Synth.Met., **48**,1992,259.

121. J.R.Reynolds, M.Pyo, Y-J.Qui, Synth.Met., **55**,1993,1388.

122. E.M.Genies, J.M.Pernault, Synth.Met., **10**,1984,117.

123. F.Chao, J.L.Baudoin, M.Costa, P.Lang, Makromol.Chem.Mackromol.Symp., **8**,1987,173.

124. M.Iseki, K.Sato, K.Kuhara, A.Mizukami, Synth.Met., **40**,1991,117.

125. H.S.Nalwa, Handbook of Organic Conductive Molecules and Polymers, John Wiley & Sons Ltd., New York,1997, p-517.

126. Q.Pei, O.Inganas, J.Physical Chem., **96(25)**,1992,10507.

127. Q.Pei, O.Inganas, Solid State Ionics, **60**,1993,161.

128. E.Smela, J.Micromech.Microeng., **9**,1999,1.

129. E.Smela, O.Inganas, Q.Pei, I.Lundstron, Adv.Mater., **5**,1993,953.

130. E.Smela, M.Kallenbach, J.Holdenried, J.Microelectromech.Syst., **8**(4),1999,373.

CHAPTER - II

Experimental

2.1. Introduction

In this chapter, a brief description of the materials used throughout this work together with general details of the experimental procedures employed for the electrochemical and chemical preparation of the conducting polymers and their applications as sensors and actuators. Also included are general details of the spectroscopic, electrochemical and other methods of characterization used for studying these polymers. The details of specific procedures used in particular case are outlined in the experimental section of each individual chapter.

2.2. Materials

The various polymeric materials and chemicals used were given in the table 2.1.

Table 2.1. Polymeric materials and chemicals used and their sources.

Material	Acronym	Source
Ammonium persulfate,A.R.	APS	S.D.Fine Chem., India.
Aniline,A.R.	-	S.D.Fine Chem., India.
Camphor sulfonic acid.	CSA	Merck Ltd., Germany.
Chloroform,G.R.	$CHCl_3$	Merck Ltd., India.
Dodecylbenzenesulfonic acid.	DBSA	Fluka Chem., Switzerland.
Hydrochloric acid (35%),G.R.	HCl	Merck Ltd., India.
p-toluene sulfonic acid.	PTSA	Loba Chem., India.
Styrene Butadiene Styrene. (Cariflex CTR 1102)	SBS	Shell Corporation, Netherlands.
Polyvinylidene fluoride.(Solef)	PVDF	Solef, 1101, Belgium.
Polypropylene film.	PP	I.P.C.L, India.
Methyl sulfonic acid.	MSA	Merck Ltd., India.

Potassium chloride.	KCl	Merck Ltd., India.
Lithium carbonate.	Li_2CO_3	S.D.Fine Chem., India.
Perchloric acid.	$HClO_4$	S.D.Fine Chem.., India.
Agar Agar powder.	-	Loba Chem., India.
Sulfuric acid.	H_2SO_4	Merck Ltd., India.
Pyrrole.A.R.	-	Merck Ltd., India.
Hytrel.	-	Dupont, Mumbai, India.
Polyethylene.	LLDPE/LDPE	I.P.C.L, India.
Polyethylene terephthalate.	PET	BHEL, (Capacitive grade), India.

Pyrrole and aniline were obtained form Merck and Aldrich chemical company, respectively. Both were distilled and stored in a freez prior to use.

Section A: Sensor Fabrication and Testing

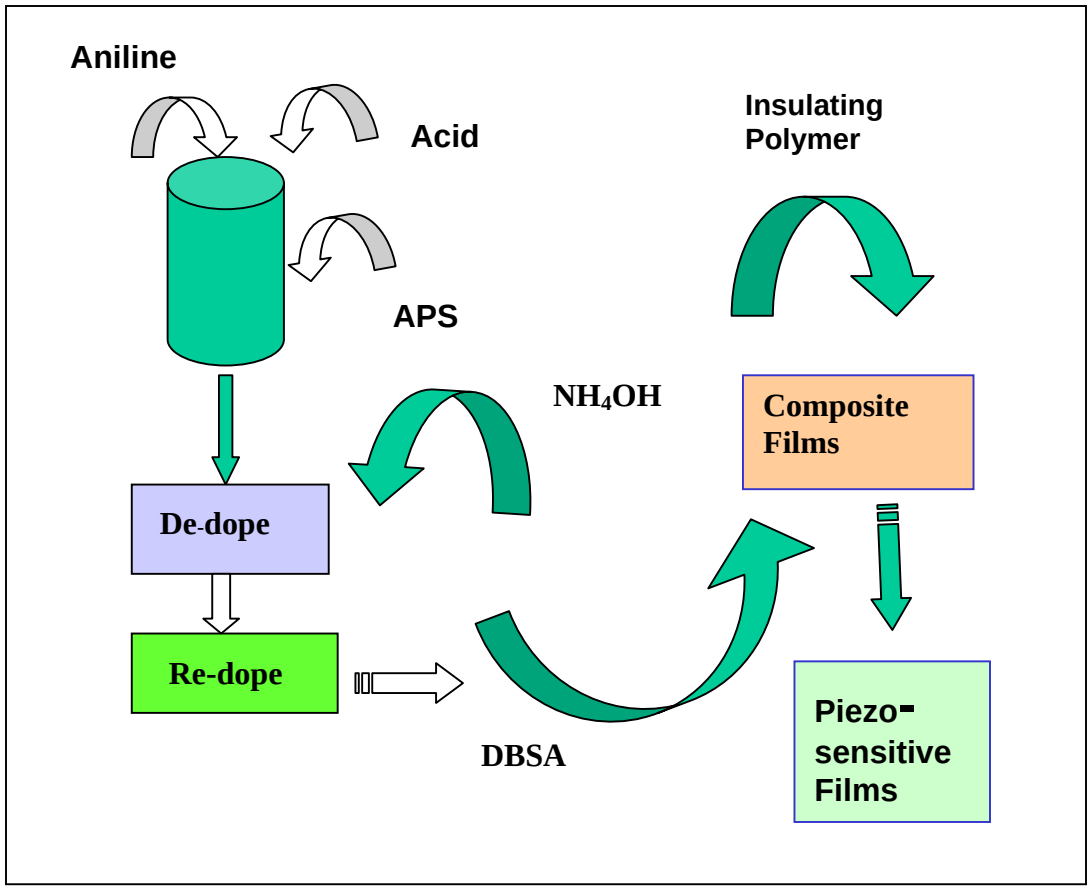

Scheme-2.1. Outline of the preparation of PANI composites films

2.3. Synthesis of Polyaniline

Polyaniline was synthesized by well known chemical routes [1] given in the section 1.7.7.1 of chapter I in this thesis. The total synthesis of polyaniline with different dopant ions was done in two different ways.

2.3.1. *Polyaniline Synthesis with Direct Doping Method*

Polyaniline was synthesized in conventional route in aqueous medium using mineral acid such as HCl as the dopant ion and oxidizing agent ammonium persulfate, $(NH_4)_2S_2O_8$, as

the initiator. Aniline monomer, acid dopant and oxidizing agent were taken in the molecular ratio of 1:1:1 [1]. Hydrochloric acid was taken in distilled water into which aniline monomer was added and stirred to get aniline-acid complex and kept in the freezing mixture to attain the reaction temperature 0-5^{o}C. In another beaker $(NH_4)_2S_2O_8$ was dissolved in distilled water and kept in the freezing mixture. When both of these solutions attained the reaction temperature, they were mixed together and stirred well, and kept for 4 hour for the completion of reaction. Polyaniline powder thus formed was filtered, washed thoroughly with water to remove excess salts and dried under the vacuum (10^{-3} torr) for 24 hr to make it moisture free. The product obtained is directly doped PANI with Cl dopant (PANI-HCl) and it was ground to fine powder by mechanical grinding in agate pestle mortar.

2.3.2. ***Preparation of Polyaniline by Indirect Doping Method***

Emeraldine base powder was first prepared by de-doping of PANI-HCl emeraldine salt obtained in the above manner. This was accomplished by stirring the emeraldine salt in a 1.0 M NH_4OH for 12 hour. The brown product was collected via suction filtration. The powder was then dried under vacuum for 24 hour at room temperature and stored in a freezer for later use. This de-doped PANI was subsequently doped with dodecyl benzene sulfonic acid (DBSA) in certain proportion (2:1) to obtain doped PANI i.e; PANI-DBSA.

2.4. Preparation of PANI Blends/Composites

For the purpose of solution blending of polyaniline with insulating materials, the stock solutions of each insulating polymer (mainly PVDF and SBS) were prepared in suitable solvents. The solvents used in this work were chloroform & dimethyl acetamide for SBS

& PVDF respectively. All these stock solutions were made with the concentration of 1g/ 30 ml. Polyaniline blends with different polymer were carried out by solution casting technique. Dedoped PANI (emeraldine base) was then re-doped with dodecylbenzene sulfonic acid (DBSA) in $CHCl_3$ for SBS–PANI and DMAc for PVDF-PANI blends. Several blend compositions (PANI doped with HCl ranging from 2 vol. % to 30 vol. % were prepared separately and mixed with stock solution of styrene-butadiene-styrene tri-block polymer (SBS) and polyvinylidene fluoride (PVDF), and an another set appropriate volume of PANI (DBSA-doped) solution was added to the same stock polymer solution separately to get PANI (DBSA-doped) blends. The whole slurry was stirred for 24 hrs to form a uniform blend of different compositions. These were cast in glass petri-dish followed by complete solvent evaporation in the ambient condition and then under vacuum to give films of SBS-PANI (470-500 μm thick) blends and PVDF-PANI films (35-50 μm thick). Outline of the preparation of PANI blends and composites were shown in scheme-2.1.

2.4.1. *Electrical Poling of PVDF-PANI Films*

The PVDF-PANI composite films were prepared in the manner described in previous section. These were placed between the two metal foil and pressed between glass slides. The two electrodes were connected to stabilized (D.C) power supply and voltage was applied for certain duration of time (poling time). The poling voltage ranged from 25 to 100 V for 35 μm thick film i.e, the poling field ranged from 10^4 to 10^5 V/cm .The poling time was 1 hr. and temperature was 25^0C in all cases.

2.5. Characterization

2.5.1. *UV-Visible Spectroscopy*

The creation of mid-gap state in the conducting polymers due to charge transfer complex can be studied by UV–visible spectroscopy. The intensity, or even the existences of bands of the solutions (polyaniline) are subjected for the scan directly gives characteristic peak of polyaniline. UV-visible spectroscopy was done using the Shimadzu UV-240 spectrometer sweeping the incident wavelengths from 900 nm to 300 nm.

2.5.2. *Infrared (IR) Spectroscopy*

FTIR studies [2] have confirmed the presence of PANI and different form of PVDF in selective PVDF-PANI blends. The PANI samples were mulled with dry potassium bromide crystals .The spectrum was recorded in the wavelength region of 400-2000 cm^{-1}. The IR of polymer films was recorded using a reflection mode on FTIR spectrometer (Shimadzu model 8201 PC) in few cases. The films were mounted in IR cell in the conventional way to record the IR spectra using Perkin Elmer model 1600.

2.5.3. *X-RAY Diffraction Studies*

Wide-angle X-RAY Diffraction (WXRD) studies were done in order to analyze the structures of synthesized polyaniline and selective blends of PVDF-PANI. The conducting polymer blends synthesized by using PVDF as matrices generally offered a semi crystalline structure. The PVDF as supplied used for this study is reported to have well defined structure. Hence, incorporation of conducting polymers is expected to show some structural changes of PVDF. These changes are studied using a well-known technique of wide angle X-RAY diffraction (WXRD) [3]. The crystalline structure of

various polymeric compositions was investigated by WXRD, using a powder X-RAY diffractometer (Phillips PW 1730 model) using CuKα source and β Ni filter. Also some of the scans were recorded on Rigaku X-RAY diffractometer, using Rint 2000 wide-angle goniometer with K-beta filter. All the scans were recorded in the 2θ region of 5-40° at a scan rate of 4°/min. From the 2θ values for the reflections, 'd' values were calculated using well-known Brag's equation,

$$2\,d \sin\theta = n\lambda. \qquad (2.1)$$

2.5.4. *Optical Microscopy*

In order to study particle size of synthesized polyaniline, an optical polarizing microscope (Leitz LaborLux 12 pol, Germany) coupled to an image analyzer system (VIDPRO 32, Leading Edge, Australia) was used in the present work. The microscope contains essentially a light source (Tungsten Lamp 25W), a condenser, a polarizer, a sample stage with controlled heating arrangement, objective assembly, an analyzer and eyepiece/ microphotography arrangement. In another arrangement, image analyzer was connected in place of microphotography. The image analysis system contains a video camera connected to a computer via a software which provide image grabbing, image storage and analysis facilities.

2.5.5. *Scanning Electron Microscopy (SEM)*

SEM studies [4] were performed to investigate the surface morphology or microstructure of the sample. Leica Stereoscan 440 model manufactured by M/s Leica Cambridge Ltd, U.K. was used in our work. Cross-section of the samples was mounted on the standard specimen mounting stubs by silver paste. These were coated with a thin layer of gold by

sputtering technique. The micrographs of the samples with 10 KV beam current were recorded by a 35 mm camera, which was attached on the high-resolution recording unit.

2.5.6. *Electrical Conductivity*

The electrical conductivity was determined at room temperature by placing the pellet or the film in a suitably designed apparatus as shown in Fig. 2.1. The apparatus consists of a sample holder, which was enclosed in an electromagnetic shielded cell, which in turn was mounted inside a glass. The change in the resistivity with blends composition were noted using an electrometer (Keithley 614 model).

2.5.7. *I-V Characterization*

The I-V characteristics were recorded for these samples using a stabilized DC power supply and Keithley electrometer (614 model) (Fig 2.1). The current was recorded as a function of the changing applied potential across the two terminals.

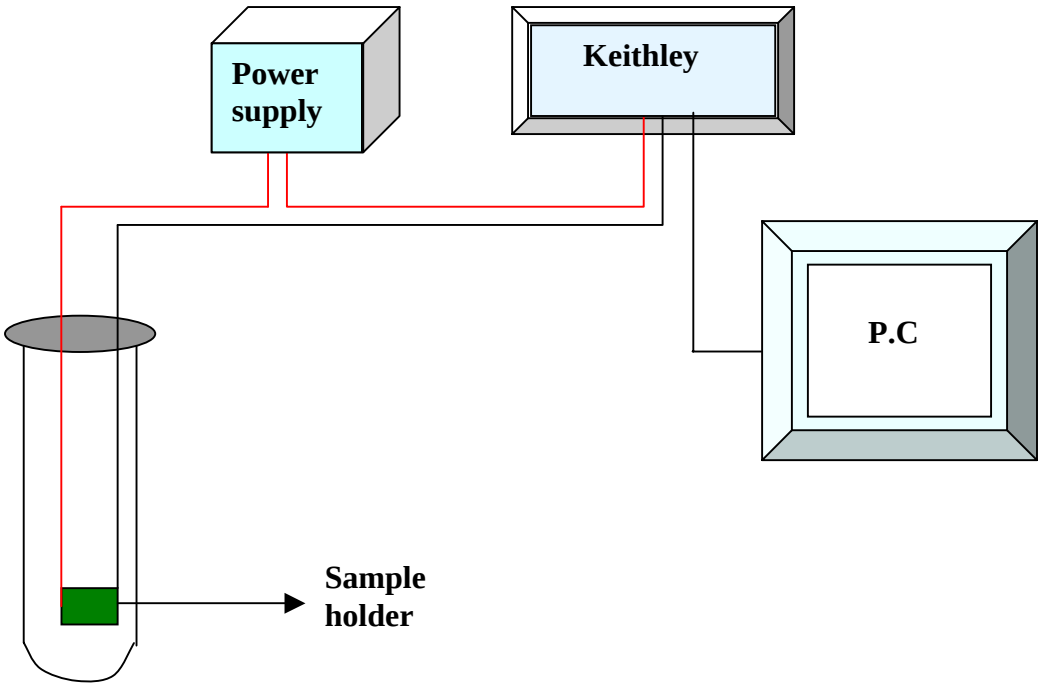

Figure-2.1. Electrical properties measurement apparatus.

2.5.8. *Piezo-sensitivity Measurements*

Details of the measurement of electrical properties and changes in these materials due to mechanical deformation were shown in Fig.2.2, same as those reported earlier for other polymers [5,6]. The piezo-resistivity was measured in these samples by placing them between two metal plates on which the mechanical load was applied. The top and bottom electrode were connected through constant voltage (D.C) power supply (typical applied potential of 2.0 V was used) and the signal (current) at different mechanical load application was measured using Keithley electrometer connected to computer. Continuous piezo-response curve with application and removal of mechanical load could be traced by this arrangement.

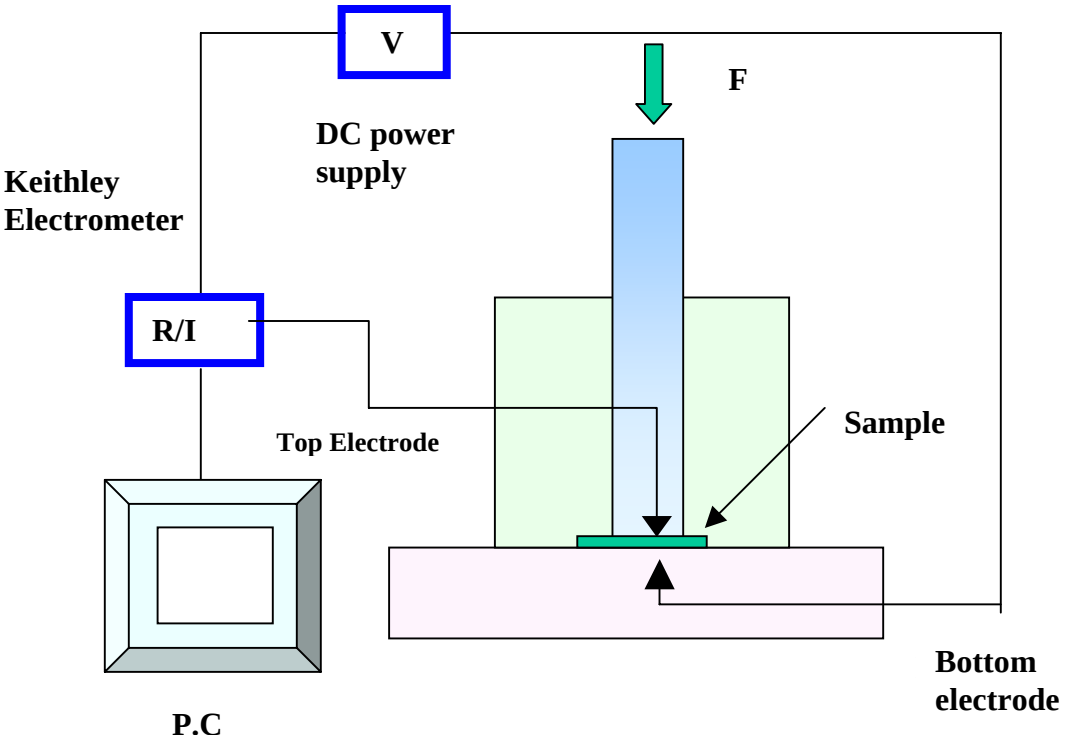

Figure-2.2. Set up for measurement of piezo-sensitivity of conducting polymer sensor.

Section B: Actuator Fabrication and Measurement of Response

2.6. Synthesis of Polypyrrole

2.6.1. *Electrodes*

A variety of electrode materials were used as working electrodes. These included PET, Hytrel, SBS, LLDPE/LDPE, and PP films. These films were gold coated by vacuum coating (12 inch Vacuum Coating unit, Model-12A4D) and used as a working electrode. Auxiliary electrodes used included platinum. Calomel electrodes obtained from SinSil Inter. Ltd. were used as reference electrodes, always in conjunction with a salt bridge.

2.6.2. *Electrochemical Polymerization*

Synthesis of polypyrrole films on various gold-coated electrode was carried by potentiostatic method, using a Vibrant Electro-chemical System (Model no-VSM /EC /2010) connected with a personal computer. The electrochemical deposition was carried out in a single compartment cell with three electrodes system as shown in Fig 2.3. The saturated calomel electrode (SCE) was connected through the salt bridge containing agar-agar/KCl mixture to the electrolytic solution. The counter electrode used was platinum and the working electrode was gold-coated substrate, on which electrochemically deposited polymer films were to be formed [7]. Solutions used for polymerization typically contained 0.1 M pyrrole and an electrolyte that provided the dopant. Appropriate dopant H_2SO_4 in 0.1 M molar concentrations was mixed in the water. Upon completion of polymerization, thin polypyrrole films were washed with distilled water before further use. PPy films were prepared by applying a potential of 0.65 V for a predetermined period of time and is given in the section 1.8.5.2.1 of the chapter I in this thesis.

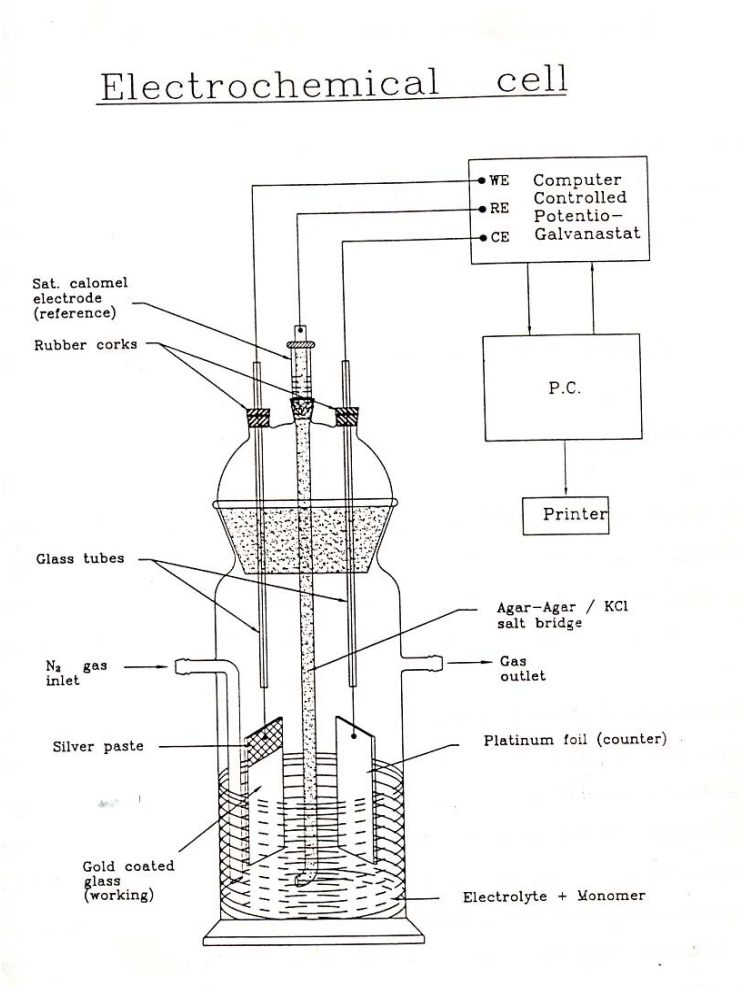

Figure-2.3. Electrochemical deposition unit.

2.6.3. *Mechanical Property*

Mechanical Property measurement of different insulating materials (films) which were used as a backing layer in bi-layer actuator, were carried out using an Instron Series IX Automated Materials Testing System 1.04. The tensile tests were done with dumbbell shaped samples. Tensile tests were done according to the standard ASTM D 882, keeping the grip distance of 150 mm, gauge length 50 mm, width 15 mm and cross-head speed 50 mm/min.

2.6.4. *Actuation Measurements*

Actuator strips of PPy/Au/backing layer with the dimension area of 2.5 cm length and 0.25 cm width were cut out from the laminate for bending test. Actuation measurement set up is presented in Fig.2.4. The above actuator films were tested for actuation by measuring bending angle (degree) in 0.1 M $LiClO_4$ aqueous solutions and a potential of –1.0 volt was applied. Various types of dopants used are also reported here.

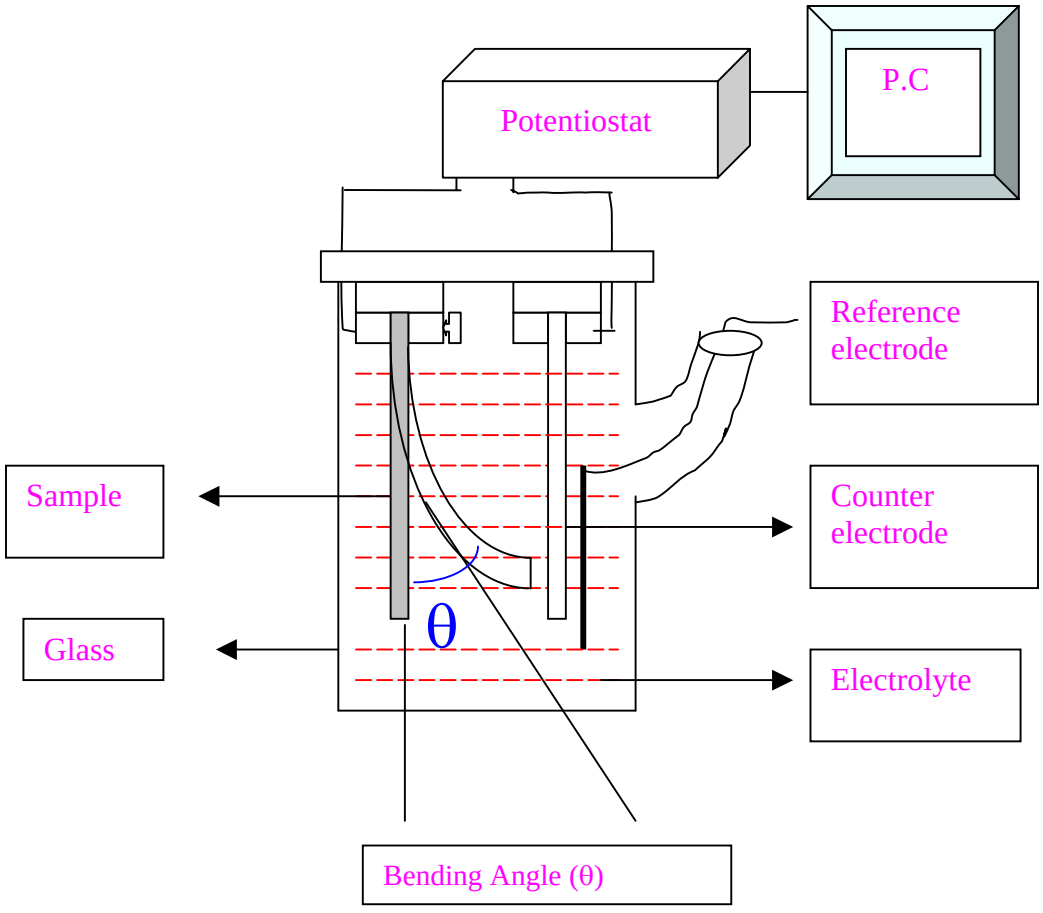

Figure-2.4. Set up for measurement of electromechanical actuation of conducting polymer actuator.

2.7. References

1. F.Lux, Polymer, **35**,1994,29.
2. H.Ishida, Fourier Transformation Infrared Characterization of Polymers, Plenum Press, New York, 1987, Ch-V.
3. N.H.Hartshorne, A.Stuart, Practical Optical Crystallography, Edward Arnold Ltd., London,1964, Ch-3.
4. D.B.Holt, M.D.Muir, P.R.Grant, I.M.Boswarva, Quantitative Scanning Electron Microscopy, Academic Press, New York, 1974, Ch-4.
5. S.Radhakrishnan, S.Unde, J.Appl.Polymer Sci., **71**,1999,2059.
6. S.Radhakrishnan, D.R.Saini, J.Mater.Sci., **26**,1991,5950.
7. S.Radhakrishnan, P.R.Somani, Chem.Phys.Lett., **292**,1998,218.

CHAPTER - III

Theoretical Model

Section I: Sensor

3.1. Introduction

There are many types of electromechanical sensors with large number of data reported in literature. In order to understand these varieties of cases, there is a need to develop a model, which gives the correlation between the experimentally observed variations with the basic underlying mechanism of the sensor. Modeling of the electromechanical sensor is essential for optimizing its performance with respect to material composition, structure, mechanical properties, dimensions, user application criteria, etc.

Carmona et al.[1] has studied piezo-resistivity of heterogeneous solids. They developed a model to predict the piezo-resistance of the conductor filled polymer composites close to threshold. The piezo-resistive effects of the materials were investigated under hydrostatic and uniaxial pressure. It was shown that piezo-resistance depends on materials composition, applied pressure and conducting particle concentration. Although his model can fit the experimental data, it has many disadvantages: (i) it is difficult to predict the effects of the influencing factors on the piezo-resistance quantitavely, especially the effects of filler particle diameter, matrix compressive modulus, etc. and (ii) it can not explain the time dependence of piezo-resistance. Xiao et al.[2] explained time dependency peizo-resistance of conductor filled polymer composites based on tunneling conduction mechanism. A model based on the change in interparticle separation under the applied stress has been developed to interpret the piezo-resistance and its time dependence. The theoretical data obtained from the model are found to agree with the experimental ones fairly well. According to this theory, piezo-resistance of the composites is arises from the

change of separation of adjacent particles, which is caused by the difference between the filler and matrix compressibility. The time dependence of piezo-resistance is due to the change of separation with time under the fixed stress, caused by the creep of polymer matrix. The influence of applied stress, filler volume fraction, filler particle diameter, and polymer creep behaviour on the time dependence of piezo-resistance have also been discussed in this model. It was found that all parameters influence the time dependence of piezo-resistance by altering the change process of interparticle separation. Therefore, to decrease the time dependence of piezo-resistance, which is important to improve the reproducibility and stability of piezo-resistance, the change process of interparticle should be controlled. Radhakrishnan et al.[3] described piezo-resistivity in terms of space charge limited conduction mechanism. They prepared conducting thermoplastic elastomer blends with various amount of oxidizing agents. These blends have phase-segregated morphology with preferential deposition of conducting polymer on domain of elastomer. These blends are very sensitive to small mechanical deformation. Radhakrishnan et al.[4] developed a model related to resistivity of filled polymer systems a function of filler concentration. This model takes into account non-ohmic conduction phenomena. It has been shown that, using a simple model that the charge carrier conduction process across the particle layer plays an important role in deciding the relationship between the overall resistivity and the filler concentration of filled polymer systems. M. Knite et al.[5] proposed a model on the basis of atomic force microscopy of the conductive surface network of the composite, which is related microstructure with piezo-sensitivity. Theoretical equations have been derived from a model based on the change

of particle separation under applied stress. Y. Pan et al.[6] developed a model based on the change in interparticle separation under applied stress for analyzing this piezo-resistance effect. In this model, the piezo-resistance of composites is proved to be caused by the difference between the filler and matrix compressibility. In addition, piezo-resistance values were calculated and the results were in good agreement with the experimental values.

There have been some reports on the piezo-resistivity of conducting polymer composites and blends in the past [7,8]. However, there are still many aspects, which need deeper understanding and more detailed investigations. For example, the effect of composition/ concentration of the additives on piezo-sensitivity is not investigated in detail as regards- the particle size, shape, nature of conducting particle (i.e. polypyrrole, polyaniline, doped with different dopants etc. vis-a-vis metal or carbon). Additionally, the deformation of the matrix polymer would be dependent on its mechanical behaviour which is not only depends on the type of polymer used viz. thermoplastics, elastomer type etc. but also on the concentration of the additive, its distribution, reinforcing effect etc. It is the purpose of the present studies to carry out detailed investigations on these various aspects and formulate a phenomenological model for understanding in depth the mechanism of piezo-sensitive effect and the peculiarities present in the piezo-sensitivity of conducting polymer composites.

3.1.1. *Background*

There are various observations made in the earlier reports on piezo-sensitivity of conducting polymer composites. It was found that the piezo-sensitivity of such

composites was dependent on the composition i.e. the concentration of the conducting additive, its nature i.e. metallic, carbon or graphite as well as the polymer matrix. Further, many of these composites exhibit non-linear conduction characteristics. It is also known that the deformation behaviour of the polymer matrix can be non-linear with mechanical load. Furthermore, the mechanical properties also get affected by incorporation of fillers, which can in some cases give reinforcement. Thus, it is essential to take into account all these factors in developing any model for explaining the piezo-sensitivity in conducting polymer composites.

3.1.2. *Assumptions*

i) Conducting particles are assumed to be incompressible, spherical and uniform in size.

ii)Conducting polymer particles are uniformly distributed throughout the polymer matrix.

iii) Matrix resistance is homogenous, the resistance of paths perpendicular to the current flow may be neglected, thus number of conducting particles between electrodes will be a factor in model derivation, together with the number of conducting paths.

iv) Conducting particle does not form aggregates.

3.1.3. *Theory*

The phenomenological model representing the piezo-sensitivity of conducting polymer composites, which incorporated both non-linear conduction process as well as mechanical properties of polymer is described as follows;

The present theory is based on the non-linear conduction model [9,3] for conducting polymer composites. The conducting polymer composite or phase separated immiscible blend can be considered as network of uniformly distributed conducting domains

with thin insulating films between them as shown in Fig. 3.1. In composites, the total resistance can be considered to be a function of both the resistance of each conducting

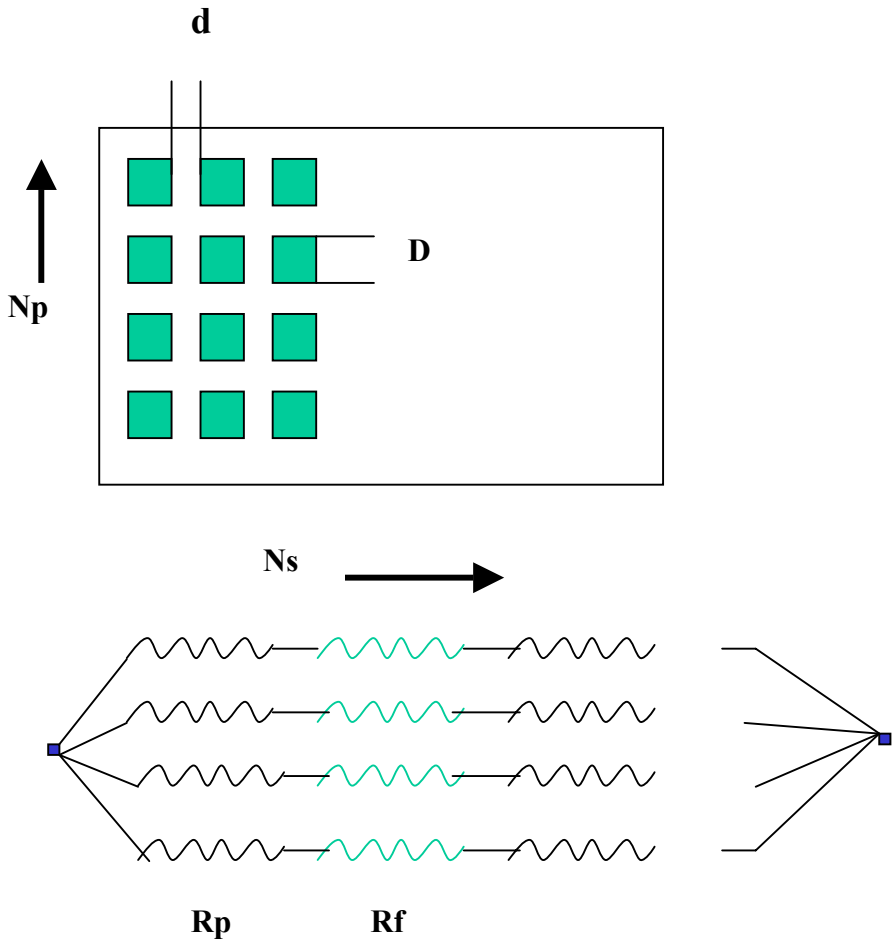

Figure-3.1. Schematic representation of polymeric composite containing conductive particle and the equivalent circuit for the same

particle (M) and the insulating layer between the two conducting particles (P). Rp and R_f are resistances of polymer matrix and conducting particle, respectively.

Rx is the net resistance of M-P-M junction.

$$Rx = [(B-d)^2/(D+d)^2]^{-1} (L-d)(Rp+R_f)/(D+d) \qquad (3.1)$$

Np and Ns are the number of M-P-M junctions in parallel and series, respectively. B^2 is the cross sectional area of the tested sample. At each of these inter-domain junctions the current voltage characteristics are non-linear. The theory of electrical conductivity or resistivity of conducting composites, taking into account of various non-linear conduction processes, has been described in details by Radhakrishnan et al.[4,10]. Amongst the different non-linear processes such as Schottky effect (SE), Fowler Nordheim tunneling (TN) of charge carrier and space charge limited conduction (SCLC); In the case of SCLC non-linear process, the current voltage relation is highly non-linear type [11] and is given by the following equations;

$$I = (9/8)(\mu\, \theta\, e)\, V_x^{n+1}/d^{2n+1} \qquad (3.1a)$$

$$Ns = (L-d)/(D+d) \qquad (3.1b)$$

$$Np = (B-d)^2/(D+d)^2 \qquad (3.1c)$$

In case of particle filled system, applying voltage (V) gets divided between the particles and the voltage present across the interparticle gap is Vx =V/Ns and the sample resistance (R_{SL} = V/I) in MKS units is given by [4];

$$R_{SL} = \frac{8}{9} \frac{10^{-13}}{\mu\, \theta\, e V_x^n} \frac{L-d}{D+d} \frac{d^{n+1}}{D^2} \qquad (3.1d)$$

Where L is the sample thickness, D is the conducting particle size, μ is the mobility, V_x is the voltage across the conducting particle and insulator junction, e is an electronic charge, n is an integer where n = 0, 1, 2, 3 and θ is a constant depending on the trap distribution, d is the inter-particulate gap which depends on the conducting particle concentration and its size given by the relation [4];

$$\phi^{1/3} = D.(L - d)/(D + d).L \qquad (3.2)$$

ϕ is the volume fraction of conducting particle in composite. It may be pointed out here that in the above equation 3.1a when n = 0, it is equivalent to ohmic case where current varies linearly with voltage.

Now the effect of external pressure on such a composite is to mainly change in d and thus cause modulation of resistivity. It may be assumed that the applied load gets dissipated through deformation of the polymer matrix and conducting particles are rigid. Non-linearity of stress-strain relationship has been mentioned in a number of cases where the system contains heterogeneous two phase components viz, foam, rubberized thermoplastic, elastomer, etc.[12 – 15]. The non-linear stress-strain relation is,

$$P / A = f(\in)K(\tfrac{v}{l_0})^{q}\, \tfrac{1}{1-q} \in^{1-q} \qquad (3.3)$$

Where, P/A is stress, P is applying load, A is cross section area on which load has been applied, $f(\in)$ is strain function, $\in$ is strain, K is constant, (v/l_0) is strain rate and it is very small, v is velocity, q is constant which is come from Boltzman superposition principle.

$$f(\in) = \frac{1}{(\in +1)} \qquad (3.4)$$

Combining equation 3.3 & 3.4 we get,

$$P = A\tfrac{1}{1+\in}K(\tfrac{v}{l_0})^{q}\, \tfrac{1}{1-q} \in^{1-q} \qquad (3.5)$$

Because the insulating matrix studied is elastomer, whose compressive modulus is much lower than that of the filler (conducting particle), so the deformation of conducting particles under load can be neglected. As a result, the change in interparticle separation along the conducting path is only due to deformation of insulating matrix. So, at small deformation, equation 3.5 gives the following form, where, the compressive strength (α)

is some what akin to inverse of tensile strength (E) [16], i.e. $\alpha = 1/E$, the change (d/d_0) in inter-particulate distance due to applied pressure (P) can be described as follows;

$$d = d_0 \left[1- (\alpha P)^{\beta} \right] \tag{3.6}$$

where, d_0 is the original distance (between two conducting particles) at dead load which is necessary to keep good contact between electrode and material surface, β is the exponent (non-linearity of mechanical properties) which depends on the polymer used. Combining the equations 3.1d and 3.6, we obtain the pressure dependence of resistance for SCLC non-linear process as follows;

$$R_{SL} = R_1 \left\{ \frac{L-d_0 [1-(\alpha P)^{\beta}]}{D+d_0[1-(\alpha P)^{\beta}]} \right\} \frac{d_0^{n+1}}{D^2} [1-(\alpha P)^{\beta}]^{n+1} \tag{3.7}$$

where, R_1 is taken as constant since it involves parameters which are independent of P or d. Sensitivity factor (S=Ro/R) is ratio of original resistance of composites (R_o) at dead weight (called zero weight) to resistance (R) after applying mechanical pressure. The sensitivity factor is derived from equation 3.7 and other equations as given below,

$$S = \frac{R_{0(SL)}}{R_{P(SL)}} = \frac{(L - d_0)\, d_0^{n+1}}{(D + d_0)\, D^2} \quad \frac{\left[D + d_0 \left\{1 - (\alpha P)^{\beta}\right\}\right] D^2}{\left[L - d_0 \left\{1 - (\alpha P)^{\beta}\right\}\right] d_0^{n+1} \left\{1 - (\alpha P)^{\beta}\right\}^{n+1}}$$

or,

$$= \frac{(L - d_0)}{(D + d_0)} \quad \frac{\left[D + d_0 - d_0 (\alpha P)^{\beta}\right]}{\left[L - d_0 + d_0 (\alpha P)^{\beta}\right] \left\{1 - (\alpha P)^{\beta}\right\}^{n+1}}$$

or,

$$= \frac{(L - d_0)}{(D + d_0)} \quad \frac{(D + d_0)\left[1 - \frac{d_0(\alpha P)^{\beta}}{(D + d_0)}\right]}{(L - d_0)\left[1 + \frac{d_0(\alpha P)^{\beta}}{(L - d_0)}\right]\left\{1 - (\alpha P)^{\beta}\right\}^{n+1}}$$

$$S = \frac{1 - \left(\frac{d_0}{D + d_0}\right)(\alpha P)^{\beta}}{1 + \left(\frac{d_0}{L - d_0}\right)(\alpha P)^{\beta}} \quad \frac{1}{[1 - (\alpha P)^{\beta}]^{n+1}} \qquad (3.8)$$

Hence, $\mathbf{S = f (D, d_0 , L , P , \alpha , n , \beta)}$

The ratio of resistance, the most important parameter for the piezo-sensitivity can then be predicted by equation 3.8. By analyzing this equation, the influence of applied load (P), matrix compressibility (α), conducting particle diameter (D), particle separation distance (d_0) or volume fraction, conduction process (n), film thickness (L), and non linear function of mechanical property (β) on the piezo-sensitivity (S) can also be interpreted quantitatively.

Piezo-sensitivity factor calculated for the above cases depends on number of effective metal-insulator-metal junction, which are available in a given composite. In conducting polymer composite, it is well known that, the electrical conductivity goes through sharp transition from almost insulating state to semi-conducting state at a critical concentration of an additive (percolation threshold) due to the formation of conducting network

(see Fig. 3.2). This implies that the number of available M-P-M junctions for pressure dependence changes with the concentration of the conducting particles and their distribution in the insulating matrix. After percolation threshold, the number of effective junctions (N_{eff}) will decrease with increase of concentration of conducting particles because the M-P-M junctions will get short circuited by particle- to-particle contacts.

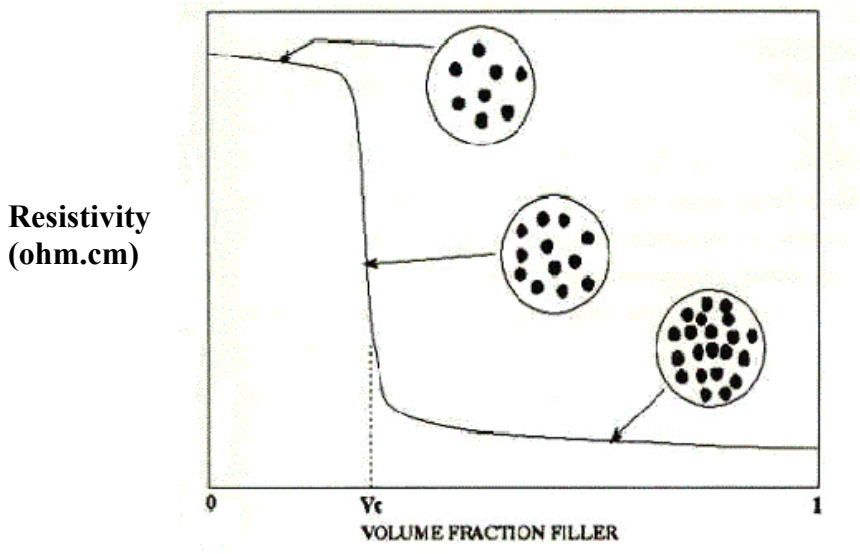

Figure-3.2. A schematic graph of resistivity vs. filler concentration

Hence, the piezo-sensitivity factor will depend on N_{eff} (number of effective junctions);

$$N_{eff} = [Ns \times Np \times f(\varphi)] \qquad (3.9)$$

Where, $f(\varphi)$ being a function (polynomial) of volume fraction(φ) of conducting phase. The net piezo-sensitivity factor will be then given as,

$$S_t = N_{eff} \times S = Ns \times Np \times S \times f(\varphi) \qquad (3.10)$$

The above equation for the piezo-sensitivity shows that the conducting polymer composites have highly non-linear pressure dependence of an electrical resistance and also the sensitivity has strong dependency on the composition.

Similar equations were derived in the other cases of non-linear charge transport viz. Fowler Nordheim tunneling of charge across the barrier at the inter-granular spaces. The final equation for (TN) is represented below. In case of Fowler-Nordheim tunneling (TN), the sample resistance (R_{TN}) is given by [4];

$$R_{TN} = \frac{(L-d)\Delta d^2}{V_X D^2 (D+d)} e^{\left|\frac{\Delta^{3/2} d(L-d)}{V_X (D+d)}\right|} \qquad (3.11)$$

Δ is the potential barrier height adjacent particles in composites. The sensitivity factor (S_{TN}) derived from above equation for tunneling is then,

$$S = \frac{R_{0(TN)}}{R_{P(TN)}}$$

$$= \frac{(L-d_0)\, d_0^2 (D+d)}{d^2 (D+d_0)(L-d)} e^{\left|\frac{\Delta^{3/2}}{V_x}\left[\frac{d_0(L-d_0)}{(D+d_0)} - \frac{d_0\{1-(\alpha P)^\beta\}\left[L-d_0\{1-(\alpha P)^\beta\}\right]}{\left[D+d_0\{1-(\alpha P)^\beta\}\right]}\right]\right|} \quad \text{or,}$$

$$= \frac{\left[1-\frac{d_0(\alpha P)^\beta}{(D+d_0)}\right]}{\left[1+\frac{d_0(\alpha P)^\beta}{(L-d_0)}\right]\left[1-(\alpha P)^\beta\right]^2} e^{\left|\frac{\Delta^{3/2}}{V_x}\left[\frac{d_0(L-d_0)}{(D+d_0)} - \frac{d_0\{1-(\alpha P)^\beta\}\left[L-d_0\{1-(\alpha P)^\beta\}\right]}{\left[D+d_0\{1-(\alpha P)^\beta\}\right]}\right]\right|} \quad \text{or,}$$

$$= \frac{\left[1-\frac{d_0(\alpha P)^\beta}{(D+d_0)}\right]}{\left[1+\frac{d_0(\alpha P)^\beta}{(L-d_0)}\right]\left[1-(\alpha P)^\beta\right]^2} e^{\left|\frac{\Delta^{3/2}}{V_x}\left[\frac{(L-d_0)}{\left(\frac{D}{d_0}+1\right)} - \frac{(L-d_0)\left\{1+\frac{d_0(\alpha P)^\beta}{(L-d_0)}\right\}}{1+\frac{D}{d_0\{1-(\alpha P)^\beta\}}}\right]\right|} \quad \text{or,}$$

or,
$$= \frac{\left\{D + d_0 - d_0(\alpha P)^{\beta}\right\}}{\left[1 + \frac{d_0(\alpha P)^{\beta}}{(L - d_0)}\right]\left[1 - (\alpha P)^{\beta}\right]^2} e^{\left|\frac{\Delta^{3/2}}{V_x}\left[\frac{(L-d_0)}{\left(\frac{D}{d_0}+1\right)} - \frac{(L-d_0)\left\{1+\frac{d_0(\alpha P)^{\beta}}{(L-d_0)}\right\}d_0\left\{1-(\alpha P)^{\beta}\right\}}{\left\{D+d_0-d_0(\alpha P)^{\beta}\right\}}\right]\right|}$$

$$S = \frac{B}{A\left[1 - (\alpha P)^{\beta}\right]^2} e^{\left|\frac{\Delta^{3/2}\, d_0(L-d_0)}{V_x}\left[\frac{1}{(D+d_0)} - \frac{A\left\{1-(\alpha P)^{\beta}\right\}}{B}\right]\right|} \qquad (3.12)$$

Hence, **$S = f(D, d_0, L, P, \alpha, \beta)$**

Zhang et al. [2] also found similar type of functional dependency in tunneling conduction process, where, A and B are representing as,

$$A = \left[1 + \frac{d_0(\alpha P)^{\beta}}{(L - d_0)}\right] \qquad B = \left\{D + d_0 - d_0(\alpha P)^{\beta}\right\}$$

Therefore,

$$S_{t\,(TN)} = N_{eff} \times S = Ns \times Np \times S \times f(\varphi) \qquad (3.13)$$

In case of Schottky emission (SE), the sample resistance (R_{SE}) is given by [10];

$$R_{SE} = \frac{V_X}{(L - d)DAT^2}\left(1 + \frac{d}{D}\right) e^{\frac{\Delta}{KT}} e^{-\left|\frac{\beta_{SE}\, V_x^{1/2}(D+d)^{1/2}}{d^{1/2}\, KT(L-d)^{1/2}}\right|} \qquad (3.14)$$

Where, T is the temperature at which measurement has been done, the sensitivity factor (S_{SE}) is derived from above equations,

$$S = \frac{R_{0(SE)}}{R_{P(SE)}} = \frac{\dfrac{V_X}{(L-d_0)DAT^2}\left(1+\dfrac{d_0}{D}\right)\ e^{\frac{\Delta}{KT}}\ e^{-\left|\frac{\beta_{SE}\ V_x^{1/2}(D+d_0)^{1/2}}{d_0^{1/2}\ KT(L-d_0)^{1/2}}\right|}}{\dfrac{V_X}{(L-d)DAT^2}\left(1+\dfrac{d}{D}\right)\ e^{\frac{\Delta}{KT}}\ e^{-\left|\frac{\beta_{SE}\ V_x^{1/2}(D+d)^{1/2}}{d^{1/2}\ KT(L-d)^{1/2}}\right|}}$$

or,
$$= \frac{(L-d)\left(1+\dfrac{d_0}{D}\right)}{(L-d_0)\left(1+\dfrac{d}{D}\right)} \frac{e^{-\left|\frac{\beta_{SE}\ V_x^{1/2}(D+d_0)^{1/2}}{d_0^{1/2}\ KT(L-d_0)^{1/2}}\right|}}{e^{-\left|\frac{\beta_{SE}\ V_x^{1/2}(D+d)^{1/2}}{d^{1/2}\ KT(L-d)^{1/2}}\right|}}$$

or,
$$= \frac{(L-d)\left(1+\dfrac{d_0}{D}\right)}{(L-d_0)\left(1+\dfrac{d}{D}\right)} e^{\left|\frac{\beta_{SE}\ V_x^{1/2}\left[D+d_0-d_0(\alpha P)^{\beta}\right]^{1/2}}{KT\left[d_0^{1/2}-d_0^{1/2}(\alpha P)^{\beta}\left\{L-d_0+d_0(\alpha P)^{\beta}\right\}^{1/2}\right]} - \frac{\beta_{SE}\ V_x^{1/2}(D+d_0)^{1/2}}{KT\ d_0^{1/2}(L-d_0)^{1/2}}\right|}$$

or,
$$= \frac{(D+d_0)(L-d_0)}{(D+d_0)(L-d_0)} \frac{\left[1+\dfrac{d_0(\alpha P)^{\beta}}{(L-d_0)}\right]}{\left[1-\dfrac{d_0(\alpha P)^{\beta}}{(D+d_0)}\right]} e^{\left|\frac{\beta_{SE}\ V_x^{1/2}\left[D+d_0-d_0(\alpha P)^{\beta}\right]^{1/2}}{KT\left[d_0^{1/2}-d_0^{1/2}(\alpha P)^{\beta}\left\{L-d_0+d_0(\alpha P)^{\beta}\right\}^{1/2}\right]} - \frac{\beta_{SE}\ V_x^{1/2}(D+d_0)^{1/2}}{KT\ d_0^{1/2}(L-d_0)^{1/2}}\right|}$$

or,
$$= \frac{\left[1+\dfrac{d_0(\alpha P)^{\beta}}{(L-d_0)}\right]}{\left[1-\dfrac{d_0(\alpha P)^{\beta}}{(D+d_0)}\right]} e^{\left|\frac{\beta_{SE}\ V_x^{1/2}(D+d_0)^2\left[1-\frac{d_0(\alpha P)^{\beta}}{(D+d_0)}\right]^{1/2}}{KT\left[d_0^{1/2}\left\{1-(\alpha P)^{\beta}\right\}(L-d_0)^2\left\{1+\frac{d_0(\alpha P)^{\beta}}{(L-d_0)}\right\}^{1/2}\right]} - \frac{\beta_{SE}\ V_x^{1/2}(D+d_0)^{1/2}}{KT\ d_0^{1/2}(L-d_0)^{1/2}}\right|}$$

or,
$$= \frac{\left[1+\frac{d_0(\alpha P)^{\beta}}{(L-d_0)}\right]}{\left[1-\frac{d_0(\alpha P)^{\beta}}{(D+d_0)}\right]} e^{\left|\frac{\beta_{SE}\, V_x^{1/2}(D+d_0)^{1/2}}{KTd_0^{1/2}(L-d_0)^{1/2}}\left[\frac{\left\{1-\frac{d_0(\alpha P)^{\beta}}{(D+d_0)}\right\}^{1/2}(D+d_0)^{3/2}}{\left\{1+\frac{d_0(\alpha P)^{\beta}}{(L-d_0)}\right\}^{1/2}(L-d_0)^{3/2}}-1\right]\right|}$$

$$S = \frac{A_1}{B_1} e^{\left|\frac{\beta_{SE}\, V_x^{1/2}(D+d_0)^{1/2}}{KTd_0^{1/2}(L-d_0)^{1/2}}\left[\frac{B_1^{1/2}(D+d_0)^{3/2}}{A_1^{1/2}(L-d_0)^{3/2}}-1\right]\right|} \qquad (3.15)$$

Hence, $\mathbf{S = f\,(D,\, d_0\,,\, L\,,\, P\,,\, \alpha\,,\, \beta\,,\, \beta_{SE})}$

Where,

$$A = \left[1+\frac{d_0(\alpha P)^{\beta}}{(L-d_0)}\right] \qquad B_1 = \left[1-\frac{d_0(\alpha P)^{\beta}}{(D+d_0)}\right]$$

Therefore,

$$S_{t\,(SE)} = N_{eff} \times S = Ns \times Np \times S \times f(\varphi) \qquad (3.16)$$

The coefficient of piezo-resistance or Gauge factor is given by [17] ;

$$G = (Ro - R) / R\epsilon$$

$$= (S_t - 1) / (\alpha P)^{\beta} \qquad (3.17)$$

where G is the Gauge factor, S is the sensitivity factor defined by Ro/R, ϵ is strain, and R is the measured resistance at applied stress (σ), S is the sensitivity factor and Ro is the resistance at zero weight.

3.1.4. *Discussions*

In the present studies, the sensitivity factor was evaluated as a function of one parameter at a time while holding other parameters fixed at their base line (original) values. The sensitivity factor (S_t) was evaluated from equation (3.10, 3.13 & 3.16 for SCLC, TN and

SE respectively) using typical values of various parameters: L = 470 μm, n = 2, P = 100 gm/cm^2, D = 10 μm, d_0 = 4.14 μm, β = 0.12, β_{SE} = 0.4, kT = 0.025 e.v (room temperature) and V_X = 1 Volt.

$E_m = (1/\alpha)$ = 30 MPa for matrix polymer without any conducting particles. Different values of modulus (E) were calculated for different conducting particles loading by using parallel model for the total modulus of the composites and which is given as [18],

$$\alpha = 1/E = \Phi_m / E_m + \Phi_c / E_c \qquad (3.18)$$

where, E is the Young modulus of resulting composite, Φ_m and Φ_c are the volume fractions of an insulating matrix and conducting particles, respectively. E_m and E_c are the Young modulus of insulating elastomer matrix and conducting polymer, respectively [19]. Values were derived from equations 3.10, 3.13 and 3.16 by putting above values and are listed in table 3.1.

Table 3.1: Calculated values of piezo-sensitivity (S) (normalized, normalization has been done by taking ratio of particular value to least value) types of conduction processes at room temperature with thermo- plastic elastomer as the matrix.

Different non-linear conduction process	Value of Piezo-sensitivity (S) (Relative)
Space charge Limited conduction (SCLC)	6
Fowler-Nordhein tunneling (TN)	2
Schottky emission (SE)	1

It is obvious that the piezo-sensitivity is highest when SCLC is present. Resistance is related to the power of an interparticle distance (d^{n+1}). Since, slope of R vs d is higher for

SCLC due to high n value, piezo-sensitivity is more for SCLC than other conduction process like TN and SE. Hence further calculations were restricted to the SCLC case only.

The set of d_0 values were calculated by using equation 3.2 with particle size (D) 10 μm for one system and 2 μm for another system, which are more realistic. The sensitivity factor (S_t) was evaluated from equation 3.10 using the $\beta = 0.12$ for D = 10 μm system and $\beta = 0.2$ for D = 2 μm system. The polynomial is $f(\varphi) = 1 - z_1(\varphi) + z_2(\varphi^2) - z_3(\varphi^3) + z_4(\varphi^4) -$ --------- $(-1)^n z_n(\varphi^n)$. In our case, $Z_1 = 15$, $Z_2 = 95$, $Z_3 = 120$ are constant and also depends upon nature of composite systems.

Case I

Figs. 3.3 and 3.4 depict the variation of piezo-sensitivity with change in composition and modulus for the two systems studied. It is quite evident from these figures that there

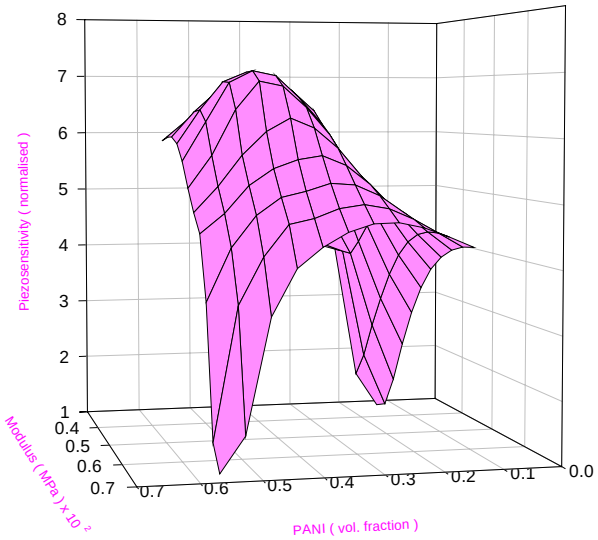

Figure-3.3. Variation of piezo-sensitivity vs concentration of conducting particles (D=10 μm). The sensitivity factor estimated from equation 3.10 with the values of the parameters .

is a similarity in the nature of the graphs, which clearly bring out the fact that there is an optimum composition of the conducting polymer blend at which the piezo-sensitivity is maximum.

The piezo-sensitivity equation is,

$$S = \frac{1 - \left(\frac{d_0}{D + d_0}\right)(\alpha P)^{\beta}}{1 + \left(\frac{d_0}{L - d_0}\right)(\alpha P)^{\beta}} \quad \frac{1}{[1 - (\alpha P)^{\beta}]^{n+1}}$$

Above equation composed of two terms where, 2nd term contains α, which is decreasing with filler loading. At constant applied pressure, S always diminished with high filler

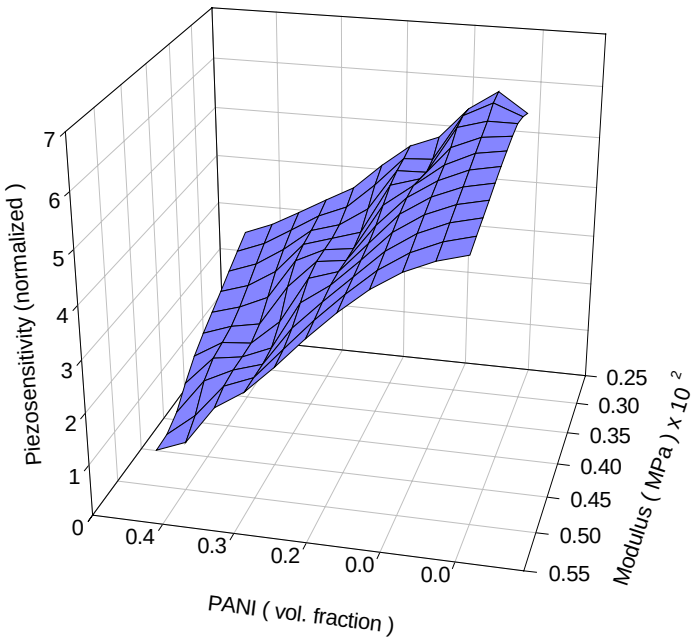

Figure-3.4. Variation of piezo-sensitivity vs concentration of PANI particles (D=2 µm). The sensitivity factor estimated from equation 3.10 with the values of the parameters

loading 1st term contains d_0, which keeps changing with conducting particle loading (equation 3.2). L is very much higher than d_0 where as D is comparable with d_0. So, piezo-sensitivity increases with decreasing d_0 (increasing particle loading). Since both are opposite trends and shows maxima at certain composition. These two figures showed the different due to different D value (conducting polymer particle size) but they are similar in one point, there is an optimum composition where piezo-sensitivity is maximum. Fig. 3.3 shows maximum near about 10 % particle loading where as Fig. 3.4 shows near about 2 % particle loading. This arises due to shifts of percolation threshold concentration, which is mainly controlled by particle size. Piezo-sensitivity decreases with increasing net modulus of the composites. Modulus of the composites increases with increasing loading of particle (equation 3.18) .The peak in the piezo-sensitivity in both cases is seen at the composition where the critical value of inter-domain distance changes with conducting particle loading (equation 3.2) occurs at which the non-linear conduction becomes predominant. Xiao et al [2] also studied two different types of polymers with same conducting particle and he observed resistance change was higher in lower modulus matrix than higher modulus matrix, which is same in Fig. 3.3 & 3.4.

Case-II

In continuation of the theoretical estimation, the piezo-sensitivity was evaluated as a function of the non-linearity term as defined by the exponent terms β and n for mechanical and electrical response. Fig. 3.5 depicts the variation of piezo-sensitivity with respect to concentration of conducting particles and different values of β while the Fig. 3.6 gives similar estimates for different values of n. It again becomes evident that the

piezo-sensitivity of these conducting polymer blends is higher when the non-linearity factors increase. It is interesting to note that there is very little piezo-sensitivity for n = 0 i.e. when the conduction process is ohmic. On the other hand, for n = 2 or higher, i.e. for SCLC type conduction, there is much higher piezo-sensitivity expected from the theory. Further, the compositional dependence of the piezo-sensitivity also becomes more pronounced when there is non-linear conduction process as well as non-linear mechanical response.

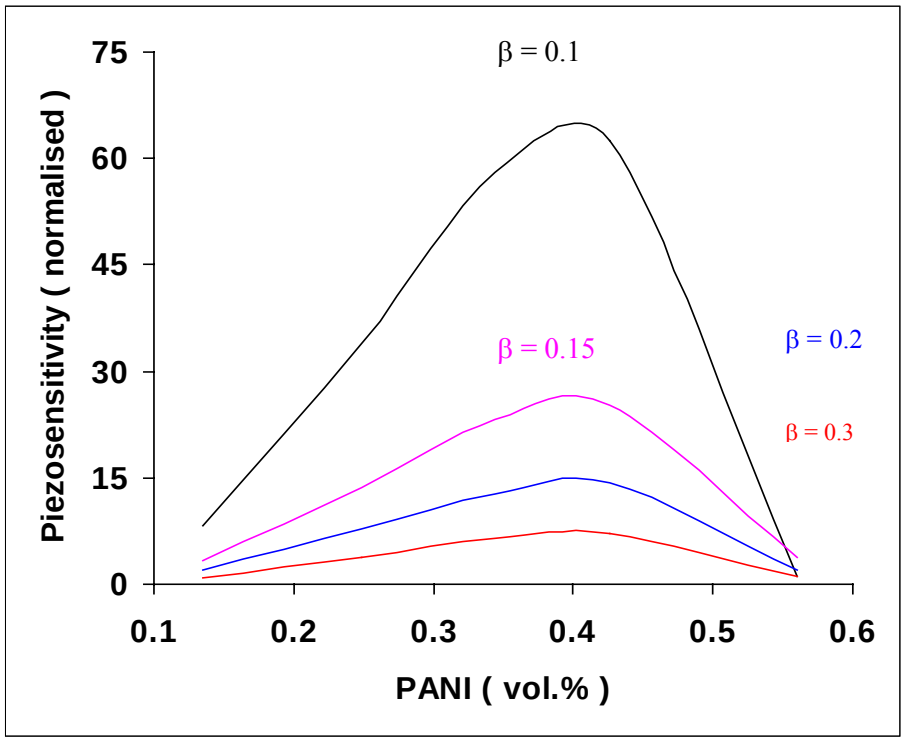

Figure-3.5. The effect of non-linear mechanical response (exponent β) on the piezo-sensitivity of conducting polymer (PANI) blend (D =10 μm)

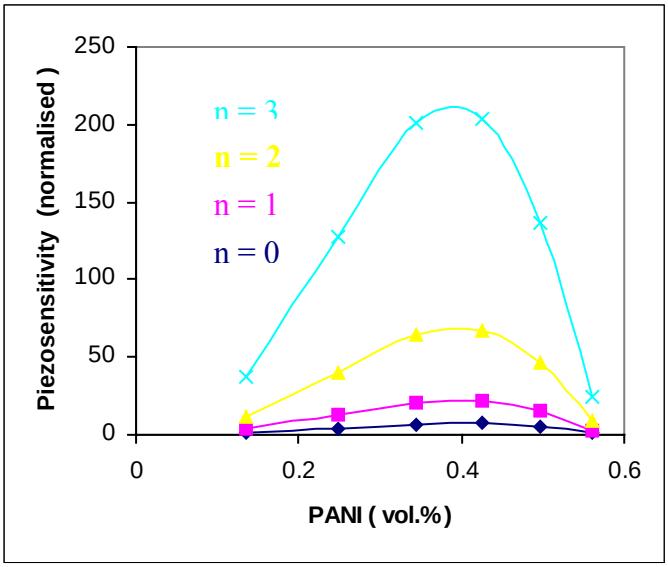

Figure-3.6. Effect of non-linear conduction process (exponent n) on the piezo-sensitivity of conducting polymer blends containing PANI particle (D=10 µm)

Case-III

It is interesting to observe that the presence of non-linear processes also affects the piezo-sensitivity of the conducting polymer blend in other ways, e.g, the piezo-sensitivity depends on the applied pressure for such cases as shown in Fig. 3.7. It can be noted that with the increase of pressure not only the compositional dependency of the sensitivity increases but also the peak in piezo-sensitivity shifts towards the lower concentration of conducting polymer in the blend. If a load is applied to the sample, the resistance will be altered due to a change in interparticle separation, which is caused by the difference in compressibility between filler particles and the matrix. As a result, the electrical conduction through the conducting paths becomes easier under stress. Thus, increase of piezo-sensitivity is attained at the cost of large variations with composition.

Radhakrishnan et al [9] also found same observation in conducting polymer composites. It is evident that the pressure of highly non-linear conduction process present at the interparticulate region can lead to high sensitivity in the piezo-sensitivity effect for conducting polymeric composites. That's why all these phenomena are related to the

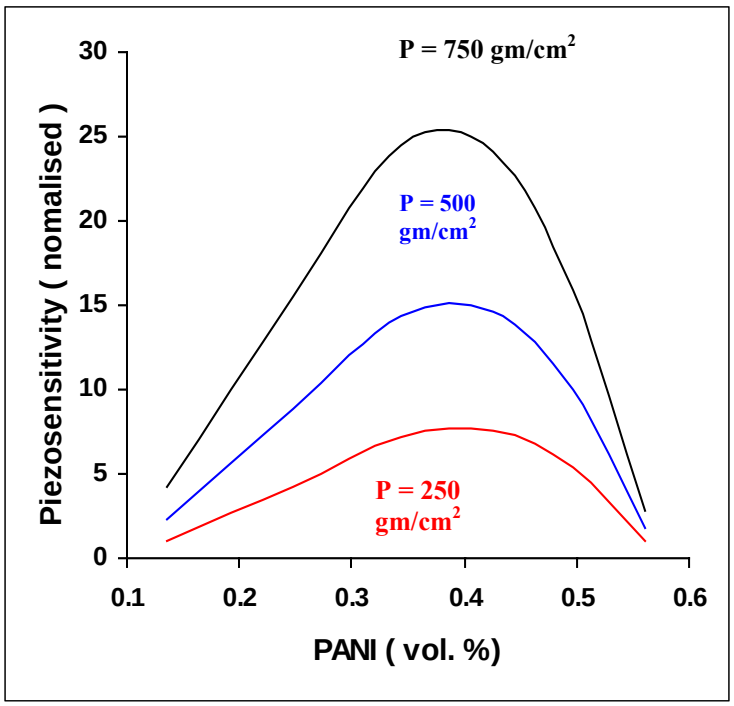

Figure-3.7. Effect of applied pressure on the piezo-sensitivity of conducting polymer blend containing PANI particle (D =10 μm) in presence of non-linear conduction process SCLC.

inter-domain junctions and the strong variation of current with voltage/inter-domain distance 'd' can be seen from Figs. 3.3 & 3.4. These figures also indicate that the phenomenological model based on the non-linear effects gives better understanding of the processes responsible for the observed behaviour for piezo-response of the conducting polymer blends / composites . Of course the exact value of the piezo-

sensitivity has not been evaluated and this is also very difficult to carry out keeping in view the differences in the various assumptions made in the theory and the actual experimentation especially as regards the uniformity of dispersion, effect of plasticizing effect of the dopant, exact change of modulus with composition, etc. None the less, a good insight can be obtained with the help of the phenomenological model as regards the overall behaviour. Thus, the non-linear effects can be the main cause of such behaviour in piezo-response of conducting polymer blends or composites.

3.2. Conclusions

The conducting polymer blends exhibit piezo-sensitivity, which is found to be dependent on composition, type of the matrix used, applied pressure, etc. A phenomenological model has been developed which takes into account the non-linear conduction processes as well as the non-linear variations of mechanical response. This theoretical model is able to explain many aspects of the piezo-sensitivity of these blends or composites. It may be of interest to mention here that some authors have recently [20] found that polyisoprene-carbon black nano-composites exhibit non-linear response of electrical resistance with tensile strain/pressure and their results can also be explained by non-linear conduction processes. The theory presented by us in the current chapter is a generalized approach taking all types of conduction processes and considers also the non-linear mechanical behaviour. Thus, the role of non-linear processes in piezo-resistivity of conducting polymers has been brought out clearly by us in the above model.

3.3. References

1. F.Carmona, R.Canet, P.Delhaes, J.Appl.Phys., **61**,1987,2550.

2. X.Zhang, Y.Pan, Q.Zheng, X.Yi, J.Polymer Sci., Part B: Polymer Phys., **38**,2000,2739.

3. S.Radhakrishnan, D.R.Saini, Polymer Int., **34**,1994,111.

4. S.Radhakrishnan, Polymer Comm., **26**,1985,153.

5. M.Knite, V.Teteris, A.Kiploka, J.Kaupuzs, Sensors and Actuators, A: Physical, **110**,2004,142.

6. X.W.Zhang, Y.Pan, Q.Zheng, X.Yi, Polymer Int., **50**,2001,229.

7. Z.X.Bao, F.Colon, N.J.Pinto, C.X.Liu, Synth.Met., **94**,1998,211.

8. V.Skalova, P.Fedorko, D.Vegh, A.Chyla, S.Ryley, D.Walton, Synth.Met., **101**,1998,399.

9. S.Radhakrishnan, S.Chakne, P.N.Shelke, Materials letters**, 18**,1994,358.

10. S.Radhakrishnan, J.Mater.Sci.Lett.**, 6**,1987,145.

11. D.A.Seanor, Electrical Properties of Polymers, Academic Press, New York, 1982, Ch-1.

12. E.A.Meinecke, R.C.Clark, Mechanical Properties of Polymeric Foams, Technomic Publication, West Port, U.S.A, 1973, p-16.

13. A.I.Medalia, Rubber Chem.Technol., **59**,1986,432.

14. I.M.Ward, Mechanical Properties of Solid Polymers, John Wiley & Sons Ltd., New York, 1983, p-37.

15. H.S.Katz, J.V.Milewski, Handbook of Fillers and Reinforcements for Plastics, Von Nostrand Reinhold Company, New York, 1978, p-34.

16. L.H.Sperling, Introduction to Physical Polymer Science, John Wiley & Sons Ltd., New York, 1992, Ch-11.

17. L.I.Maissel, R.Glang, Handbook of Thin Film Technology, International Business Machines Corporation Components Division, Hopewell Junction, New York, 1970, Ch-15.

18. L.E.Nielsen, Mechanical Properties of Polymers and Composites II, New York, Marcel Dekker, 1974, p–34.

19. P.C.Rodrigous, G.P.de Souza, J.D.Da Motta Neto, L.Akcelrud, Polymer, **43**,2002,5493.

20. M.Knite, V.Teteris, A.Kiploka, J.Kaupuzs, Sensors and Actuators, A: Physical, (in press)

Section II: Actuator

3.4. Introduction

In order to understand the performance limits as well as to predict their response for design purpose, it is important to have mathematical models that describe actuator behaviour. These provided a physical insight into mechanism of electromechanical response of these materials. Modeling is considered as an effective approach in investigating the significance of design parameters.

The conducting polymer (C.P) system can be modeled according to two substantially different approaches: a continuum physical model and a discrete phenomenological model and it can be instrumental for the implementation of control and driving methods for a CP actuating device.

We can be built up a model starting from the Biot poro-elastic theory and its application to polyelectrolyte gels [1], it has been applied also to our system. The C.P system is modeled as a biphasic system. The first phase is the polymeric matrix, which is elastic and porous (at least 10 % porosity). The second phase is the electrolyte fluid, completely filling the pores. A review of the literature [2-4] shows that several models have been proposed to explain the actuation behaviour of PPy in various oxidation states.

A novel method, in which the bending beam method (BBM) was introduced by O. Inganas et al.[5] to measure bending angle in an electro-active polymer, polypyrrole (PPy). Volume changes in PPy are studied by observing the bending behaviour of a bi-layer laminate strip, made of a PPy layer and a polyethylene layer, during electrochemical redox of the PPy. One of the first models proposed in this field was the theory of

bi-layer strip model by Q. Pei et al. [6]. They assume bi-layer strip made of PPy layer and polyethylene layer bound together responds by bending and volume changes in the PPy layer during its electrochemical doping and un-doping. They gave a correlation between the local linear strain and the curvature change of the strip. Mathematical models of the cation insertion, salt draining, and bending behaviour are given. An attempt was made to develop a theoretical model able to predict experimental results by Otero et al. [7]. A double layer will be considered: an electro-active homogeneous and electro elastic film of a poly-conjugated material stuck to a non-electroactive, and flexible film. He assumed volume change due to solvated counter ions and charged polymer–charged polymer, charged polymer-anion, anion-anion, polymer-solvent and anion–solvent interaction. The relative increase or decrease of length of actuator is proportional to the electrical charge consumed during the concomitant oxidation or reduction process. The self–induced bending of a bi-layer strip, the so-called bending beam method (or bending cantilever, or bending strip method, depending on the geometry and positioning of the strip), like a bimetal, has been shown to be a simple yet sensitive method for the study of small volume change in one of the layer by S. Timoshenko et al. [8]. In an effort by J. D.W. Madden et al. [9] to provide a model of a full description of the relationship between load, displacement, voltage and current of an actuator system. Stress-strain tests are performed at constant applied potential to determine PPy stiffness. The relationship between strain and charge was investigated, showing that strain is directly proportional to charge via the strain to charge density ratio. D.De Rossi et al.[10] proposed two different approaches to the electro - mechanical modeling to the conducting polymer electrolyte system and

discussed about foreseen improvements in the implementation of actuating structures. T. A. Betts et al.[11] propose a bi-layer strip model for chemical sensor, where a thin layer of polymer coating was applied in one side of the cantilever. Sensitivity was measured by measuring bending of cantilever beam, and it depends upon film thickness.

The common mechanisms behind these applications are doping and /or un-doping, charge compensation, and associated conformation change (or phase transition) in the conjugated polymer phase. Models of actuator response were developed [12, 13]. Some workers reported model for designing conducting polymer actuators [6, 14-17]. However, these did not throw any light on how bending of actuator depends on mechanical property of backing layer which supported the active conducting polymer.

The goal of our investigation is to establish a phenomenological model, which relates the bending angle of actuator with the backing layer modulus and thickness together with the conducting polymer modulus and thickness. This can lead to optimization of the design of these actuators to produce large force. Such optimal design is essential to produce practically viable artificial muscle.

3.4.1. *Background*

There are various observations made in the earlier reports on actuation of conducting polymer actuators. Magnitude of actuation was dependent on mechanical properties of polymer. Polymer expansion is mainly associated with ion insertion. The magnitude of strain depends upon modulus of individual layer of bi-layer strip. The magnitude of strain depends upon thickness of individual layer of bi-layer strip. The magnitude of strain

depends upon dimension of bi-layer strip. Thus, it is essential to take into account all these factors in developing any model for explaining the actuation in conducting polymer.

3.4.2. *Assumptions*

1. Conducting polymer is porous, allowing easy diffusion of ions and small molecules with in it.
2. The plane surface cross section remains plane on macroscopic scale.
3. Both conducting polymer and backing layer are isotropic and elastic. The strain in the C.P layer is homogenous along planes parallel to the interlayer junction.
4. The change in Young's modulus of the conducting polymer layer is negligible during the doping/un-doping process.
5. The bending force which arises from the ion insertion is uniformly exerted along length of the film.
6. Force (h.ρ.g) due to water is negligible, where h is height of water on top of the film, ρ is density of liquid and g is gravity.

3.4.3. *Theory*

The phenomenological model representing the actuation of conducting polymer, which considered mechanical properties of polymer is described as follows. The challenges are now to represent the phenomena mathematically. The equations representing the bending of bi-layer beam actuator are now derived. The model names stems from the assumption that volume change of one layer have to accommodated by other layer which is chemically inert, behaves like support materials.

The construction and positioning of a bi-layer actuator made up by one layer was conducting polymer and other was any non-reactive and non-conducting polymer which was called backing layer. Conductive polymer is generally deposited by electrochemical method on metallized flexible polymer films as substrates. Conducting polymer film is stimulated by electrochemical technique using appropriate dopant electrolyte. The configuration to be modeled is shown in Fig. 3.8. A strip of polymer has a length *L*, a width b and d_1 & d_2 be the thickness of two layer in bi-layer strip, in contact with an electrolyte over a surface area A = *L*.b, and one end is strongly hold & another free. It is assumed that *L* >> b.

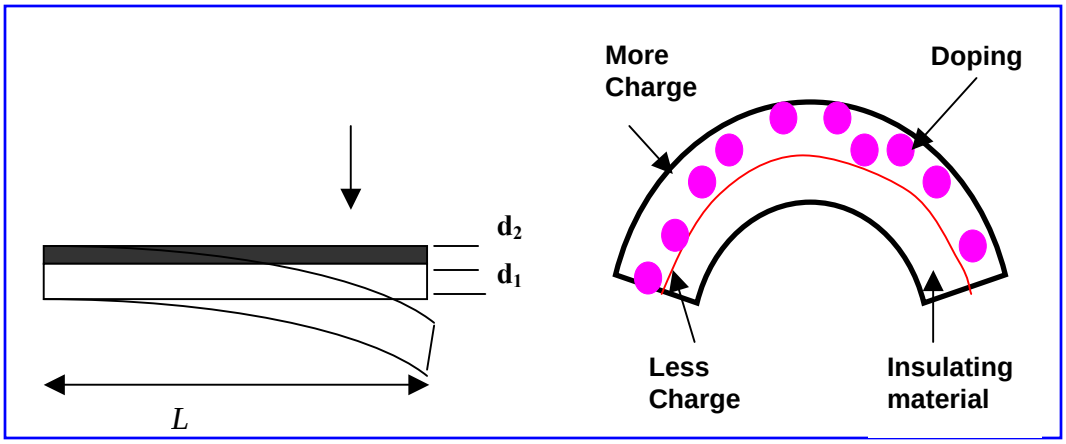

Figure-3.8. Schematic diagram of bi-layer actuator bending

The bi-layer strip is then considered as a cantilever comprising of two materials with different modulus and thickness values E_1, d_1 and E_2, d_2, respectively. The bending force is given by ;

$$F = \int_o^{d2} \alpha .dy + \int_o^{\infty} i.dt \qquad (3.19)$$

For constant applied potential the total charge (q = i.t) i.e. the second term becomes constant and hence it is not considered in the following formulation.

For uniform volume change perpendicular to the cross section of bi-layer equation 3.19 turns to

$$\text{Therefore,} \qquad F = \alpha\, d_2 \quad \text{or, } W = Z\, d_2$$

Where, α is the lateral linear strain perpendicular of the cross section from backing side, Z is constant and F and W are numerically same.

The constituent basic equations, which are useful for correlating the various parameters, are discussed below [18-20].

Suppose bi-layer actuator is a cantilever with a uniformly distributed load (force arises due to all cumulative factors in time of actuation) on it.

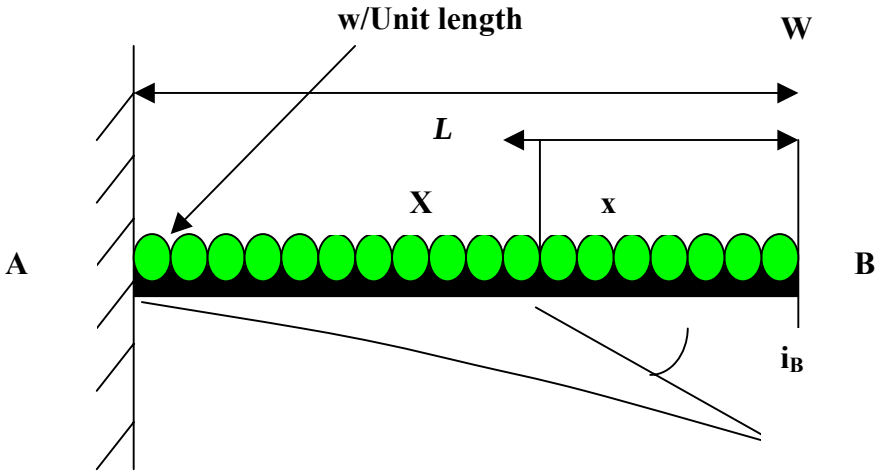

Figure-3.9. A beam with uniformly distributed load

Consider a cantilever AB of length *L*, and carrying distributed load of w per unit length as shown in Fig. 3.9. Consider a section X, at a distance x from the free end B.

The bending angle ($i_B = \theta$) of cantilever due to load (W) is given by ;

$$\theta = W L^2 / 6E I \quad (3.20)$$

Where, I is the moment of inertia, E is the modulus of beam,

Moment of inertia of any rectangular beam expressed as,

$$I = m (L^2 + b^2)/12 \quad (3.21)$$

Where, b is width of the bi-layer, m is the mass of film.

Substituting the value of I in equation 3.20 we get,

$$\theta = \frac{2WL^2}{E\, m\left(L^2 + b^2\right)} \quad (3.22)$$

Mass of the beam is

$$m = \{\rho L\, b\, (d_1+d_2)\} \quad (3.23)$$

Where, ρ is the density, $d_1$and d_2 are thickness of backing layer and conducting polymer respectively,

Combining equations 3.22 & 3.23 we get,

$$\theta = \frac{2WL}{E\, \rho\, b\, (d_1 + d_2)\left(L^2 + b^2\right)} \quad (3.24)$$

E is the modulus of that film as a whole of the beam can be expressed in terms of series model [20] of modulus.

$$E = d_1E_1 + d_2 E_2 \quad (3.25)$$

Where, E_1 & E_2 are the modulus values of backing layer and conducting polymer, respectively. Which are considered as series to each to form the total system.

Combining equations 3.24 & 3.25 we get,

$$\text{or,} \quad \theta = \frac{2W}{\rho\, b\left(L^2 + b^2\right)\left(d^2{}_1 E_1 + d_1 d_2 E_2 + d_1 d_2 E_1 + d^2{}_2 E_2\right)} \tag{3.26}$$

$$\text{or,} \quad \theta = f\left(W, \quad , \rho, b, d_1, d_2, E_1, E_2\right)$$

Usually, in time of bending film moves upwards (against gravitation and water pressure). One part of the force (arises due to oxidation reaction of conducting polymer) would be spent to overcome gravitation and water pressure on top of the film. So effective force would be (W-p), where p is the combined force of gravitation and water pressure.

The relation between backing layer thickness (d_1) and bending angle (θ) when others parameters are held constant

$$\boldsymbol{\theta = (\, X\, d_2\,) / A + B d_1 + C d_1{}^2\,)} \tag{3.27}$$

Where, X = 2(W-p) L/ρ b (L^2+b^2) and A = $d^2{}_2$ E_2, B = (d_2E_1 + d_2 E_2), C = E_1 all are constant and values of constant could be calculated.

The relation between modulus of backing layer (E_1) and bending angle (θ) when conducting polymer thickness is same and others parameters are held constant

$$\boldsymbol{\theta = (\, X\, d_2\,) / (\, D + F\, E_1\,)} \tag{3.28}$$

Where, D = d_2 (d_1E_2 + d_2 E_2), F = ($d^2{}_1$+ d_1d_2)

The relation between the bending angle (θ) with conducting polymer layer thickness (d_2) with backing layer being same and when others parameters are held constant

$$\boldsymbol{\theta = (\, X\, d_2\,) / (G + H d_2 + I\, d_2{}^2\,)} \tag{3.29}$$

Where, G= $d^2{}_1$ E_1, H = (d_1E_1 + d_1 E_2), I = E_2

The relation between modulus of conducting polymer layer (E_2) and bending angle (θ) when backing layer is same and others parameters are held constant.

$$\theta = (X d_2) / (J + K E_2) \quad (3.30)$$

Where, $J = d_2 (d_1E_1 + d_2 E_1)$, $K = (d^2_1 + d_1d_2)$

The relation between the Bending angle with width of actuator, when others parameters are held constant.

$$\theta = M. L/b (L^2+b^2) \quad (3.31)$$

Where, $M = \dfrac{2W}{\rho\left(d^2_1E_1 + d_1d_2E_2 + d_1d_2E_1 + d^2_2E_2\right)}$

A-M is constants related to E_1, E_2, d_1 and d_2 and evaluated by using proper value of the same.

3.4.4. *Discussions*

In this study, in order to quantify the influence of the important model parameters, for every calculation, one parameter is changed from its baseline value (initial value) while the other parameters are held fixed at their base line values. The bending angle was estimated using the above equations for different conditions. The backing layer was considered as flexible elastomer or thermoplastic having lowest to highest modulus values 20–1500 MPa. The modulus of the conducting polymer was taken as 1500 MPa, which has been measured experimentally in our laboratory and as well as reported by D. De Rossi et al [10]. The thickness range of backing layer was varied from 0.025 mm. – 0.30 mm., and the thickness range of conducting polymer from 0.001 mm. - 0.15 mm. that are typical to experimentally possible and practically used.

The bending angle was estimated from the phenomenological model equations described above with respect to various important factors such as backing layer thickness, modulus of the backing layer polymer, thickness of the electroactive polymer, etc.

Case I

Equation 3.27 shows that the bending angle (θ) is inversely proportional to quadratic function of backing layer thickness (d_1) where as equation 3.28 shows bending angle is inversely proportional to linear function of modulus of backing layer. Fig 3.10 depicts the variation of bending angle (normalized) for different values of modulus of the backing layer polymer as its thickness is varied. Bending angle was estimated from the equation

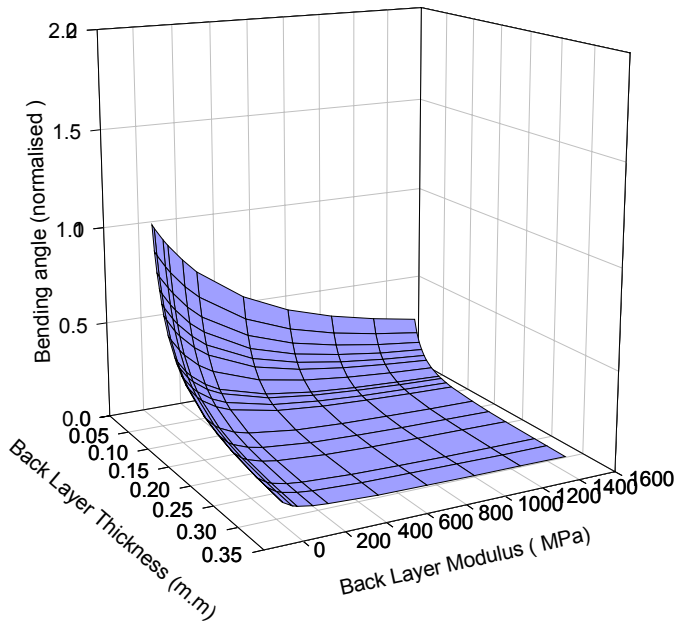

Figure-3.10. Variation of bending angle (normalized) vs modulus of backing layer and different thickness of the same

3.27. Fig. 3.10 depicts the variation of bending angle (normalized) for different values of modulus of the backing layer polymer as its thickness is varied. In this case the C.P

(PPy) was considered to be constant and kept at 10 μ m. It is evident that as the backing layer thickness is decreased the bending angle increases for any modulus value. Also, the bending angle decreases with increase of backing layer modulus. Due to quadratic function dependency of bending angle with thickness it changes with high slope, whereas with modulus lower slope due to linear dependency. Similar types of observations were observed by K. J. Kim et al.[17]. It is also interesting to note that the modulus of the backing layer plays vital role in obtaining good actuation. Back layer e.g. PET which has quite high modulus as compared to low modulus e.g. SBS or Hytrel shows least bending angle while the elastomers give very good actuation – bending angle increases to more than 90 degrees for some cases (backing layer thickness less than 20 μm).

Case-II

In order to study the effect of conducting polymer layer thickness on the actuation effect, the above equation 3.29 was used for estimation of the bending angle of the bi-layer having same backing layer thickness but different materials/or modulus values on which various thickness of conducting polymer (PPy) have been deposited.

In this configuration, the bending force would increase with the increase of conducting polymer layer thickness but only up to certain value since beyond the critical limit, there will be opposite force due to self-recovery. The backing layer will add to the recovery force and hence the bending angle will be maximum at certain thickness of the conducting polymer. These expectations are clearly reflected in the nature of the graph obtained from above calculations and depicted in Figs. 3.11 and 3.12.

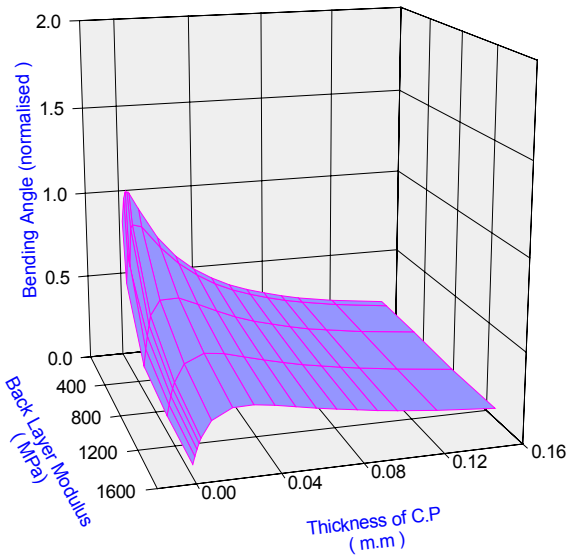

Figure-3.11. Variation of bending angle (normalized) vs modulus of backing layer and different conducting polymer thickness

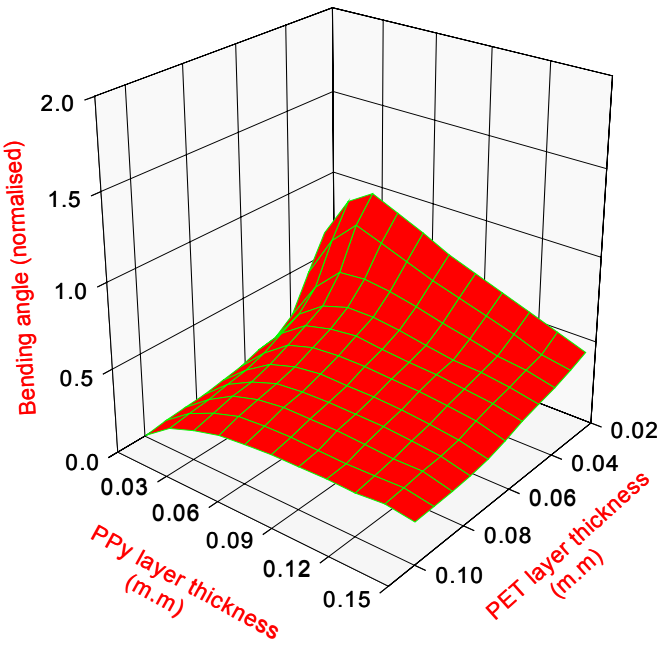

Figure-3.12. Variation of bending angle (normalized) vs thickness of backing layer and different conducting polymer thickness

Case-III

Equation 3.30 shows that bending angle varies with conducting polymer modulus with linear function. Figs. 3.13 & 3.14 depicts variation of bending angle with modulus and thickness of conducting polymer layer and backing layer, respectively. Bending angle always decreases with modulus of C.P for any thickness of the same.

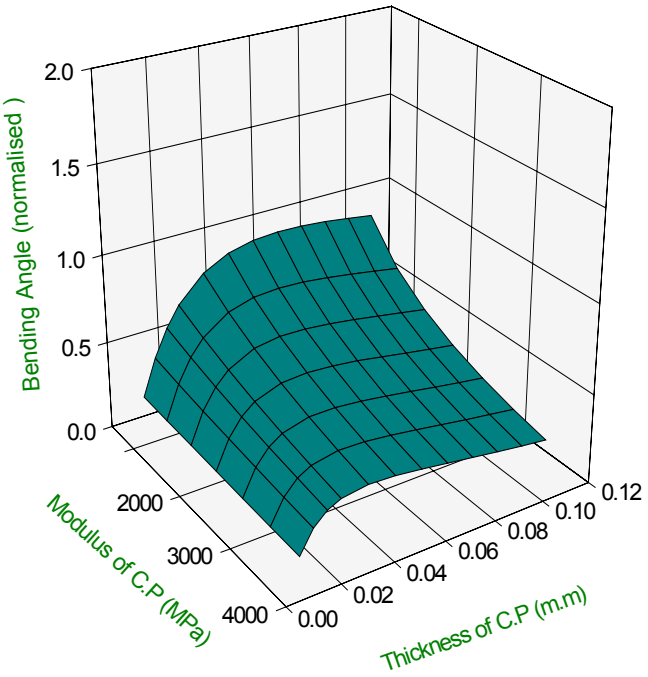

Figure-3.13. Variation of bending angle (normalized) vs modulus of C.P layer and different C.P thickness

With increasing conducting polymer layer modulus actuator system turns to more rigid in nature, so more force required to bend it. $d(\theta)/d(d_1)$ is higher and more prominent when backing layer thickness (d_1) is lower (Fig.3.14).

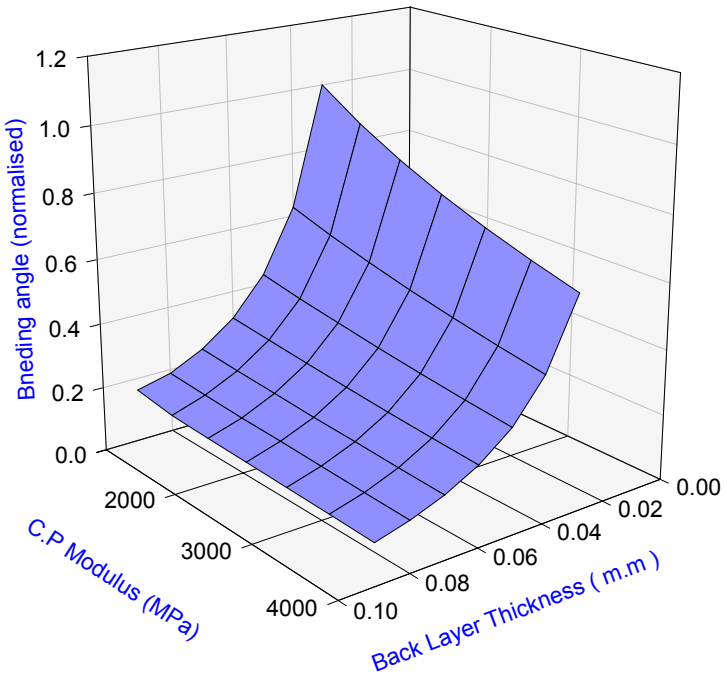

Figure- 3.14. Variation of bending angle (normalized) vs modulus of C.P layer and PET back layer thickness

Case-IV

Finally equation 3.30 shows that the bending angle of actuator system is dependent on width (b) and length (L). Generally, L is very much large quantity with respect to b. Bending angle proportional to L/b ratio, while it is inversely proportional to square of width. Fig. 3.15 presents the effect of dimension on the bending of an actuator. Bending angle was calculated by using equation 3.31 when others parameters are held constant. Bending angle increases with increasing L/b ratio. Since, actuator seems to be a rectangular beam, L/b ratio should be > 1. It is clear that the actuator width (b) is an important parameter when bending performance of actuators within the operating

conditions. There is critical value of the width below, which the bending angle increases sharply. This indicates that the scaling down of the material dimension can provide great improvements to the device response.

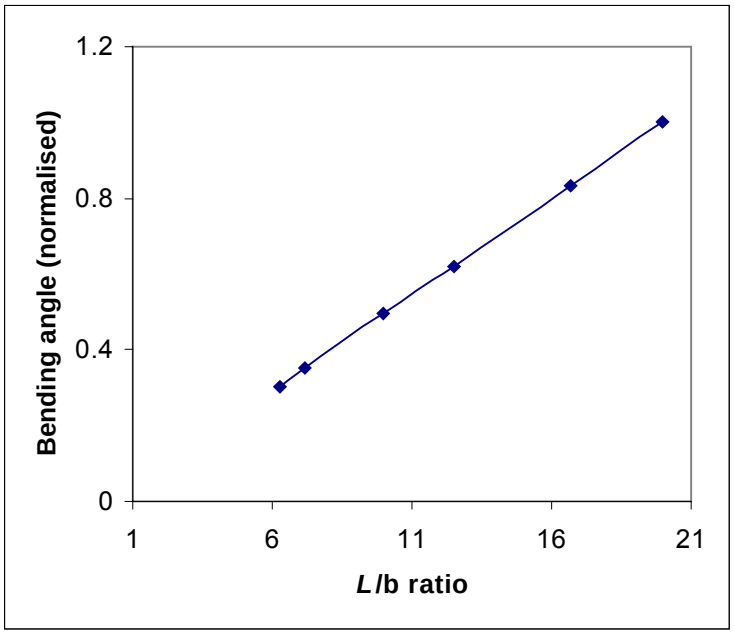

Figure-3.15. Bending angle vs *L*/b ratio

3.5. Conclusions

A phenomenological model has been proposed for a conducting polymer based bi-layer type actuator which takes into account the nature of backing layer and gives the correlation between the modulus, thickness of the supporting substrates on the actuation efficiency. It clearly brings out the fact that for a given condition of dopant ion, applied potential and conducting polymer, there is an optimum thickness of the backing layer, its modulus as well as the thickness of the conducting polymer at which the actuation is maximum. It is clearly found that model results are more influential with smaller

thickness of backing layer and modulus of the same. The optimal design parameters are investigated to estimate the effect of varying experimental conditions of the response of actuator. Thus, using this information, it is possible to adjust the parameters and choose appropriate materials for good actuating effect.

3.6. References

1. M.R.Gandhi, P.Murray, G.M.Spinks, G.G.Wallace, Synth.Met., **73**,1995,247.

2. C.K.Baker, R.A.John Reynolds, J.Electroana.Chemistry, **251**,1988,307.

3. E.W.H.Jager, E.Smela, O.Inganas, Science, **290**,2000,1540.

4. E.T Jones, E.Chao, M.J.Wrihton, J.Am.Chem.Soc., **109**,1987,5526 .

5. Q.Pei, O.Inganas, Solid State Ionics, **60**,1993,161.

6. Q.Pei , O.Inganas, J.Physical Chemistry, **96**,1992 ,10507.

7. H.S.Nalwa, Handbook of Organic and Conductive Molecules and Polymers, John Wiley & Sons Ltd., Chichester, **4**,1997,517.

8. S.Timoshenko, J.Opt.Soc.Am, **11**,1925,233.

9. I.W.Hunter, J.D.W.Madden, P.G.A.Madden, The Home Automation and Healthcare Consortium, Progress Report No.2-3, March 31,1999.

10. D.De Rossi, A.D.Santa, A.Mazzoldi, Synth.Met., **90**,1997,93.

11. T.A.Betts, C.A.Tipple, M.J.Sopaniak, P.G.Datskos, Anal.Chimica Acta, **422**,2000,89.

12. Li.Xiaoping, W.Y.Shih, I.A.Aksay, Wei-Heng, J.Am.Ceram.Soc., **82(7),**1999,1733.

13. Q.M.Wang, Q.Zhang, X.baomin, L.Rubin, C.Eric, J.Appl.Phys., **86(6)**,1999,3352.

14. H.S.Nalwa, Handbook of Organic Conductive Molecules and Polymers, John Wiley & Sons Ltd., Chicheste, England, **4**,1997,545.

15. E.Smela, M.Kallenbach, J.Holdenried, J.Microelectromechanical Sys., **8(4),**1999,373.

16. D.Haronian, Sensors and Actuators, A: Physical, **50**,1995,223.

17. J.Chung-Hwan, K.J.Kim, Sensors and Actuators, A: Physical, **112(1)**,2004,107.

18. A.C.Ugural, S.K.Fenster, Advanced Strength and Applied Elasticity, American Elsevier Publishing Company Inc, New York,1975, Ch-5.

19. J.G.Williams, Stress Analysis of Polymers, Ellis Harwood Ltd, New York, 1980, Ch-4.

20. L.E.Nielsen, Mechanical Properties of Polymers and Composites II, Marcel Dekker, New York,1974, p-34.

CHAPTER- IV
Sensor

Piezo-sensitivity studies have been mostly conducted on polymer-matrix composites with fillers that are electrically conducting. For this purpose, we have studied separately two different systems particularly PVDF-PANI and SBS-PANI, where PVDF and SBS were used as an insulating matrix and PANI was conducting filler. All detailed characterization and properties of PVDF-PANI and SBS-PANI blends are discussed in this chapter.

Piezo-Sensitivity of PVDF-PANI Blends

4.1. Introduction

First, we are discussing about PVDF-PANI composites system in details. The semi-crystalline fluoropolymers are widely popular as piezo-polymers. The partially crystalline poly(vinylidene fluoride) (PVDF) is one such example of these polymer [1]. PVDF (Fig. 4.1) is known to exist in different crystal forms: phase I is polar β phase [2], phase II is anti-polar α phase [3], and phase III and IV are denoted as γ and δ phases, respectively.

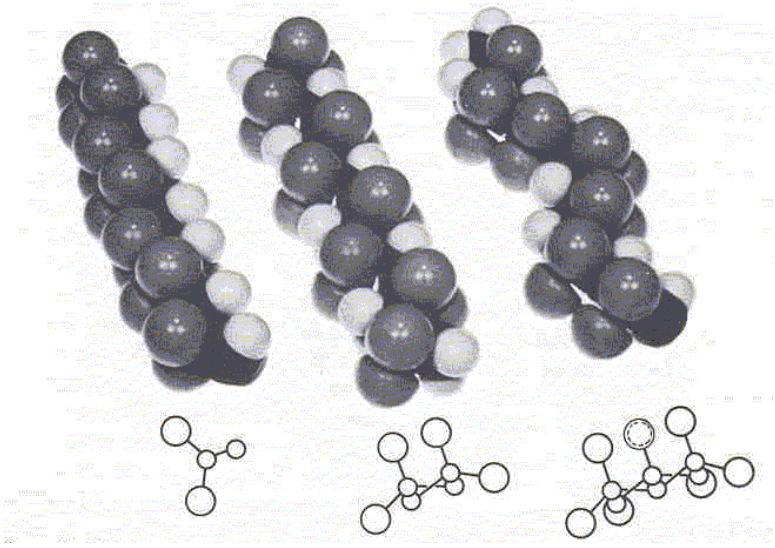

Figure- 4.1. Schematic view of various crystal structure of poly(vinylidene fluoride)

Due to high piezo-electric coefficient, PVDF has gained much importance. This feature is attributed to the β or the polarized crystalline phase. To prepare PVDF containing β crystalline phases, either of the following techniques are used: (a) stretching the polymeric film (four times its original size in two dimensions) [4], (b) heat treatment [5] and (c) poling, i.e. charging the films by applying high electric fields [6]. These techniques normally induce desired structural deformation i.e. orientation of molecular dipoles leading to drastic changes in the physical properties. PVDF films containing predominantly anti-polar form II were poled and exhibited a piezoelectric response about one half that of form I films [7]. However, to obtain anti polar form II i.e, β-crystalline phase, which exhibits high piezoelectric effect, PVDF has to be specially treated at very high electric fields (>$5X10^5$ V/cm) [8]. Such films are typically utilized for generation and detection of acoustic pulse signals for underwater transmission. Although, piezo-resistive ceramic, such as lead zirconate titanate (PZT) can well function as the sensing elements due to its large piezo-electric coefficient and large dielectric permitivity. Its performance is limited by a large acoustic impedance mismatch between the ceramic and water and its brittleness character. On the other hand, PVDF has its own limitation especially concerning processing difficulties and a number of steps such as high temperature stretching, high electric poling, etc. required to induce the proper β-crystalline phase and piezo-properties. Apart from this, PVDF is also highly insulating material, which is not easy to couple with other electronic devices. Hence, considering drawbacks of existing piezo-materials, scientists are in search for a suitable alternative. It would advantageous if PVDF is made semi-conducting by blending with conducting polymers [9-13]. The effect of

compressive stress on resistivity of conducting polymer composites was studied by many workers [9-12]. E. T. Kang et al.[13] prepared semi-conducting blends of PVDF and polyaniline by phase inversion in an aqueous solution of dopant. He found PANI chains dispersed uniformly in the doped PVDF-PANI blends, which have an asymmetric structure with a dense skin layer and a porous inner layer. PVDF films, filled with various mass fractions of $MgCl_2$, were prepared by A.Tawansi et al.[14]. They investigated effect of crystalline and electronic structural variations, on d.c electrical conductivity as a function of concentration of filler particles and found enhancement in degree of crystallinity of PVDF increased by loading of $MgCl_2$. Blends of poly(o-methoxyaniline) (POMA) and PVDF of various compositions were prepared from organic solvent phase by L. F. Malmonge et al.[15]. Despite the presence of the conductive host, the blends displayed a crystalline spherulitic morphology and a β crystalline phases characteristics of pure PVDF. Radhakrishnan et al.[9] reported high piezo-resistive effect of metal filled semi-conducting PVDF. The origin of such high sensitivity lies in the non-linear conduction process controlling the charge transport at the inter-particulate region. Conducting composites were made with different conducting filler and PVDF. They obtained typical response from these composites when subjected to low pressure (0.15 to 0.8 kg/cm^2). Some research groups found that the presence of α and/or β crystalline phases were enhanced by loading PVDF with certain mass fractions of the copper chlorides [16]. PVDF and (vinylidenefluoride-trifluoroethylene) (PVDF-TrFE) co-polymers have been used as the sensing elements [1]. Blends of PVDF with conducting polymer were exploited in membrane applications [13] due to its high degree of flexibility,

good mechanical property, durability, and low acoustic impedance, which facilitates good impedance matching with water and human tissues.

In order to investigate the role of non-linear process in piezo-sensitivity of conducting polymer blend/composites, PVDF-PANI system was chosen. This is particularly important since the promising electromechanical properties of PVDF combined with its excellent processibility makes PVDF a ideal choice for therefore its use in micro-electromechanical system (MEMS). Moreover composites of PVDF with conducting filler like PANI may possess some interesting properties. In the present scope of work, we have prepared and analyzed piezo-sensitivity of PVDF-PANI composites.

4.2. Experimental

PVDF-PANI composite films used for studying piezo-sensitive properties were prepared by the following method.

4.2.1. *Polyaniline (PANI) Synthesis*

Polyaniline (PANI) was synthesized by well known chemical route by oxidative coupling procedure [17, 18]. 19.61 gm.of ammonium persulphate was added to 8 ml of aniline as the oxidant in 1 M aqueous HCl acidic solution. As obtained PANI was in emeraldine salt (doped) form and it was additionally doped with 2 M HCl and then dried for 24 hr. in ambient condition under vacuum. In another set of experiment, the PANI powder obtained was treated with 2 M aqueous ammonium hydroxide (NH_4OH) solution for 2 hr. so as to neutralize the salt form. The emeraldine base form of PANI thus formed was then re-doped with DBSA in dimethylacetamide (DMAc) medium.

4.2.2. *Preparation of PVDF-PANI Blends*

Blends of PVDF-PANI were casted from solution containing varying amounts of PANI in PVDF solution. Both PVDF and PANI (either HCl-doped or DBSA-doped) solutions were prepared in DMAc. The desired quantity of PANI ranging from 2-25% were added to PVDF solution. The whole slurry was stirred for 24 hr. to form a uniform PVDF-PANI dispersions which were then poured in a glass petri-dish. The solvent was then evaporated at 50^0C and then resulting PVDF-PANI films (40-50 μm thick) were dried under vacuum. These dried films were placed between two metal electrodes and potential ranging from 25 V to 100 V was applied for duration of 30 to 180 min. at various temperatures. The maximum temperature was limited to 100^0C. These films were examined for beta crystalline phase content by WXRD and FTIR.

Details of the measurement of electrical properties (resistance, I-V characteristics) and resistance changes in PVDF-PANI films due to mechanical deformation are same as those reported for other polymers [11, 19, 20]. The piezo-sensitivity was measured in these samples by placing them between two metal plates on which the mechanical load was applied through top electrode. The top and bottom electrode were connected in a circuit diagram (Fig.2.2, chapter-II) through constant voltage D.C power supply and Keithley electrometer. The signal (current) was measured on application of pressure. Similar type of set up (Fig.2.1, chapter-II) was used for poling PVDF-PANI composite films by applying electrical field (25-100 volt) for different duration without applying any pressure. Details of experimental procedures of other characterization techniques like UV-visible, FTIR, WXRD are explained in chapter-II.

4.3. Results and Discussions

Before preparing PVDF-PANI blends, the PANI (as synthesized) was characterized by different analytical techniques. Two samples particularly HCl-doped and DBSA-doped PANI was used and results are discussed throughout this chapter.

4.3.1. *Polyaniline Characterization*

UV-visible spectra were carried out to characterize polyaniline prepared in two methods. UV-visible spectra of PANI (doped with DBSA and HCl) in DMAc solution are shown in Fig. 4.2. In each case, the absorption peak in the range of 320-330 nm is assigned to л – л* excitation of benzene ring of doped PANI [21]. The broad band around 600 nm wavelength region for doped PANI is indicative of protonation on acid doping and it also apparently corresponds to polaron–bipolaron transition [22]. It was also found that the

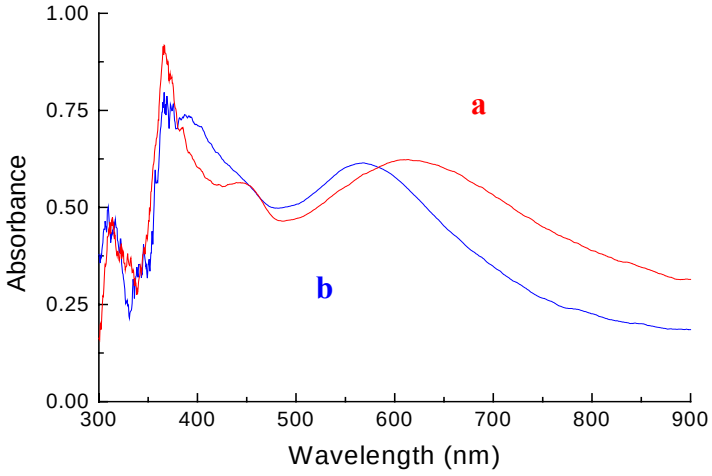

Figure-4.2. UV-visible spectra of solutions of polyaniline doped with different dopant in DMAc (a) PANI-HCl, and (b) PANI-DBSA

solubility of the PANI improves when doped with DBSA dopant. UV visible spectra of

PANI (doped with DBSA, HCl) were also recorded in $CHCl_3$ medium and similar peak (with little shift.) as that of DMAc were noticed in the spectra. The IR spectra of HCl-doped and DBSA-doped PANI are given in the Fig. 4.3. Infrared spectra of these polyaniline powders were recorded from 400 cm^{-1} to 2000 cm^{-1} to analyze mainly the fingerprint region. The peaks at 1015 and 1045 cm^{-1} appearing only in the case of DBSA-doped PANI correspond to the aromatic rings present in the dopant acids. On the other hand the sharp peak around 540 cm^{-1} is ascribed to the halogens (Cl) appears for HCl-doped PANI. The intensity of benzenoid and quinoid vibrations are almost seen to be equal in both the cases suggesting polyaniline is in emeraldine form.

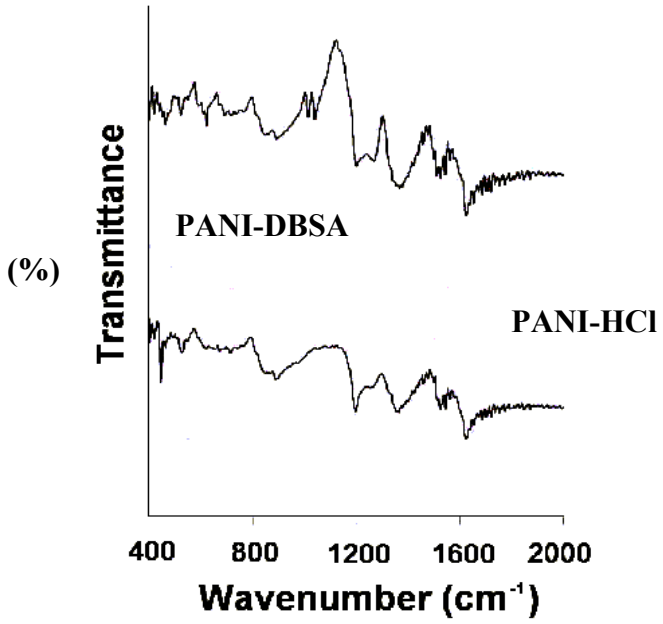

Figure-4.3. IR spectrum of PANI doped with different dopant ions

Wide angle X-RAY diffraction (WXRD) analysis was carried out for HCl and DBSA-doped polyaniline to understand the structural behavior (Fig. 4.4). These patterns were analyzed to get the effect of dopant acid used on the crystallinity of polyaniline formed.

PANI is known to be semi-crystalline as it exhibits sharp peaks in the diffraction angle (2θ) region of 15 to 35 degrees [23]. It can be noted that the HCl-doped polyaniline (Fig. 4.4 curve-a) showed higher crystallinity than DBSA-doped polyaniline (Fig. 4.4 curve-b). The lower crystallinity of DBSA-doped polyaniline might be attributed to interaction of long chain present in DBSA with the lattice. This interaction especially leads to disturb the crystalline order of PANI.

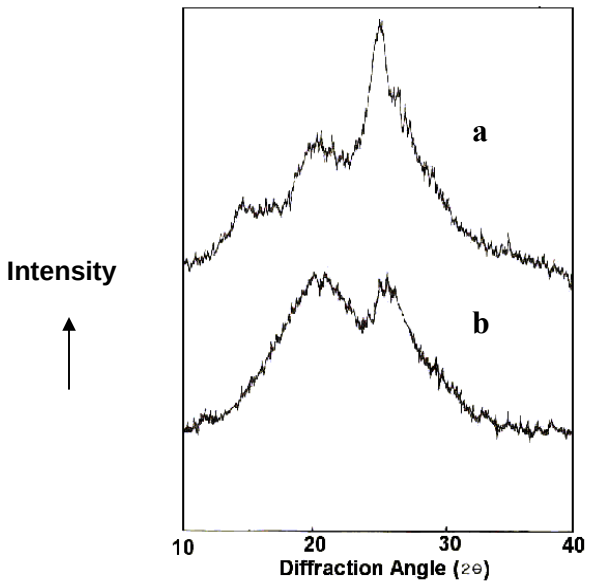

Figure-4.4. X-RAY diffraction scans for PANI with different dopant ions (a) PANI-HCl, and (b) PANI-DBSA

4.3.2. *Compositional Dependence of Resistivity*

The host polymer (PVDF) was found to be highly insulating [24] (resistivity $>10^{14}$ ohm-cm at room temperature). However, upon addition of PANI there was a sharp decrease in the resistivity of PVDF by several orders of magnitude. Fig. 4.5 shows the decrease in the

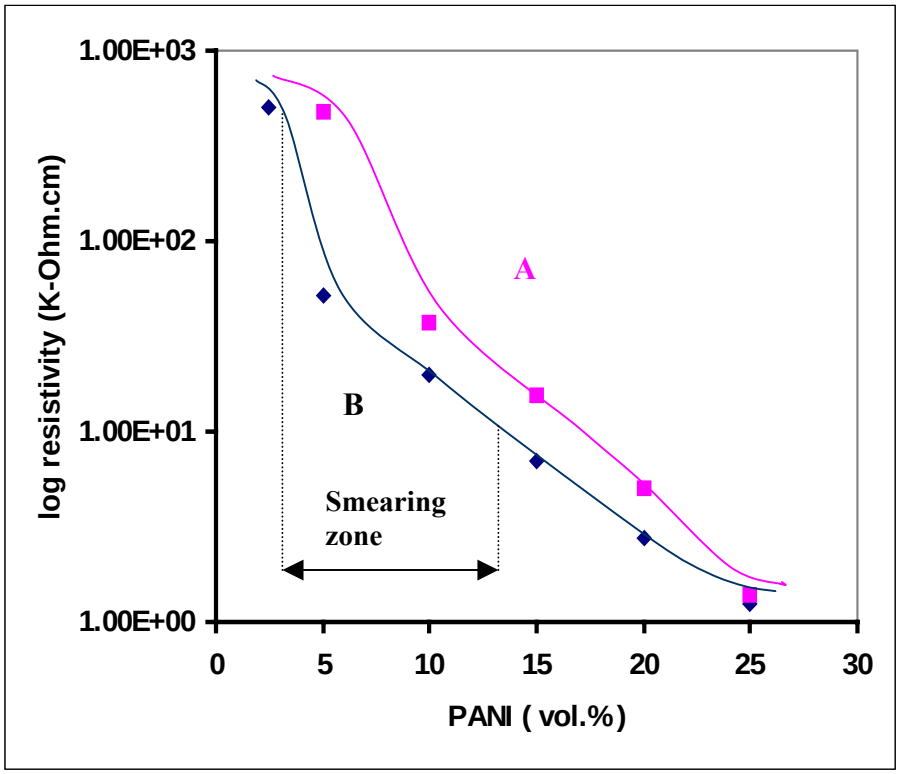

Figure-4.5. Electrical resistivity with composition of the PVDF-PANI blends for the two types of PANI (A)HCl-doped and (B) DBSA-doped, PANI

resistivity as a function of volume fraction of polyaniline in PANI-PVDF blends. In case of blend containing HCl-doped PANI (Fig. 4.5, curve-A) percolation threshold appears at about 10% PANI loading in the PVDF matrix while that for DBSA system (Fig. 4.5 curve-B), percolation attains at much lesser content of PANI (<5%) in PVDF matrix. Moreover on visual comparison DBSA-doped PVDF-PANI, films look more uniform and semi-transparent especially at lesser loading of PANI fillers than that HCl-doped PVDF-PANI films. Since DBSA-doped PANI gives better solubility in any organic solvent than conventional HCl-doped PANI, the difference in appearances of these two blends is self-explanatory. In conducting polymer particle-filled polymer composites, the particles can

be separated by thin polymer inter-layers, whose thickness may vary from 10 to 100 Å depending on the physicochemical properties of the polymer matrix, on the filler concentration and on the conditions of composite preparation. Their conductivity is determined by interlayer thickness, physicochemical properties, temperature, and strength of external field attributed to electron tunneling or ionic conductivity. While forming a composite, these inter-layers may be squeezed from the inter-particle region. In this case, particles are brought into a direct contact whose surface area is much smaller than that of their cross sections. The contact area is responsible for the so-called transient resistance. The presence of thin isolating inter-layers in the particle contact zone and the transient resistance lead to the appearance of a wide spectrum of resistance values inside the system. Because of the distribution of the values of contact resistance, a region of so-called smearing appears [25]. This region is assumed to be the width of "smearing" of critical transition from the non-conducting to conducting state (Fig. 4.5). Large gap-width between the conducting particles stand as physical barriers to flow of electrons/charges through the polymer matrix, thereby resulting in a relatively high level of electrical resistivity. Very fine dispersion and uniformity of the blend leads to effective and progressive lowering in the gap-width [26] between the conducting particles and as a result the barrier or hindrance to electron mobility drops sharply. This causes a sharp decrease in the percolation threshold for the DBSA-doped PANI.

4.3.3. *I-V Characteristics*

The I-V characteristics of these blends were investigated without applying any mechanical load to the sample. These are depicted in Fig. 4.6 (A) to (E) and Fig. 4.7 (A)

to (F) for different concentrations of HCl-doped PANI as well as DBSA-doped PANI in the blends, respectively.

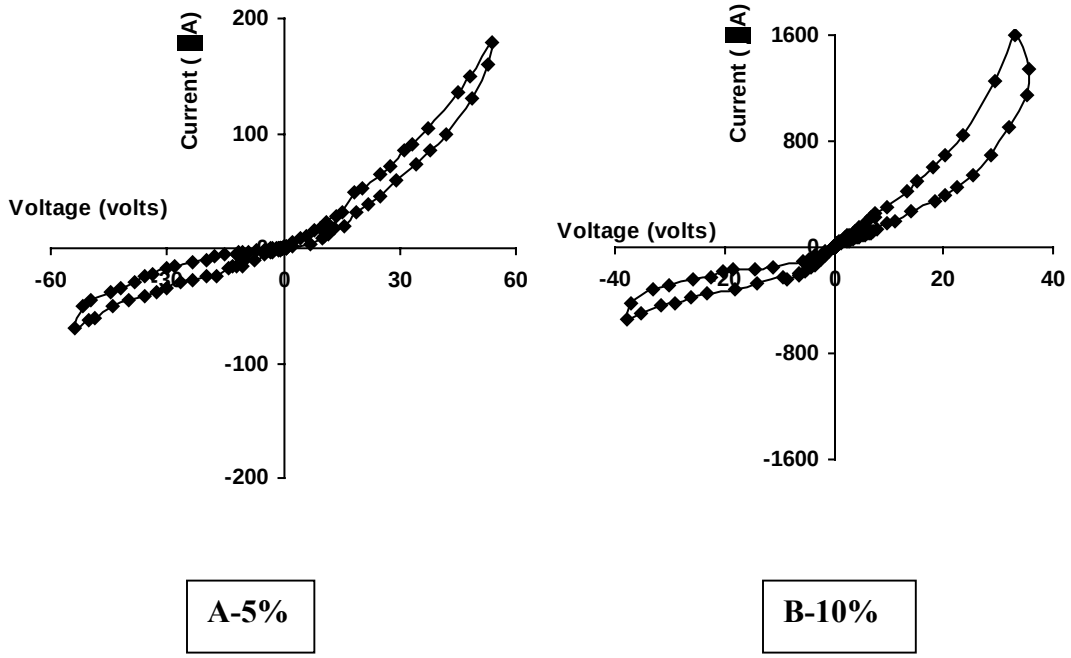

Figure–4.6. I-V characteristics for PVDF-PANI blends containing (A) 5% (B) 10% HCl-doped PANI

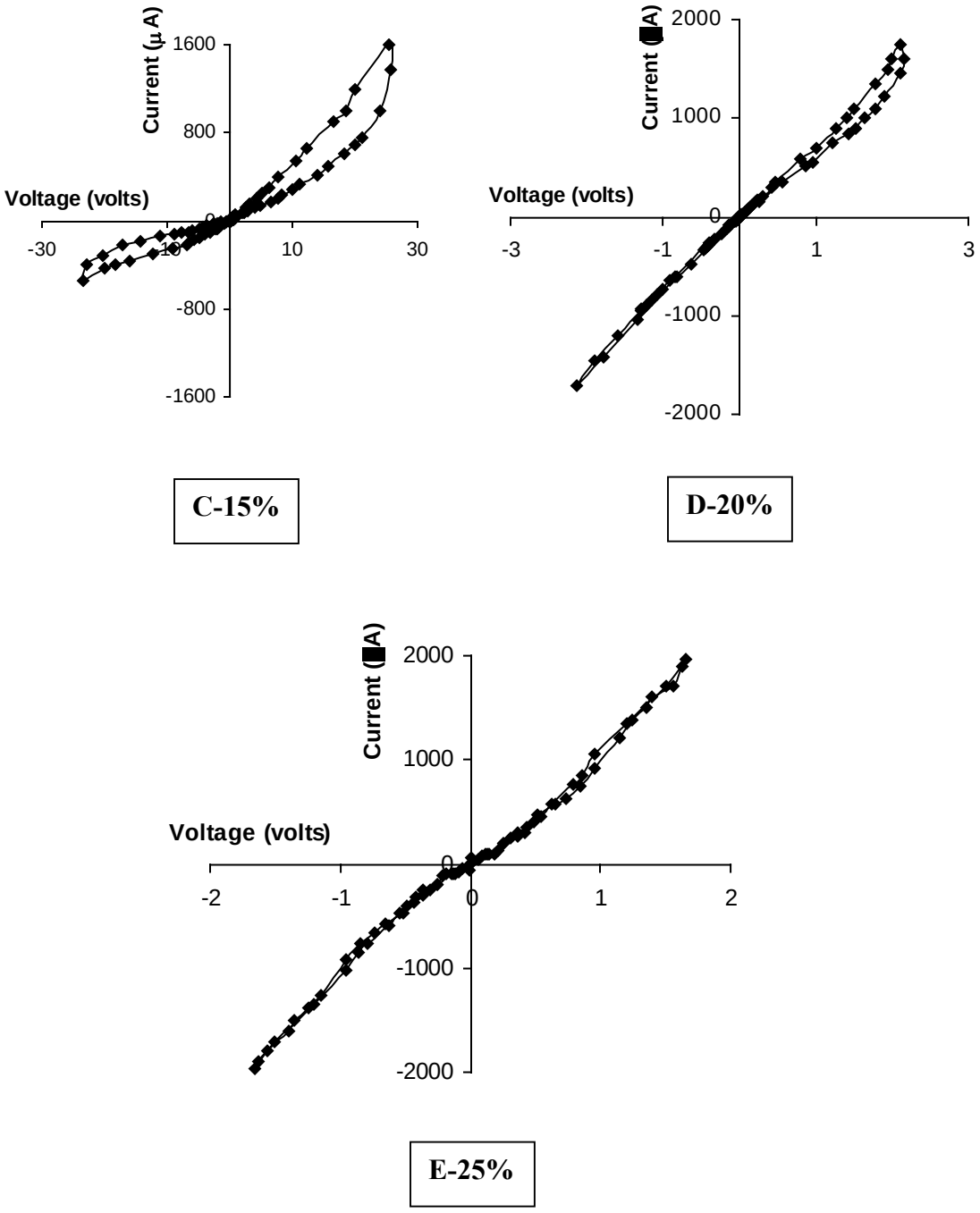

Figure–4.6. I-V characteristics for PVDPANI blends containing (C) 15%, (D) 20%, (E) 25% HCl-doped PANI

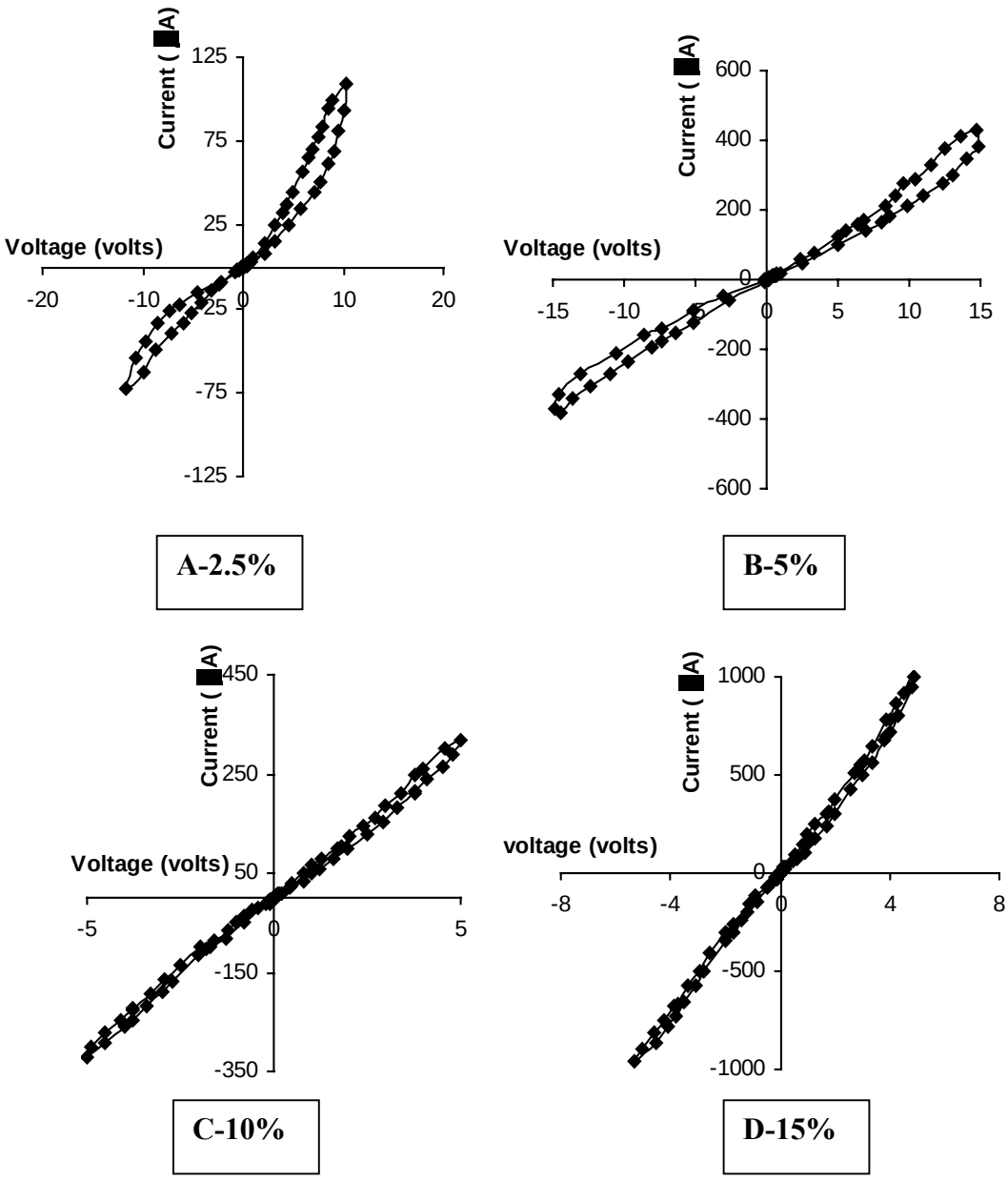

Figure–4.7. I-V characteristics for PVDF-PANI blend containing (A) 2.5%, (B) 5%, (C) 10%, (D) 15% DBSA-doped PANI

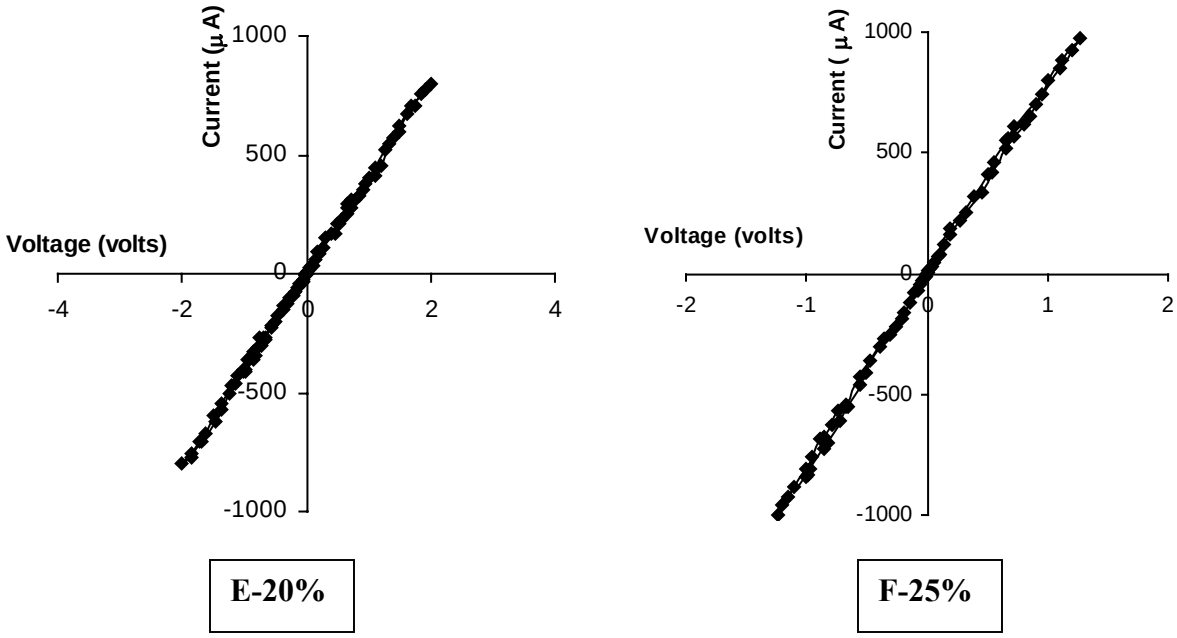

Figure– 4.7. I-V characteristics for PVDF-PANI blends containing (E) 20%, (F) 25% DBSA-doped PANI

In all cases, the I-V curves are non linear in nature and the non-linear character depends on the concentration of PANI [27]. At low concentration of PANI the I-V curves are slightly non-linear ; at intermediate levels these become highly non-linear while at high levels of PANI these become linear. Noteworthy, here is that PANI concentration in PVDF matrix plays important role in governing I-V characteristics. From Fig. 4.6, it is very much clear that by increasing concentration of PANI a systematic transition from nonlinear to linear conduction process occurs in these blends. The I-V characteristics for the PVDF-PANI (HCl-doped PANI) blends are found to be non-linear in nature with hysteresis in the rising and return part of the curves A, B, C, D corresponding to 5%, 10 %, 15 %, and 20 % PANI content as shown in the Fig. 4.6, respectively.

On the contrary for the blends containing higher amount of PANI, the I-V characteristics are seen to be linear in nature as depicted in Fig. 4.6 (curve-F, PANI 25%). The I-V characteristics of PVDF-PANI (DBSA-doped PANI) blends also reveal similar trend except that the transition from non-linear to linear behaviour occurs at much lower loading of 5% (Fig. 4.7). In most of these blends I-V characteristics are symmetric i.e. current observed in forward and backward bias are same barring exception 5%, 10%, 15% PVDF-PANI (HCl-doped PANI) composites.

Such non-linear characteristics can arise from a number of non-ohmic charge transport processes such as space charge limited conduction (SCLC), Tunneling (TN), and Schottky [28] effect. A detailed discussion on these along with the theoretical model for the conductivity especially in the context of conducting polymeric composites is given elsewhere [9, 10, 26, 29]. In brief, this essentially considers the composites as a series of junctions formed by the conducting-insulating-conducting elements and, I-V characteristics at each of these junctions, which when added together gives rise to an overall non-linear characteristics for the composites at the macroscopic level. In order to determine exact mechanism of the charge transport, a detailed analysis of the I-V characteristics was carried out.

In general for SCLC type conduction mechanism, the current–voltage relationship (equation- 4.1) is given by ;

$$I = I_o \mu \theta [V^{n+1}/d^{2n+1}] \qquad (4.1)$$

Where, I is the current, V is the voltage, 'd' is the thickness (here inter-particulate distance), μ is the mobility of charge carrier, θ is a parameter depending on the trap

distribution centers, I_o is a constant, and n is an integer. Forward bias of the I-V curves were then analyzed by making a plot of log I against log V.

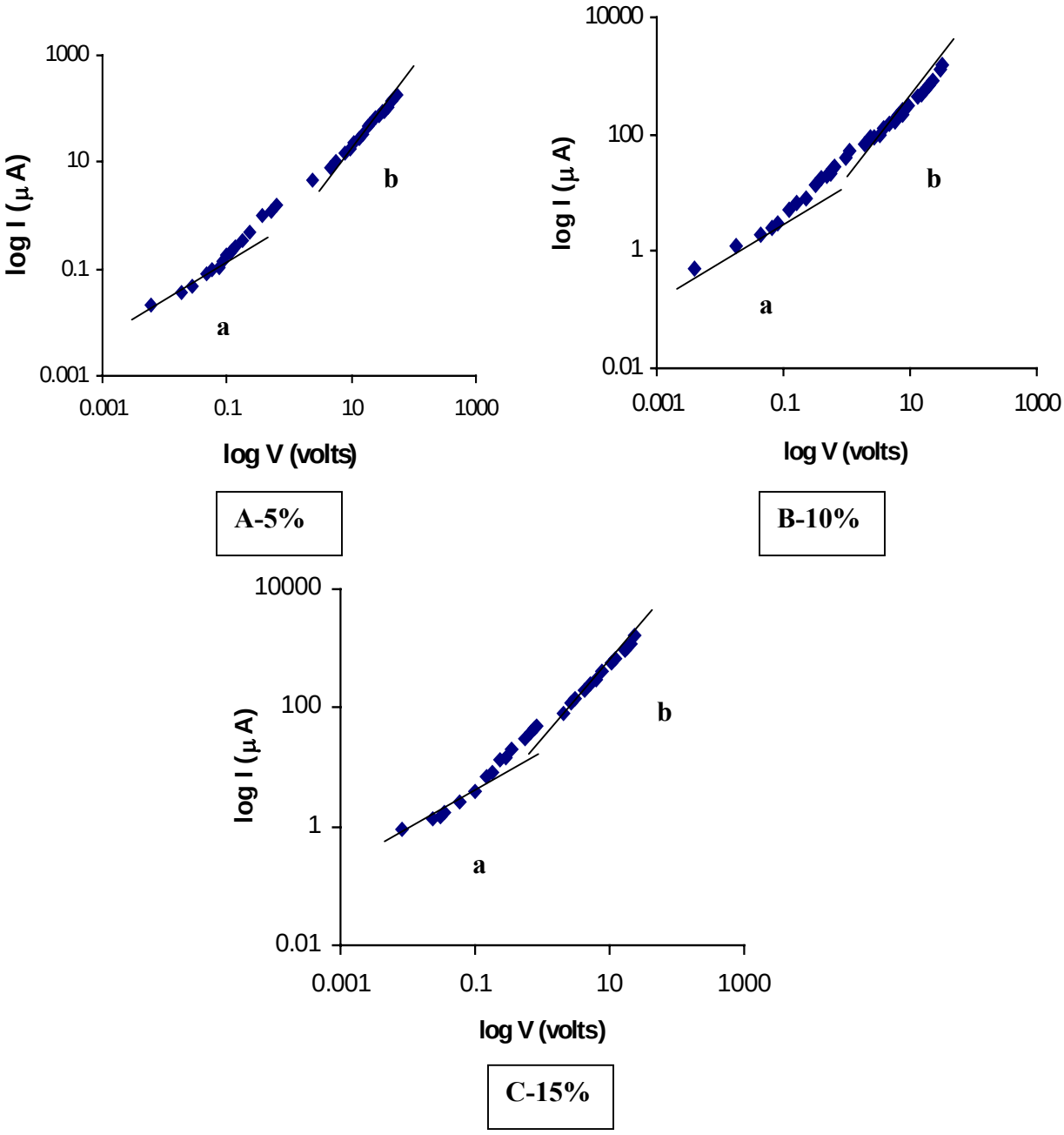

Figure–4.8. log-log plot of I-V characteristics for PVDF-PANI blends containing (A) 5%, (B)10%, (C)15%, HCl-doped PANI

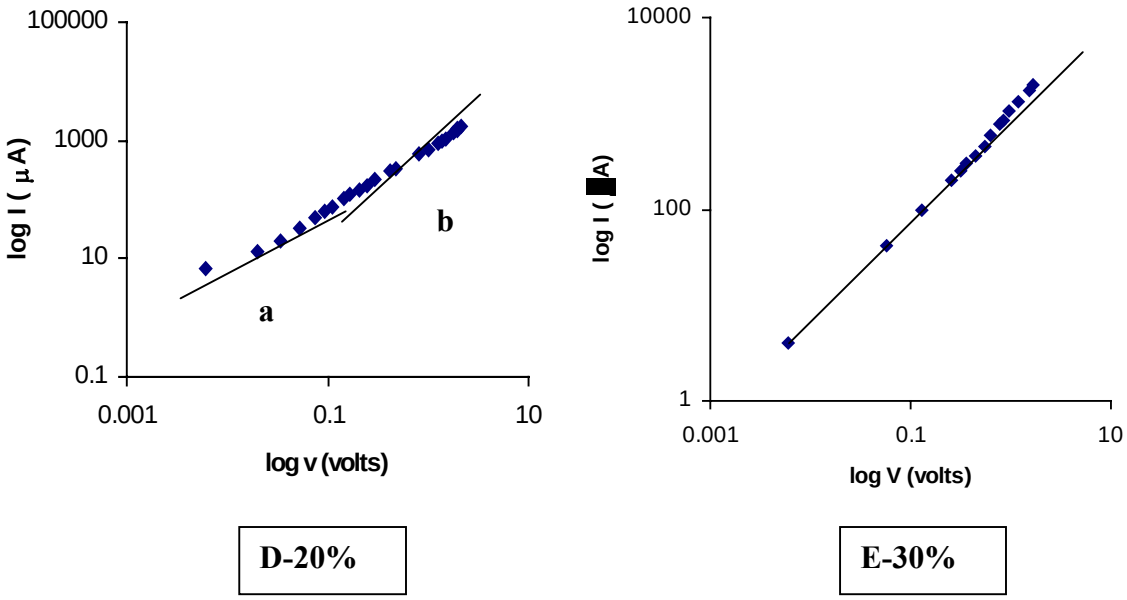

Figure–4.8. log-log plot of I-V characteristics for PVDF-PANI blend containing (D) 20%, (E) 25% HCl-doped PANI

Fig.4.8 reveals two different slopes in the I-V curves of A, B, C, and D samples. Whereas for curve E plot of log I vs log V varies linearly without any deviation in the slope value. The voltage dependence of current appears to follow the power law $I \propto V^n$. At low voltage, corresponding to an ohmic region ($J\alpha V$), (n=1), [a], which then becomes space-charge limited with a single discrete set of shallow traps ($J\alpha V^2$), (n= 2), [b]. These regions can be well explained using standard space charge limited current (SCLC) theory [30]. Charge transport through a thin polymer film may be an electrode limited process or a bulk limited process. SCLC process is confined to a bulk limited process.

It is well known that, the behaviour of the injected carriers in a semiconductor through an ohmic contact is affected, to some extent, by the physical properties of materials in which the carriers are flowing. The trapping centers created by impurities (dopant) and defects

will capture there and thereby immobilize a fraction of injected carriers, thus controlling the current transport process. For this reason, shape of I-V characteristics is not only controlled by the contacts but strongly dependent on the concentration and energy distribution of trapping centers inside the materials. The assumption of single discrete energy for all the traps is an oversimplification of this situation, since it is well known that, the trapping sites would not be identical in nearest, next nearest environment and so on. In fact, the existence of two trapping levels distributed in energy around levels E_1 and E_2 ($E_1 < E_2$) simultaneously acting in the SCLC conduction mechanism has been observed in some semiconductor materials. For the I-V characteristics presented here, they are considered as the case of two trapping levels and the thermal equilibrium Fermi level [31] (F_0) lying between E_1 & E_2. In this case, the current follows ohm's law at low voltage up-to the first (trap filling limited) TFL voltage, which corresponds to the end of trap filling around E_1. If voltage exceeds TFL voltage then, traps around E_2 level dominate and current changes slowly up-to the second TFL voltage, which corresponds to the end of the trap filling around E_2. After second TFL voltage, current increases very sharply and is denoted as trap free region.

The critical voltage at which the curve passes from the ohmic to the non-ohmic region is given in earlier reports [32, 33]. As the PANI content in the composite increases, the value of the V_{crit} shifts to lower voltage side and the curve becomes more and more non-linear (equation-4.2).

$$V_{crit} = 8/9\{d^{2n}/\mu\theta\, e\} \qquad (4.2)$$

Somani et al. [34] also found same observation about shifting of V_{crit} with composition. The

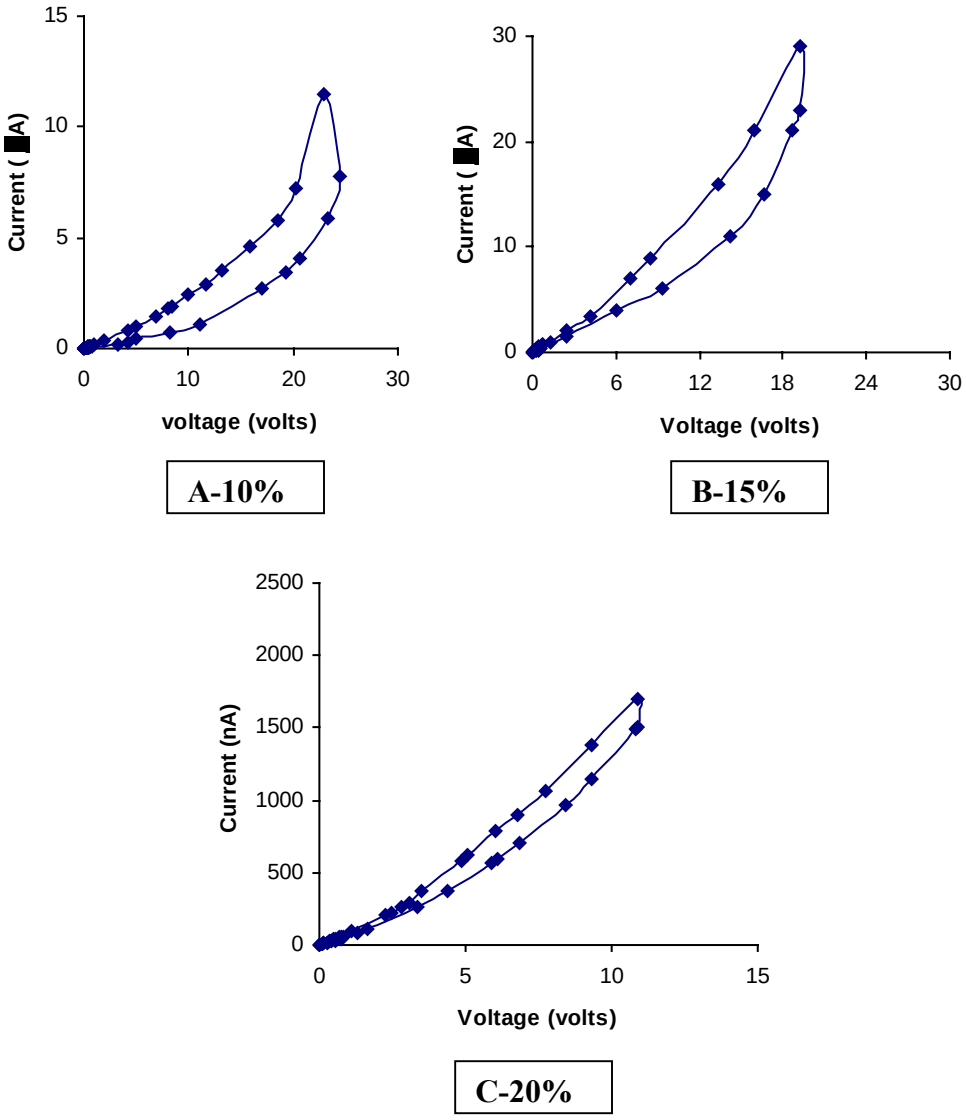

Figure-4.9. I-V characteristics for PVDF-PANI blends (HCl-doped) after poling at R.T

change of slope might be arising due to filling of the traps. Hence, it can be said that a space charge region is created at the interface of PANI/PVDF that gives rise to the SCLC behaviour. If the contacts to the electrode a re ohmic, then the electrode acts as an abundant source of charge carrier which can be injected into the solid. The hysteresis

observed in the I-V characteristics may be associated with the charge storage in the sample. The charge storage can be due to the ferroelectric nature of PVDF and/ or due to the space charge at the PVDF/PANI interface. It is interesting to note that as the sample becomes more and more conducting with an increase of PANI content in it, the charge gets dissipated and the hysteresis in the I–V characteristics decreases. The I-V characteristics of DBSA-doped PVDF-PANI in log-log scale showed linear nature and hence not present here.

Fig. 4.9, depicts the I-V characteristics of selective PVDF-PANI (HCl-doped PANI) composites after poling. The non-linear conduction process is observed in these samples. This process increasingly becomes SCLC type for certain concentration of PANI (10%) and then decreases. Comparison of Fig. 4.6 and 4.9 indicates that the current values at a particular voltage drops down by poling of the sample. It can be explained well on the basis that the sample being ferroelectric, the poling creates an internal field in the sample itself by orienting the electric dipoles. This especially opposes the external applied field and hence the current values drops down considerably after poling as compared to those before poling of the sample.

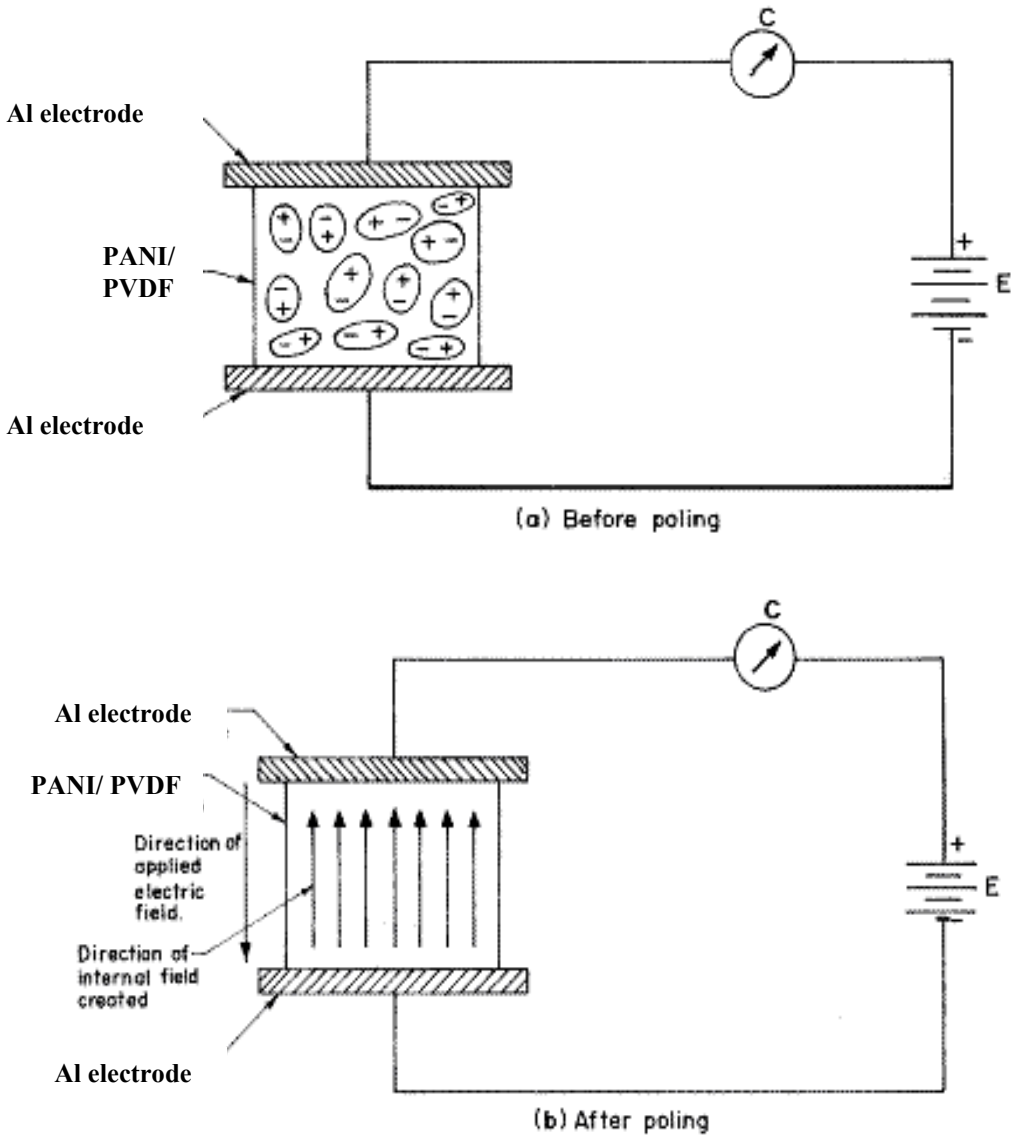

Figure-4.10. Effect of poling the PVDF-PANI composites showing the creation of internal field in a direction opposite to that of extremely applied electric field

For a ferroelectric material alone, current is limited by space charge, in the region of weak fields, and it is in accordance with Child's law normally applicable for linear semiconductors. Non-linearity in the ferroelectric material appears in the region of the

strong fields where the dielectric non-linearity normally appears. When the field reaches the value of the coercive field, the spontaneous polarization changes its sign because of the polarization reversal and the SCLC declines continuously. The results of the PVDF-PANI composites can be explained on similar arguments applicable in case of ferroelectric material PVDF alone. This is quite logical since here in the composite, PVDF being ferroelectric in nature undergoes poling and other such effects and the matrix polymer is not supposed to play any role in it. The poling process in PVDF in general is accompanied by charge injection. As a result of field ($1.8X10^4$ V/cm) application, there is a homogeneous dipole orientation and compensation charges located at the sample surfaces, then charge injection. The charges get accumulated at the left and right at the boundaries of a central polarization zone with time and this might be the reason for the predominant existence of SCLC process after poling.

4.3.4. *FTIR Characteristics*

Poling in the sample by applying electric field can also lead to appearance of new crystalline phases such as polar α phase and highly polar β phase. In order to confirm this, FTIR spectra were recorded and presented in Fig. 4.11.

On comparing these spectra significant changes in the regions of 800 cm^{-1} to 900 cm^{-1} are noticed. The bands at 610 cm^{-1} and 530 cm^{-1} in the spectra reflects α form [35] and these bands are very weak or subdued in curves B, C (Fig. 4.11). The intensity of peak at 976 cm^{-1} corresponding to α phase decreases with increasing poling field (Fig.4.11,curve-D).The peak appearing at 510 cm^{-1} (Fig.4.11, curve-D), belonging to the β phase are assigned to CF bending and wagging. These spectral differences reflect the different

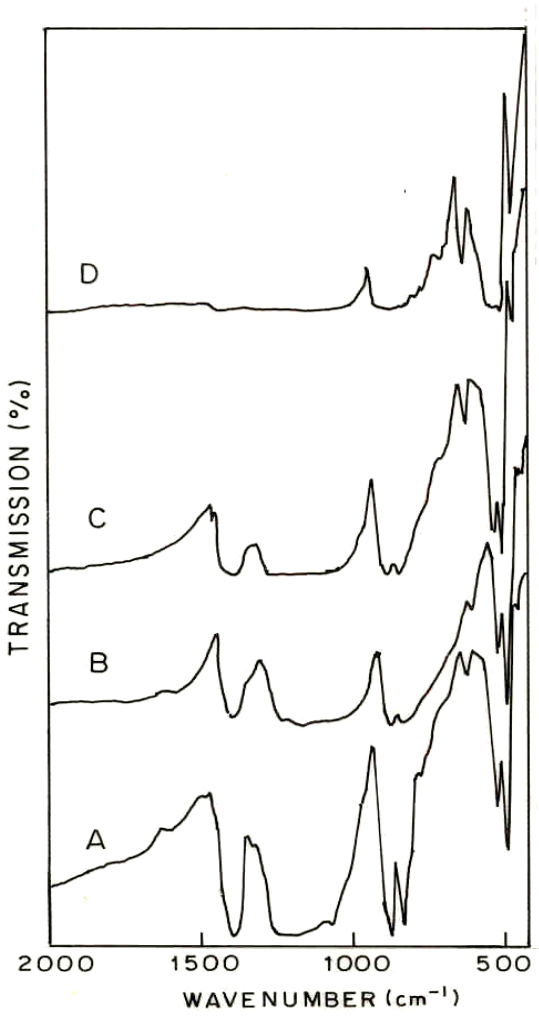

Figure-4.11. FTIR curves of PVDF-PANI blends containing 5% PANI (HCl-doped) loading (A) without poling (B) poled 0.6 X10^4 V/cm, 2 hr. (C) poled 1.8 X10^4 V/cm, 2 hr. (D) poled 2.4 X10^4 V/cm, 2 hr.

intermolecular and intra-molecular interactions which exist in the structural conformations of the two crystalline phases. Such new phases are normally seen at very high electric fields [36, 37].

4.3.5. *WXRD Characteristics*

The strong influence of an electric field on α phase of the polymer can also be seen from

the XRD of selected sample (Fig. 4.12). All the XRD patterns reveal presence of a semi-crystalline structure. PVDF alone (0% conducting particle loading) shows peaks at 2θ value of 16.8, 17.43, and 18.6 corresponding to existence of α phase [38]. On addition of

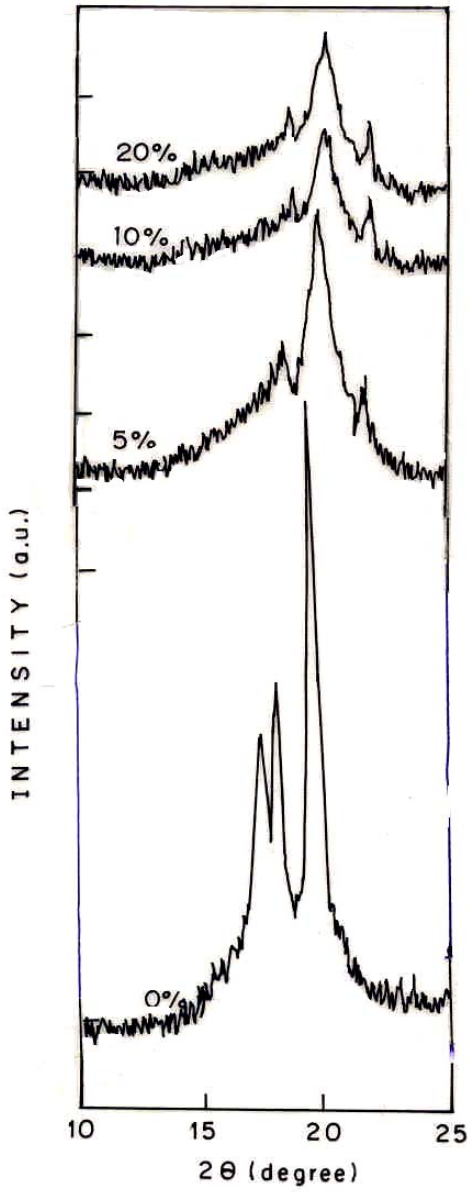

Figure-4.12. WXRD of PVDF-PANI blends containing various PANI (HCl-doped) loading (0–20%) poled 2 hr, at R.T.

PANI, the peaks at 2θ value of 16.8 disappear completely whereas the peak intensity of peak at 2θ value of 17.43 corresponding to α phase decreases systematically. Additionally, it comes shift in peak present at 18.6 towards higher 2θ side, the peak value at 20.5 correspondence to β phase.

We can explain this type of phase change of PVDF in PVDF-PANI blends by considering it M-I-M junction. The conducting particles act as electrode and the inter-granular distance is of sub-micron order giving rise to high electric fields in all these junctions (M-I-M) even when external voltage applied is comparatively low. This potential was to some extent sufficient to rotate C-F bond in PVDF matrix to give more order form of PVDF (such as polar α phase and highly polar β phase). The relative amount of polar β

Table-4.1. Amount of β phase produced in blends compositions.

Composition (%) PANI (HCl-doped)	Treatment	2θ	d	β (%)
0 (%)	Poled	17.43 18.08	5.07 4.89	0
5 (%)	Poled	19.86 20.40	4.46 4.34	40
10 (%)	Poled	19.85 20.50	4.46 4.32	47
20 (%)	Poled	19.92 20.40	4.46 4.34	43

crystalline phase, i.e. the ratio of the amount of the β crystalline phase to the total amount of the α & β phases, can be determined by using peak height of α & β phases in

Fig. 4.12. Table- 4.1 shows that β crystalline phase could be generated after poling and it depends on conducting polymer loading. PVDF-PANI blends with 10% HCl-doped sample shows maximum β phase [39], which will directly reflects on piezo-sensitivity i.e. higher β phase higher will be the piezo-sensitivity. However when conducting polymer loading exceeds more than 10%, the formation of β phase in PVDF-PANI blend is found to be decreased.

4.3.6. *Piezo-Sensitivity*

4.3.6.1. *Dependence of the Piezo-Sensitivity on Pressure*

The effect of deformation on electrical resistance of PVDF-PANI blends were studied in only compression mode. Fig. 4.13 and 4.14 showed the change of electrical resistance with applied mechanical load of PVDF-PANI blends on log-log scale, containing different amount of HCl and DBSA-doped PANI, respectively.

The sample and electrode (platinum) dimensions have been retained the same (1 cm^2) in all cases studied. In all measurements, the mechanical load was always applied in a direction parallel to electrical current flow. It can be seen that the resistance of all samples decreases monotonically with increasing mechanical load. The decrease in resistance as a function of mechanical load is rather rapid in case of 10 % and 15 % PANI than the other samples (Fig. 4.13).

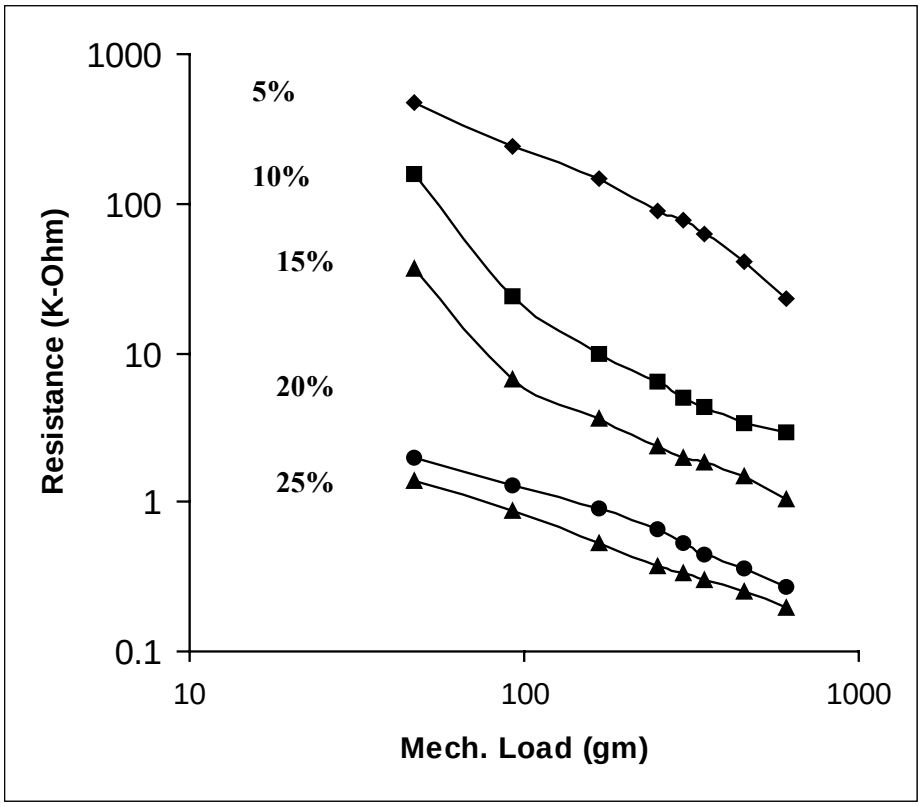

Figure-4.13. Effect of Compressive load on the sample resistance for PVDF-PANI blends with HCl dopant. Curves correspond to PANI concentration of 5%, 10%, 15%, 20%, and 25% respectively.

Similar trends are obtained for DBSA-doped PANI blends, except the fact that the decrease of resistance becomes weaker for 10% to 25% PANI loading (Fig. 4.14).

most of the above samples, the pressure (P) dependence of resistance (R) obeys power law $R = KP^{-m}$ where, K is a constant and m is an exponent which depends on sensitivity of the sample [40], i,e. higher the m value greater will be the sensitivity. Since pressure is directly proportional to applied compression, the values of m are obtained by plotting the data on log-log scale. These values of m are given in table 4.2.

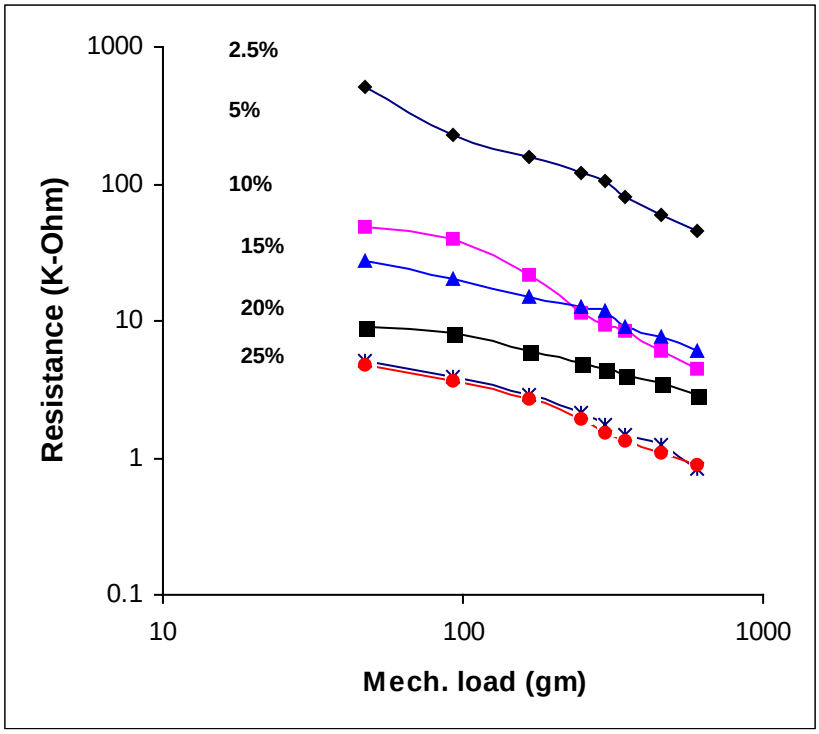

Figure-4.14. Effect of mechanical load on the electrical resistance of blends of PVDF-PANI with DBSA system. Curves correspond to PANI concentration of 2.5%, 5% , 10%, 15%, 20%, and 25% of PANI respectively.

Table-4.2. Different values of exponent m & K with composition of blends.

System	PANI loading (%)	Value of K *	Value of (m) *
PVDF +PANI (HCl doped)	5	40058	1.1254
	10	31732	1.5127
	15	3386	1.2905
	20	404	0.6814
	25	47	0.4735
PVDF +PANI (DBSA doped)	2.5	15710	0.9011
	5	3010	1.0440
	10	267	0.5725
	15	70	0.6925
	20	50	0.456
	25	35	0.2989

* The exponent values in the equation $R = K P^{-m}$ obtained by curve fitting.

It is seen from the table 4.2 that PVDF-PANI blend containing 10% PANI (HCl-doped) shows maximum piezo-sensitivity as compared to other blends including DBSA dopant system [27]. In fact, the latter type shows hardly any piezo-sensitivity.

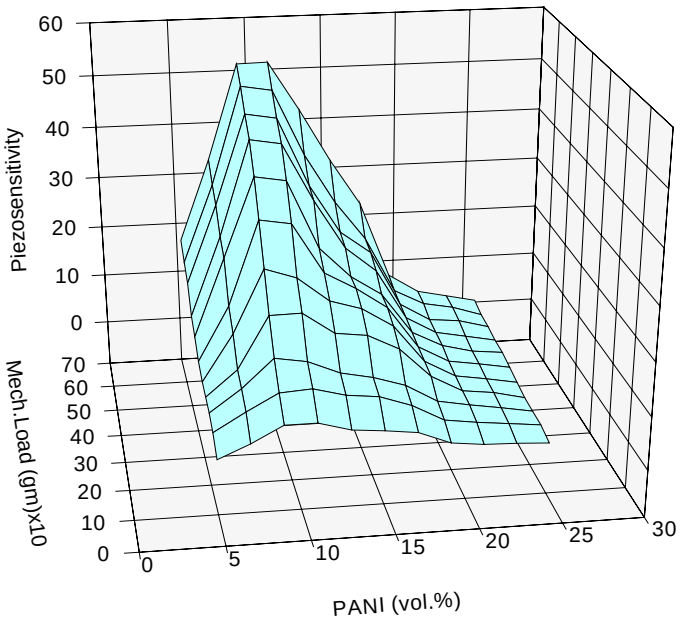

Figure-4.15. Piezo-sensitivity with respect to mechanical load as well as volume fraction of HCl-doped PANI of PVDF-PANI blends.

Fig. 4.15 showed that piezo-sensitivity pass through maximum at certain concentration at any load and maxima will shift to lower PANI concentration with increasing load. Piezo-sensitivity increases with increasing load and rate is higher at particular PANI concentration (10%). Somani et al.[41] also reported similar observation. This effect is little at higher PANI concentration (25%) & it may be due to the charge stored under constant applied field can get liberated during the application of pressure due to overlap of the levels & /or increase of contact area giving rise to additional current in forward direction.

4.3.6.2. *Dependence of the Piezo-Sensitivity on Composition*

A prominent feature which has been brought in to consideration from the present result is that the dependence of piezo-sensitivity factor on the concentration of the conducting phase. This has been presented in Fig. 4.16. It depicts that, piezo-sensitivity increases upto certain loading and by further raising PANI concentration it decreases considerably. Value of piezo-sensitivity steadily increases with mechanical loading at any blend composition. The average interparticle distance 'd' as determined from the equation 4.3

$$\phi^{1/3} = D.(L-d) / (D +d).L \qquad (4.3)$$

given for an uniformly dispersed two phase system described in the phenomenological model [42]. As the concentration of the conducting phase (ϕ) increases, the inter-particle distance 'd' decreases according to the relation (equation 4.3).

Resistance of the sample changes non-linearly with respect to 'd'. During application of external pressure (mechanical load), the interparticle distance changes giving rise to rapid change in electrical resistance as $R \propto (d)^{p+1}$, p being constant having value ≥ 1. Thus, small change in 'd' gives large change of R. To get maximum piezo-sensitivity, the value of 'd' should be optimum since its variation with applied mechanical load will decide the change in the sample resistance. For low polyaniline loading, 'd' will be large but change in 'd' will be small while at high PANI concentration, 'd' tend to zero as the particles touch each other. Accordingly, the piezo-sensitivity will also change with respect to the composition and it shows maximum at certain critical composition at which 'd' is optimized. Thus, one obtains critical concentration of the conducting additive at which the piezo-sensitivity is maximum.

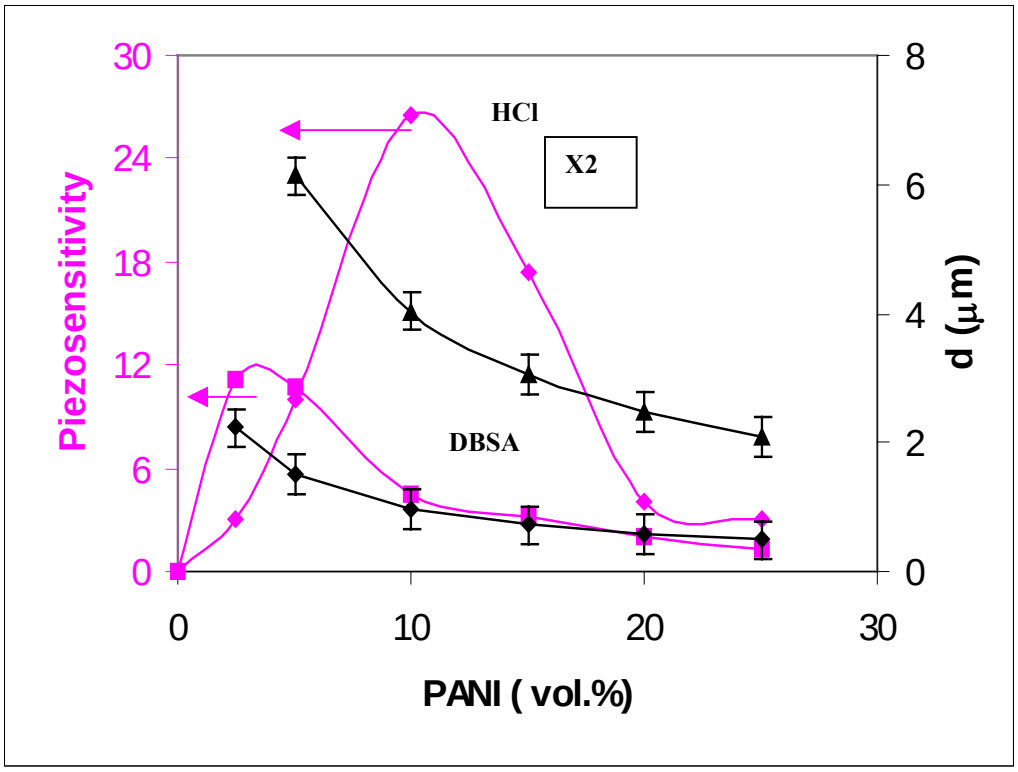

Figure- 4.16. Compositional variation of piezo-sensitivity and interparticle distance 'd' in PANI-PVDF blends with HCl and DBSA system, X 2 is the multiplication factor

4.3.6.3. *Effect of Poling on Piezo-Sensitivity*

I-V characteristics of selectively poled PVDF-PANI (HCl-doped) composites are non-linear and which becomes increasingly SCLC type. Piezo-sensitivity is highly dependent on the charge transport phenomena. In the case of space charge limited conduction, it has been shown earlier [43] that the piezo-sensitivity of the conducting polymer composites is much higher than that obtained in ohmic type conduction. The present studies also suggest that the piezo-sensitivity is higher for the compositions having SCLC type charge transport than ohmic type conduction. The effect of internal charge storage / electrical poling on the piezo-sensitivity is depicted in Fig. 4.17 & 4.18 for HCl and DBSA-doped

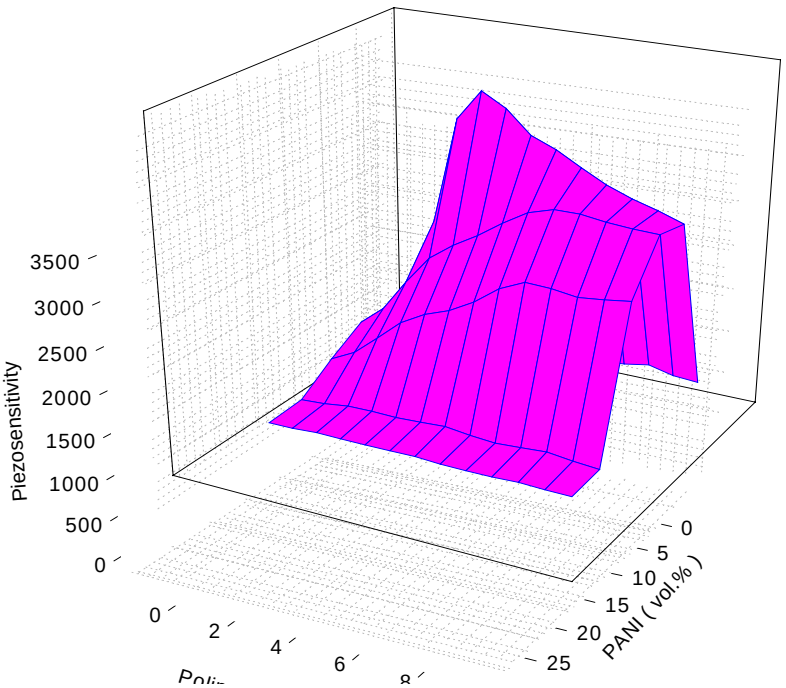

Figure-4.17. Plot of piezo-sensitivity vs PANI (HCl-doped) and as well as poling time

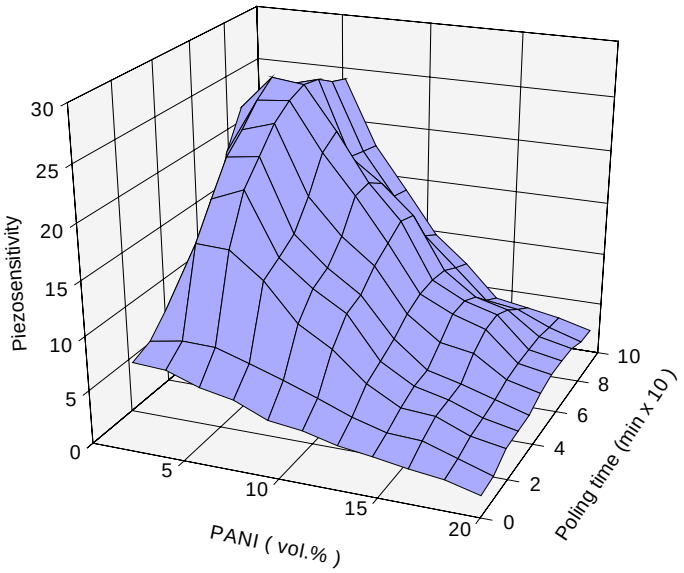

Figure-4.18. Plot of piezo-sensitivity vs PANI (%) (DBSA-doped) and as well as poling time

PVDF-PANI composites, respectively. It is evident (Fig. 4.17) that there is tremendous increase in the piezo-sensitivity by subjecting the samples to electric poling treatment. The composites containing 10% HCl doped PANI in PVDF matrix shows high piezo-sensitivity after poling [27, 44].

These results can be explained with the help of model suggested by Radhakrishnan et. al [45] on the basis of the nature of contact at the inter-granular interface and the conduction process at these junctions. This is basically due to charge storage and newly generated β phase in PVDF. Poling is not so much effective for DBSA-doped composites. Although DBSA-doped PVDF-PANI blends are compatible and uniform, the piezo-sensitivity remains low in these composites even after poling them. Contrary to this HCl-doped PANI blends can store charge during poling .The same charge gets liberated under application of mechanical load leading to high piezo-sensitivity in HCl-doped PVDF-PANI composites.

4.4. Conclusions

These studies demonstrates that PVDF-PANI conducting blends are useful candidates as piezo-sensors. The blends containing 10% to 15% of PANI appear to be best for such applications. The dopant ion plays an important role. Dopant with semi-compatible nature with insulating matrix is the best for showing good piezo-sensitivity. Composite, which stored more charge during poling and get liberated on application of load shows high piezo-sensitivity. The charge storage in such composites is confirmed from non-linear current voltage (SCLC) characteristics. Piezo-sensitive state in a semi-conducting PVDF is brought by electrical poling. Permanent dipoles of the CF_2 group reoriented with

respect to the film surface. When the film was subjected to the process the molecules is transformed to the planner Zig-Zag for phase I**,** which produces high piezo-resistive property. Semi-conducting PVDF can be used for piezo-sensor but their composition has to be optimized for good performance.

4.5. References

1.W.Chirhua, M.Adreas, K.Patrick, A.U.Ieong, Sensors and Actuators, B: Chemical, **73**,2001,100.

2. B.Mazurek, S.Rozecki, D.Kowalczyk, T.Janiczek, J.Electrostatics, **52**,2001,180.

3. W.W.Doll, J.B.Lando, J.Macromol.Sci.Phys., **B4**,1970,309 .

4. A.J.Lovinger, Developments in Crystalline Polymers, Applied Science, London, 1982, p-195.

5. K.Yamada, M.Die, M.J.Takayanagi, Polymer Sci., Polymer Phys., **21**,1983,1063.

6. K.Doughty, D.I.Das-Gupta, Thin Solid Films, **112**,1984,303.

7. H.Ohigashi, J.Appl.Phys., **47**,1976,949.

8. B.A.Newman, C.H.Yoon, K.D.Pae, J.I.Scheinbein, J.Appl.Phys., **50**,1979,6095.

9. S.Radhakrishnan, S.Chakne, P.N.Shelke, Materials letters, **18**,1994,358.

10. E.K. Sichel, Carbon Black Polymer Composites, Marcel Dekker, New York, 1982, p-103.

11. S.Sivaram, Polymer Science Contemporary themes, Tata McGraw- Hill Publishing Company Ltd., New Delhi, **2**,1991,761.

12. B.Lumberg, B.Sundquist, J.Appl.Phys., **60**,1074,1986.

13. P.Wang, K.L.Tan, E.T.Kang, K.G.Neoh, Applied Surface Science, **193**,2002,36.

14. A.Tawansi, A.H.Oraby, E.M.Abdelrazek, M.Abdelaziz, Polymer Testing, **18**,1999,569.

15. L.F.Malmonge, L.H.C.Mattoso, Synth.Met., **69**,1995,123.

16. A.Tawansi, E.M.Abdelrazek, H.M.Zidan, J.Mater.Sci., **32**,1997,6243.

17. F.Lux, Polymer, **35**,1994,2915.

18. Y.Cao, A.Andreatta, A.J.Heeger, P.Smith, Polymer, **30**,1989,2305.

19. S.Radhakrishnan, G.Joshi, J.Macromol.Sci.Phys., **B27**,1988,291.

20. S.Radhakrishnan, D.R.Saini, Polymer Int., **34**,1994,111.

21. W.Meixiang, Synth.Met., **31,**1987,51.

22. J.Huang, M.Wan, J.Polymer Sci., **37**,199,151.

23. H.K.Chaudhari, D.S.Kelkar, J.Appl.Polymer Sci., **62**,1996,15.

24. H.S.Nalwa, K.Tashiro, Ferroelectric Polymers, Marcel Dekker, New York, 1995, Ch-2.

25. V.I.Roldughin, V.V.Vysotskii, Progress in Organic Coatings, **39**,2000,81.

26. A.I.Medalia, Rubber Chemistry Technology, **59**,1986,432.

27. S.Radhakrishnan, S.B.Kar, SPIE–2002, p-23.

28. J.G.Simsons, L.I.Maissel, R.Glang, Handbook of Thin Film Technology, Tata McGraw-Hill Publishing Company Ltd., New York ,1976, Ch-14.

29. S.Radhakrishnan, S.P.Khedkar, Synth.Met., **79**,1996,219.

30. M.A.Lampert, P.Mark, Current Injection in Solids, New York, Academic Press, 1970, Ch-7.

31. A.Rizzo, G.Micocci, A.Tepore, J.Appl.Phys., **48(8)**,1977,3415.

32. F.Gutman, L.E.Lyons, Organic Semiconductors, John Wiley & Sons Ltd., New Work, 1967, Ch-10.

33. D.A.Seanor, Electrical Properties of Polymers, Academic Press, New York, 1982, Ch-1.

34. P.R.Somani, R.Marimuthua, AB.Mandaleb, Polymer, **42**,2001,2991.

35. J.P.Luongo, J.Polymer Sci., Polymer Phys., **10**,1972,1119.

36. N.Murayama, T.Oikawa, U.S.Pat., 3931446.

37. N.W.Tester, U.S.Pat., 4340786.

38. G.T.Davis, J.E.McKinney, M.G.Broahurst, S.C.Rath, J.Appl.Phys., **49**,1978,4998.

39. S.Radhakrishnan, S.B.Kar, U.S.Pat. 0127573 A1.

40. S.Radhakrishnan, S.B.Kar, Sensors and Actuators, A: Physical, **12**,2005,474.

41. P.R.Somani, R.Marimuthu,U.P.Mulik, S.R.Sainker, D.P.Amalnerkar, Synth.Met., **106**,1999,45.

42. S.Radhakrishnan, S.B.Kar, Sensors, (Communicated).

43. J.Kpst, M.Narkis, A.Foux, J.Appl.Polym.Sci., **29**,1984,3937.

44. S.Radhakrishnan, S.B.Kar, U.S.Patent. 0065280 A1.

45. S.Radhakrishnan, Polymer Comm., **26**,1994,153.

Piezo-Sensitivity of SBS-PANI Blends

4.6. Introduction

Piezo-sensors are useful in variety of applications as mentioned previously in this chapter. Piezo-sensors developed using thermoplastic elastomer (SBS) (Fig.4.19) play an important role because of their flexibility, lightweight, toughness, availability in different thicknesses and surface areas, ease of fabrication/processing and integration with other devices. Another key feature, which makes piezo-sensors valuable, is the relatively low

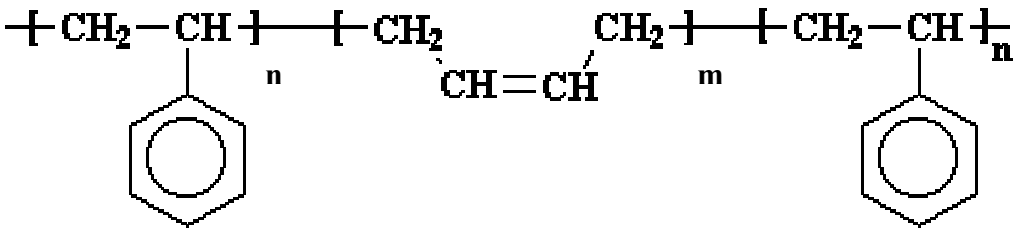

Figure-4.19. Styrene butadiene styrene

acoustic impedance and its close match to those of water, human tissue, and other organic matter. A close impedance match allows acoustic signals to pass through the film without being distorted. When it is laminated to a vibrating structure, it does not significantly distort the motion of the structure. Due to low permitivity value of 12 (PZT is 12,000) the "g" or stress constant of piezo film is significantly greater. It operates over an extremely wide frequency range-from the tapping of one's finger on a simple touch panel switch to transducer arrays for ultrasonic imaging that operate in the 1-10 MHz range. In fact, the film detects GHz frequencies . Up till now polymeric piezo-sensors produced

commercially are mainly based on polyvinylidene fluoride (PVDF) or its co-polymers, which exhibit piezoelectric properties. However, such sensors have very high resistance and require high input impedance (>10^{12} ohms) devices for further data handling. Moreover these PVDF sensors are very difficult to process and produce, they are expensive and not easily available.

Taking into consideration these drawbacks, the present work is an attempt to develop flexible semi-conducting piezo-sensors using conducting polyaniline incorporated SBS blends.

The effect of mechanical stress on the electrical properties of composites made either by using SBS as insulating matrix or conducting polyaniline as filler particles in different insulating matrix has been studied in details [1-2]. In recent past number of articles are available in literature [3-5] mentioning influence of mechanical stress on resistivity of conducting polymeric materials.

Hassan et al.[6] have studied the effect of tensile deformation on the electrical conductivity of conducting carbon black loaded styrene-butadiene rubber and showed that the equilibrium value of the electrical conductivity increased with deformation upto an elongation of 110% and then decreased with further increase in the extension. Radhakrishnan et al.[7] made the efforts to evaluate dependence of the electrical resistivity of semi-conducting SBS composites on mechanical deformations both in compression and extension modes. They have concluded that, origin of high piezo-sensitivity lies in the nonlinear conduction process controlling the charge transport at the interparticulate region. Bao et al.[8,9] monitored electrical conductivity of polyaniline as a function of

pressure. According to them, primary effect of applying pressure is simple compression, and it leads to reduce interchain separation with increasing pressure. The data obtained in their work shows asymmetry in resistance against pressure measurements pointing out towards irreversible structural changes in the sample. Origin of high piezo-sensitivity of polyaniline/TiO_2 system has been reported by Somani et al.[10]. They have synthesized highly piezo-resistive conducting polyaniline–titanium oxide (PANI/TiO_2) composites. These composites exhibited high piezo-sensitivity at a certain polyaniline/TiO_2 composition. Radhakrishnan et al.[11] also studied piezo-resistivity of polyaniline and $BaTiO_3$ composites. These composites exhibited high piezo-sensitivity at a certain composition. Recently, Hong-Quan et al.[12,13] reported piezo properties of SBS-PANI composites. They made conductive thermoplastic elastomer of SBS-PANI by using emulsion polymerization technique. However, any did not perform piezo-resisitive measurement. In order to investigate the role of non-linear process in piezo-sensitivity of conducting polymer blend/composite, SBS-PANI system was chosen. This is particularly important since it offers a flexible matrix, which has non-linearity in mechanical properties, and because of block copolymer nature it gives phase-segregated domains of conducting polymer.

4.7. Experimental

For investigating piezo-sensitive properties, SBS-PANI composites were prepared by following method.

4.7.1. *Polyaniline (PANI) Synthesis*

Polyaniline (PANI) was synthesized by the same method [14,15] as described in section 4.2.1 of this chapter.

4.7.2. *Blends Preparation*

Preparation of SBS-PANI blends (A) vol.% stock solution of SBS was prepared by dissolving appropriate quantity of SBS in chloroform. To a fixed volume of (A) vol.% SBS solution a desired amount of PANI was added so that the final concentration of PANI in the blend would not be lower less than 5% or exceed more than 30% .The whole slurry was stirred for 24hr. at room temperature. The blend solution was then poured in a glass petri dish and solvent was evaporated completely at ambient conditions. The 470 to 500 μm thick SBS-PANI blend films were then vacuum dried and subjected for the electrical property measurements.

These properties were measured in the same manner as described in section 4.2.2 of this chapter [16,17]. The piezo-sensitivity in SBS-PANI blend film was measured by sandwiching the film between two metal plates on which the mechanical load was applied through top electrode. The top and bottom electrodes were connected through constant voltage (D.C) power supply (typically applied potential of 2.0 V was used) and the current output was monitored using Keithley electrometer connected to computer. Continuous piezo-response curve with application and removal of mechanical load was determined by this arrangement.

4.8. Results and Discussions

4.8.1. *Compositional Dependence of Resistivity*

The SBS thermoplastic elastomer used in the present work is known to be highly insulating with resistivity at room temperature being greater than 10^{13} ohm.cm [18]. The resistivity as a function of vol.% of PANI in SBS elastomer is presented in Fig.4.20

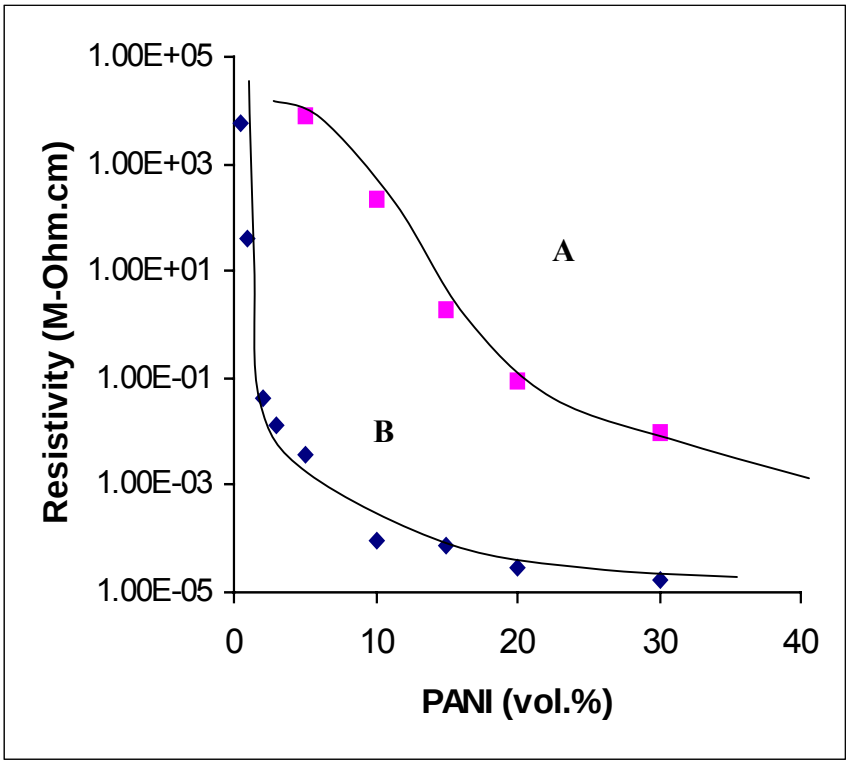

Figure-4.20. Electrical resistivity with composition of the SBS-PANI blends for the two types of polyaniline. (■) HCl-doped, and (♦) DBSA-doped PANI.

In case of DBSA doped PANI system, the decrease in resistivity is very sharp whereas in case of HCl doped PANI resistivity decreases steadily. This type of curve is typical in most of the CPC reported in the literature [11, 19]. However, the interesting feature of the

present case is that the resistivity range remains in the semi-conducting region. At the same PANI content the resistivity of SBS-PANI (HCl doped) blend is greater than SBS-PANI (DBSA-doped) blend. The percolation threshold appears at about 10% PANI for HCl-doped case while it is about 1.5% for DBSA doped PANI. Hong–Quan Xie et al.[13,20] also reported percolation threshold near 3 % for SBS-PANI (BDSA doped) blends, of course their blends preparation methods were different from the present case.

The sharp decrease in resistivity could be explained on the basis of the percolation theory [21] (section 4.3.2) which is widely used to describe the properties of such systems and to establish the quantitative relationship between the composite structure and its conductivity. There can be several reasons for these observations viz. the particle size of the PANI used, the distribution of the added component, compatibility of the PANI with SBS etc. It is known that DBSA has plasticizing effect on PANI [22] which makes it sticky, rubbery and soluble in chloroform. The solubility of PANI-DBSA in $CHCl_3$ is enhanced mainly because of structural similarities between SBS and DBSA group in PANI-DBSA system. Dodecylbenzene sulfonic acid gets incorporated between the PANI chains and (like intercalation to make nanoparticle) due to its bulky size it increases PANI-PANI interchain layer distance to enhance the solubility in the resulting solvent. Thus, the uniformity of mixing/dispersion is much better for PANI-DBSA than PANI-HCl. For the latter case, the blend is likely to be highly phase segregated due to incompatible nature (see SEM figure). Also, the inter-domain distance is related to the particle size and concentration of the conducting additive. The particle size being very much smaller (confirmed by optical microscopy) for PANI-DBSA, the inter-domain distance is much

smaller for the same concentration of PANI in this case than for HCl doped PANI.

4.8.2. *Scanning Electron Microscopy*

In order to understand the conducting particle (PANI) distribution in SBS matrix, cross section morphology of SBS-PANI blends films were investigated by scanning electron microscopy. The micrographs were taken by sectioning blend films along the transverse direction. Fig.4.21 (A, B, C, and D) & 4.22 (E and F) depicts the SEM micrographs for fractured surface of the films (selective composition) containing 5%, 10%, 15% and 20%

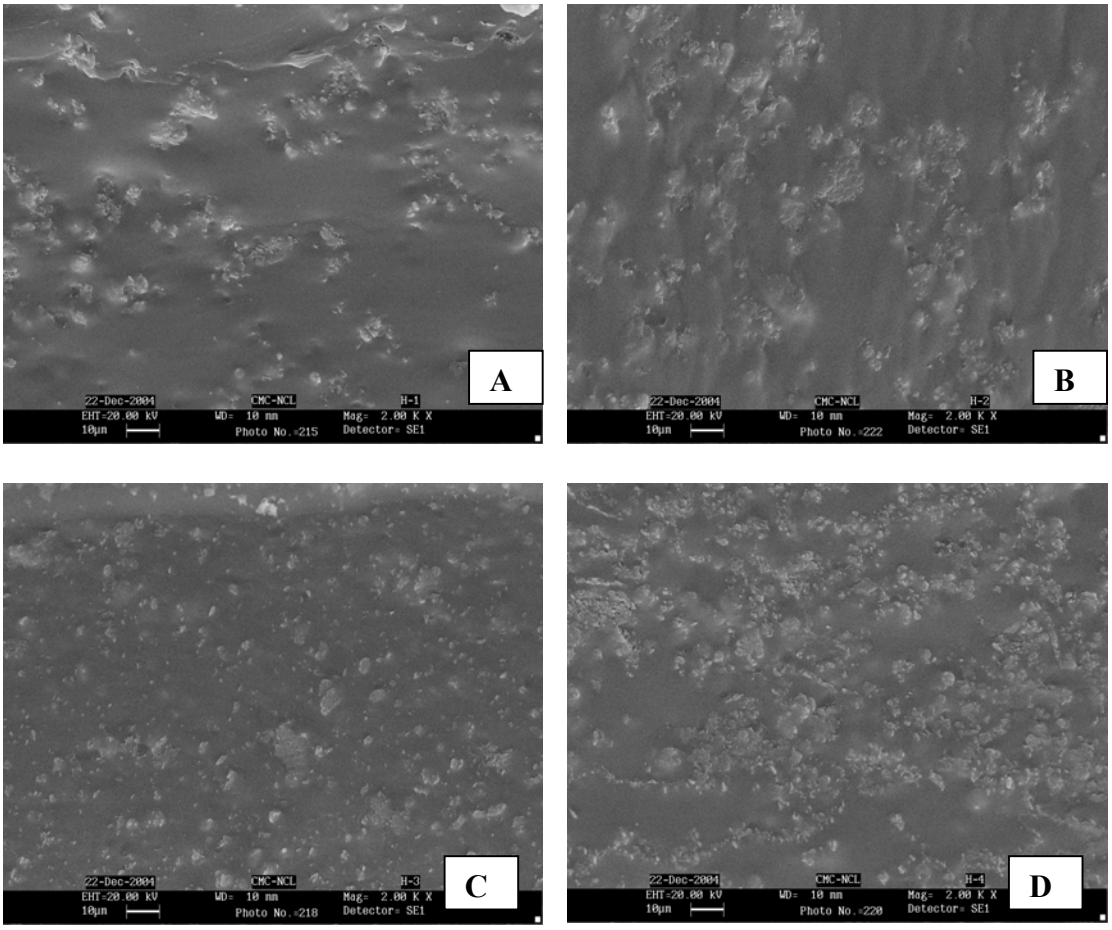

Figure-4.21. Scanning electron micrographs for SBS-PANI blends containing (A) 5%, (B) 10%, (C) 15 %, and (D) 20 % HCl-doped PANI

HCl-doped & 5%, 15% DBSA-doped PANI, respectively. Morphology was controlled by nature of dopant ion and it changes with the same. In the case of DBSA-doped PANI, the dopant acts as plasticizer and gives more compatible/finely dispersed blends, (Fig.4.22) where as HCl-doped PANI gives heterogeneous phase segregated morphology (Fig.4.21). The existence of two phases is distinctly noticed especially at low concentration of PANI (5%, Fig 4.21 micrograph-A). The regions rich in PANI appear as white agglomerate clusters, and these PANI clusters are surrounded by the SBS matrix (darker zone in

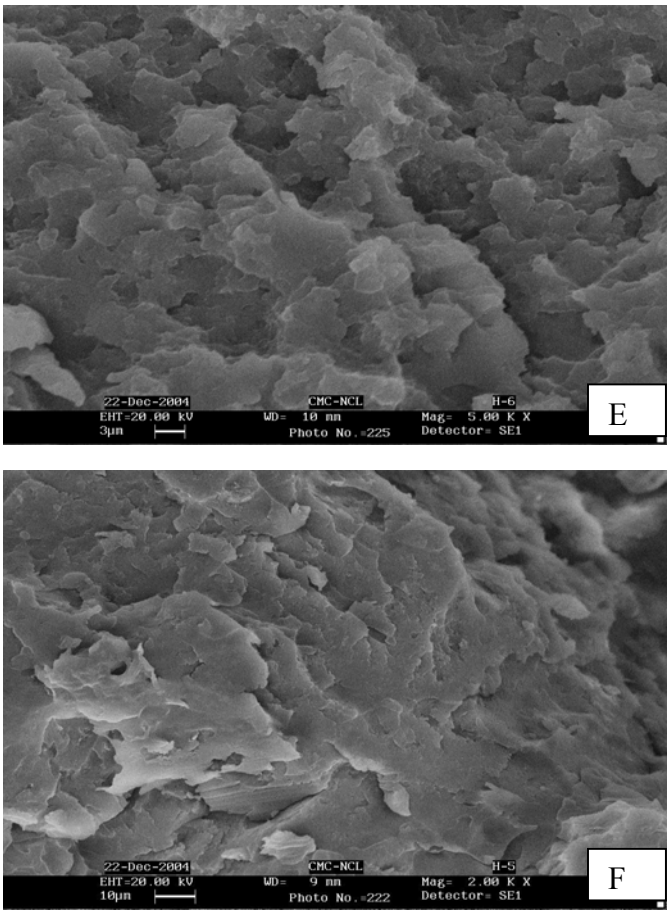

Figure-4.22. Scanning electron micrographs for SBS-PANI blends containing (E) 5% and (F) 15% DBSA-doped PANI

micrograph, Fig 4.21 micrograph-A). Although, at low PANI concentration in SBS matrix the PANI appears to exist as distinct, unconnected regions, a degree of connectivity must also exists between the visible conducting zones in order to facilitate the electrical conduction. By increasing PANI content in the SBS matrix (Fig.4.21, micrograph D), the interconnected nature of the PANI phase is much more apparent. Indeed, few distinct regions of SBS can be seen and the PANI phase appears continuous. More specifically, PANI particles in the SBS-PANI composites are seen to be distributed as small spherical granules in the matrix. On the contrary, the micrographs in Fig.4.22 reveal the fracture substrate without any particulate nature. In this case phase separation still remains even as the interfacial tension is acted between the DBSA protonated PANI and SBS matrix. In spite of the lower content of PANI, the PANI particles within the SBS matrix are well distributed due to the effect of sulfonation [13].

The average PANI particle size as determined by optical microscopy for the PANI (HCl & DBSA-doped) is found to be 10 μm & 2 μm, respectively (Fig. not shown). We have already explained in section 4.3.1 that, solubility of DBSA-doped PANI is much higher than that of HCl-doped PANI. Obviously, the particle size of PANI doped with DBSA is lower than that of HCl-doped PANI. We have considered that, conducting particles are well distributed in insulating matrix (in theoretical discussion chapter III, section-I). Here, we have measured interparticle distance 'd' between two PANI particle from micrographs of HCl-doped SBS-PANI composites and we have compared it with theoretical value calculated by using equation 4.3 (in section 4.3.6.2).

Table-4.3. Theoretical and experimental 'd' value of SBS-PANI (HCl-doped system) by using equation 4.3 and Fig.4.21.

System	PANI loading (%)	Theoretically calculated 'd' (μm) equation (4.3)	Experimentally measured 'd' (μm) Fig.4.21
SBS +PANI (HCl-doped) (D = 10 μm)	5	9.10	9.125
	10	5.71	6.33
	15	4.14	4.52
	20	3.20	3.41

The distance between two PANI particles determined experimentally matches well with that of theoretically calculated d value.

4.8.3. *I-V Characteristics*

The effect of morphology on the electrical properties of these conducting polymers is also manifested in the linear and non-linear both type of current-voltage (I-V) characteristics. The I-V characteristics of these blends were investigated without applying any mechanical load to the sample. These are depicted in Fig.4.23 (A) to (E) and Fig.4.24 (A) to (G) for different concentrations of HCl-doped PANI as well as DBSA-doped PANI in the blends, respectively. It is clearly seen that the I-V characteristics are not non-linear in all cases and their non-linearity changes with PANI concentration [23]. At low concentrations of PANI the I-V curves are slightly non-linear; at intermediate levels these become highly non-linear while at high levels of PANI these become linear.

The I-V characteristics for the HCl-doped SBS-PANI blends are found to be non-linear in nature when PANI content is limited upto 20 % as shown in Fig.4.23. Further increase in

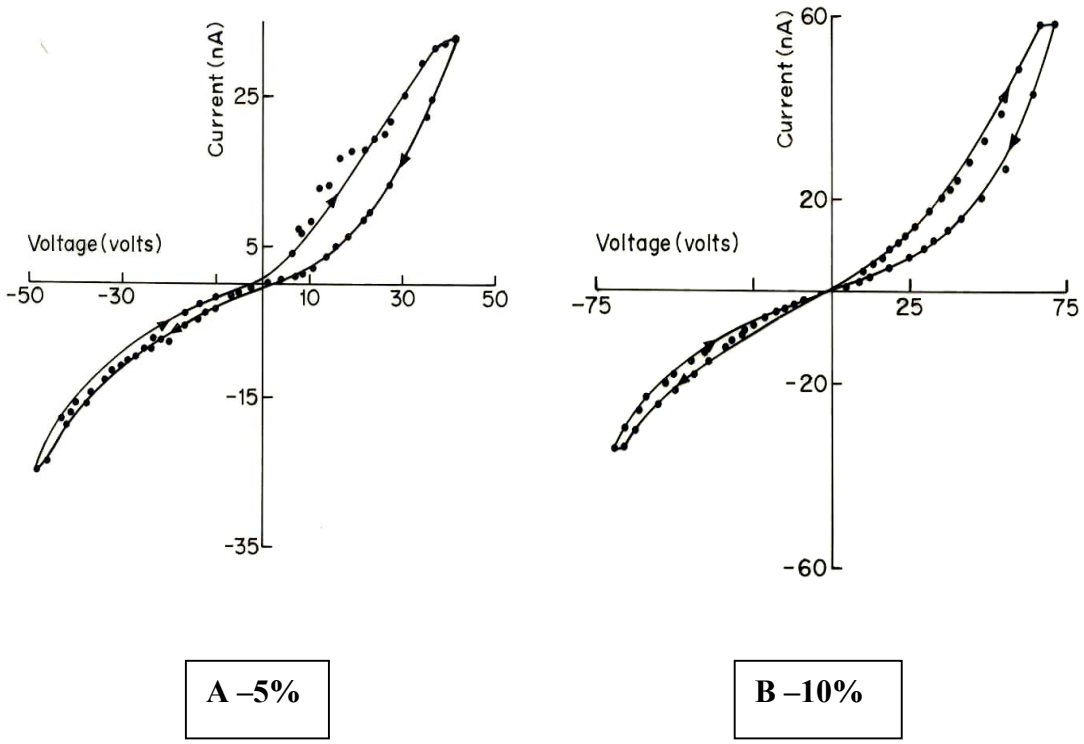

Figure. 4.23. I-V characteristics for SBS-PANI blend containing (A) 5%, (B)10% HCl-doped PANI

the concentration of PANI tends to exhibit linear I-V characteristics as depicted in Fig.4.23, curve-E. On the other hand, the DBSA-doped SBS-PANI shows non-linear I-V plot when PANI content in SBS elastomer kept to be as low as 3% (Fig. 4.24, curves- A, & B). Higher loading of PANI than 3% linearity is observed in I-V characteristics (Fig.4.24, curves-C-G). Moreover, the degree of non-linearity was found to depend on PANI concentration, and it shows maxima (non-linearity) in certain composition of these blends. The non-linear I-V characteristics for the conducting polymer blends or

composites arise from the various types of charge transport processes present at the inter-domain gaps. Such non- linear characteristics can arise from non-ohmic charge transport

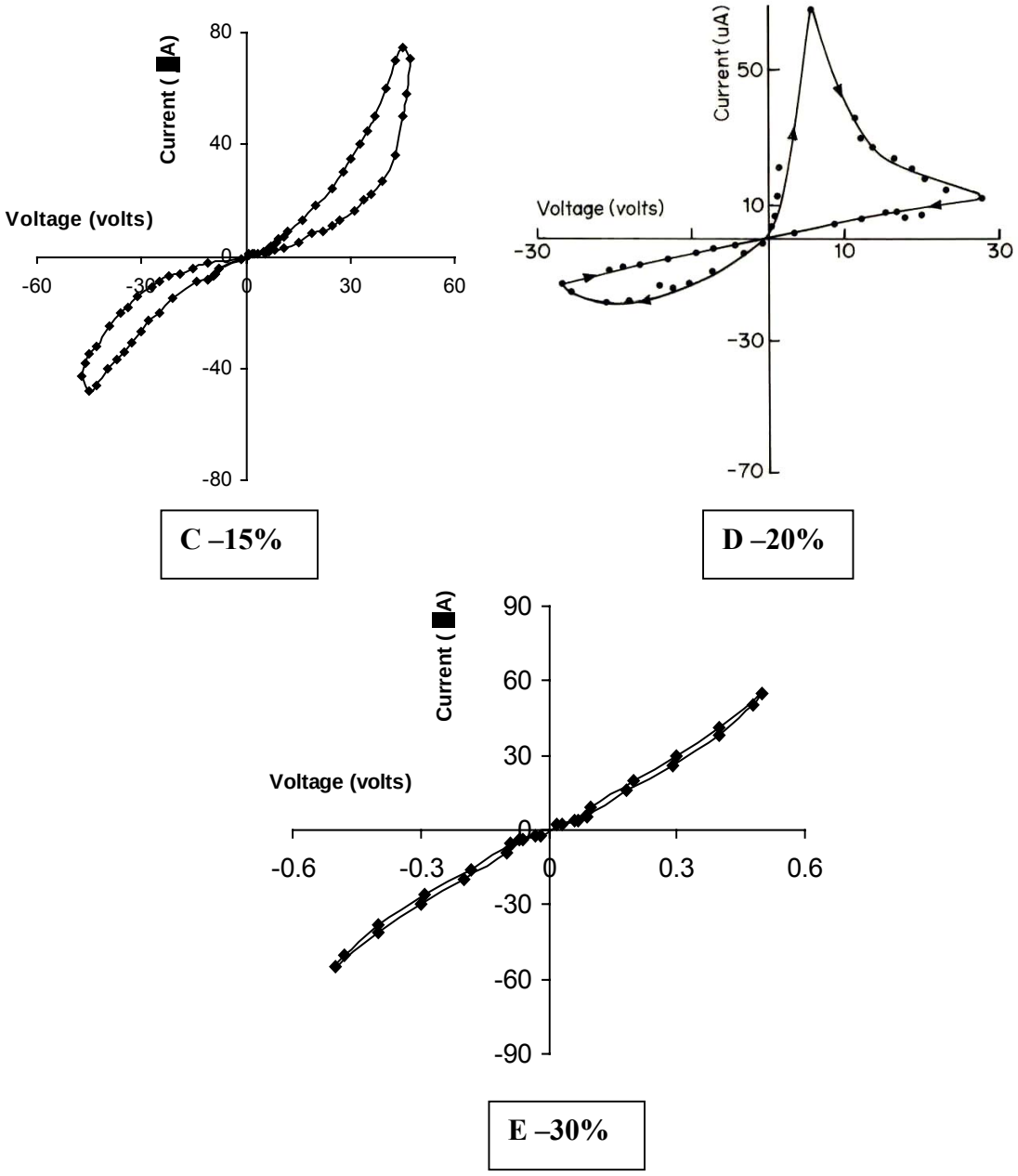

Figure-4.23. I-V characteristics for SBS-PANI blends containing (C) 15%, (D) 20%, (E) 30%, HCl-doped PANI

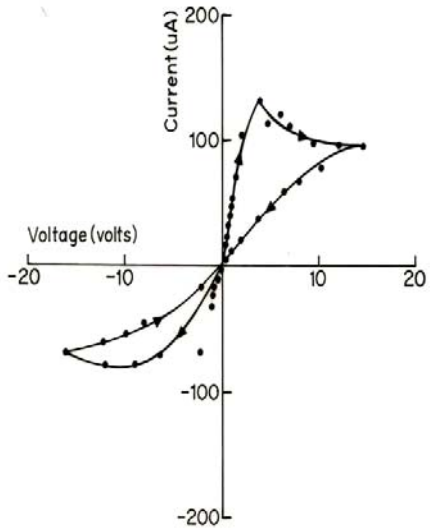

A -2%

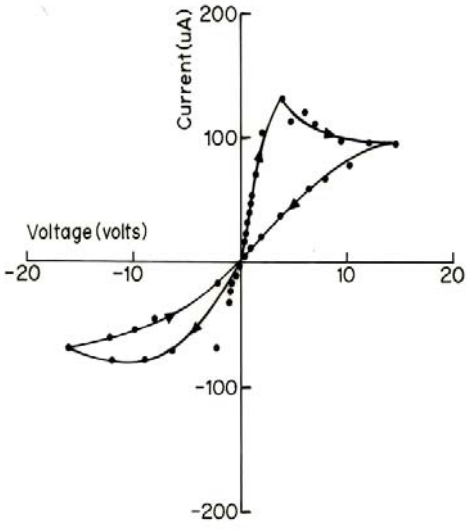

B -3%

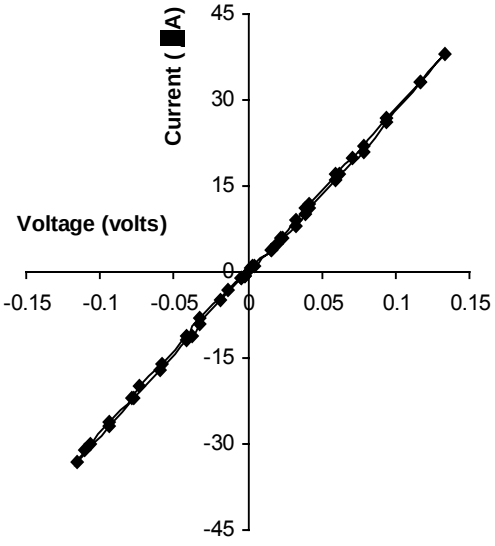

C -5%

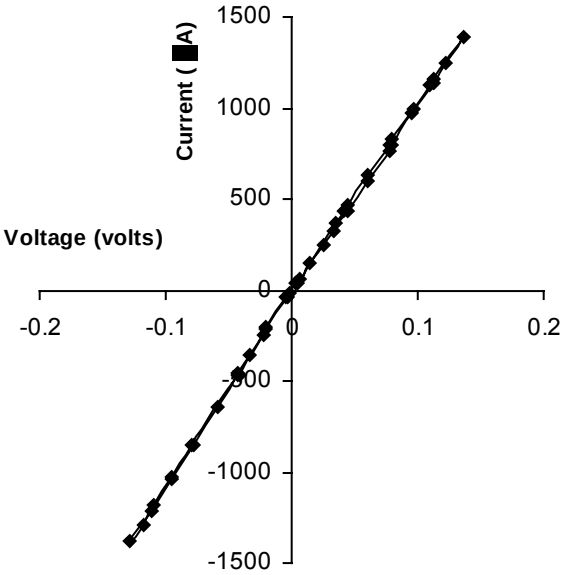

D -10%

Figure-4.24. I-V characteristics for SBS-PANI blend containing (A) 2%, (B) 3%, (C) 5%, (D) 10% DBSA-doped PANI.

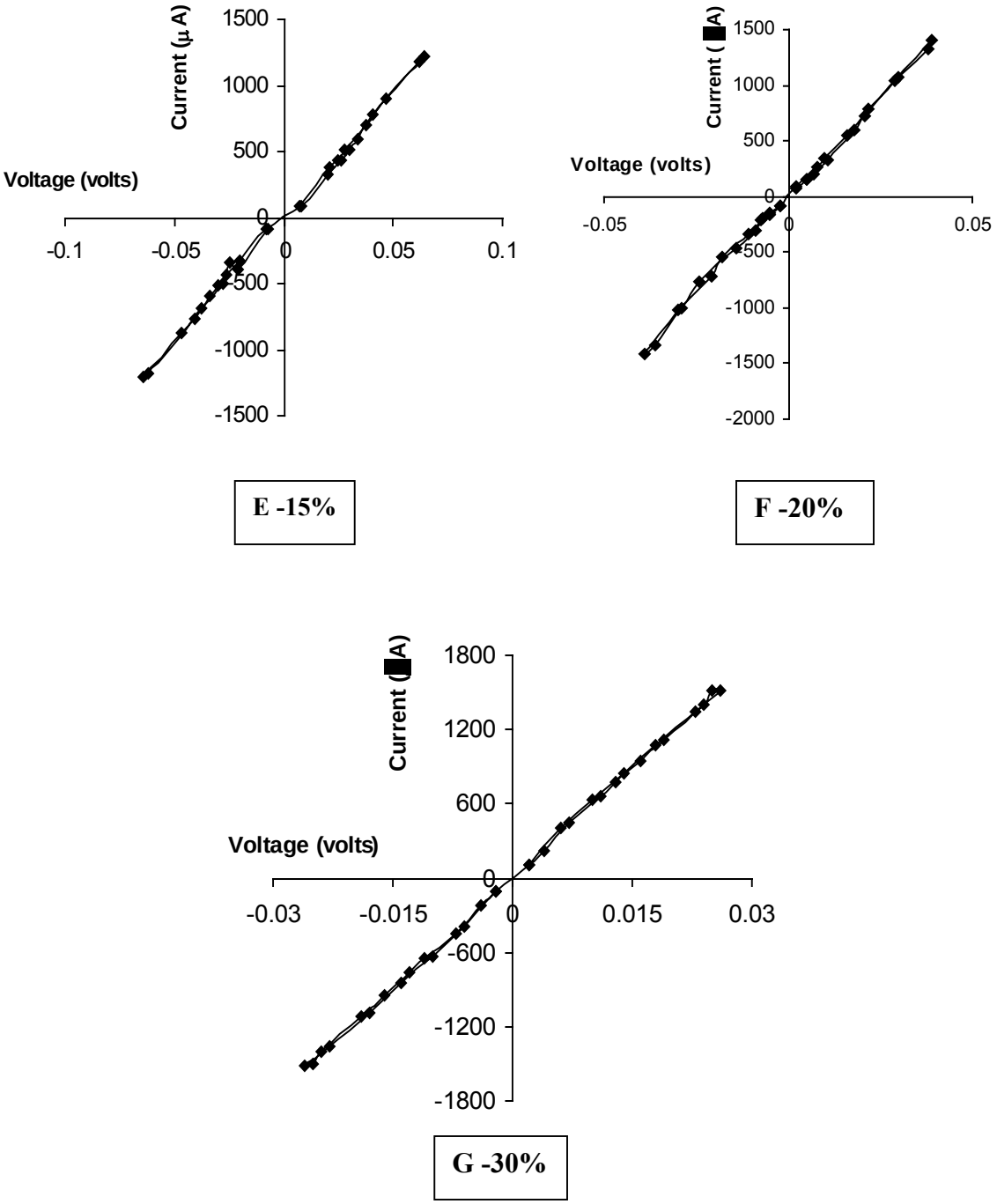

Figure–4.24. I-V characteristics for SBS-PANI blends containing (E) 15%, (F) 20%, (G) 30%, DBSA-doped PANI.

process such as space charge limited conduction (SCLC) [24]. A detailed discussion on these along with the theoretical model for the conductivity especially in the context of conducting polymeric composites is given earlier (chapter III, section-I) of this thesis and elsewhere [25-28, 29] in which it was described that such non-linear phenomena can have profound effect on the piezo-sensitivity of the material. In brief, this essentially considers the composites as a series of junctions formed by the conducting-insulating-conducting elements and, at each of these, the current is non-ohmic in nature which when added together gives rise to an overall non-linear characteristics for the composites at the macroscopic level. In order to determine exact mechanism of the charge transport, a detailed analysis of the I-V characteristics was carried out.

The I-V characteristics were analyzed in detail in section 4.3.3. The I-V curves were then analyzed for charge transfer process by making a plot of log I against log V. The plots were found to delineate into two straight lines as exhibited by Fig. 4.25 (curves A-C). The slopes of the plots were found to change from 1 to 2 i.e. at low voltage, corresponding to an ohmic conduction (n = 1) [a], which then becomes SCLC type with a single discrete set of shallow traps (n = 2) [b], finally trap-filled region [c] [30]. The V_{crit} is the critical voltage at which the curve passes from the ohmic to the non-ohmic region and it is given in chapter-I to be dependent on the interparticulate distance 'd' [31,32]. As the PANI content in the composite increases, the value of the V_{crit} shifts to lower voltage side and the curve becomes more and more non-linear (equation-4.2), which is in accordance with these expectations.

Somani et al.[23] also found same observation about shifting of V_{crit} with composition. This

type of behaviour is encountered in the case of SCLC type of conduction mechanism as discussed in 1.7.8.3.3. The change in the slope of log I versus log V plot thus can be ascribed to filling of the traps. Hence, it is reasonable to state that the SCLC behaviour observed in case of SBS-PANI blends arises due to a space charge region developed at the interface of SBS/PANI blends.

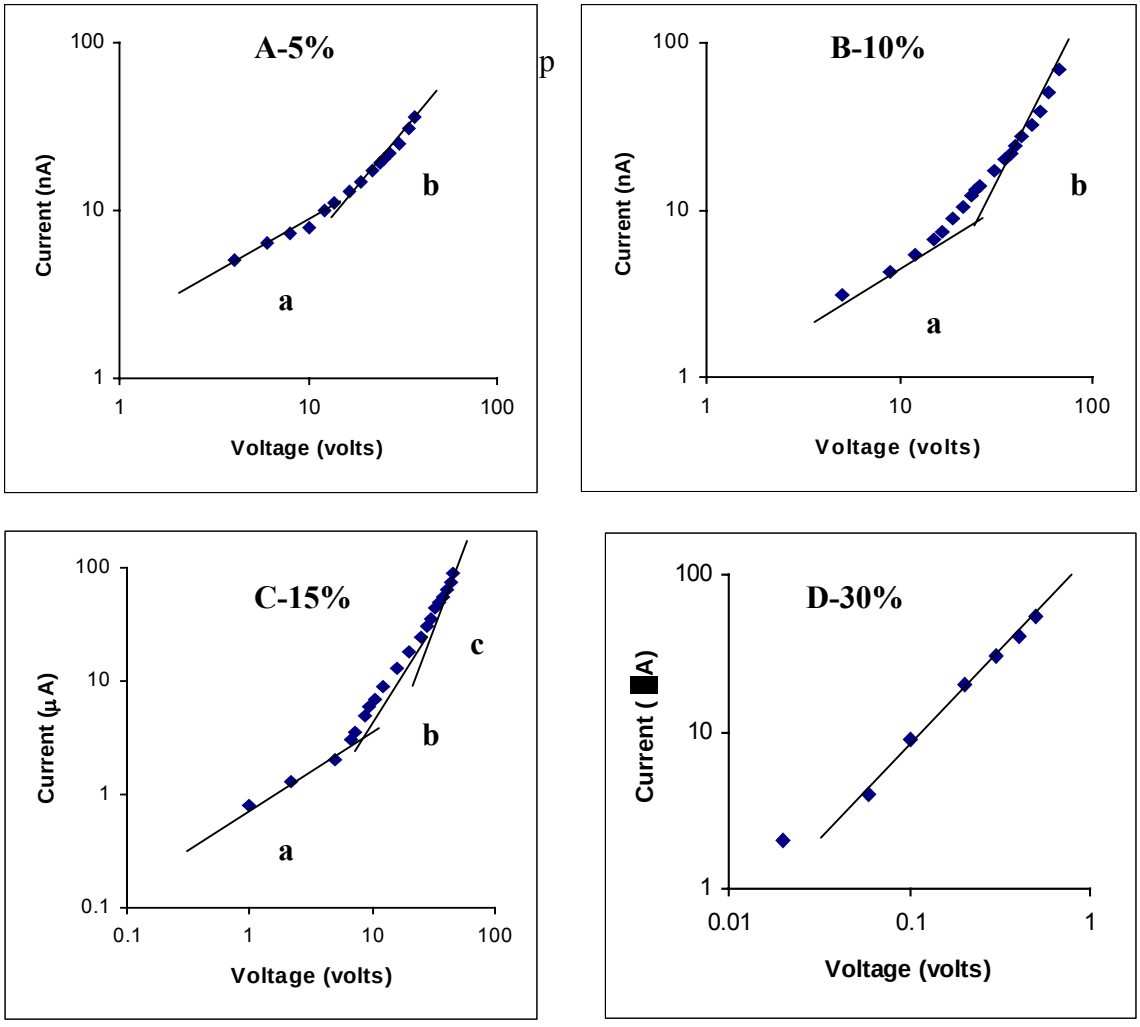

Figure–4.25. log-log plot of I-V characteristics for SBS-PANI blend containing (A) 5%, (B) 10%, (C) 15%, (E) 30% HCl-doped PANI

If the contacts to the electrode are ohmic, then the electrodes acts as an abundant source of charge carrier which can be injected into the solid. At sufficiently high fields, the blend unable to transport all the injected charge and a build up of charge begins within the solid. Traps are generated in the PANI owing to the dopant ions. The conduction proceeds by filling up of these traps depicting SCLC behaviour. This causes a change in the conduction behaviour from ohmic at lower voltage to a square law at higher voltages (explained in 4.3.3). This explanation holds good in the case of blends wherein each PANI particle is presumed to form a junction at the SBS interface and these junctions when connected in series and parallel exhibit a net effect as in the I-V characteristics. The hysterisis in the I-V characteristics clearly implies charge storage in the sample. It can be concluded from the above studies that the blend system consists of several discrete junctions, which are connected together giving rise to a multiple junction effect. These junctions exist only till the percolation threshold where after they form particle-to-particle contacts giving rise to a polyaniline network. The conduction occurs by hoping process in the blends containing higher PANI and shows linear I-V characteristics (though these may have some frequency dependent conductivity).

Apart form non-linear I-V characteristics observed in the present work, some peculiar features like appearance of peak in I-V plot, negative resistance value above certain applied voltage are also noticed. These characteristics are reminiscent of tunneling type behaviour in thin film semiconductor/insulator structures [33, 34]. The Fowler Nordheim type tunneling (equation4.4) takes place only at high concentration of the conducting phase (or very small inter-particle distance) and the resistance is given by ;

$$V/I = R_{TN} = \frac{(L-d)\Delta d^2}{3.38 X 10^{10} V_X D^2 (D+d)} \exp \frac{0.69 \Delta^{3/2} d(L-d)}{V_X (D+d)} \quad (4.4)$$

where all the symbols have their usual meaning.

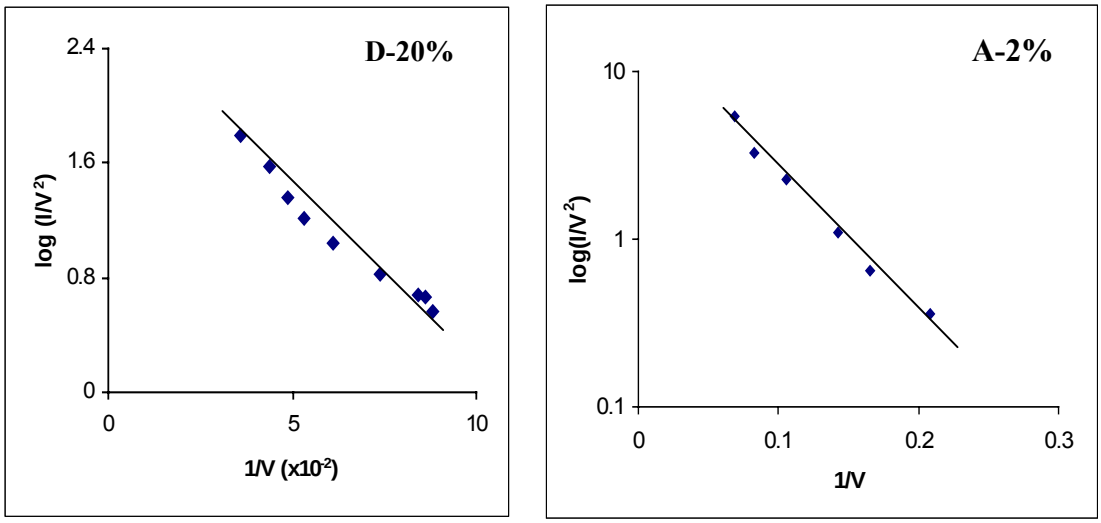

Figure-4.26. I-V Characteristics for SBS-PANI blend containing (D) 20% HCl-doped PANI and (A) 2% DBSA-doped PANI

Fig. 4.26, curve-D and A, shows the Fowler Nordheim plot, log (I/V^2) against (1/V) for the 20 % and 2% loading of HCl and DBSA-doped PANI in SBS matrix, respectively. Tunneling will be effective when two conducting particles are placed at certain minimum distance 'd' for high probability for tunneling of carriers. However, at higher loading of PANI in the matrix, there is no barrier left and the I-V characteristics become more linear. This has been well reflected in our results where in at

higher loading of PANI such as 30% for HCl-doped (Fig. 4.25) and 5 or 10% for DBSA doped (Fig. 4.27), the I-V characteristics are found to obey ohms law. Here, it is

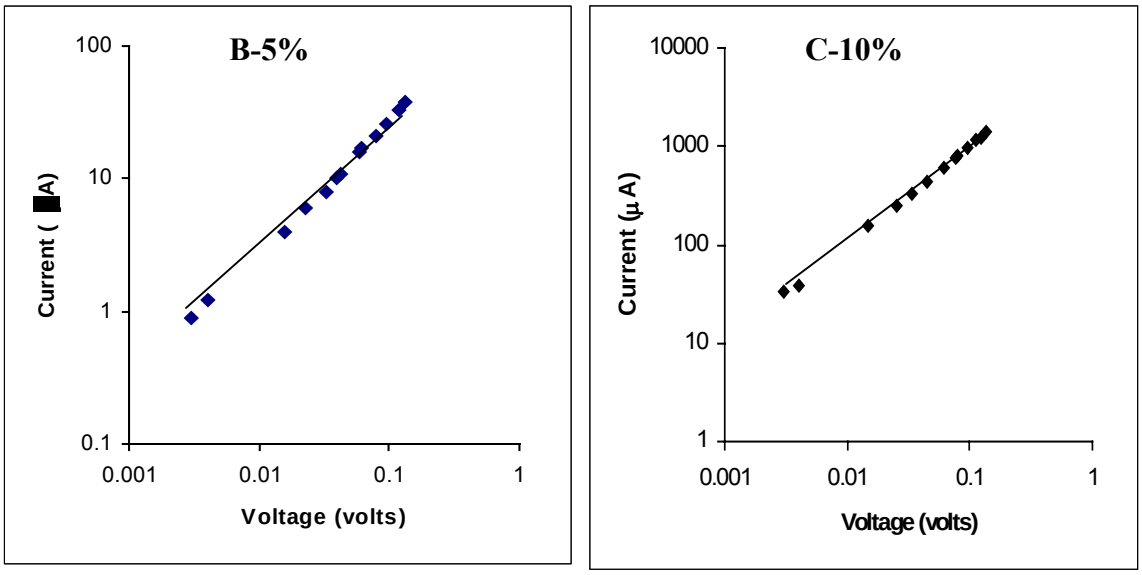

Figure-4.27. I-V Characteristics for SBS-PANI blend containing (B) 5%, (C) 10% DBSA doped PANI

important to recollect that this amount of PANI loading lies well above the percolation threshold and conduction occurs mainly via continuous phase of PANI embedded in SBS matrix. As a consequence shorting of SBS /PANI barriers occur preferentially resulting in to linear I-V characteristics. The results clearly suggested that at low PANI concentrations, the electrical properties of SBS-PANI blends are mainly governed by SCLC mechanism whereas increasing amount of PANI loading tunneling type characteristics plays important role.

4.8.4. *Piezo-Sensitivity*

4.8.4.1. *Dependence of the Piezo-Sensitivity on Pressure*

The effect of mechanical pressure on electrical resistance of these blends was studied only in compression mode. Logarithmic plot of pressure dependence of resistance of the SBS-PANI blends, containing different amount of HCl & DBSA-doped PANI are shown in Fig. 4.28 & 4.29. The sample and electrode dimensions were kept same in all the

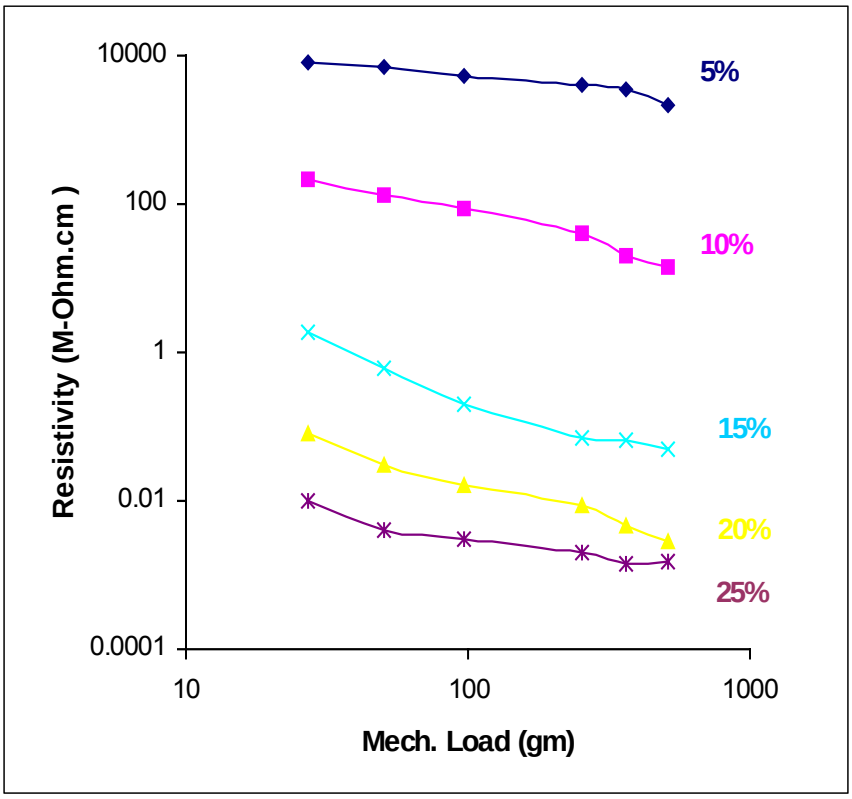

Figure-4.28. Pressure dependence of electrical resistivity of SBS-PANI (HCl) blends on log-log scale

samples studied. During piezo-resistivity measurements, the load was always applied in a direction parallel to electrical current flow . It can be seen that in all samples , the

resistivity decreases monotonically with increase of mechanical load, but the extent of decrease with samples having 10% & 15% PANI (HCl-doped) are larger than remaining samples (Fig. 4.28). Similar results are obtained for DBSA-doped PANI blends except

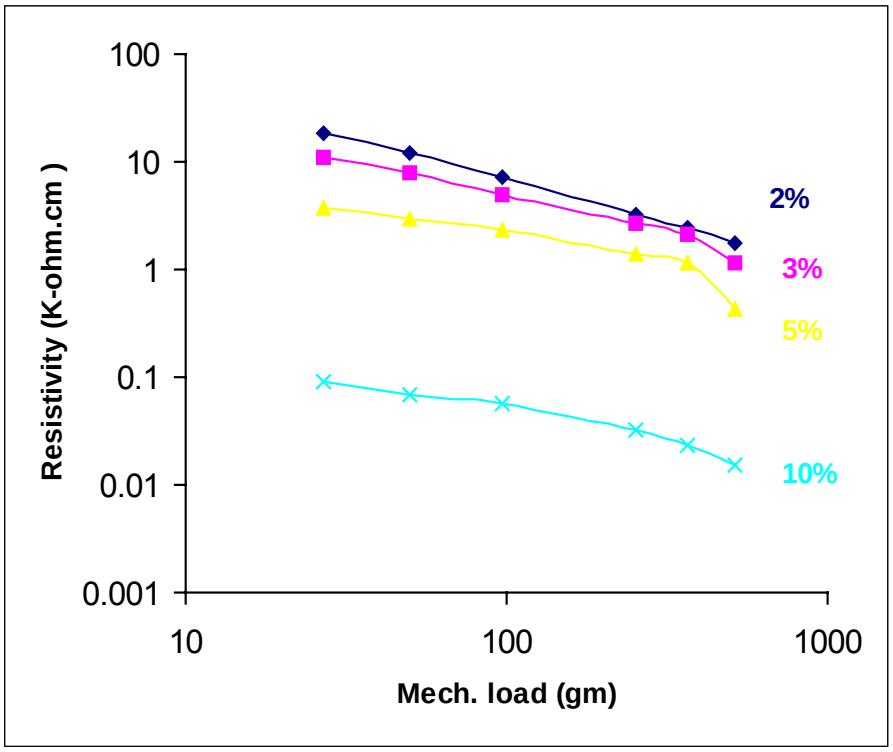

Figure-4.29. Pressure dependence of electrical resistivity of SBS–PANI (DBSA) blends on log-log scale

that decrease in resistivity is sharper at much lower PANI-DBSA content (i.e. 2 to 5%) (Fig. 4.29). It is evident from these curves that the pressure (P) dependence of resistance (R) in all the samples followed the power law $R = KP^{-m}$ where, K is a constant and m is an exponent which depends on the composition of the sample [35]. Both K & m were determined for all the samples by fitting the log-log plots of resistivity versus pressure values are given in table 4.4. SBS-PANI blends containing 15% HCl-doped PANI and

Table-4.4: Calculated values of K & m in SBS-PANI blends

System	PANI loading (%)	Value of K *	Value of (m) *
SBS+PANI (HCl- doped)	5	33048	0.4003
	10	4910	0.9159
	15	74	1.215
	20	2.14	1.044
	30	0.055	0.6068
SBS+PANI (DBSA-doped)	2	265	0.7916
	3	128	0.7118
	5	34	0.6294
	10	0.701	0.5855

* The exponent values in the equation $R = K P^{-m}$ obtained by curve fitting.

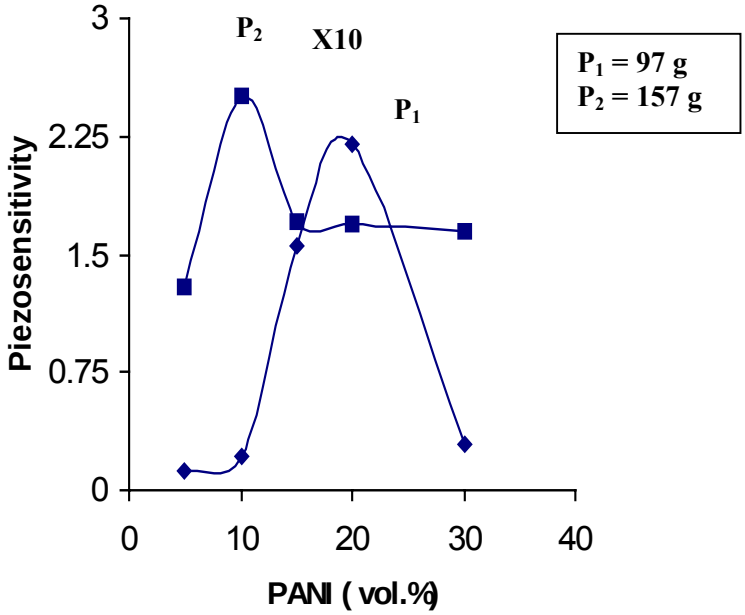

Figure-4.30. Effect of applied pressure on the maximum of piezo-sensitivity factor for different compositions in HCl-doped SBS-PANI blends.

2% DBSA-doped PANI shows higher m values than rest of the compositions. Higher the value of m higher will be piezo-sensitivity and the results obtained in the present work are in accordance with this observation. Moreover, it suggests that the pressure

dependence of the electrical resistance is non-linear and depends very much on the composition as well as the type of PANI incorporated in the blend. Our results matches well with reported one [12].

Fig. 4.30 showed that piezo-sensitivity pass through maximum at certain concentration at any pressure (load) and that maxima will shift lower particle concentration with increasing load [10]. This might be due to the charge stored under constant applied field is getting liberated during the application of pressure due to overlap of the levels and /or increase of contact area giving rise to additional current in forward direction.

4.8.4.2. ***Dependence of the Piezo-Sensitivity on Composition***

A prominent feature which imerges from the results described in previous section that the piezo-sensitivity factor is highly governed by the concentration of the conducting phase. In this section we will see how the piezo-sensitivity varies by varying interparticle distance 'd'. The interparticle distance is directly related to conducting phase (ϕ) by equation 4.3. Using this equation we have determined interparticle distance for our uniformly disperse two phase systems described in the phenomenological model [29] and plotted in Fig. 4.31 as a function of volume % of PANI in SBS matrix.

It has been already shown that the resistance of the sample changes non-linearly with respect to 'd' . During application of external mechanical pressure load, the interparticle distance changes giving rise to rapid change in electrical resistance as $R \propto (d)^{p+1}$. Thus, small change in 'd' gives large change of R. To get maximum piezo-sensitivity, the value in 'd' will be small while at high PANI concentration, 'd' tend to zero as the particles touch each other . Accordingly , the piezo-sensitivity will also change with the

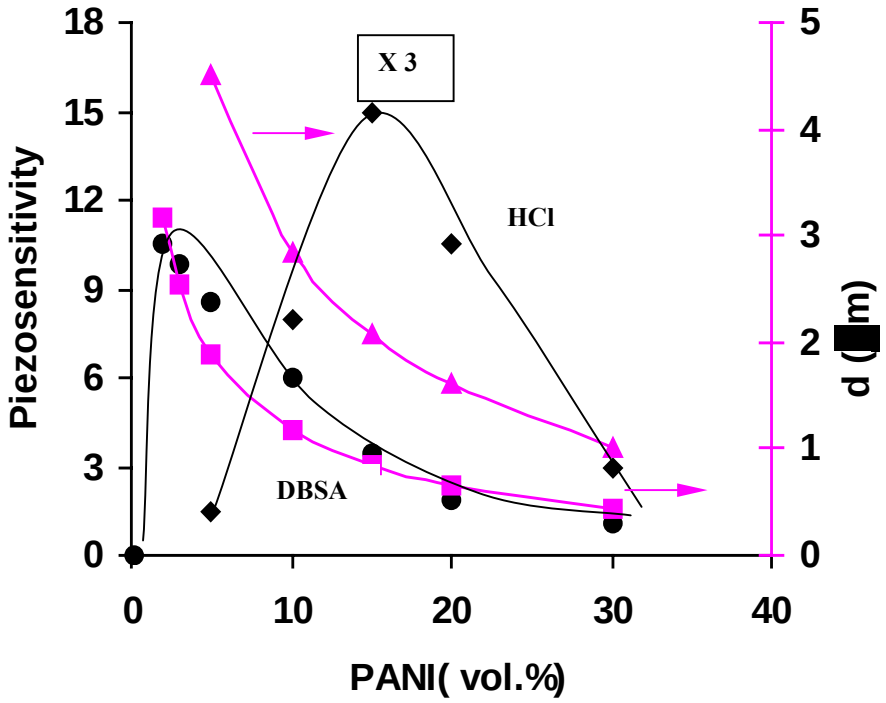

Figure-4.31. Compositional variation of piezo-sensitivity and interparticle distance (d) in SBS-PANI blends with HCl and DBSA system.

composition & it shows maxima at certain critical composition at which 'd' is optimized. of 'd' should be optimum since its change with applied mechanical pressure will decide the change in sample resistance. For low polyaniline loading, 'd' will be large but change in 'd' will be small while at high PANI concentration, 'd' tend to zero as the particles touch each other. Accordingly, the piezosensitivity will also change with the composition and it shows maxima at certain critical composition.

4.8.4.3. ***Dependence of the Piezo-Sensitivity on Non-linear I-V Characteristics***

Piezo-sensitivity is highly dependent on the charge transport phenomena. In the case of space charge limited conduction (SCLC) it has been shown earlier [29] that the piezo-

resistivity of the conducting polymer composites is much higher than that obtained in ohmic type conduction. The present studies are well in agreement with this observation. In fact it reveals that piezo-sensitivity is higher when charge transport is SCLC type than the tunneling type conduction. This may arise from the lower dependence of current on thickness (here inter-particle gap 'd') and lack of charge storage in the latter as compared to the SCLC case.

4.8.4.4. ***Comparison Between Theoretical and Experimental Values of Piezo-Sensitivity***

The piezo-sensitivity factor (S) for various compositions is shown in Fig. 4.32 and 4.33 for the HCl and DBSA-doped PANI, respectively. The theory of electrical conductivity or resistivity of conducting composites, taking into account for the various conduction process, has been described in details elsewhere [25-28] in the thesis. Sensitivity factor S is derived and mentioned in section-I in chapter III.

$$S = \frac{1 - \left(\frac{d_0}{D + d_0}\right)(\alpha P)^{\beta}}{1 + \left(\frac{d_0}{L - d_0}\right)(\alpha P)^{\beta}} \quad \frac{1}{[1 - (\alpha P)^{\beta}]^{n+1}} \qquad (4.5)$$

The piezo-sensitivity factor will depend on N_{eff}, where N_{eff} = [Ns x Np x f(φ)], and f(φ) is a function (polynomial) of (φ) the volume fraction of conducting phase. The net piezo-sensitivity factor will be then given as,

$$S_t = N_{eff} \times S = Ns \times Np \times S \times f(\varphi) \qquad (4.6)$$

The net sensitivity factor (S_t) was evaluated from equation (4.6) using typical values of

various parameters: L = 470 μm, n = 2, P = 100 gm, E = 1/α = 30 MPa for matrix polymer without any conducting particles and different E values are calculated for each PANI loading by using parallel model for evaluating the modulus of composites [36],

$$E = \Phi_m / E_m + \Phi_c / E_c \qquad (4.7)$$

where, E is the Youngs modulus of resulting composite, Φ_m and Φ_c is the volume fraction of insulating matrix and conducting particles respectively, E_m and E_c is the Young modulus of insulating elastomer matrix (30 MPa) and conducting polymer (here polyaniline, 2200 MPa), respectively [37]. The set of d_0 values were calculated by using equation 4.3. The net sensitivity factor (S_t) was evaluated from equation 4.6 using the β = 0.12 for PANI-HCl system and β = 1 for PANI-DBSA system, respectively. The polynomial is $f(\varphi) = 1 - z_1(\varphi) + z_2(\varphi^2) - z_3(\varphi^3)$ where, $Z_1 = 15$, $Z_2 = 95$, $Z_3 = 120$, respectively. Fig. 4.32 (A) and (B) and Fig.4.33 (A) and (B) depict the variation of piezo-sensitivity with composition and modulus for the two systems studied.

The experimentally determined graphs are also shown in these figures for comparison. These figures showed that there is very strong similarity in the nature of the graphs, which clearly brings out the fact that there is a composition of the conducting polymer blend at which the piezo-sensitivity is maximum. These figures also indicate that the phenomenological model based on the non-linear effects gives better understanding of the processes responsible for the observed behaviour for piezo-response of the conducting polymer blends. Dopant concentration influences the total resistance, and the piezo-sensitivity. Increasing dopant concentration increases the number of carriers, however if dopant concentration is too high the sensitivity decreases. In addition, high

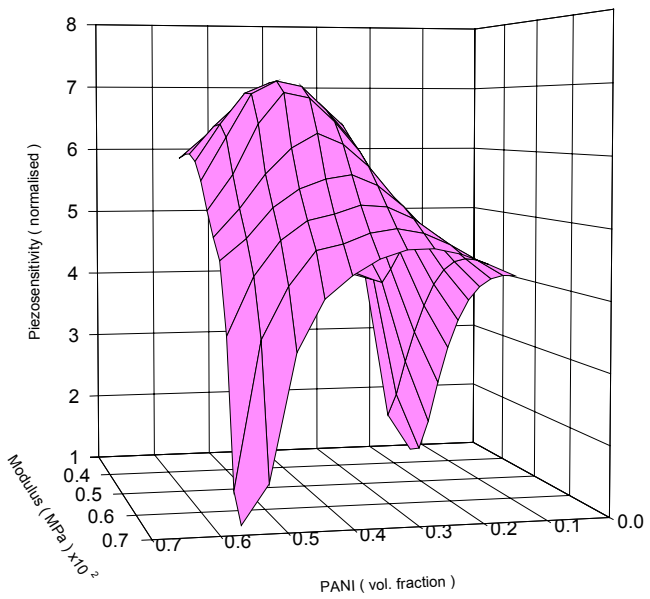

A

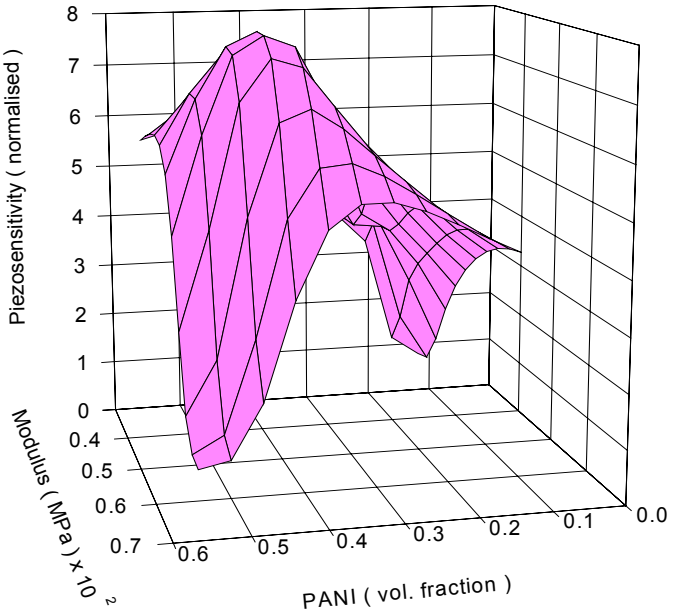

B

Figure-4.32. Comparison of (A) theoretical with (B) experimental values of piezo-sensitivity with respect to modulus of blends as well as volume fraction of HCl-doped PANI.

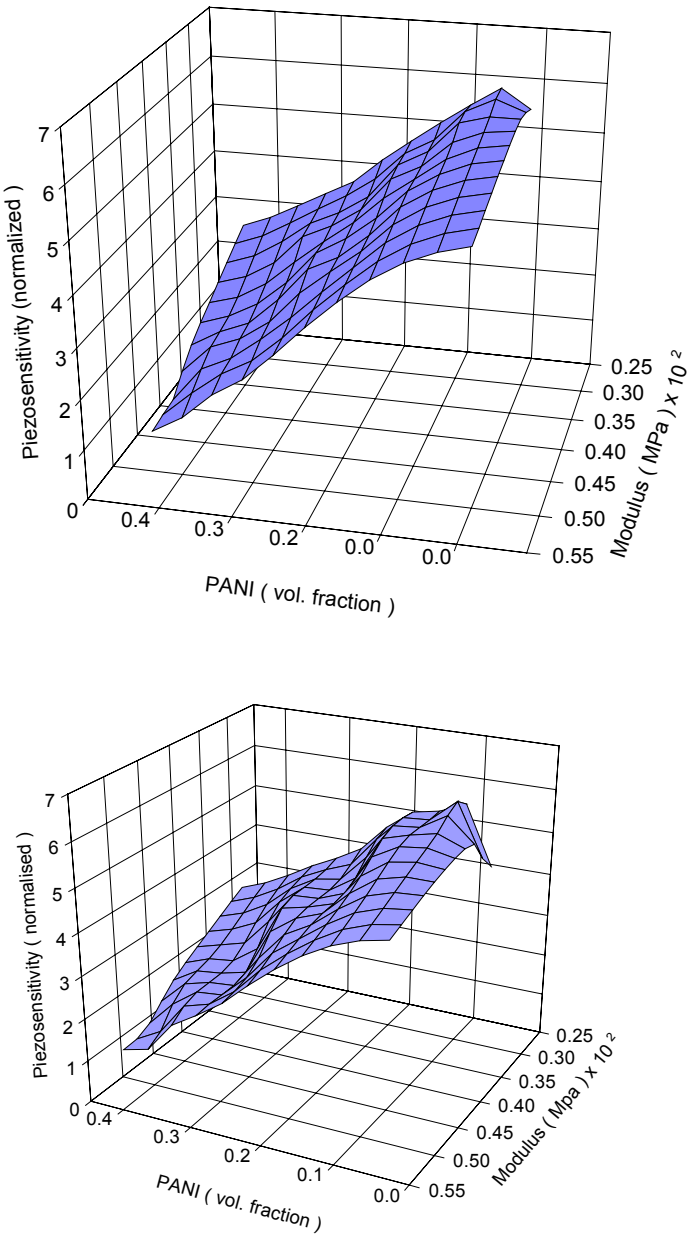

Figure-4.33. Comparison of (A) theoretical with (B) experimental values of piezo-sensitivity with respect to modulus of blend as well as volume fraction of DBSA-doped PANI.

dopant concentration also lowers total resistance and consequently increases the power consumption for a fixed bias voltage, which reduces the sensitivity further. Therefore choice of appropriate doping level is necessary for getting optimum piezo-sensitivity. This conclusion is also in agreement with the results obtained by Harley and Kenny who got high piezo-sensitivity at the optimum dopant concentration [38]. Of course the exact value of the piezo-sensitivity has not been evaluated and this is also very difficult to carry out keeping in view the differences in the various assumptions made in the theory and the actual experimentation especially as regards the uniformity of dispersion, affect of plasticizing effect of the dopant, exact change of modulus with composition, etc. None the less, a good insight can be obtained with the help of the phenomenological model as regards the overall behaviour.

It is evident from these that there is an overall agreement between the nature of the graphs i.e. the piezo-sensitivity in these blends is optimum at certain composition and the modulus of the matrix as well as the particle size of the dispersed conducting phase are important factors in determining the sensitivity factor.

4.8.4.5. *Typical Piezo-resistor Design*

PANI was dispersed in matrix polymer viz. elastomeric materials (SBS). Thin sheets were either casted or were films deposited in patterned array. Piezo-sensitivity was determined as a function of pressure, by measuring the output voltage. Fig. 4.34 shows the typical piezo-resistor device made from SBS-PANI blend (HCl-doped), It acts as an one of the resistance of four-arm resistance circuit. Specification of this device is given below.

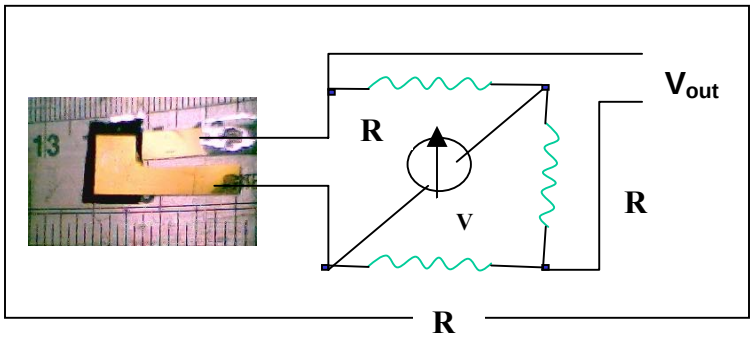

Figure-4.34. Schematic view of piezo-resistor device

Table- 4.5: Peizo-sensor specification

Electrical

Output voltage	0 – 3.0 V (depending on pressure)
Supply voltage	3 Volts DC
Supply voltage sensitivity	< 0.1%
Typical current consumption	10 µA
Minimum load resistance	5 K-ohm.
Load range	20-500 gm/cm^2
Best performance load	50-200 gm
Response time	< 1 Sec

Mechanical

Materials	SBS-PANI (HCl-doped) film
Area of Sensor	1 cm^2
Thickness of Sensor	200 µm
Wight of Sensor	< 1 gm

Others

Electrical Connection – Open
Free mounting
Environmentally Stable

4.8.4.6. *Quasi-Static Sensing Property of Piezo-resistor Device*

The experimental set up was such that the tip of the lever of mechanical load as shown in Fig.4.35 was mechanically pressed and released, and the corresponding output resistance was recorded. When films are disturbed by means of a shock or loading, an electrical response is observed as shown in Fig. 4.35. It shows the typical response curve for SBS–PANI (HCl-doped) composite with applied mechanical pressure and release of pressure. From the Fig. 4.35 it is clearly evident that the response is reproducible, fast and recovery is quick with practically no hysteresis. Further, the sample has sensitivity even at low mechanical pressure. The height of the peak depends on the actual weight applied. From these curves, one can also calculate the sensitivity factor. This particular property of films may find a large number of applications in large pressure sensing devices for a variety of industrial applications. Since these materials can also be cut as small as one desires, they present a tremendous potential to micro-electro-mechanical systems (MEMS) sensing applications.

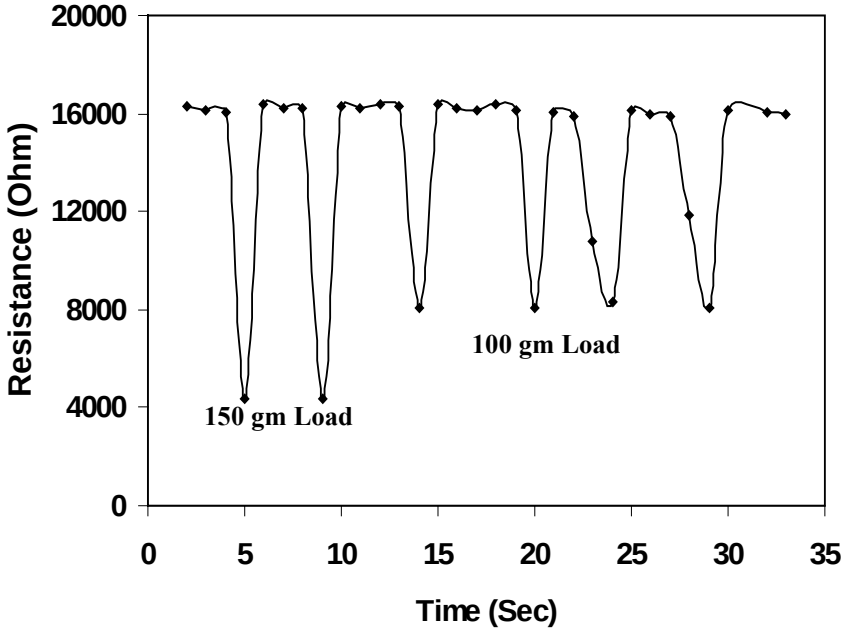

Figure-4.35. Resistance changes in SBS-PANI (HCl-doped) with loading-unloading cycle of mechanical load

4.9. Conclusions

SBS-PANI conducting blends are good candidates for piezo-sensor application. However for obtaining good performance one has to use optimum concentration of PANI. The blends containing 15% of HCl doped and 2% DBSA doped PANI appears to be best for giving higher piezo-sensitivity. In the case of DBSA-doped PANI, the dopant acts as plasticizer and gives more compatible/finely dispersed blend. This type of morphology is not amenable for obtaining high piezo-sensitivity whereas the HCl-doped PANI gives phase segregated morphology and better piezo-sensitivity. It may be pointed out that the conducting polymer blends which are essentially non-compatible behave more akin to composites and the results reported on such materials reported earlier by other authors are in keeping with the observations made in the present thesis. For example, the detailed

analysis of the data reported by others authors when analyzed fit the SCLC type behaviour and show similarity to our experimentally determined values for K & m. Pressure dependence of the electrical resistance is non-linear and depends very much on the composition as well as the type of PANI incorporated in the blend. The present studies indicate that the piezo-sensitivity is higher for the compositions having SCLC type charge transport than ohmic or even the tunneling type conduction.

4.10. References

1. A.C.Partridge, M.L.Jansen, W.M.Arnold, Materials Science and Engineering C, **12**,2000,37.

2. P.Bruschi, F.Cacialli, A.Nannini, Sensors and Actuators, A: Physical, **32**,1992,313.

3. A.Das, K.C.Santra, J.Sound and Vibrations, **197**,1996,515.

4. L.Cui, J.Swann, AGlidle, J.R.Barker, J.M.Cooper, Sensors and Actuators, B: Chemical, **66**,2000,94.

5. M.Shikida, T.Shimizu, K.Sato, K.Itoigana, Sensors and Actuators, A: Physical, **103**,2003,213.

6. H.H.Hassan, S.A.Khairy, S.EI–Guiziri, M.Eabdel–Moeim, J.Appl.Polym.Sci., **42**,1991,2883.

7. S.Radhakrishnan, D.R.Saini, Polymer Int., **34**,1994,111.

8. Zhong-Xing Bao, C.X.Liu, N.J.Pinto, Synth.Met., **87**,1997,147.

9. Zhong-Xing Bao, F.Colon, N.J.Pinto, C.X.Liu, Synth.Met., **94**,1998,211.

10. P.R.Somani, R.Marimuthu, U.P.Mulik, S.R.Sainker, D.P.Amalnerkar, Synth.Met., **106**,1999,45.

11. R.C.Patil, S.Radhakrishnan, S.Pethkar, R.Vijaymohanan, J.Mater.Res., **16**,2001,1982.

12. Hong-Euan Xie, Yong-Mei Ma, J.Appl.Polym.Sci., **77(10)**,2000,2156.

13. Hong-Euan Xie, Yong-Mei Ma, Jun-Shi Guo, Polymer, **40**,1998,261.

14. F.Lux, Polymer, **35**,1994,2915.

15. Y.Cao, A.Andreatta, A.J.Heeger, P.Smith, Polymer, **30**,1989,2305.

16. S.Radhakrishnan, S.Unde, J.Appl.Polym.Sci., **71**,1999,2059.

17. S.Radhakrishnan, D.R.Saini, J.Mater.Sci., **26**,1991,5950.

18. A.K.Bhowmick, H.L.Stephens, Handbook of Elastomers, Marcel Dekker, New York, 1988, Ch-26.

19. S.Radhakrishnan, Polymer Commun., **26**,1985,153.

20. H.Q.Xie, Y.M.Ma, J.Appl.Polym.Sci., **77**,2000,2156.

21. V.I.Roldughin, V.V.Vysotskii, Progress in Organic Coatings, **39**,2000,81.

22. G.M.Spinks, G.G.Wallace, Li.Liu, D.Zhou, Macromolecular Symposia, **192**,2003,161.

23. P.R.Somani, R.Marimuthua, A.B.Mandaleb, Polymer, **42**,2001,2991.

24. J.G.Simsons, L.I.Maissel, R.Glang, Handbook of Thin Film Technology, Tata McGraw-Hill Publishing Company Ltd., New York,1976, Ch-14.

25. S.Radhakrishnan, S.P.Khedkar, Synth.Met., **79**,1996,219.

26. S.Radhakrishnan, S.Chakne, P.N.Shelke, Materials Letters, **18**,1994,358.

27. AI.Medalia, Rubber Chem.Technol., **59**,1986,432.

28. E.K.Sichel, Carbon Black Composites, Marcel Dekker, New York, 1982, p-103.

29. S.Radhakrishnan, S.B.Kar, Sensors (Communicated).

30. S.Besbes, A.Bouazizi, H.Ben Ouada, H.Maaref, A.Haj Said, F. Matoussi, Materials Science and Engineering C, **21**,2002,273.

31. F.Gutman, L.E.Lyons, Organic Semiconductors, John Wiley & Sons Ltd., New Work,1967, Ch-10.

32. D.A.Seanor, Electrical Properties of Polymers, Academic Press, New York, 1982, Ch-1.

33. K.L.Chopra, Thin Film Phenomena, Tata McGraw-Hill Publishing Company Ltd., New York,1969, Ch-8.

34. J.G.Simsons, J.Appl.Phys., **34**,1963,1793.

35. S.Radhakrishnan, S.B.Kar, Sensors and Actuators, A: Physical, **12**,2005,474.

36. L.E.Nielsen, Mechanical Properties of Polymers and Composites II, Marcel Dekker, New York,1974, p-34.

37. P.C.Rodrigous, G.P de Souza, J.D.Da Motta Neto, L.Akcelrud, Polymer, **43**,2002,5493.

38. J.A.Harley, T.W.Kenny, J.Microelectromech.Syst., **9(2)**,2000,226.

CHAPTER- V

Actuator

5.1. Introduction

Actuators convert electrical energy to mechanical energy via charge induction, the common examples being muscles, touch me not plant, etc [1]. Intrinsically conducting polymers show actuation as a result of molecular level insertion of dopant ions [2] as there can be driven between the conducting and insulating states reversibility through electrochemical charging-discharging cycles in an electrolyte solution or a gaseous atmosphere [3]. Among the conducting polymers, polypyrrole (PPy) is one of the most widely investigated material for actuator applications due to its observed contractile strength [4,5], strain rate, ease of production and reaction time [6]. The volume change of polypyrrole can be controlled by an applied potential [7]. The volume change is thought to be governed primarily by insertion and de-insertion of ions and solvent that occurs during oxidation and reduction [8-10]. A few researchers studied these in the form of bi-layer actuator in which a differential expansion between two thin, adjoining layers results in bending. The performance of such bi-layers could be increased in terms of their electrical and mechanical response voltage inputs [11-16] by using different solvent medium, electrolytes [17] , and conducting polymers, etc. [18-20]. However, these did not throw any light on how bending of actuator depends on mechanical property and geometry of backing layer which supported the active conducting polymer. Hence, in the present studies we have considered various polymers such as PET, SBS, Hytrel, LDPE/LLDPE, PP having large span of modulus and thickness values.

The main aim of the present investigation is to explain the response characteristics of bi-layer actuator in terms of mechanical properties of backing layer, applied voltage, various

dopant, etc. This can lead to optimization of design of these actuators to produce large force. Such optimization is essential to produce practically viable electromechanical devices.

5.2. Experimental

Bi-layer type actuators were fabricated as follows: The conducting polymer coated flexible substrates were prepared by electrochemical polymerization of pyrrole in a single compartment three electrode cell connected to computerized potentio-galvenostat. The PPy film deposition technique was standard conventional one, which has been described elsewhere (see chapter II, 2.6.6). It essentially consisted of placing gold coated (vacuum deposited) polymer films in an electrochemical bath (aqueous) containing 0.1 M pyrrole and 0.1 M sulphuric acid along with platinum as counter electrode, saturated calomel as reference electrode (SCE) and applying 0.65 V (vs SCE) constant potential for variable time period. Supporting polymer film was made from PET (Polyethylene terephthalate), Styrene Butadiene-Styrene (SBS) tri-block copolymer, Hytrel, Polypropylene (PP), and Linear low-density polyethylene/low-density polyethylene (LLDPE/LDPE). The working electrodes with PPy films were removed, rinsed in distilled water and dried. The strips of PPy/Au/backing layer polymer actuators with 2.5 cm length (*L*) and 0.25 cm width (b) were cut out from the multilayer films for studies on response characteristics. The above actuator films were tested for actuation by measuring bending angle (degree) in solution of 0.1 M $LiClO_4$ applying -1.0 volt potential. Fig. 5.1 shows experimental observation of bending of PPy actuators in our laboratory.

5.3. Results and Discussions

Polypyrrole has been reported to exhibit actuation under low applied potential in electrochemical mode. In order to use this effect for actuators or electrochemical device such as remote control valve, etc., it is essential to have appropriate design parameters such as bending angle and actuation force with respect to applied potential, dopant type, geometrical parameters such as length, breadth, thickness, porosity, and other structural features of the films.

Actuation was measured in terms of the bending angle and its variation with respect to (i) polypyrrole deposition potential (ii) applied potential (iii) nature of dopant (iv) time response of actuation (v) backing layer & conducting polymer layer thickness (vii) backing layer modulus (ix) dimension of actuator.

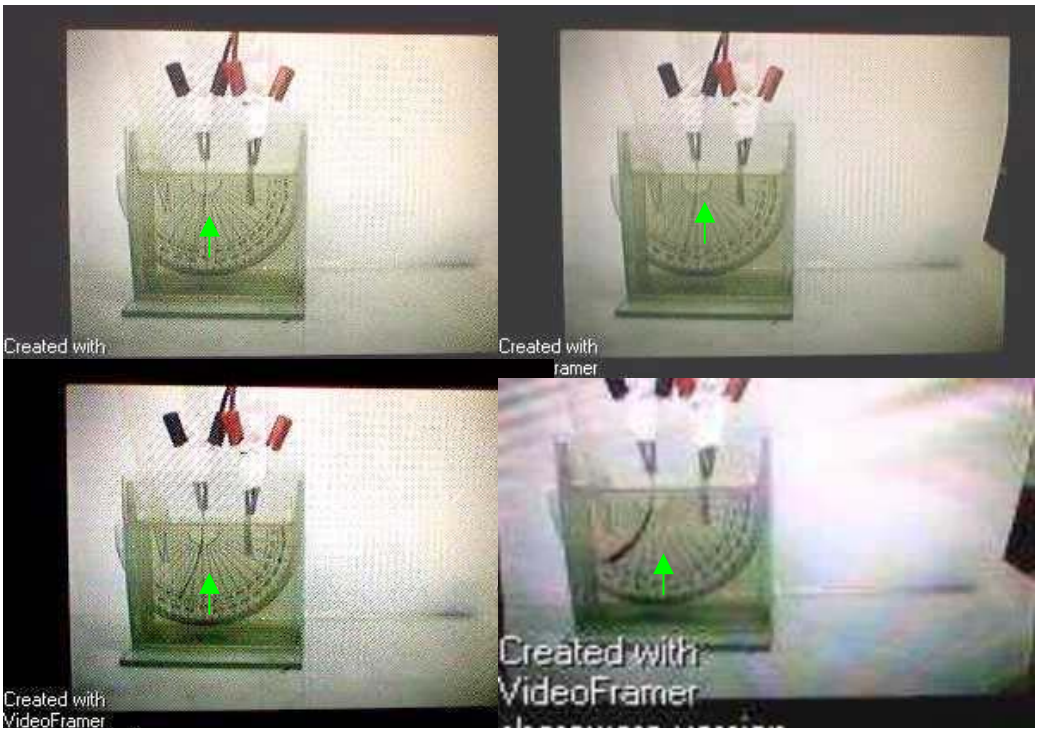

Figure-5.1. Experimental observation of bending angle in our laboratory

5.3.1. *Polypyrrole Deposition Potential*

It has been reported that production or synthesis parameters such as the deposition potential significantly affect various properties of PPy films [21-23]. Electrochemical polymerization of pyrrole was carried out in the same manner as described in chapter II, section-2.6.2, using flexible gold-coated PET substrate by potentiostatic method. Applied potential was varied from 0.5 V to 0.75 V SCE. Deposition time or duration changed from 1 min to 20 min, depending on deposition potential value to get equal PPy thickness. The resulting bi-layer actuators were subjected to voltage stimulation waveforms, and the film movements were recorded as a function of time at constant

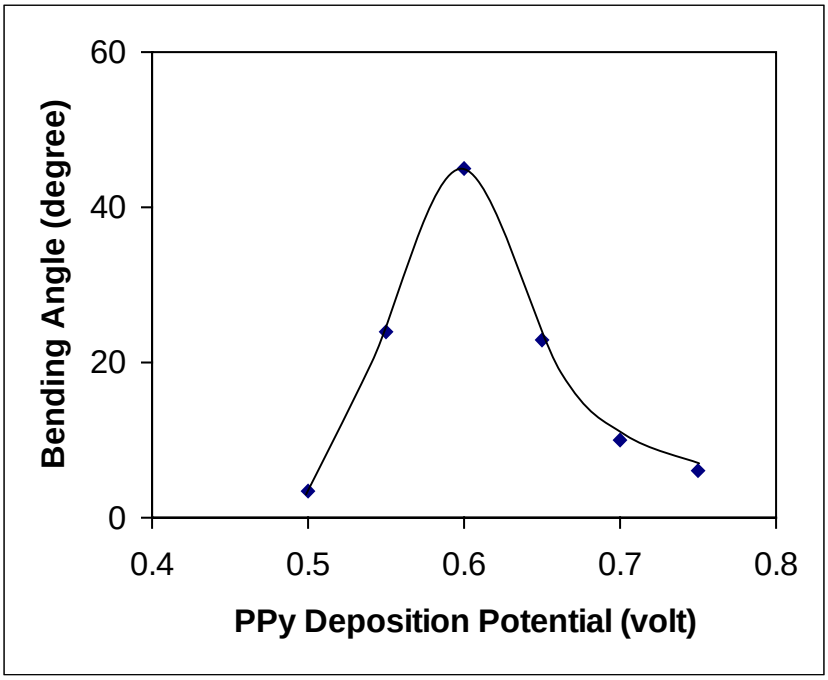

Figure-5.2. Variation of bending angle with deposition potential of PPy [PPy thickness 2.72 μm, 25 μm PET back layer]

potential. Fig. 5.2 shows that the bending angle increases to reach maximum and then

decreases with increasing deposition potential. At lower deposition potential, the deposition rate is very slow and the deposited polypyrrole layer would be very dense, compact, and highly conducting [24]. On the other hand, at higher deposition potential it can be rough, fluffy (highly porous), and soft. Thus the modulus of the film depends on the deposition potential or rate of polymerization under potentiostatic condition.

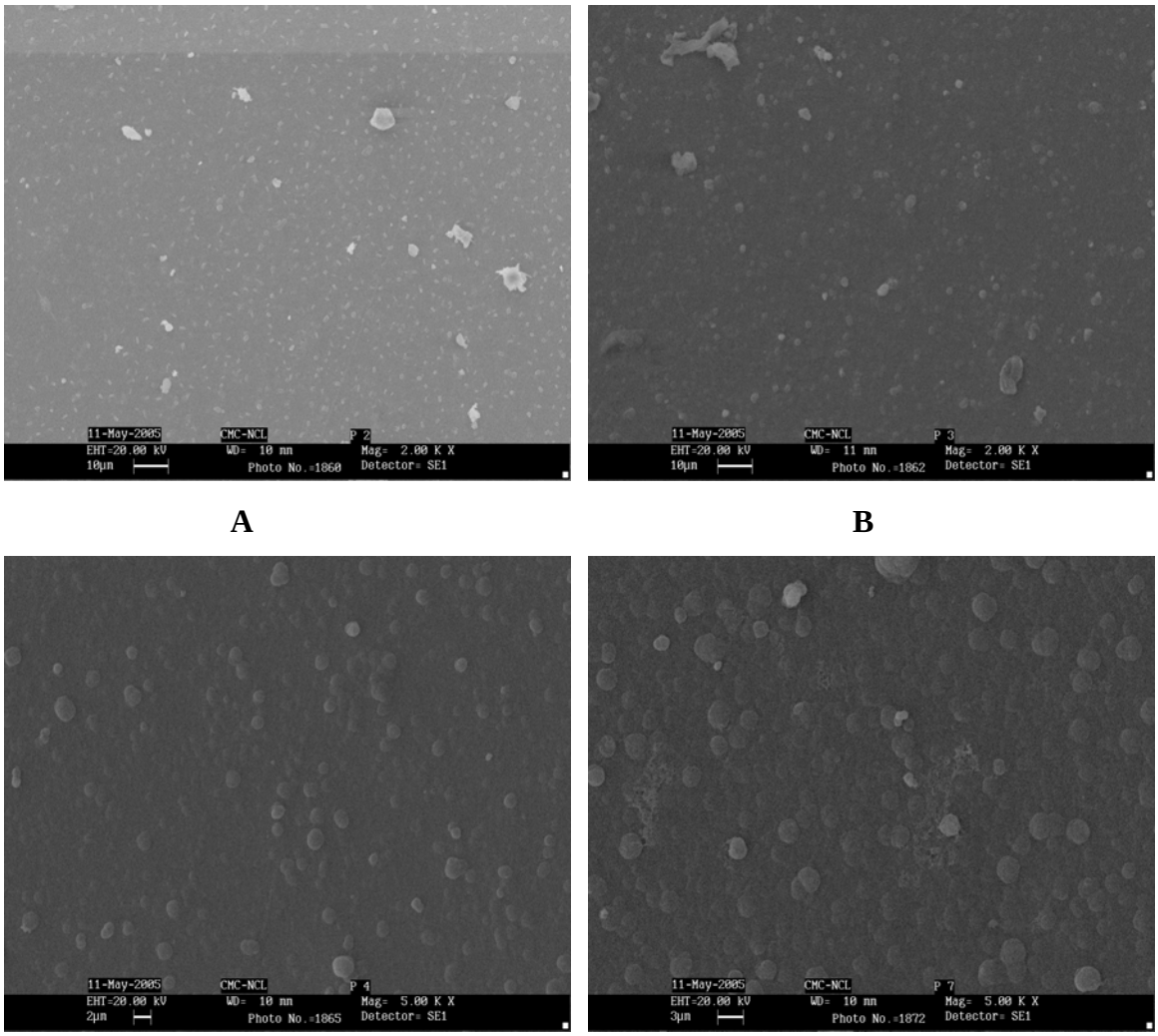

Figure-5.3. SEM images of PPy films (A, B, C, D) of different deposition potential 0.55 V, 0.60V, 0.65 V, and 0.75 V, respectively showing roughness variation

It has been shown (in chapter III, section-II) that in the case of bi-layer actuator, the bending angle depends on the modulus of active conducting polymer films as well the backing layer and there is an optimum combination of both at which the bending angle is maximum. In the present case, the backing layer modulus was kept same while the conducting polymer film's modulus value changed by varying the deposition potential, the electroactive films have the optimum modulus value for maximum bending. Additionally, the morphology also affects the ionic transport through the film. The deposition potential also affects the morphology (see Fig. 5.3) due to change in rate of polymerization. As the PPy films become more porous, ionic diffusion and ejection (in redox cycles) becomes easy. As morphology of the PPy film plays an important role in the actuation of PPy bi-layer actuator, conducting PPy films of varying deposition potential were prepared. Fig. 5.3 shows the SEM for the polypyrrole deposited at the four deposition potential (micrograph A: 0.55 volts, B: 0.60 volts, C: 0.65 volts, and D: 0.75 volts). Surface morphology of the film was found to contain nodular structure, typical of conducting polymers [25-27]. It is evident that the film surface goes from very smooth (Fig. 5.3, micrograph A) to very rough (Fig. 5.3, micrograph D) as the deposition potential is increased. This is mainly associated with the high current or the rate of deposition of PPy under potentiostatic condition. In particular, the films grown at higher potential or current density show larger features (i.e. granular structure) than the films grown at the lower settings (compare micrographs A and C). In this case the larger features may be the result of the more rapid and less ordered growth of the polymer under the greater driving force of higher potential or current density. The porosity on the film also increases with

increase of deposition potential. Nature of polypyrrole produced under different synthesis conditions is different. One deposition potential (0.65 volts) was used in all cases studied throughout in this thesis.

5.3.2. *Backing Layer & Conducting Polymer Layer Thickness*

The bi-layer type actuators were fabricated with conducting polypyrrole deposited on different types of gold-coated substrates viz. PET, SBS, Hytrel, LDPE/LLDPE films

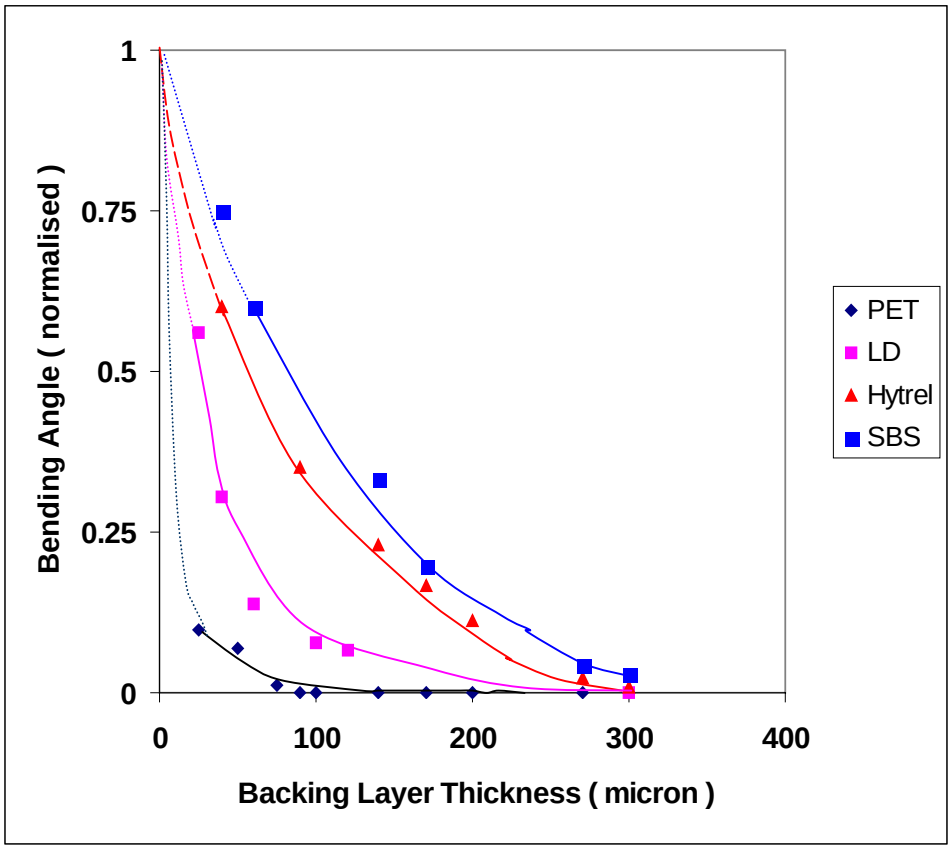

Figure- 5.4. Variation of bending angle (normalized) vs thickness of different backing layer [PPy thickness 2.45 μm]

having thickness values in the range of 12 to 300 μm. Here, PET, SBS, Hytrel, LDPE/LLDPE used as a backing layer. Experimentally observed bending angles were

normalized by dividing all values (bending angle) with respect to least value (bending angle). Fig. 5.4 depicts the variation of bending angle for different values of backing layer thickness. In these cases, thickness of conducting polymer (PPy) was considered to be constant. It is evident that, as the backing layer thickness is decreased the bending angle increases for all types of backing polymer. SBS shows maximum bending angle in comparable thickness of Hytrel, LLDPE /LDPE and PET. In each case, bending angle

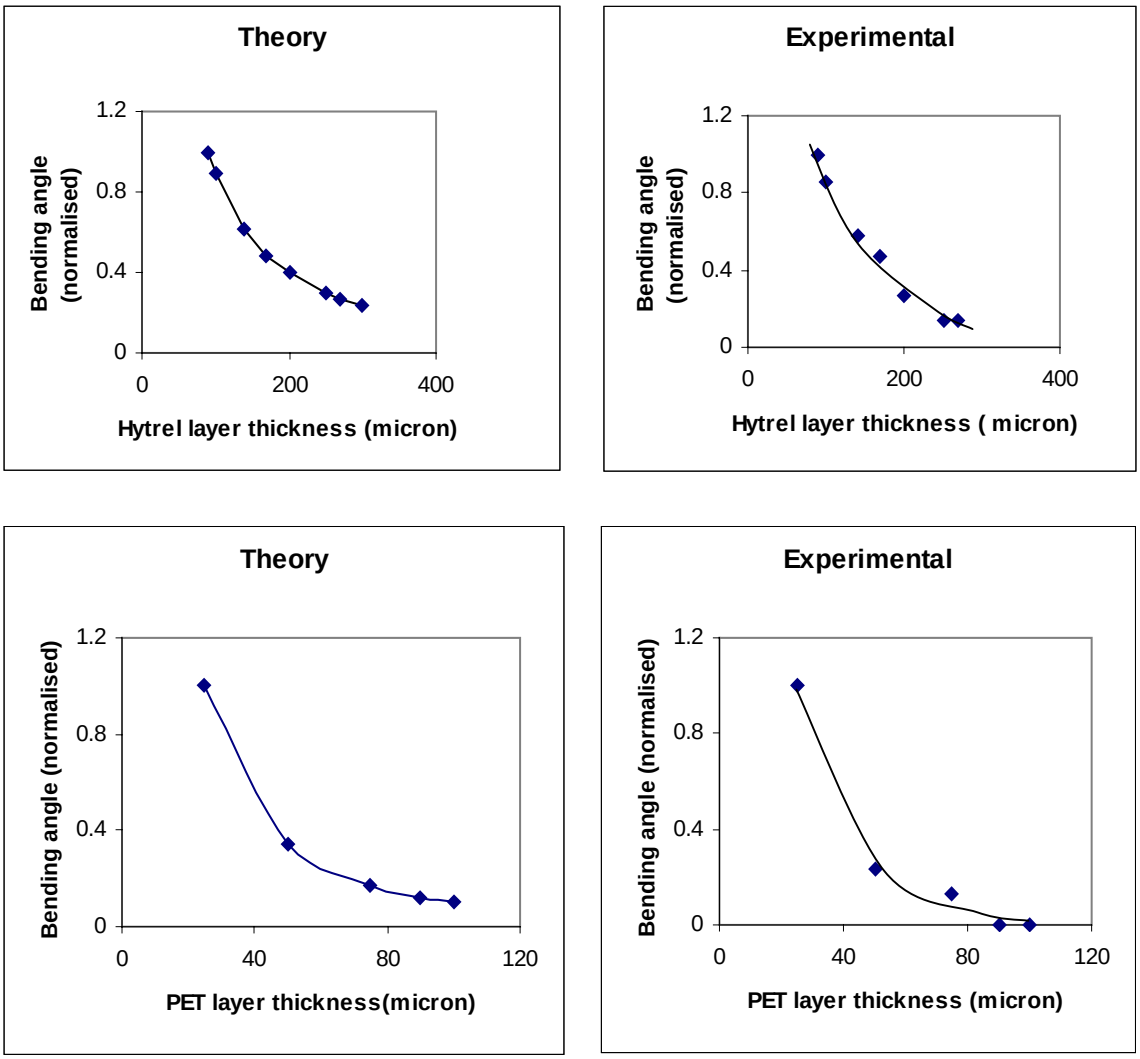

Figure-5.5. Comparison of theoretical and experimental values for bending angle for different backing layer thickness in Hytrel & PET.

increases very rapidly below certain artificial thickness depending on the polymer used, which is called optimum thickness. In order to confirm the experimental observations with theory described in the chapter III (section II), bending angle was estimated from the phenomenological model described in chapter III (section II). Theoretical values were calculated by using equation 3.27 (chapter III) for Hytrel and PET backing layer and plotted in Fig. 5.5. Fig. 5.5 shows a comparison between theoretical and experimental data. It is clearly seen that in each case there is critical value of the backing layer below which the bending angle increases sharply. Above this thickness value, the bending angle becomes low and almost independent of the backing layer. Similar type of observations were made by K. J. Kim et al.[28]. Further, the theoretical estimates are quite close to the experimental data at lower thickness values but little deviations are seen for higher thickness of the backing layer. These small deviations could arise from the fact that it has been assumed that the modulus of the backing layer does not depend on its thickness. However, it is known that bulk modulus and the film modulus could be quite different due to changes in processing conditions as well as structure development during processing. None the less, there is a good match in the nature of the curves in all cases between the theory and experiment. Figs. 5.6, 5.7, & 5.8 showed the effect of conducting polymer (PPy) layer thickness on the bending of actuator, the bending angle of the bi-layer having different backing layer PET, PP , and LLDPE/LDPE respectively on which various thickness of conducting polymer (polypyrrole) have been deposited. The thickness is controlled by polymerization time [29] at constant applied potential

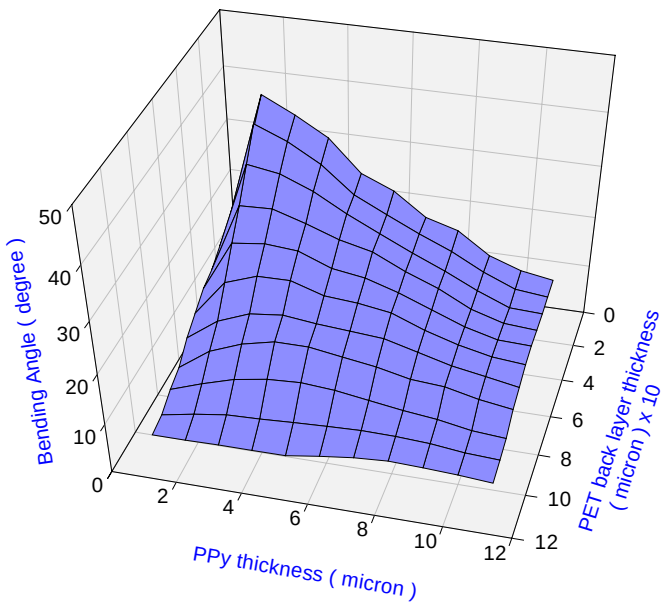

Figure-5.6. Variation of bending angle vs thickness of backing layer (PET) and PPy different thickness

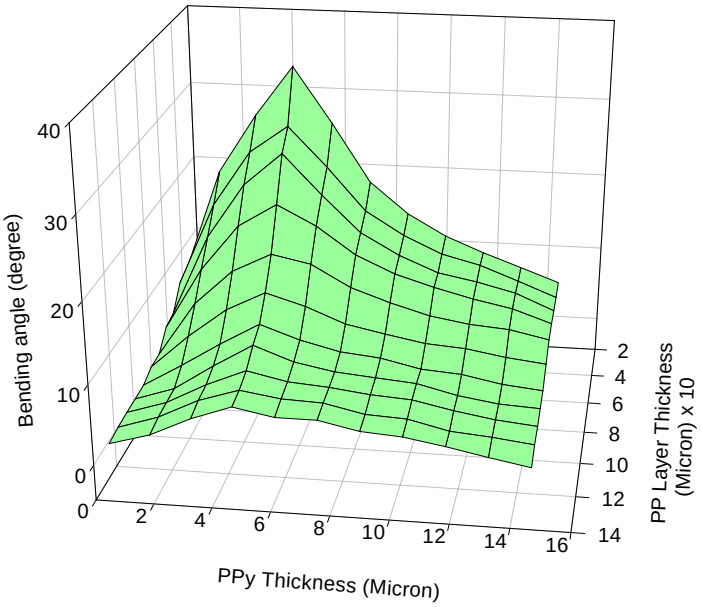

Figure-5.7. Variation of bending angle vs thickness of backing layer (PP) and different PPy thickness

(table-5.1). In this configuration, the bending force would increase with the increase of conducting polymer layer thickness but only up to certain value since beyond the critical limit, there will be opposite force due to self-recovery. The backing layer will add to the recovery force and hence the bending angle will be maximum at certain thickness

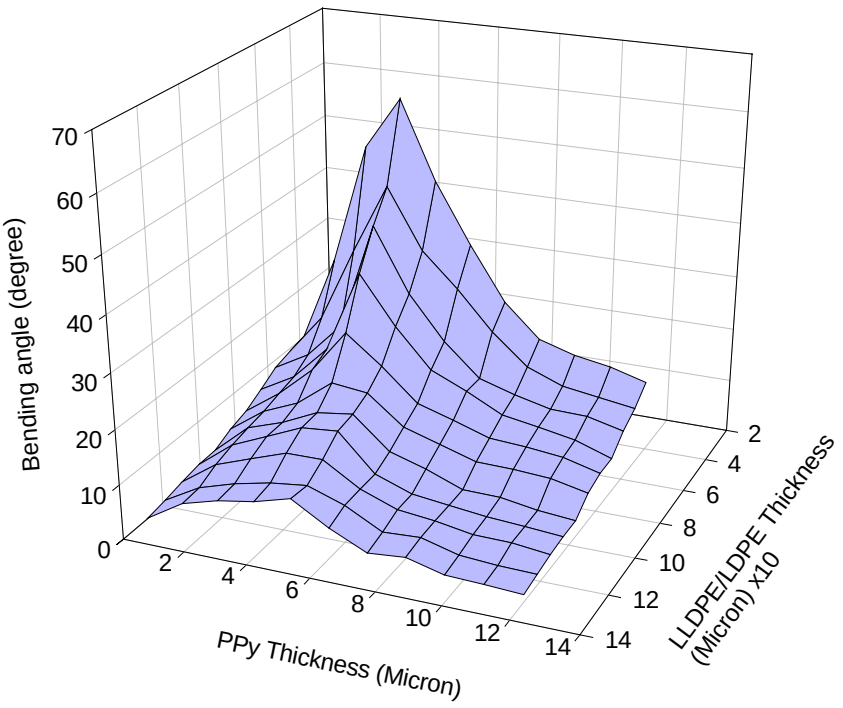

Figure-5.8. Variation of bending angle vs thickness of backing layer (LLDPE/LDPE) and different PPy thickness.

of the conducting polymer [30]. In another way, charge passed during the redox reaction of the PPy film also decreased for thickest film. This indicates that the redox reactions are slowed by diffusion of ions through and/or the iR (i is current and R is the resistance of the PPy film) drop across the film thickness as the film thickness increases. G. M. Spinks et al.[7,18] also observed similar type of behaviour where P Py has been deposited on

PVDF backing layer. Susumu Hara et al.[31] also claimed that, PPy thickness should be smaller so that PPy actuation occurred more efficiently. In all cases, there is specific thickness for conducting polymer layer at which maximum bending angle is obtained. For LLDPE/LDPE back layer actuator, maxima shifts towards higher conducting polymer layer thickness. For the higher thickness of C.P layer the electrochemical stretching of films would be very slow and small due to slow diffusion of dopant ions in the films.

`Table-5.1. Effect of deposition/polymer growth time on polypyrrole thickness

Deposition time (Sec)	**PPy layer thickness (μm)**
10	0.197
30	0.640
60	1.129
90	1.580
120	1.790
150	2.450
180	3.080
240	3.500
270	3.920
300	4.720
360	6.500
420	8.220
480	9.040
540	10.50

5.3.3. *Backing Layer Modulus*

Fig. 5.9. shows experimentally measured bending angle (normalized) decreases with

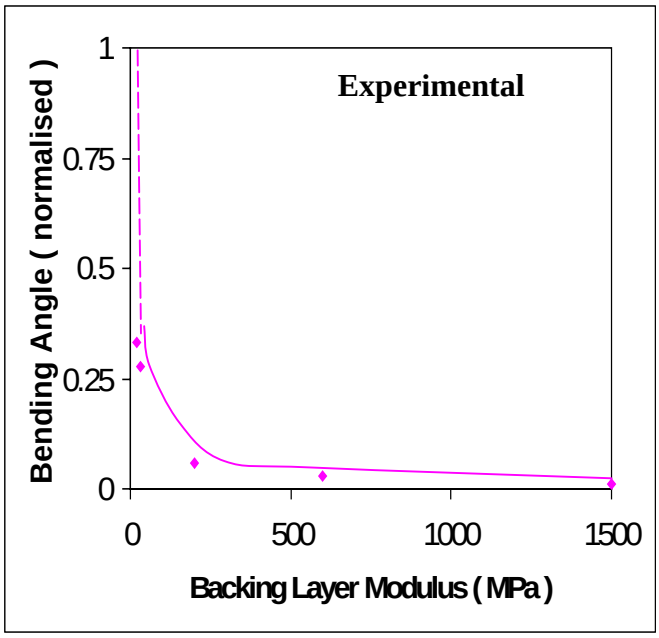

Figure-5.9. Variation of bending angle (normalized) vs modulus of backing layer [PPy thickness 2.45 μm]

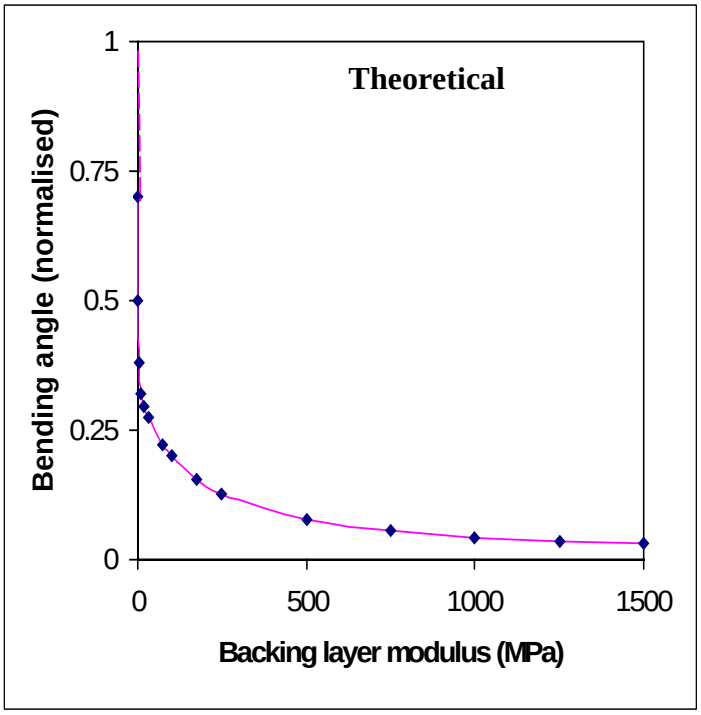

Figure-5.10. Variation of bending angle (normalized) vs modulus of backing layer [PPy thickness 2.45 μm]

increase of backing layer modulus. Bending angle attains steady value after certain modulus value (500 MPa). It is also interesting to note that the modulus of the backing layer plays vital role in obtaining good actuation. PET, which has quite high modulus (1500 MPa) as compared to SBS (20 MPa) or Hytrel shows least bending angle while the elastomers give very good actuation/bending angle which increases to more than 90 degrees for some cases [32].

In this case the conducting polymer (PPy) and backing layer thickness were considered to be constant. In order to confirm the experimental observations with theory, theoretical value was calculated by using equation 3.28 (chapter-III) for the range of modulus (20 MPa to 1500 MPa) of backing layer and plotted in Fig. 5.10. It shows quite good resemblance in the nature of curves with small deviation in higher modulus, where as theoretical bending angle is expected to be slightly higher than experimental bending angle. The exact bending angle at these modulus values could not be determined accurately due to limitation in experimental set up which could go up-to one degree. For lower bending angle one may have to use lower deflection methods.

5.3.4. *Geometry of Actuator*

Actuation of bi-layer actuators was highly influenced by geometry of actuator. Fig. 5.11 shows the effect of ratio of actuator length (L) and width (b) on the performance of actuator. Bending angle increases with L/b ratio. Actuator width is more influential than actuator length. It is clear that the L/b ratio is an important design parameter when improving the bending performance of actuators with in the operating conditions.

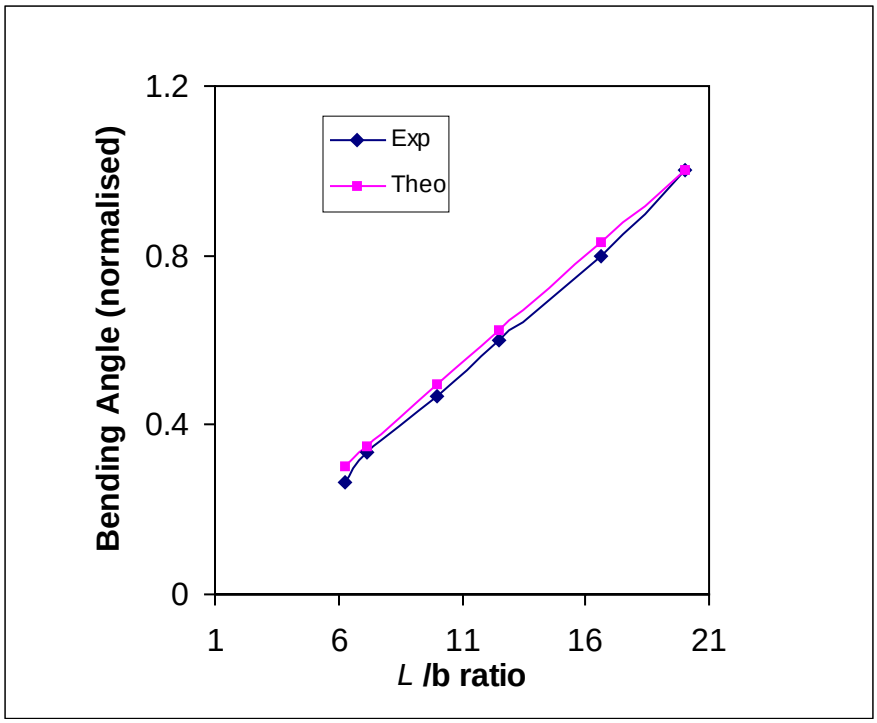

Figure-5.11. Variation of bending angle with *L*/b ratio of PPy/Au/PET actuator [PET thickness 25 μm, PPy thickness 1.86 μm]

K. J. Kim et al. [28] also observed same behaviour in biodegradable cellophane paper actuator and also confirmed in the fiber actuator [31].

5.3.5. *Effect of Dopants*

To study the effect of various dopants on the actuation produced; actuators were prepared with PPy films containing small, medium and large dopants. For this purpose such as, MSA (methyl sulfonic acid), PTSA (*p*-toluene sulfonic acid), DBSA (dodecyl benzene sulfonic acid), CSA (camphor sulfonic acid) were used. All practical purposes, PPy actuator films doped with various dopants were tested in aqueous $LiClO_4$ under –1.0 volts potential for constant time. From the Fig. 5.12, it is clear that bending angle produced by

the actuator made with small anions for MSA is very small. Furthermore, the bending angle produced when medium sized anion for PTSA is involved is larger than that produced with surfactant anions for (DBSA or for CSA). It has been reported that the type and size of the dopant anion used during the polymerization changed morphology [33]. We have explained earlier bending angle of bi-layer actuator depends upon conducting polymer modulus. Modulus of conducting polymer layer highly depends on nature of dopant used. Modulus also depends on crystallinity of the film and crystallinity varied with dopant ions. It has also been found that PPy film made with small anions movement does not make significant volume change due to lower volume and it does not drag much

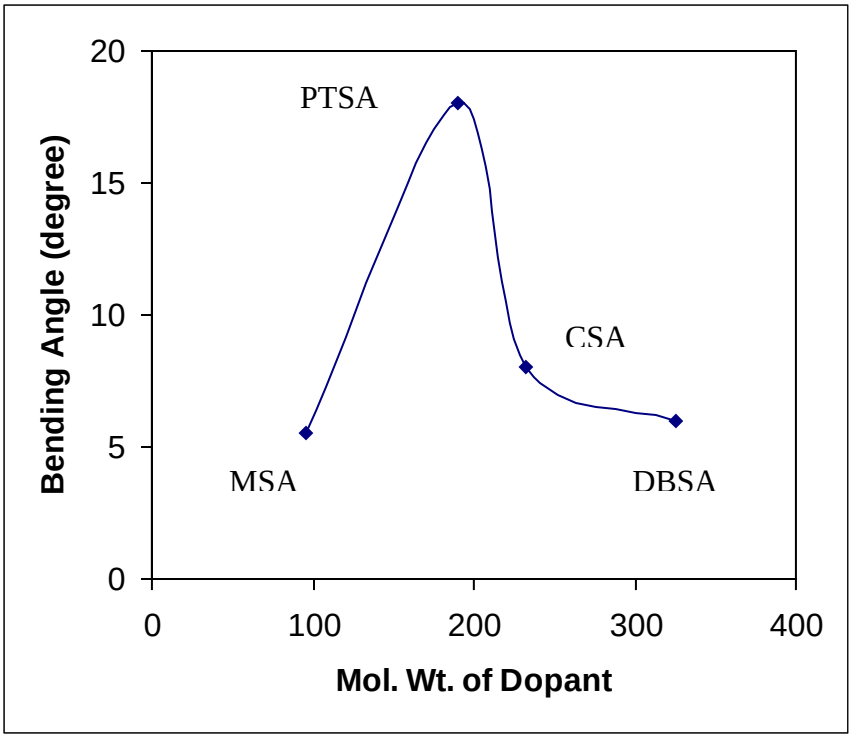

Figure-5.12. Variation of bending angle with molecular weight dopants [(SO_4^{-2} doped PPy) thickness 2.04 μm & 25 μm PET back layer]

amount of solvent [34]. Volume of ions is in increasing order for these dopants as MSA < PTSA < DBSA < CSA. Since, bending angle is directly connected with the volume change in the PPy film, it becomes evident that angle was shown by the PPy actuator made with small anions (smaller size dopant) is low. According to Fig. 5.12, the actuator made with *p*-toluene sulfonic acid dopant shows much higher bending angle than other dopants. It is believed that large anions are trapped inside the polymer structure and will not participate in the redox process [35]. It has been found further that cation movement dominates in the redox process of PPy films containing large surfactant anions [15] . It is reasonable to believe that large surfactant anions get trapped inside the polymer matrix partly due to their large size and partly due to the interaction of the polar ends of the surfactant with the matrix of polymer, and therefore the polypyrrole films formed with surfactant anions become more stable. Large anions would not come out easily from PPy matrix. So, considering both reverse factors (modulus and volume of anion) bending angle showed by PPy films made with large surfactant would be low. Shimidzu et al.[36] have explained anion mobility in PPy film decreases with increasing molecular weight of the same. Hence, lower bending angle showed by actuator made with PPy films containing very small and large dopants are understandable.

Fig. 5.13 shows bending angle of PPy films (curves.-A, B, C, D represents H_2SO_4, PTSA, DBSA, CSA doped, respectively) vs PPy layer thickness under above experimental condition . It is very clear from the Fig. 5.13, though H_2SO_4 doped PPy shows initially (lower PPy thickness) high bending angle but it starts saturation with increasing PPy thickness, but incase of PTSA doped PPy initial angle is lower (compare with H_2SO_4

doped PPy) in same PPy thickness interval but it increases with increasing PPy thickness. DBSA and CSA doped PPy showed lower angle and gets saturated with PPy thickness. It is reasonable to understand that smaller anions could come out very fast and easily from

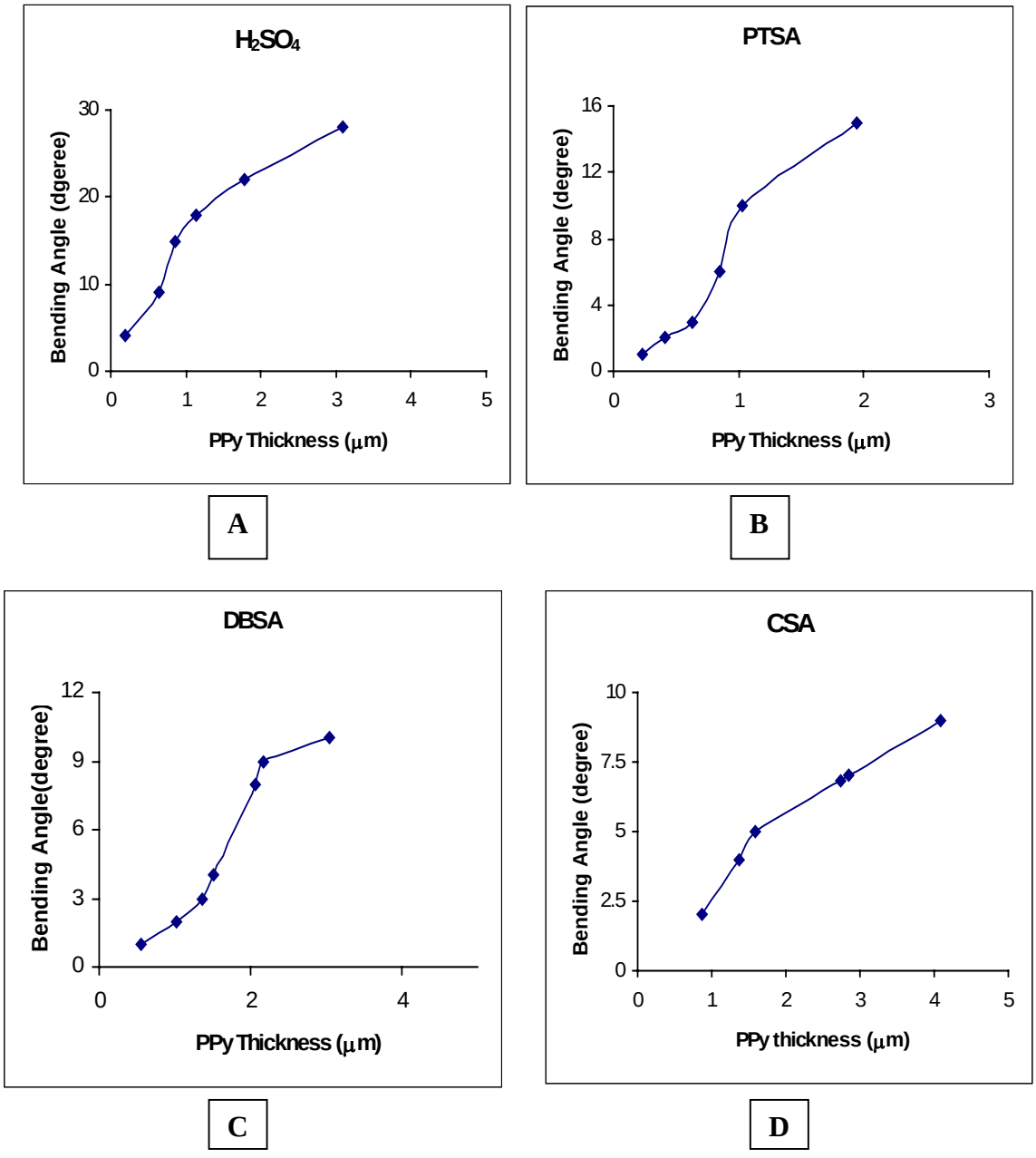

Figure 5.13. Variation of bending angle with PPy layer thickness of PPy actuator doped with (A) H_2SO_4 (B) PTSA (C) DBSA (D) CSA [25 μm PET back layer]

lower thickness PPy layer than larger anions. That's why H_2SO_4 doped PPy film shows saturation in lower PPy thickness with respect to remaining dopants. The critical or optimum thickness where bending angle would be maximum, depends on nature of dopants and it shifts towards higher PPy thickness with increasing dopant size.

5.3.6.*Time response*

Upon reduction in an aqueous solution of electrolytes, polypyrrole actuator undergoes shrinking and continuous slow shrinking. The volume changes in actuator films are dependent on time and it was controlled by different factors.

5.3.6.1. *Applied Potential*

Fig. 5.14 depicts the variation of bending angle at different applied potential with time of actuation measurement. Initially bending angle increases very fast after that attains saturation with increasing time. However, as the applied potential is increased the upper limiting value of the bending angle also increases. In case of a reduction potential < 0.5 volts vs calomel, the time required for maximum bending was shorter or the response speed of actuator was faster, by making the potential larger the speed of un-doping PPy becomes faster. It (angle) decreases slightly in 0.8 volt and then increases with increasing potential rather than steady increase. Higher applied potential shows higher bending angle [37]. At applied potential lower than – 0.4 volt vs calomel, the bending behaviour could be hardly being observed. G. M. Spinks et al [14] showed that, the amount of actuator strain of PPy (doped with benzenesulfonate) increases with an increase of the applied potential range. Which suggests that bending angle should be higher at higher potential. At higher potential water electrolysis is likely to be taking place with oxygen gas

produced at the anode and hydrogen gas at the cathode. This is not the main cause of bending [38] (since deformation is observed at lower potential – 0.4 volt). Electric field is

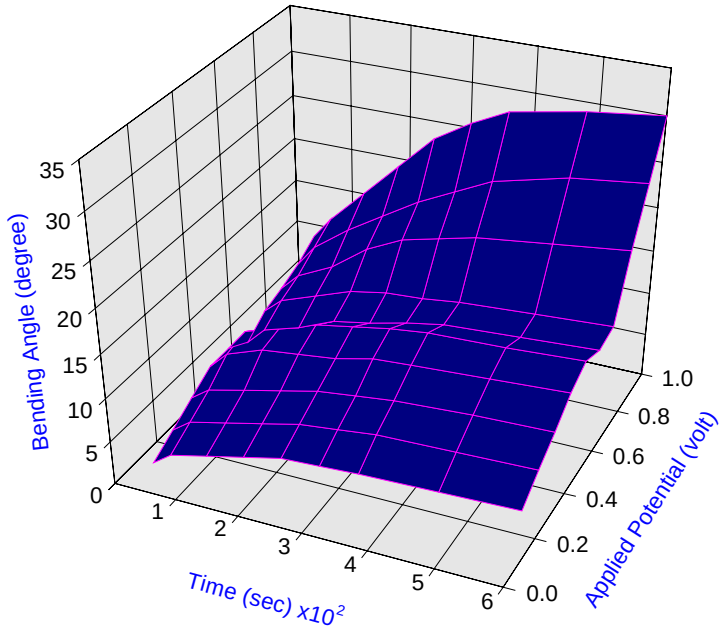

Figure-5.14. Variation of bending angle vs time and different applied potential [PPy thickness 1.98 μm, 25 μm PET back layer]

also likely to cause electrochemical reaction. The standard potential for the hydrolysis

$$H_2O_{(l)} = H_{2\,(g)} + ½\ O_{2(g)}$$

reaction is 1.23 volt, therefore large applied potential voltage that exceeds the potential level. However, no work has been done regarding the application of larger voltages where electrochemical reactions and deviation from linear behaviour are likely to occur. Higher potential can cause blistering of the coating as well as de-bonding. Tetsuya et al.[9] also obtained similar trends of actuation of PPy film with increasing potential. The initial

transient response is due tocharging of the PPy films, which behave as capacitor via ionic diffusion. At higher potential, capacitance of the PPy films increases so bending angle increases . Fig. 5.15 shows surface morphology of selective PPy / Au / PET

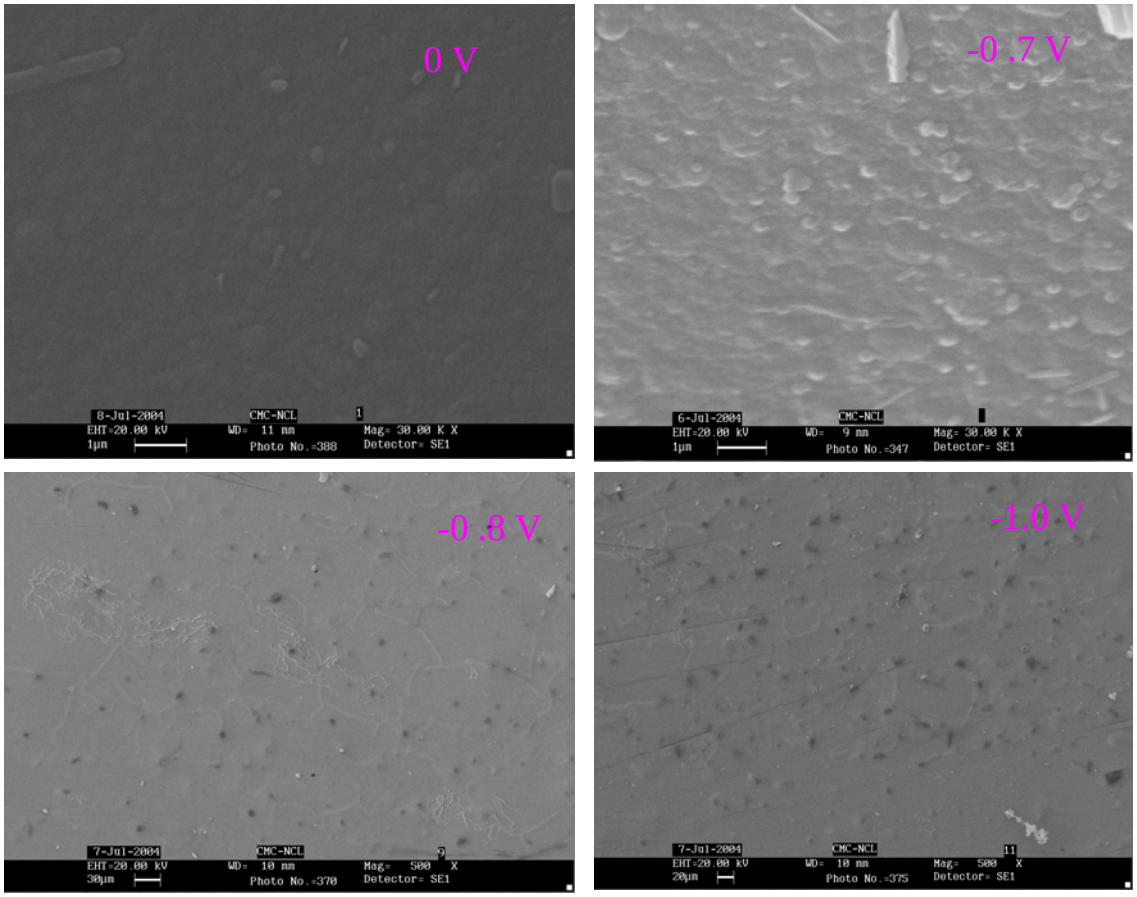

Figure-5.15. SEM images of PPy actuator subject to different applied potential showing porosity variation

actuators, which undergoes actuation experiment in different potential. Separate actuators are used for each applied potential. It is very clear form the SEM micrographs, PPy film does not show any holes before actuation (0 volt potential) where as it forms

hole after actuation and number of holes increases with increasing potential. This may be due to ejection of SO_4^{-2} ions during reduction [39, 40]. At Higher potential more ions will come out, so number of holes will increase. More anions ejection means more volume changes and it is shown in Fig. 5.14 where bending angle increases with increasing potential. G. G. Wallace et al.[41] also observed similar observation in PPy film doped with PTSA. There was no complete agreement about the morphological changes associated with the reduction of PPy. PPy bi-layer actuator shows large bending in –1.0 Volts potential, so we have selected that potential for all actuation measurements.

5.3.6.2. ***Effect of Dopants***

As we have seen in earlier discussion, bending angle dependent on nature of dopants, so we are trying to analyze here, how it influences the actuation mechanism. Fig. 5.16 shows variation of bending angle of PPy/Au/PET actuator doped with different dopant (A) MSA, (B) PTSA, (C) DBSA, with time of actuation in log-log scale. Each curve indicates different slope and slope corresponding to rate of bending. Slope difference might be due to different diffusion coefficient of dopants and dopant dependent conductivity of PPy film.

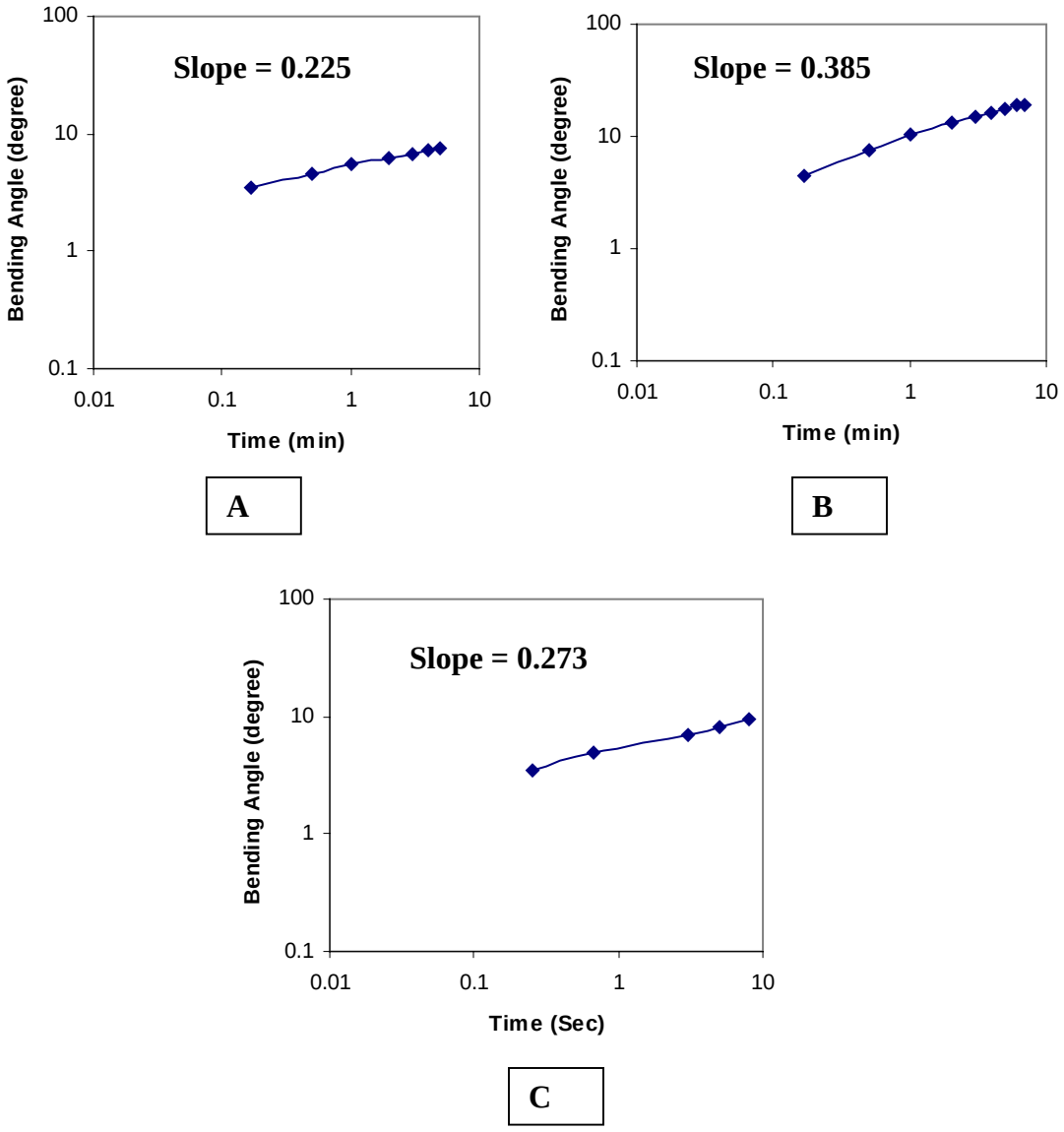

Figure-5.16. Variation of bending angle of PPy actuator containing different dopants (A) MSA, (B) PTSA, (C) DBSA [PPy thickness 2 μm & 25 μm PET back layer]

5.3.6.3. *Effect of Conducting Polymer Layer Thickness*

Upon electrochemical reduction in an aqueous solution of 0.1 M $LiClO_4$ at a constant potential –1.0 volts, PPy/Au/PET actuator was bent to the PPy side. Both bending angle

and time scale dependent on the PPy (SO_4^{-2}) layer thickness. Fig. 5.17 shows the bending angle change during the reduction of a actuator with different PPy layer thickness. For a constant time bending angle passes through maxima like Fig. 5.6. Here, bending angle

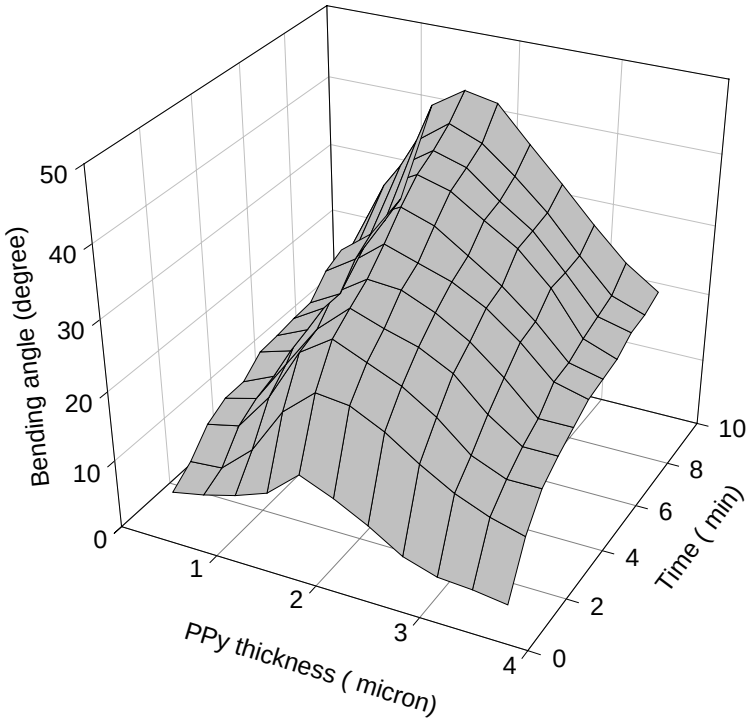

Figure-5.17. Variation of bending angle PPy layer thickness and time of actuation [12 µm PET back layer]

also shows two slopes with time axis. Dopant extraction out of PPy layer is diffusion controlled and its time scale closely related to the PPy layer thickness [42]. With thinner PPy layer thickness the rate of bending is obviously dependent on the number of dopant ions extracted during reduction. However, as the PPy thickness increased further the

rate of bending angle decreased owing to hindered transport through the thicker PPy film. The rate is then diffusion controlled and would be slow [39], will take more time to get saturated.

5.4. Conclusions

Experimental results of PPy actuator indicated that, it could provide as an artificial muscles. Actuation in PPy bi-layer actuator can be controlled during manufacture of PPy films. Management of the deposition potential PPy resulted in different qualities of PPy film. Thus, deposition potential can and should be carefully considered in the design of PPy bi-layer actuator. Electrochemical actuation of PPy was affected by the nature of dopants. Anions used during polymerization of PPy films have a greater effect on the actuation produced by bi-layer actuators. Higher bending angle can be obtained with medium size of anions. The type of ions is very important in optimizing the bending angle of PPy actuator. More bending angle can be obtained (in reduction) from medium size dopant. The potential limits suitable for application to PPy bi-layer actuator was investigated. It requires a delicate balance between extending the potential limits as far as possible to allow redox reaction, while ensuring that the potential at which over-oxidation will occur are not reached. In order to enhance the effect of electromechanical deformation, the system design, such as structure of conducting polymers and morphology of the co-operative contribution of these mechanisms, is important.

The actuation mechanisms during the reduction are deduced nicely by considering electrostatic repulsion and diffusion controlled ion exchange phenomena. Diffusion of ions dependent on PPy layer thickness, nature of ions (size of ions), and merely on backing layer thickness.

5.5. References

1. S.S.Pandey, W.Takashima, M.Fuchiwaki, K.Kaneto, Synth.Met.,**135**,2003,59.

2. Rajesh, S.S.Pandey, D.Kumar, W.Takashima, K.Kaneto, Thin Solid Films, **467**,2004,227.

3. Q.Pei, O.Inganas, Synth.Met., **55-57**,1993,3739.

4. P.I. Lazarev, Micro-Electromechanical Actuators based on Conducting Polymers, Molecular Electronics, Kluwer Academic Publishers, Dordrecht, 1991, p-267.

5. I.W.Hunter, S.Lafontaine, IEEE Solid- State Sensors and Actuators Workshop Technical Digest, Hilton Head Island, USA, 21-25 June, 1992, p-178.

6. J.D.Madden, R.A.Cush, T.S.Kanigan, I.W.Hunter, Synth.Met., **113**,2000,185.

7. T.W.Lewis, S.E.Moulton, G.M.Spinks, G.G.Wallace, Synth.Met., **85**,1997,1419.

8. M.Onoda, T.Okamoto, K.Tada, Synth.Met.,**119**,2001,279.

9. T.Okamoto, Y.Kato, K.Tada, M.Onoda, Thin Solid Films, **393**,2001,383.

10. M.F.Suarez, R.G.Compton, J.Electroanal.Chemistry, **462**,1999,211.

11. Y.Bar-Cohen, SPIE, Electroactive Polymer Actuators a Artificial Muscles, Washington,USA, 2001,Ch-7.

12. A.D.Santa, D.De Rossi, A.Mazzoldi, Smart Materials and Structures, **6**,1997,23.

13. S.Maw, E.Smela, K.Yoshida, P.Sommer–Larsen, R.B.Stein, Sensors and Actuators, A: Physical, **89,** 2001,175.

14. G.M.Spinks, Lu.Liu, G.G.Wallace, D.Zhou, Advanced Functional Materials, **12**,2002,437.

15. S.Shimoda, E.Smela, Electrochim.Acta, **44(2-3)**,1998,219.

16. G.M.Spinks, Xi.Binbin, D.Zhou, V.T.Troung, G.G.Wallace, Synth.Met., **140**,2004,273.

17. S.S.Pandey, W.Takashima, K.Kaneto, Sensors and Actuators, B: Chemical, **102**,2004,142.

18. A.S.Hutchison, T.W.Lewis, S.E.Moulton, G.M.Spinks, G.G.Wallace, Synth.Met., **113**,2000,121.

19. S.Skaarup, K.West, W.K.Gunaratne, K.P.Vidanapathirana, M.A.Careem, Solid State Ionics, **137**,2000,577.

20. G.Han,G.Shi, Sensors and Actuators, B: Chemical, **99**,2004,525.

21. R.Bilger, J.Heinz, Synth.Met., **55-57**,1993,1424.

22. T.F.Otero, J.Rodrigous, Synth.Met., **55-57**,1993,1418.

23. P.Dyreklev, M.Granstrom, O.Inganas, L.M.W.K.Gunaratne, G.K.R.Senadeera, S.Skaarup, K.West, Polymer, **36(6)**,1995,1275.

24. M.F.Suarez, R.G.Compton, J.Electroanal.Chemistry, **462**,1999,211.

25. O.A.Sememikhin, L.Jiang, T.Iyoda, K.Hashimoto, A.Fujishima, J.Physical Chem., **100**,1996,18603.

26. M.Gandhi, G.M.Spinks, R.P.Burford, G.G.Wallace, Polymer, **36**,1995,4761.

27. S.Paschen, M.Carrard, B.Senior, F.Chao, M.Costa, L.Zuppiroli, Acta Polymer, **47**,1996,511.

28. J.Chung-Hwan, K.J.Kim, Sensors and Actuators, A: Physical, **112(1)**,2004,107.

29. M.Schroedner, H.K.Roth, M.Heinemann, M.Kallenbach, WWEAP Newsletter, **1(2)**,1999,4.

30. H.S.Nalwa, Handbook of Organic Conductive Molecules and Polymers, John Wiley and Sons Ltd., Chicheste, England, **4**,1997,550.

31. S.Hara, T.Zama, W.Takashima, K.Kaneto, Synth.Met., **146**,2004,47.

32. S.Radhakrishnan, S.B.Kar, Sensors and Actuators, B: Chemical.(in press, 2005)

33. J.Y.Lim, W.K.Paik, L.H.Yeo, Synth.Met., **69**,1995,451.

34. H.Yang, J.Kwak, J.Physical Chem., **101**,1997,4656.

35. T.Matencio, M.A.De Paoli, R.C.D.Peres, R.M.Torresi, S.I.C.De.Torresi, Synth.Met., **72**,1995,59.

36.T.Shimidzu, A.Ohtani,T.Iyoda, K.Honda, J.Electroanal.Chem., **224**,1987,123.

37. S.Radhakrishnan, S.B.Kar, World Wide Electroactive Polymer News letters**,** **6(2)**,2004,17.

38. J.N.Barisci, R.Stella, G.M.Spinks, G.G.Wallace, Electrochimica Acta, **46**,2000,519.

39. A.F.Diaz, K.K.Kanazawa, J.Chem.Soc.Chem.Comm.,1979,635.

40. A.F.Diaz, Chem.Scripta, **17**,1981,145.

41. H.Zhao, W.E.Price, G.G.Wallace, J.Electroanal.Chem., **334**,1992,111.

42. Q.Pei, O.Inganas, J.Physical Chem., **96**,1992,10507.

CHAPTER- VI

Summary and Conclusions

Summary and Conclusions

Conducting polymers have become important materials in large number of applications: chemical sensors for pollution control and electromagnetic shielding and static electronic safety devices protection etc. Preliminary investigations show that these polymers also exhibit electromechanical response viz. piezo-sensitivity and actuation effect. In order to utilize these materials in electromechanical devices having industrial importance such as remote control valves, smart systems, robotics, etc. It is essential to obtain deeper understanding of material characteristics, performance as well as appropriate design for the device. The present studies have been aimed towards these aspects of electroactive polymers.

The conducting polymer blends exhibit piezo-sensitivity, which is found to be dependent on composition, type of the matrix used, applied pressure, etc. A phenomenological model has been developed which takes in to account the non-linear conduction processes as well as the non-linear variations of mechanical response. This theoretical model is able to explain many aspects of the piezo-sensitivity of these blends or composites. The theory presented in the current thesis is a generalized approach taking into account all types of conduction processes and considers also the non-linear mechanical behaviour. Thus, the role of non-linear processes in piezo-resistivity of conducting polymers has been brought out clearly by us in the above model.

These studies indicate that PVDF-PANI conducting blends can be used for piezo-sensors. The blends containing 10 to 15% of PANI appear to be best for these applications. The dopant ion plays an important role since the phase of insulating matrix changes with the

same. Dopant with semi-compatible nature with insulating matrix is the best for showing good piezo-sensitivity. Composites stored more charge during poling and get liberated in application of mechanical load, and also this shows non-linear current voltage characteristics. Piezo-resistive state in a semi-conducting PVDF is brought about by electrical poling. The CF_2 groups get reoriented with respect to the film surface when the films are subjected to the poling process and form permanent dipoles. This leads to higher content of β crystalline phase, which is essential for piezo-sensitivity. Semi-conducting PVDF can be used for piezo-resistor especially at the optimum composition of PVDF-PANI blends with poling which have very high sensitivity (>3000) at 100 gm load.

These studies indicate that SBS-PANI conducting blends can be used for piezo-sensors but their composition has to be optimized for good performance. The blends containing 15 % of PANI appear to be best for these applications. However, the dopant ion also plays an important role since the phase morphology changes with the same. In the case of DBSA-doped PANI, the dopant acts as plasticizer and gives more compatible/finely dispersed blend. This type of morphology is not amenable for obtaining high piezo-sensitivity whereas the HCl-doped PANI gives phase segregated morphology and better piezo-sensitivity. It may be pointed out that the conducting polymer blends which are essentially non-compatible behave more akin to composites and the results about such materials reported earlier by other authors are in keeping with the observations made in the present thesis. For example, the detailed analysis of the data reported by others authors when analyzed fit the SCLC type behaviour and show similarity to our

experimentally determined values for K & m. Pressure dependence of the electrical resistance is non-linear and depends very much on the composition as well as the type of PANI incorporated in the blend. The present studies indicate that the piezo-sensitivity is higher for the compositions having SCLC type charge transport than ohmic or even the tunneling type conduction.

Thus, the non-linear characteristics of the electrical conduction as well as the mechanical deformation of the conducting polymer blend and composite affect the piezo-response leading to optimum composition for highest sensitivity which depends on the modulus of the major matrix, particle/domain size of the dispersed phase as well as the type of conduction process.

A phenomenological model has been proposed for a conducting polymer based bi-layer type actuator which takes into account the nature of backing layer and gives the correlation between the modulus, thickness of the supporting substrates on the actuation. It clearly brings out the fact that for a given condition of dopant ion, applied potential and conducting polymer, there is an optimum thickness of the backing layer, its modulus and also the thickness of the conducting polymer at which the actuation is maximum. The results derived from the model clearly indicate higher sensitivity of the various factors at small thickness of the backing layer and/or its modulus. The optimal design parameters were investigated to estimate the effect of varying experimental conditions of the response of actuator. Thus, using this information, it is possible to adjust the parameters and choose appropriate materials for good actuation effect.

The experimental results of PPy actuator indicated that , the actuation response

characteristics depend on several factors: (a) backing layer thickness and its modulus, (b) conducting polymer thickness, (c) applied potential, (d) nature of dopant, (e) morphology of the conducting polymer, etc. these various findings are in keeping with the behaviour expected from the theoretical model described in this thesis. Actuation in PPy based bi-layer actuator can be controlled during manufacture of PPy films. Management of the deposition potential of PPy resulted in different qualities of PPy film. Thus, deposition potential can and should be carefully considered in the design of PPy bi-layer actuator. Electrochemical actuation of PPy was effected by the nature of dopants. Anions used during polymerization of PPy films have a greater effect on the actuation produced by bi-layer actuators. Higher bending angle can be obtained with medium size of anions. The potential limits suitable for application to PPy bi-layer actuator was investigated. It requires a delicate balance between extending the potential limits as far as possible to allow redox reaction, while ensuring that the potential at which over-oxidation will occur are not reached. In order to enhance the effect of electromechanical deformation, system

Table-6.1. Piezo-sensitivity coefficient (m) & non-linear charge transport coefficient (n) of SBS-PANI & PVDF-PANI blends.

System	PANI loading (%)	Value of n	Value of (m)
SBS+PANI (HCl-doped)	5	1	0.6805
	10	1.6	1.2429
	15	2.5	1.6178
	20	1.84	1.3140
	30	1	0.8092
SBS+PANI (DBSA-doped)	2	1.5	0.9716
	3	1.33	0.9118
	5	1.1	0.7894
	10	1	0.7655

System	PANI loading (%)	Value of n	Value of (m)
PVDF+PANI (HCl-doped)	5	1.15	1.0214
	10	2.29	1.5127
	15	1.53	1.2905
	20	1.08	0.8814
	25	1	0.7735
PVDF+PANI (DBSA-doped)	2.5	1	0.8011
	5	1.05	1.0040
	10	1	0.6890

design, such as structure of conducting polymers and morphology of the cooperative contribution of these mechanisms, are important.

The actuation mechanisms during the reduction are deduced nicely by considering electrostatic repulsion and diffusion controlled ion exchange phenomena. Diffusion of ions dependent on thickness of PPy layer thickness, nature of ions (size of ions), applied potential, and merely on backing layer thickness.

As seen from the table-6.1 the non-linear charge transport coefficient (n) and the piezo-sensitivity factor exponent (m) are correlated. When the non-linearity becomes higher, the piezo-sensitivity also increases. It should be noted that non-linear charge transport arises from the space charge limited conduction process, which suggests that for this type of transport process one would expect higher piezo-sensitivity. This is observed in all the conducting polymer dispersed system studied in this thesis.

The present studies have given deeper understanding regarding the various parameters, which play important role in governing the electromechanical response of conducting polymers dispersed or deposited on common polymers. It has brought forward the controlling factors which need to be optimized for best performance from a given

combination of conducting polymer with commodity polymer. The importance of the choice of material is also clearly brought forth. In certain cases, the same combination can be used for piezo-sensor as well as actuator. This is essential for smart systems which is self regulating. Typically, if one takes the example of flow control valve, one requires separating devices, materials and electronics for sensing, giving feedback and regulating the open area / aperture. All these functions can be carried out simply by using smart materials/system. The piezo-sensor and the actuator function can be performed by the diaphram made of electroactive polymer combined with flexible polymer. Single controlling circuit can be coupled with this to obtain the desired control for flow, pressure, etc. In order to build such devices/systems, the present studies will be certainly useful. Soft actuators can be used where the requirements of pressure, load, voltage, etc., one desired to be in the low range for example, in biomedical applications. The data obtained for materials studied in this thesis are useful in these areas for future applications.

List of U.S.Patents

1. Process for Preparing Conducting or Semi-Conducting Polymer with high Piezo- sensitivity.

S. Radhakrishnan and **Swarnendu B. Kar**

Pub No: US 2005/0065280 A1.

2. A Process for the Preparation of Semi-Conducting Polymer Film Containing Beta Crystalline phase of Poly-vinylidene fluoride.

S. Radhakrishnan and **Swarnendu B. Kar**

NF-354/ 2003, Appl. No- 10/810304.

List of Publications

S. Response Characteristics of Conducting Polypyrrole Bi-layer Actuators: Role of Backing Layer Polymer.

S.Radhakrishnan and **Swarnendu B.Kar**

Sensors and Actuators B. (in press, 2005)

2. Dual Phenomena in Response Time of Conducting Polymer Bi-layer Actuator.
S.Radhakrishnan and **Swarnendu B.Kar**

World wide Electroactive Polymer News letters, **Vol-7, No-1 June. 2005, P-15**

3. Enhancing Piezo-sensitivity in Polyvinylidene Fluoride /Conducting Polymer Composites.

S.Radhakrishnan and **Swarnendu B.Kar**

World wide Electroactive Polymer News letters, **Vol-7, No-1 June. 2005, P-16**

4. Role of Non-linear Processes in Conducting Polymer Blends for Piezo- sensors:2 . SBS/Polyaniline blends.

S.Radhakrishnan and **Swarnendu B.Kar**

Sensors and Actuators A : Physical, **12, 2005, 474.**

5. Response of Conducting Polymer bi-layer Actuators.
S.Radhakrishnan and **Swarnendu B.Kar**

*World wide Electroactive Polymer News letters***, Vol-6, No-2 Dec. 2004, P-17.**

6. Role of Backing Layer on Actuator performance of Conducting Polymer Bi-layer Actuators : A Phenomenological Model.

S.Radhakrishnan and **Swarnendu B.Kar** (***Proc, SPIE* 2004**)

7. Effect of Dopant ions on Piezo-response of Polyaniline- PVDF blends.

S. Radhakrishnan and **Swarnendu B. Kar, *Proc. SPIE*- 4934, 2002. P-23.**

8. Conducting polymer blends for piezosensors : Role of Non-linear Processes in sensitivity: Part-I

S.Radhakrishnan and **Swarnendu B.Kar.**

***Sensors* (Communicated)**

Symposia Presentations

1.Conducting Polyaniline/Elastomer Blends for Piezo-sensors.

Swarnendu B. Kar and S.Radhakrishnan.

Presented at the 9th National Symposium on Applied Physics and Sensors 2002 held at Institute of Engineers.

2. Conducting Polyaniline - Poly(vinylidine fluoride) blends for piezo-sensor.

Swarnendu B. Kar and S.Radhakrishnan.

Presented at the International Seminar on Frontiers of Polymer Science and Engineering (Macro-2002) I,I,T Kharagpur, India .

3. Low Electric Field Induced High Piezo-sensitive semi-conducting Polyvinylidene fluoride.

Swarnendu B.Kar and S.Radhakrishnan.

Presented at the International seminar on advances in Polymer Technology, Cochin University, Jan 2004.

4. Conducting Polymers as a Novel Materials for Bi-layer Actuators.

Swarnendu B.Kar, S.Radhakrishnan and B.D.Kulkarni.

Presented at the seminar on the foundation day Society of Polymer Science, India, July 2004.

5. Optimization of bi-layer Polymeric Actuator Design.

Swarnendu B.Kar and S.Radhakrishnan.
Science day symposium at NCL, Pune, India, on Feb -2004, 2004 Poster presentation.

6. Conducting Polymer Based Piezosensors.

Swarnendu B. Kar and S. Radhakrishnan

Presentated at the Workshop on NPSM , Bangalore , March, 2004.

7. Polyvinylidene Fluoride Films for Piezoelectric Applications.

Swarnendu B. Kar, S. Radhakrishnan, and S. Navale.

Presentated at the Workshop on NPSM , Bangalore , March, 2004

8. Optimization of conducting polymer based tactile sensor design.

Swarnendu B. Kar and S. Radhakrishnan.

Science day symposium at NCL, Pune, India, on Feb –2005.